THE IMPACT OF HEAT-MOISTURE TREATMENT ON THE MOLECULAR STRUCTURE AND PHYSICOCHEMICAL PROPERTIES OF NORMAL AND WAXY POTATO STARCHES

VARATHARAJAN VAMADEVAN

THE IMPACT OF HEAT-MOISTURE TREATMENT ON THE MOLECULAR STRUCTURE AND PHYSICOCHEMICAL PROPERTIES OF NORMAL AND WAXY POTATO STARCHES

by

©Varatharajan Vamadevan

A thesis submitted to the School of Graduate Studies in partial fulfillment of the requirements for the degree of Master of Science

Department of Biochemistry

Memorial University of Newfoundland

November 2010

St. John's Newfoundland and Labrador

ABSTRACT

Heat-moisture treatment (HMT) is a physical modification technique that modifies starch structure and properties without destroying its granular structure. HMT has been shown to cause starch chain interactions and crystallite disruption/reorientation within the amorphous and crystalline domains. However, the part played by amylose (AM) during HMT of starches is not properly understood. Furthermore, a systematic study has not been carried out to examine how variations in HMT temperatures influence molecular structure, physicochemical properties and digestibility of normal potato (NP) and waxy potato (WP) starches. Thus, the objective of this study was to determine changes to molecular structure, physicochemical properties and digestibility of NP and WP starches on HMT at different temperatures (80, 100, 120 and 130°C) for 16 h at 27% moisture. Structural changes on HMT were monitored by scanning electron microscopy (SEM), confocal laser scanning microscopy (CLSM), polarized light microscopy (PLM), wide angle X-ray scattering (WAXS), attenuated total reflection-Fourier transform infrared (ATR-FTIR) spectroscopy, fluorophore assisted capillary electrophoresis (FACE) and K/S spectra. Changes to physicochemical properties on HMT were determined by granular swelling, amylose leaching, gelatinization parameters and pasting properties. Digestibility of normal and waxy potato starches before and after HMT by porcine pancreatic α-amylase (PPA) was monitored by measuring initial velocity and by examination of the granular structure at different stages of hydrolysis by SEM, CLSM and PLM. The results showed that structural changes on HMT were influenced by differences in starch chain mobility at different temperatures of HMT. Starch chain mobility, in turn, was influenced by the interplay between the extent to which B-type crystallites were transformed into A+B-type crystallites, kinetic energy imparted to starch chains and amylose content. The main type of structural changes

influencing physicochemical properties at different temperatures of HMT were starch chain interactions (at 80 and 100°C), disruption of hydrogen bonds between amylose-amylopectin and amylopectin-amylopectin (at 120 and 130°C), disorganization of amylopectin chains near the vicinity of the hilum (at 100, 120 and 130°C) and formation of interrupted helices (at 130°C). The susceptibility of NP and WP starches towards α-amylase decreased at 80°C, but increased in the range 100 to 130°C. NP and WP starches exhibited heterogeneity in degradation (NP>WP) in both their native and HMT states.

ACKNOWLEDGEMENTS

I would like to express my sincere appreciation for the invaluable guidance and advice of my supervisor, Dr. R. Hoover. I also appreciate Dr. F. Shahidi and Dr. V. K. Booth for serving on my supervisory committee and for the time and effort that they spent on my behalf. I would like to acknowledge the Department of Biochemistry and the School of Graduate Studies for providing financial assistance. Financial support from Dr. R. Hoover is also acknowledged.

I would like to express my sincere thanks to Dr. K. Seetharaman, Dr. Q. Liu, Dr. T. Vasanthan, Dr. R. N. Chibbar, Ms. E. Donner, Dr. L. Jihong, K. K. M. Nantanga and Dr. S. Jaiswal for their help with some of the analytical techniques described in the thesis.

I wish to express my sincere thanks to Dr. A. Yethiraj (Department of Physics and Physical Oceanography) for assistance with confocal laser scanning and polarized microscopy. Thanks are also extended to my colleagues H. Lan, T. Hughes and A. Priyatharani.

Finally, I thank my wife, daughter, parents and friends for helping me in all possible ways to succeed.

TABLE OF CONTENTS

LIST OF TABLES

LIST OF FIGURES

LIST OF ABBREVIATIONS

AFM	Atomic force microscopy
AM	Amylose
AML	Amylose leaching
AMP	Amylopectin
APTS	Aminopyrene trisulfonic acid
ATR-FTIR	Attenuated total reflectance Fourier transform infrared spectroscopy
a_w	Water activity
BFM	Bright field microscopy
^{13}C-CPMAS-NMR	Cross-polarization magic angle spinning carbon-13 - nuclear magnetic resonance
CL	Chain length
CLSM	Confocal laser scanning microscopy
Cps	Counts per second
db	Dry basis
DMSO	Dimethyl sulfoxide
dp	Degree of polymerization
DSC	Differential scanning calorimetry
FACE	Fluorophore-assisted capillary-electrophoresis
HMT	Heat-moisture treatment
MALDI-TOF MS	Matrix assisted laser desorption ionization - time of - flight mass spectroscopy
NP	Normal potato
PLM	Polarized light microscopy

PPA	Porcine pancreatic α-amylase
RDS	Rapidly digestible starch
RS	Resistant starch
RVA	Rapid Visco Analyser
SCLCP	Side chain liquid crystalline polymer
SDS	Slowly digestible starch
SEM	Scanning electron microscopy
SF	Swelling factor
TEM	Transmission electron microscopy
Tg	Glass transition temperature
Tm	Melting temperature
XRD	X-ray diffraction
WP	Waxy potato

CHAPTER 1

INTRODUCTION

Starch is an important functional ingredient in many food products. However, native starches usually do not meet industrial needs in which starch should be able to withstand low acidity, high temperatures and high shear forces. Consequently, starches have been modified physically and chemically in order to extend the range of starch applications in the food and non-food sectors (Hoover, 2010). Heat-moisture treatment (HMT) is a physical modification technique wherein starch granules at low moisture levels (<35% H_2O, w/w) are heated at a temperature above the glass transition temperature (Tg) but below the gelatinization temperature for a fixed period of time (15 min to 16 h). HMT has been shown to change starch properties by facilitating starch chain interactions within the amorphous and crystalline domains and/or by disrupting starch crystallites, the extent of these changes being influenced by starch composition, organization of amylose and amylopectin within the native granules, and by the conditions (temperature, moisture, time) prevailing during HMT (Hoover, 2010). Regardless of the origin of the starch, HMT increases the gelatinisation transition temperature, widens the gelatinisation temperature range, decreases granular swelling and amylose leaching, and increases thermal stability. Depending on the starch source, changes to the X-ray pattern (B to A + B), formation of amylose-lipid complexes, disruption of crystallinity, and an increase or decrease in enzyme susceptibility have also been shown to occur on HMT (Gunaratne and Hoover, 2002; Hoover and Vasanthan, 1994a).

Most studies have been on the impact of HMT on the thermal properties, crystallinity and pasting properties of normal starches. Some researchers (Hoover and Manuel, 1996; Kweon *et al.*, 2000;

Zavareze *et al.*, 2010) have attempted to explain the impact of HMT on the structure and physicochemical properties of starches varying in amylose content. However, the part played by amylose during HMT of starches is still not properly understood. Unlike in cereal starches, amylose has been shown to be co-crystallized with amylopectin in normal potato starch (Hoover and Vasanthan, 1994a; Saibene *et al.*, 2008; Zobel, 1988a). Therefore, it is hypothesized that amylose may have a significant impact on the extent to which double helical chains forming the crystalline lamellae of potato amylopectin move and rearrange during HMT.

HMT has been conducted mainly at a fixed temperature and moisture content for periods varying from 15 min to 24 h. No attempt has been made to investigate the influence of varying temperature and moisture content during HMT on starch structure and properties. Furthermore, the impact of HMT on starch digestibility has received only scant attention. Kweon *et al.* (2000) and Zavareze *et al.* (2010) studied the influence of moisture content during HMT on the digestibility of normal, waxy and high amylose maize (110°C/16 h) and rice (110°C/1 h) starches, respectively. Digestibility of HMT maize starches by porcine pancreatic α-amylase (PPA) was shown to decrease in the moisture range of (15-21%) but to increase at 27% moisture (Kweon *et al.*, 2000). However, Zavareze *et al.* (2010) reported increased PPA hydrolysis with an increase in moisture content (15 to 25%) in HMT rice starches. Hoover and Manuel (1996) reported decreased PPA hydrolysis on HMT (100°C, 30% moisture, 16 h) of normal, waxy and high amylose maize starches. In pulse (Hoover and Manuel, 1995) and tuber (Gunaratne and Hoover, 2002) starches, PPA hydrolysis was shown to increase on HMT (100°C, 30% moisture, 16 h). The results from all of the above studies showed that the impact of HMT on PPA hydrolysis is influenced by starch moisture content and by structural (crystallite disruption,

change in polymorphic form, crystallite reorientation, amylose-lipid interaction, starch chain interaction) and morphological (formation of fissures and cracks on the granule surface) changes on HMT. However, no systematic study has been carried out to investigate the susceptibility to PPA of starches subjected to HMT at different temperatures but at the same moisture level and time period of heat treatment. It is hypothesised, that under the above conditions, structural changes within the amorphous and crystalline domains of starch granules will vary at different temperatures of HMT, due to differences in starch chain mobility. Consequently, this would influence the accessibility of PPA to the amorphous and crystalline domains of the starch granule. Thus, a comparison of the action pattern of PPA on native normal and waxy potato starches with those of their HMT counterparts may provide deep insight into the influence of starch structure on the rate and extent of α-amylolysis.

The objectives of this study were as follows: 1) to determine the structural and property changes of normal and waxy potato starches subjected to heat-moisture treatment at 80, 100, 120 and 130°C at 27% moisture for 16h and 2) to determine the impact of structural changes on the susceptibility (monitored by determination of the rate and extent of hydrolysis and degradation pattern) of normal and waxy potato starches to PPA hydrolysis.

CHAPTER 2

LITERATURE REVIEW

2.1 General

Starch is a natural biopolymer produced by many plants as a source of stored energy. It is the second most abundant biomass material in nature. Starch is stored in seeds, tubers, roots, stems, leaves, fruits and pollen. The most important sources of starch are cereal grains (e.g., rice, maize, wheat, barley, sorghum and others), tubers (e.g., potato, sweet potato, yam), storage roots (e.g., cassava, taro) and seeds of beans and peas. Worldwide, the main sources of starch are maize (82%), wheat (8%), potatoes (5%) and cassava (5%) (Le Corre *et al.*, 2010).

The unique physical properties and behaviour of starch makes it an important functional ingredient in many food products. Starch contributes 50-70% of the energy in the human diet (Copeland *et al.,* 2009). In addition to being an important source of energy in the human diet, starch is also utilized in many different industrial processes because it is abundant, renewable, biodegradable and safe (Table 2.1). However, native starches from various plant species have poor functionality, and are thus not directly suitable for food applications. Consequently, to meet industrial demands, modification of starch is often needed (Hoover, 2010).

2.2 Starch granule morphology

2.2.1. Granule size and shape

Starch occurs in granules that are relatively dense, and the granules from different botanical sources vary in their size and shape (Jane *et al.,* 1994; Svegmark and Hermansson, 1993).

Table 2.1 Food and non-food applications of starches

Application area	Uses of native and modified starches
Food	Bakery products, batters and breadings, beverages, confectionery, gravies and creams, syrups and desserts, fat mimetics, yoghurts, cheese and imitation cheese, meat binders, cereals and snacks, puddings, instant meals, dressings, soups, sauces, viscosity modifiers, glazing agents, stabilizing agents
Functional foods	Ingredient (e.g., slowly digestible starch [SDS], resistant starch [RS]), encapsulant
Pharmaceutical	Diluent, binder, drug delivery, dusting agent, pill coating
Medical	Plasma extender/replacement (hydroxyethyl starch plasma), organ preservation, absorbent sanitary products, plasters and dressings
Biotechnology	Substrate for growing microorganisms
Fuel	Bioethanol (e.g., corn starch)
Adhesive	Hot-melt glues, stamps, book binding, envelopes, labels, wood adhesives, lamination, paper bags
Agrochemical	Mulches, pesticide delivery, seed coatings
Cosmetics	Dusting powder, make-up, soap filler/extender, face cream, tooth paste
Detergent	Bio-surfactants, builders, co-builders, bleaching agents, bleaching activators
Paper	Binding, internal sizing, surface sizing, filler retention, paper coating, carbonless paper stilt material, disposable diapers, feminine products
Plastics	Biodegradable filler
Biologically-degradable materials	Biodegradable plastic film (e.g., food packaging materials)
Textiles	Warp sizing, fabric finishing and printing, fire resistance
Ceramics	Filler
Metals	Foundry core binder, sintered metal additive, sand casting binder
Construction	Concrete block binder, paint filler, plywood/chipboard adhesive, asbestos, clay/limestone binder, fire resistant wallboard, gypsum board binder
Purification	Flocculent for wastewater treatment
Mining	Viscosity modifier (oil), ore flotation, ore sedimentation, oil well drilling muds
Explosives	Wide range binding agent, match-head binder
Miscellaneous	Dry cell batteries, printed circuit boards, leather finishing

Adapted from Burrell (2003), Davis *et al.* (2003), Galliard (1987), Satin (1998 and 2001).

The morphology of starch granules depends on the biochemistry of the chloroplast or amyloplast, as well as the physiology of the plant (Badenhuizen, 1969). In some sources, the age of the starch could cause differences in the size of the starch granules (French, 1984; Shannon and Garwood, 1984). Diameter of starch granules varies from less than 1 μm (e.g., amaranth, small pigweed) to more than 100 μm (e.g., canna) (Hoover, 2001; Jane, 2009; Pérez and Bertoft, 2010). Light microscopy, scanning electron microscopy (SEM), transmission electron microscopy (TEM) and atomic force microscopy (AFM) are widely used to characterize the size and shape of starch granules (Baker *et al.,* 2001; Baldwin *et al.,* 1997; Gallant *et al.,* 1992; Glaring *et al.,* 2006; Juszczak *et al.,* 2003; Ridout *et al.,* 2002; Sujka and Jamroz, 2009).

Tuber starches are generally large, ellipsoid or spherical with apparent shells around an eccentric hilum. Cereal starches are generally small and polyhedric with a concentric hilum (Gallant *et al.,* 1992; Hoover, 2001; Tester and Karkalas, 2002). Wheat, triticale, barley and rye starches have bimodal size (large A- and small B-type) distributions (Peng *et al.,* 1999; Stoddard, 1999). High amylose maize starch exhibits filamentous granules (budlike protrusions) (Jane, 2009). Legume starches are kidney-like or ovoid with well-defined shells centred along an elongated hilum (Hoover *et al.,* 2009). The general characteristics of starch granules are presented in Table 2.2.

2.2.2. Pores, channels and cavities

Surface pores, cavities and channels are important characteristic features of starch granules. They are large enough that they can be seen by SEM (Fannon *et al.,* 1992, 2004; Sujka and Jamroz, 2007). Pores have been observed on the granule surface of the following starches: corn,

Table 2.2 Size and shape of starch granules from different botanical origins

Starch source	Shape	Size (μm)	Source of information
Potato			
Normal	Oval, spherical,	5-100	Tester and Karkalas (2002)
Waxy	Round, oval	5-100	ELIANE™ (2006)*
High amylose	Rough	-	Glaring *et al.*, (2006)
Sweet potato	Round, oval, polygonal	2-42	Lim *et al.* (1994)
Yam (*D. alata*)	Oblong, oval	12-100	Gunaratne and Hoover (2002)
Cassava	Spherical, truncated, round	7-25	Mishra and Raj (2006)
Canna	Elliptical	6-79	Peroni *et al.* (2006)
Arrowroot	Round, oval	9-42	Peroni *et al.* (2006)
Ginger	Polygonal	3-34	Peroni *et al.* (2006)
Barley	Round, elliptical	2-25	Davis *et al.* (2003)
Corn			
Normal	Spherical, polyhedral	2-30	Tester and Karkalas (2002)
Waxy	Spherical, polyhedral	2-30	Tester and Karkalas (2002)
High amylose	Irregular	2-30	Tester and Karkalas (2002)
Oat	Polyhedral	3-10 (single), 80 (compound)	Tester and Karkalas (2002)
Rice	Polyhedral	3-8 (single), 150 (compound)	Tester and Karkalas (2002)
Sago	Oval	20-40	Tester and Karkalas (2002)
Sorghum	Spherical	5-20	Tester and Karkalas (2002)
Rye	Lenticular (A-type)	10-40	Tester and Karkalas (2002)
	Spherical (B-type)	5-10	Tester and Karkalas (2002)
Triticale	Spherical	1-30	Tester and Karkalas (2002)
Wheat	Lenticular (A-type)	15-35	Tester and Karkalas (2002)
	Spherical (B-type)	2-10	Tester and Karkalas (2002)
Lentil	Oval, round, ellipsoidal	15-30	Hoover, *et al.* (2009)
Smooth pea	Oval, round, irregular, rentiform	2-40	Hoover *et al.* (2009)
Wrinkled pea	Round	17-30	Hoover *et al.* (2009)

* ELIANE™ is a waxy potato starch marketed by the starch company AVEBE

sorghum, millet (over the entire granule surface), wheat, rye, and barley (along the equatorial groove of large granules). Granules of potato, tapioca, rice, oat, canna, and arrowroot appear to have no pores, but there is disagreement about the presence of pores on the surface of potato starch granules (Fannon *et al.*, 1992). The occurrence of pores on the potato starch granular surface was reported by Sterling (1973). AFM images showed depressions and protrusions (ranging up to 1 μm in size) on the surface of potato and tapioca starch granules (Juszczak *et al.*, 2003). Singh *et al.* (2006) have also reported the presence of some small nodules or protuberances, and surface fragmentation, on potato starch granules. This suggests that the structure of starch granules is more complicated than can be seen in photographs made by conventional SEM techniques. Li *et al.* (2007) have shown that pores on maize starch granules develop during a late maturation stage, i.e. 30 days after pollination (DAP). Starch granules isolated from maize kernels harvested 30 DAP showed few or no pores, whereas those from kernels harvested 45 DAP (fully matured and dried in the field) showed a large number of pores (Li *et al.*, 2007). Apart from surface pores, Huber and BeMiller (1997) observed central cavities in normal maize, waxy maize and sorghum starch granules and they proved that the cavities were not formed by drying but could be enlarged by this process.

The pores were shown to be openings to channels (5-400nm in diameter) connecting an internal cavity at the granule hilum to the external surface (Fannon *et al.*, 1993; Huber and BeMiller, 1997, 2000). It is still unclear how pores and channels are formed in certain starch granules. Jane *et al.* (1993) isolated starch granules from different parts of the corn kernel. They reported that starch granules near to the germ contained more pores than granules from other parts of the kernel, and suggested that this was a consequence of active *in situ* amylase(s). Fannon *et al.*

(2004) hypothesized that amyloplasts of maize and sorghum endosperm tissue contained microtubules that radiated from the locus of the hilum outward to the plastid periphery and that the granule develops around the radially oriented microtubules, which become the granule channels that terminate in openings to the outside surface of the granule. Benmoussa *et al.* (2010) also believed that the channels in maize starch granules are remnants of amyloplast microtubules. Microtubules may serve at least two purposes in amyloplasts and granules in which they occur: (1) they may facilitate starch polymer and granule biosynthesis and, (2) they may function to provide variation in the rate of granule breakdown during seed germination (Benmoussa *et al.,* 2010).

The channels of corn starch granules have been shown to be lined with proteins and phospholipids (Benmoussa *et al.,* 2010; Fannon *et al.,* 2004; Gray and BeMiller, 2004; Han *et al.,* 2005; Han and Hamaker, 2002). Han *et al.* (2005) found that Bt1 protein, the major translocator of ADP-glucose (Cao and Shannon, 1997; Shannon *et al.*, 1998) into the amyloplast for starch synthesis, was missing after digestion of starch granules with thermolysin and concluded that Bt1 protein is present in channels. Further investigations of the nature of channels were done by Gray (2003), who found that the binding of silver ions was completely removed only after treatment with both thermolysin and phospholipase C, and not by treatment with either one alone, indicating the presence of both proteins and phospholipids in channels. Subsequently, phospholipid was identified by matrix assisted laser desorption ionization-time-of-flight mass spectroscopy (MALDI-TOF MS) as lysophosphatidyl choline with either palmitic acid [16:0] or linoleic acid [18:2, n-6] fatty acid moieties (Lee and BeMiller, 2008).

The number of individual channels in corn starch granules varies from granule to granule, and the average number of channels per granule in a population of granules is a function of the genetic makeup of the parent plant (Fannon *et al.,* 2004; Widya *et al.*, 2010). In wheat starch, A-type granules contain two types of channels: larger channels located on the equatorial groove and smaller channels located throughout the granule. B-type wheat starch granules contain only one type of channel: large, void-like channels that are less defined than the channels of A-type granules (Kim and Huber, 2008). The presence of pores, channels and cavities increases the granule surface which is potentially available for chemical and enzymatic reactions (Sujka and Jamroz, 2007 and 2009).

2.3 Starch structure

Starch is a semicrystalline biopolymer, which displays a hierarchical structural periodicity. It is considered to be structured on five different length scales: the whole granule architecture (1-100 μm), growth rings (120–400 nm), blocklets (20–500 nm), amorphous and crystalline lamellas (9 nm) and amylopectin and amylose chains (0.1–1.0 nm) (Copeland *et al.*, 2009; Perez and Bertoft, 2010; Tester *et al.*, 2004; Vandeputte and Delcour, 2004).

2.3.1 Major structural components

Native starches from different botanical sources vary widely in structure and composition (Hoover, 2001). Starch consists of two main structural components, amylose and amylopectin. Amylose is a relatively long, linear α-glucan with few branches, containing approximately 99% α-(1,4) and up to 1% of α-(1,6) linkages, whereas amylopectin is a heavily branched structure, built from

Fig 2.1 Schematic diagram of amylose (A) and amylopectin (B) (adapted from Tester and Karkalas, 2002).

A

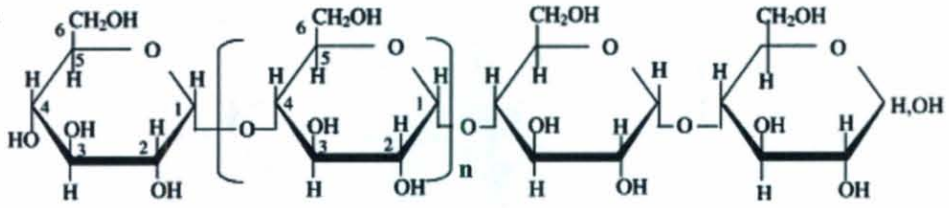

B

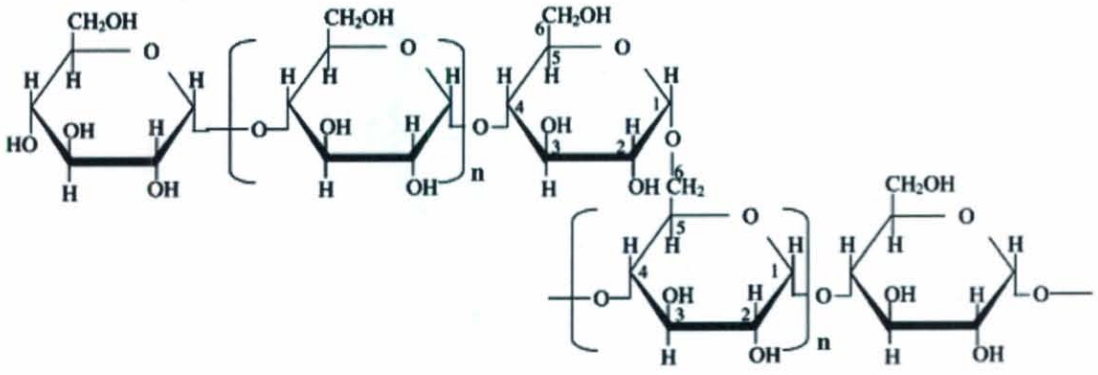

about 95% α-(1,4) and 5% α-(1,6) linkages (Fig 2.1) (Buléon *et al.*, 1998; Pérez and Bertoft, 2010). Normal starches consist of 20-30% amylose and 70-80% amylopectin, but waxy (amylose-free) starches contain essentially 100% amylopectin. High amylose starches (e.g., amylomaize V and VII and wrinkled pea) contain less than 30% amylopectin. The ratio of these two polysaccharides influences the functional properties of starch (Hoover, 2001). The proximate composition of starches of different botanical origin is presented in Table 2.3.

Amylose has a molecular weight range of approximately 10^5-10^6 g/mol (Buléon *et al.*, 1998; Mua and Jackson, 1997), degrees of polymerization (dp) of 324-4920 monomer units and 9–20 branch points equivalent to 3-11 chains per molecule (Hizukuri, *et al.*, 1981; Mua and Jackson, 1997; Takeda *et al.*, 1987; Wang and White, 1994; Yashushi *et al.*, 2002; Yoshimoto *et al.*, 2000). Each chain contains approximately 200-700 glucose residues (Tester and Karkalas, 2002). Amylopectin is a much larger molecule than amylose with a molecular weight of 10^7-10^9 (Biliaderis, 1998; Buléon *et al.*, 1998; Morrison and Karkalas, 1990; Mua and Jackson, 1997). The dp of amylopectin is generally within the range 0.7 to 26.5 × 10^3 (Pérez and Bertoft, 2010).

A third component, intermediate materials, has been identified, especially in starches from plants with modified starch biosynthesis and in low amounts in normal starches (Banks and Greenwood, 1967, Klucinac and Thompson, 1998; Lansky *et al.*, 1949; Wang *et al.,* 1993; Yoon and Lim, 2003). High amylose maize genotypes (Buléon *et al.,* 1998; Yuan *et al.,* 1993) and wrinkled pea (Bertoft, 1993) are best known for their content of intermediate materials.

Table 2.3 Proximate composition (%) of starches of different botanical origin

Starch source	Amylose	Lipid	Nitrogen	Phosphorus	Reference
Potato					
Normal	28.1	0.20	0.09	0.1	Gunaratne and Hoover (2002)
Waxy	0.0	-	-	0.066	McPherson and Jane (1999)
High amylose	59-72	-	-	-	Schwall *et al.* (2000)
Sweet potato	22.6	0.14	0.02	0.014	Peroni *et al.* (2006)
Yam	32.6	0.10	0.01	0.022	Peroni *et al.* (2006)
Cassava	19.8	0.15	0.03	0.007	Peroni *et al.* (2006)
Arrowroot	20.8	0.17	0.02	0.018	Peroni *et al.* (2006)
Canna	31.7	0.19	0.02	0.031	Peroni *et al.* (2006)
Ginger	26.5	0.24	0.05	0.007	Peroni *et al.* (2006)
Wheat	27.3	0.7	0.04	-	Hoover and Vasanthan (1994a)
Oat	19.4	1.13	0.05	-	Hoover and Vasanthan (1994a)
Maize					
Normal	29.9	0.75	0.02	-	Hoover and Manuel (1996)
Waxy	1.2	0.22	0.02	-	Hoover and Manuel (1996)
Amylomaize V	65.5	0.95	0.03	-	Hoover and Manuel (1996)
Barley					
Normal	23.6-29.0	0.91	0.3	-	Li *et al.* (2001)
Waxy	0-6.44	0.48	0.25	-	Li *et al.* (2001)
High amylose	41.7-44.5	1.34	0.41	-	Li *et al.* (2001)
Lentil	25.3-32.3	0.01-0.08	0.03-0.09	-	Hoover *et al.* (2009)
Smooth pea	24-49	0.02-0.08	0.02-0.07	-	Hoover *et al.* (2009)
Wrinkled pea	60.5-88.0	0.8-0.84	0.05-0.08	-	Hoover *et al.* (2009)

These intermediate materials have structures and properties intermediate to those of amylose and amylopectin (Jane, 2009).

2.3.1.1. Amylose

2.3.1.1.1 Fine structure of amylose

Although all amylose molecules were once considered to be linear, many amylose molecules cannot be completely hydrolysed by β-amylase [β-amylase cannot hydrolyse or by pass α-(1,6)-linkages; its action stops at the branch points (see section 2.4.7.1)]. The incomplete β-amylolysis indicates that a certain degree of branching is present in some amylose molecules (Greenwood and Thompson, 1962; Hizukuri *et al.,* 1981; Takeda *et al.,* 1987). The β-amylolysis limit of amylose varies from 72-95% compared to 55-61% for amylopectin (Jane, 2009).

The amylose fraction of starch occurs in double-helical A- and B-amyloses and the single-helical V-amylose. Both A and B forms feature left-handed helices with six glucose units per turn and seem to differ only in the packing of the starch helices (Buléon *et al.,* 1998). The latter contains a channel-like central cavity that is able to include molecules such as iodine, dimethyl sulphoxide (DMSO), alcohols or fatty acids (Rappenecker and Zugenmaier 1998; Godet *et al.,* 1995; Saitô *et al.,* 1991; Imberty *et al.,* 1991). In the single helical form, the interior surface of amylose is built up by C-H groups and glycosidic oxygen atoms forming a lipophilic core, whereas all the polar hydroxyl groups are positioned on the outer surface of the helix (Hoover, 1998). The inner diameter of the amylose helix is controlled by the size of the complexing agent. Predominant in the V amylose family is the common form of V_6 amylose, characterized by six glucose units per turn (Cardoso *et al.,* 2007: Jouquand *et al.,* 2006: Yamashita, *et al.,*

1971). However, for some guest molecules (e.g., iso- and tertiary butyl alcohols, benzoic acid, dimethyl sulphoxide, 1-napthol) the helix exhibits a different structure (e.g., V_7 [7 glucose residues per turn] and V_8 [8 glucose residues per turn]) (Helbert *et al.,* 1994; Shogren *et al.,* 2006).

Formation of the double helix requires an alignment of two amylose molecules. Without the presence of complexing agents, the linear portion of amylose molecules gradually associate and form double helices. Kinetic studies have shown that the rate of double helix formation depends on the molecular size of the amylose, its concentration and the temperature (Jane, 2009). Gidley and Bulpin (1987) demonstrated with a model system of oligosaccharides that the minimum chain length required to form starch double helices is 10. However, in the presence of longer chains, short chains (dp>6) can participate in the formation of double helices (Gidley and Bulpin, 1987).

2.3.1.1.2 Conformation of amylose

In a freshly prepared aqueous solution, amylose is present as a random coil (Hayashi *et al.,* 1981). However, the random coil conformation is not stable. Amylose tends to form either single helical (inclusion) complexes with suitable complexing agents or to form double helices among themselves when no suitable complexing agent is available (French and Murphy, 1977; Jane 2009; Zobel, 1988a, 1988b). Both single and double helices result in lower energy states and are thermodynamically favourable (Jane, 2009). However, the local conformation of an amylose chain in an aqueous environment is a matter of dispute. Three different molecular models (Fig 2.2) (Banks and Greenwood, 1971, 1975; Cowie, 1961; Fujii *et al.*, 1973; Kitamura

and Kuge, 1989; Nguyen *et al.,* 1976; Rao and Foster, 1963; Senior and Hamori, 1973; Yamamoto *et al.,* 1982) have been proposed for amylose on the basis of data analysis of conformation-dependent properties in aqueous solvents and DMSO: 1) random coil with no helical nature (Fig 2.2a), 2) interrupted helix composed of helix regions (helical segment) with intervals of short regions of random coils between them (Fig 2.2b) and 3) deformed helix (loosely wound helical chain [Fig 2.2c]). Cheetham and Tao (1998b) have shown by ^{13}C NMR, optical rotation and viscosity measurements that amylose conformation in 100% DMSO is helical rather than a random coil. With the addition of water, the intramolecular hydrogen bonding in amylose is gradually replaced by amylose-water intermolecular hydrogen bonds, leading to conformational changes. When the concentration of DMSO is decreased from 100% to 66.6%, amylose conformation changes from tight helix to loose helix. A further decrease in DMSO concentration (66.6 to 33.3%) causes a conformational change from loose helix to random coil (Cheetham and Tao, 1998).

2.3.1.1.3 Location of amylose

The exact location of amylose in starch granules still remains unresolved. Jane *et al.* (1992) showed, by cross-linking studies on potato and corn starches using epichlorohydrin, that amylose appears to be interspersed among the amylopectin molecules rather than being located in bundles. bundles. Surface gelatinization studies (Jane and Shen, 1993) have shown that amylose is heterogeneously distributed within the granule. In potato and maize starches, amylose has been found to be concentrated mainly at the peripheral regions of the granules (Jane and Shen, 1993). However, Tatge *et al.* (1999) have shown, by studies of amylose synthesis in transgenic potato granules, that amylose is mainly present in the central region of the granule.

Fig 2.2 Proposed models for amylose structure in aqueous solution (adapted from Banks and Greenwood, 1975; Yamamoto *et al.*, 1982).

(a) random coil structure
(b) interrupted helical structure
(c) deformed helix structure

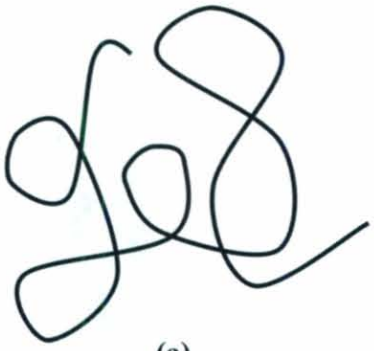

(a)

(b)

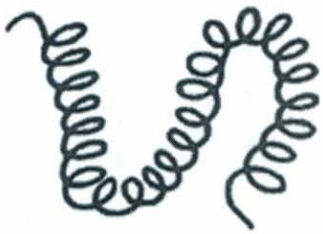

(c)

Based on small angle X-ray scattering studies on barley, pea and maize starch granules, Jenkins and Donald (1995) postulated that in these starches amylose is mainly located in the amorphous growth rings. Atkin *et al.* (1999) have shown by enzyme-gold labeling and iodine staining studies on hydrated maize and potato granules that amylose is localized in distinct amorphous regions around the hilum. Distribution of amylose in starch granules of different botanical origin has been extensively investigated by many researchers (Blennow *et al.,* 2003; Glaring *et al.,* 2006; Wei *et al.,* 2010) using APTS (8-amino-1,3,6-pyrenetrisufonic acid) coupled with confocal laser scanning microscopy (CLSM). These results also indicated that a high concentration of amylose is present in the granule center (region around the hilum).

Several studies have shown that in potato starch, amylose is co-crystallized (Fig 2.3) with the outer branches of amylopectin chains, forming double helices (Hoover and Vasanthan, 1994a; Jenkins and Donald, 1995; Saibene *et al.,* 2008; Saibene and Seetharaman, 2010; Zobel, 1988a). However, the location of amylose relative to the amylopectin molecules in common corn starch is contradictory. Based on cross-linking studies, Jane *et al.* (1992) and Kasemusuwan and Jane (1994) suggested that amylose and amylopectin are closely associated in normal maize starch. Zobel (1988a) suggested that amylose may be partly co-crystallized with amylopectin chains in potato starch but they are separated in maize starch granules. Gerard *et al.* (2002) used mild acid hydrolysis to investigate the location of amylose with respect to the amorphous and/or crystalline regions in maize starch mutants. They observed a greater interaction of amylose and amylopectin in high-amylose maize starches than in common corn starch. Co-crystallization of amylose and amylopectin has also been reported in wheat starches (Yuryev *et al.,* 2007). .

Fig 2.3 Proposed model for co-crystallization of amylose with amylopectin (Jenkins and Donald, 1995, Copyright Elsevier, reproduced with permission).

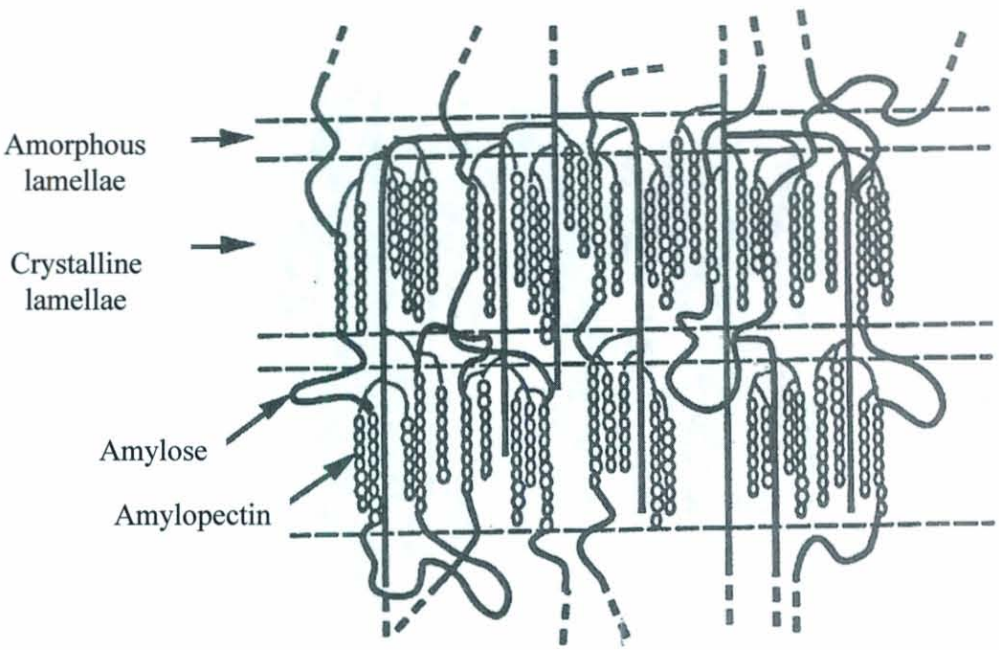
Amorphous lamellae
Crystalline lamellae
Amylose
Amylopectin

2.3.1.1.3 Amylose iodine inclusion complex

Amylose molecules are believed to be arranged in a left handed helix of an outer diameter of 13A°, a 5.0A° central cavity, and a pitch of 8A°, with each turn of the helix corresponding to six anhydroglucose units (Gidley and Bulpin, 1987; Rundle and French, 1943; Rundle, 1947). The cavity provides enough space to accommodate iodine atoms that are more or less linearly arranged with an internuclear distance of about 3.1A° (Fig 2.4a). This was first suggested by Hanes (1937) and later confirmed by X-ray diffraction analysis by Rundle *et al.* (1943). During inclusion complex formation, an iodine molecule presumably enters into the cavity of the extended helix (Fig 2.4b), followed by its polarization by the oxygen atoms (Davis *et al.,* 1994), which in turn helps the other iodine molecules to align within the cavity. The interaction of a polyiodide unit with the extended helix may form a tighter helix (Fig 2.4c), thereby providing greater stability to the polyiodine complex (Davis *et al.,* 1994). Even though the amylose-iodine complex has been extensively studied, the mechanism of its formation remains controversial. Several researchers (Knutson *et al.,* 1982; Saenger, 1984; Thoma and French, 1960; Yu *et al.,* 1996) have shown that iodide ions (polyiodide units) are involved with the amylose-iodine complex. Calabrese and Khan (1999) suggested that the amylose-iodine complex can be explained by merely considering the presence of the I_6 unit. However, there is ample evidence that in aqueous solution, the concentration of iodide ion is an important factor determining the extent to which iodine is bound by starch and that a significant fraction of bound iodine is iodide ion (Rendleman, 2003). Yu *et al.* (1996) have demonstrated that the primary structures of the polyiodide chains are composed of I_3^- and I_5^- subunits, which combine to form four dominant polyiodide chains such as I_9^{3-}, I_{11}^{3-}, I_{13}^{3-} and I_{15}^{3-}. These polyiodide chains

Fig 2.4 Proposed model for (a) amylose-iodine inclusion complex, (b) two extended helical segments of amylose joined by random non-helical structure and (c) two tighter helical segments of amylose joined by random non-helical structure (adapted from Calabrese and Khan,1999; Davis *et al.*, 1994).

(a)

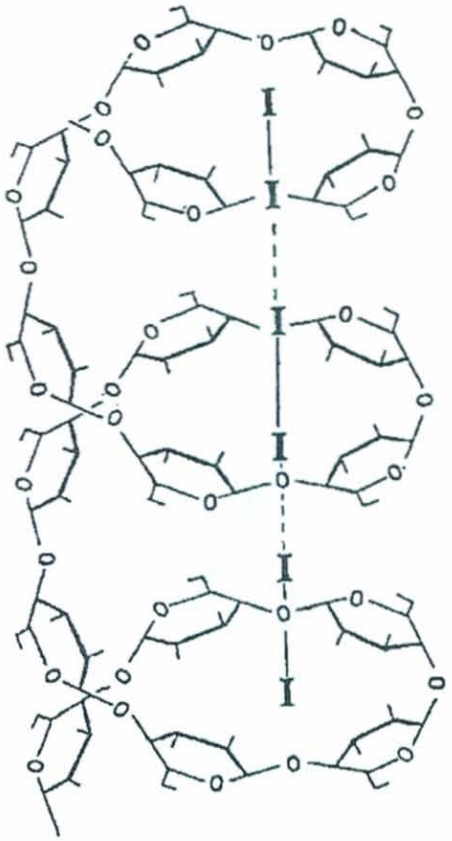

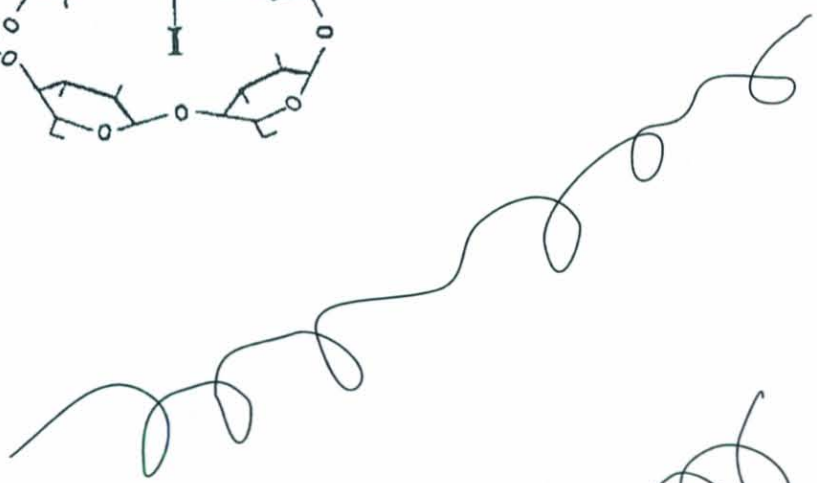

(b)

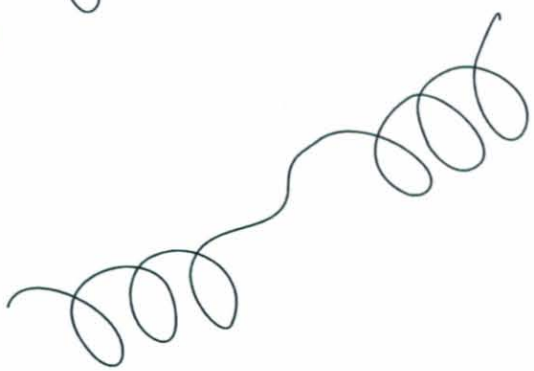

(c)

give different absorbance spectra (480-510, 610-640, 690-720 and 730-760 nm, respectively) when complexing with amylose. The average I----I distances of 3.1A between these units are shorter than van der Waals radii. This facilitates electron delocalization along the polyiodide chain and explains the amylose-iodine spectrum (Saenger, 1984). However, the polyiodide units are not stable without the helix structure around (Davis and Khan, 1994).

The iodine binding capacity of pure amylose is reported to be 19-22% of its weight (Banks, *et al.,* 1971), whereas for amylopectin it is about 1% (Gerard *et al.,* 2001). Spectrophotometric and potentiometric methods are widely used for determining the amylose contents of starches. The color and wavelength of maximum absorbance of the amylose-iodine complex vary according to the degree of polymerization (dp) of the amylose helix: brown (dp 21-24), red (dp 25-29), red-violet (dp 30-38), blue-violet (39-46) and blue (dp>47) (John *et al.*, 1983). This indicates that as the length of the helical segment in the unit of dp increases, the number of iodine molecules which can be accommodated also increases. The increased iodine binding has been shown to result in a shift in the wavelength of maximum absorbance; $1/\lambda_{max}$ has been shown to be directly proportional to 1/dp up to a dp of about 100 (Banks *et al.,* 1971; Bailey and Whelan, 1961). Yamamoto *et al.,* (1982) have shown, by amylose-iodine interaction studies on potato amylose that a helical segment of amylose consists of fewer than 60 anhydroglucose residues. On this basis, they proposed that the interrupted helix (helical regions with intervals of random coils between them) is a good model for the amylose structure in aqueous solution.

Saibene and Seetharaman (2006) used iodine to study the architecture of the starch granule and reported the ability of granular corn starches to bind iodine at moisture contents as low as 8%.

Iodine binding in a starch granule requires a certain minimum level of mobility of the linear molecules, and that the water content plasticize the starch, thus increasing the ability to bind iodine by the formation of single helices. (Saibene and Seetharaman, 2006; Waduge *et al.*, 2010). K/S spectra (the ratio of the absorption and scattering coefficients) and WAXS (wide angle X-ray scattering) have been used in these studies to investigate the intensity of the colour developed in granular starch when it is bound with iodine and to measure the effect of iodine binding to the crystallinity of the granules, respectively. The ability of iodine molecules to penetrate the starch granule likely depends also on the surface features of the granule, such as the presence of pores and channels (Wadugae *et al.,* 2010).

2.3.1.2. Amylopectin

The structure of amylopectin is generally defined in terms of the cluster model (Robin *et al.,* 1974; French, 1984) with polymodal chain length distribution (Figure 2.5) (Hizukuri, 1986) and a non-random nature of branching (Thompson, 2000). The cluster model for the amylopectin molecule describes the alternating amorphous and crystalline layers in starch (Robin *et al.,* 1974).

2.3.1.2.1 Fine structure of amylopectin

Amylopectin unit chains are relatively short compared to amylose molecules and have a broad distribution file. The individual chains can be specifically classified in terms of their lengths and consequent position within starch granules (Hizukuri, 1985, 1986). In the classical nomenclature of Peat *et al.* (1952), A-chains are defined as unsubstituted by other chains and connected through an α-(1,6) linkage to the rest of the macromolecule, whereas B-chains are substituted by

one or several other chains (A- and/or B-chains). In addition, each macromolecule contains a single C-chain that carries the sole reducing end group. Hanashiro *et al.* (2002) described the distribution of C-chains after labelling with a fluorescent dye. The chains covered the dp range 10-130, possessing a peak in size exclusion chromatograms at dp 40 for several amylopectin samples. B chains are classified as B1, B2, B3 or B4, depending on their length and the number of clusters they span (Hizukuri, 1986). B1 chains are short chains, being components of the unit clusters, whereas B2, B3 and B4 are long chains that act as connecting chains in the amylopectin molecule. Bertoft (1991) isolated groups of chains from maize amylopectin of intermediate length between the long chains and the major group of short chains. These were considered as subgroups of the originally defined B1 group and named B1b and B1c, whereas the shorter, major group was B1a. The chain lengths of A, B1, B2, B3 and B4 chains of amylopectin from different starch sources have been shown to be in the range of 12-16, 20-24, 42-48, 69-75 and 101-119, respectively (Hizukuri, 1986; Wang and White, 1994). The ratio of A- to B-chains depends on the starch source and is typically of the order of <1.1 to >2.1 on a molar basis, or <0.5:1 to >1:1 on a weight basis (Morrison and Karkalas, 1990; Tester and Karkalas, 2002). The ratio of the long to short branch chains affects the shape of AMP (e.g., cylindrical versus conical shapes), which influence their packing and, in turn, the morphology and size of the starch granule (Jane, 2007). The average chain length ($\overline{CL}$) of amylopectin is typically 18-25 units (glucose residues) (Hizukuri, 1985, 1986) and depends on the type of crystallinity of the granular starch (see section 2.3.3.2). A-type crystalline starches typically possess shorter chain length than B-type crystalline starches (Hizukuri, 1985). Pérez and Bertoft (2010) suggested that the $\overline{CL}$ value gives only a poor description of the true structure of amylopectin, because both A- and B-type crystalline starches possess short and longer chains.

Fig 2.5 A cluster model of amylopectin proposed by Hizukuri (1986). A and B denote nomenclature of branch chains, Φ = reducing end, c.l. = chain length as degree of polymerization (Hizukuri, 1986, Copyright Elsevier, reproduced with permission).

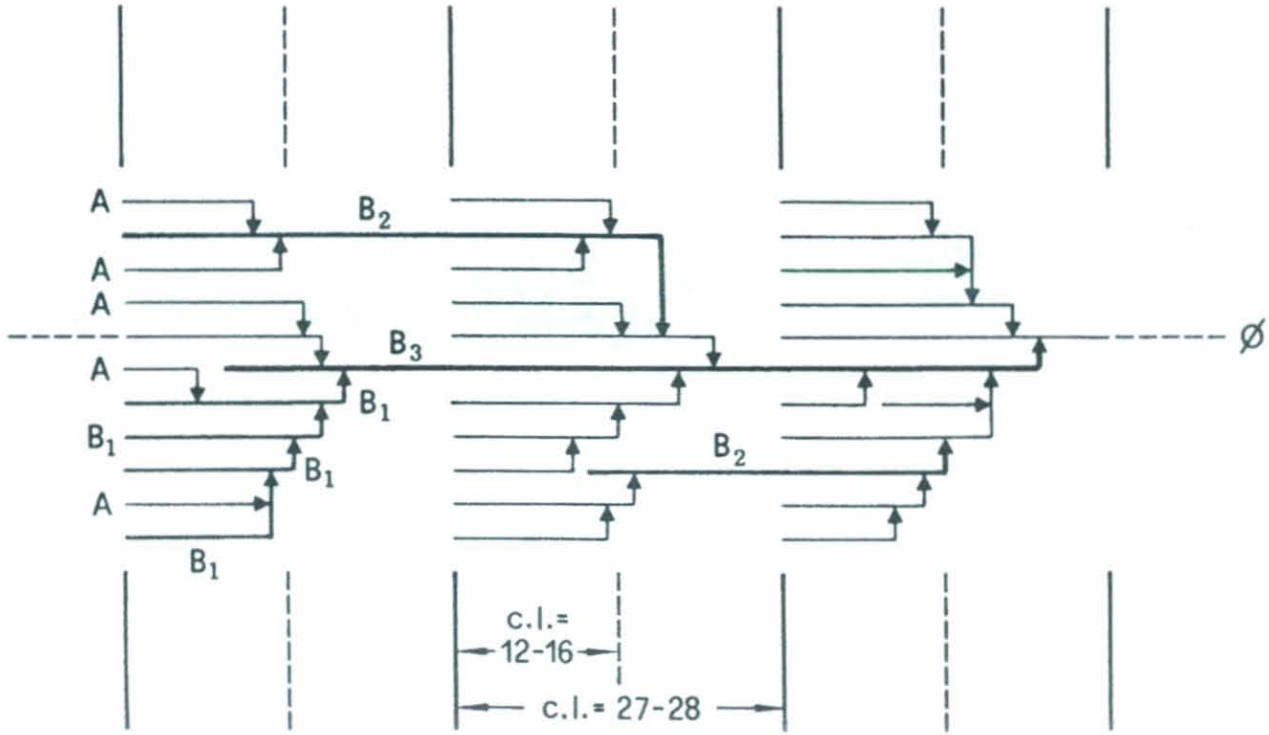
A
A
A
A
B1
B1
A
B1
B2
B3
B1
B2
Ø
c.l.=
12-16
c.l.= 27-28

2.3.1.2. Amylopectin-iodine complex

Blue colour is characteristic of the complex of iodine with amylose, whereas a reddish violet colour is characteristic of the amylopectin-iodine complex. This fact is explained by the different structures of the above complexes. Amylopectin-iodine complex formation primarily involves A-chains (Davis and Khan, 1994). Davis and Khan (1994) found that for four iodine atoms, there were 11 cyclic glycoside fragments in the formation of a chromophore group in the amylopectin–iodine complex, whereas this ratio varied from 6 to 17 in the amylose–iodine complex. However, studies showed that the linear A-chains have an average chain length of 12-16 anhydroglucose units (see sec. 2.3.1.1). Davis and Khan (1994) postulated that longer A-chains in amylopectin may not be available for iodine binding if pairs of them are involved in double helix formation.

2.3.2 Minor components

2.3.2.1 Phosphorus

Phosphorus is one of the non-carbohydrate constituents present in starches which significantly affects their functional properties (Karim *et al.,* 2007; Lim *et al.,* 1994; Lin and Czuchajowska, 1998; McPherson and Jane, 1999). Phosphorus is present as phosphate monoesters and phospholipids in various starches. The phosphate monoesters are covalently bound to the amylopectin fraction of the starch (Blennow *et al.,* 2000; Schoch and Maywald, 1956; Schoch, 1942). Inorganic phosphate is present in some starches (Kasemsuwan and Jane, 1996; Lim *et al.,* 1994). Tuber starches such as potato have been shown to have a higher phosphate monoester content (upto 0.09%) than cereal starches (Blennow *et al.,* 1998; Hizukuri *et al.*, 1970; Lim *et*

al., 1994; Kasemsuwan and Jane, 1996; Mcpherson and Jane, 1999). Takeda and Hizukuri (1982) have shown, in studies on potato, that amylopectin contains one phosphate monoester group per 317 glucose residues, equivalent to one phosphate group per 13 branch chains.

The phosphate groups are located mainly on C-6 and C-3 of the glucose units of amylopectin (Hizukuri *et al.*, 1970). The enzyme α-glucan water dikinase (GWD) is responsible for the phosphorylation at the C-3 and C-6 positions. Approximately 60-70% of the phosphate groups are bound as monoesters to the C-6 position of the glucosyl units, whereas 30-40% are monoesterified to the C-3 position (Tabata and Hizukuri, 1971; Bay-Smidt *et al.*, 1994). A small fraction (1%) may be linked to the C-2 position (Hizukuri *et al.*, 1970; Jane *et al.,* 1996). It is believed that amylose is not an efficient acceptor of phosphate groups (Kotting *et al.,* 2005; Lorberth *et al.,* 1998; Ritte *et al.,* 2006; Ritte *et al.*, 2002). Longer chains (dp 30-100) of amylopectin act as better substrates for GWD (Ritte *et al.*, 2002; Mikkelsen *et al.,* 2004) and the degree of phosphorylation is correlated to the chain length of amylopectin (Blennow *et al.,* 1998). A unit chain may contain one or more phosphate groups (Blennow *et al.*, 1998) but no phosphate groups are located on the non-reducing end (Takeda and Hizukuri, 1981) or closer than nine glucosyl units from an α-(1,6) branch point (Takeda and Hizukuri, 1982). On a molar basis, approximately 50% of the phosphorylated chains belong to the category of long B-chains (CL>35) and the rest are B_1-chains, whereas A-chains apparently are non-phosphorylated (Noda *et al.,* 2005). Surface gelatinization studies have shown that phosphate monoesters are more concentrated at the core (hilum) than in the periphery of the potato starch granule (Jane and Shen, 1993). This is explained by the fact that amylopectin, at the core, has longer B-chains (B2 and B3) than that at the periphery (Pan and Jane, 2000). Furthermore, studies showed that small

granules have greater phosphate content than larger granules (Jane and Shen, 1993; Noda *et al.*, 2005).

The phosphorus content in potato starch has been reported to be influenced by growing conditions, temperature and storage (Smith, 1987). In potato starch, the high phosphate monoester content contributes to high viscosity, high transparency, water binding capacity and freeze thaw stability (Craig *et al.*, 1989; Swinkels, 1985). This has been attributed to repulsion between negatively charged phosphate groups on adjacent amylopectin chains that hinders strong interactions between double helices (Hoover, 2010). Furthermore, studies showed that the phosphate monoester content of potato starch is inversely proportional to the crystallinity (Muhrbeck *et al.*, 1991) and the gelatinization enthalpy (Muhrbeck and Eliasson, 1991) of the starch. This indicates that the phosphate monoesters are present within the crystalline region of the starch granule (Jane 2009).

2.3.2.2 Lipid

The lipid content and composition of starch granules vary from plant to plant (Morisson, 1988). Lipids associated with cereal starch granules have been found to occur on the surface as well as inside the granules (Morrison 1981). Surface lipids are occasionally referred to as non-starch lipids, which consist of triacylglycerols, polar lipids (glycolipids and phospholipids) and small amounts of diglycerides and free fatty acids (Morrison 1981, Galliard and Bowler 1987). Lipids present on the surface of cereal starches, particularly in the case of small granules (10 μm), are able to encapsulate the granules with a thin lipid film (Galliard and Bowler, 1987). Lee and BeMiller (2008) postulated that what has been reported to be non-starch lipid of starches

containing channels (maize, sorghum, millet, wheat, rye, barley) is the lipid lining the channels, i.e., lipid at least primarily associated with internal surfaces rather than the external surface of granules. Internal lipids are mainly monoacyl lipids (lysophospholipids) and free fatty acids (Acker, 1977; Morrison, 1981). These two groups of lipids (surface and internal lipids) differ in extractability from granules with common lipid solvents. Surface lipids are extractable with cold solvents (chloroform and ether), whereas internal lipids can be extracted with hot aqueous alcohol (propanol-water 3:1 [v/v]) (Vasanthan and Hoover, 1992). Surface and internal lipids have been shown to be present in the free state as well as bound to starch components, either in the form of amylose inclusion complexes or linked via ionic or hydrogen bonding to hydroxyl groups of the starch components (Morrison, 1988; Morrison, 1995; Vasanthan and Hoover, 1992). The major fatty acids in neutral lipid fractions are palmitic acid (wheat, corn, potato and cassava) and linoleic acid (rice and lentil). The glycolipid fractions of cereal and cassava starches have been reported to contain linoleic acid and palmitic acid, respectively. However, in phospholipid fractions, all starches contain palmitic acid as major fatty acid (Vasanthan and Hoover, 1992).

Generally, cereal starches (e.g., corn, wheat, rice) contain relatively high levels of lipid (0.2-0.8%) whereas, tuber (e.g., potato) and root (e.g., tapioca) starches have lower levels of lipids (0.1-0.2%). The amount of lipid-complexed amylose ranges from less than 15 to more than 55% of the amylose fraction in cereal starches (Morrison, 1995). In most cereal starches, there is a strong correlation between the amylose and lipid contents. Most waxy starches have comparatively low amount of lipids (Morrison, 1984; South *et al.,* 1991).

2.3.2.2.1 Amylose-lipid inclusion complex

As discussed earlier (sec 2.3.1.1.1), amylose is known for its ability to form inclusion complexes with hydrophobic ligands (guest molecules). Lipids and linear alcohols form complexes with six glucose residues per turn with an inner diameter of 0.48 nm. Consecutive turns of helices are stabilised by numerous intra- and interhelical van der Waals bonds and hydrogen bonds (Biliaderis and Galloway, 1989; Rappenecker and Zugenmaier, 1981). In the amylose-lipid inclusion complex, the aliphatic part (hydrocarbon chain) of the lipid is located inside the lipophilic core of the amylose helix, whereas the polar group lies outside of the helix (Fig 2.6) (Carlson *et al.,* 1979).

DSC thermograms of normal cereal starches (e.g., maize and wheat) show an additional thermal transition peak at a higher temperature than the starch gelatinization peak (Donavon and Mapes, 1980; Kugimiya *et al.,* 1980). This peak has been attributed to the melting of the amylose-lipid complex (Biliaderis *et al.,* 1985; Bulpin and Welsh, 1982; Donavon and Mapes, 1980; Eliasson and Krog, 1985; Hoover and Hadziyev, 1981; Kugimiya and Donavan, 1981). NMR (^{13}C-cross-polarization/magic angle spinning [^{13}C-CP-MAS] NMR spectroscopy) studies have provided evidence for the existence of amylose-lipid complexes in native barley, maize, rice and oat starches (Morrison *et al.,* 1993a, 1993b). ^{13}C-CP-MAS NMR produces a broad resonance with a chemical shift of 31.2 ppm, a characteristic of mid-chain methylene carbons of fatty acids in the V-amylose complex (Fig 2.7). The results showed that up to 43% of the amylose in non-waxy rice starch, 33% in oat starch and 22% in normal maize and wheat starch granules are complexed with lipids. Based on this observation, Morrison *et al.* (1993a) postulated that amylose in cereal starches occurs as two fractions, lipid amylose and free amylose.

Fig. 2.6 Schematic illustration of amylose-lipid complex (adopted from Carlson *et al.,* 1979).

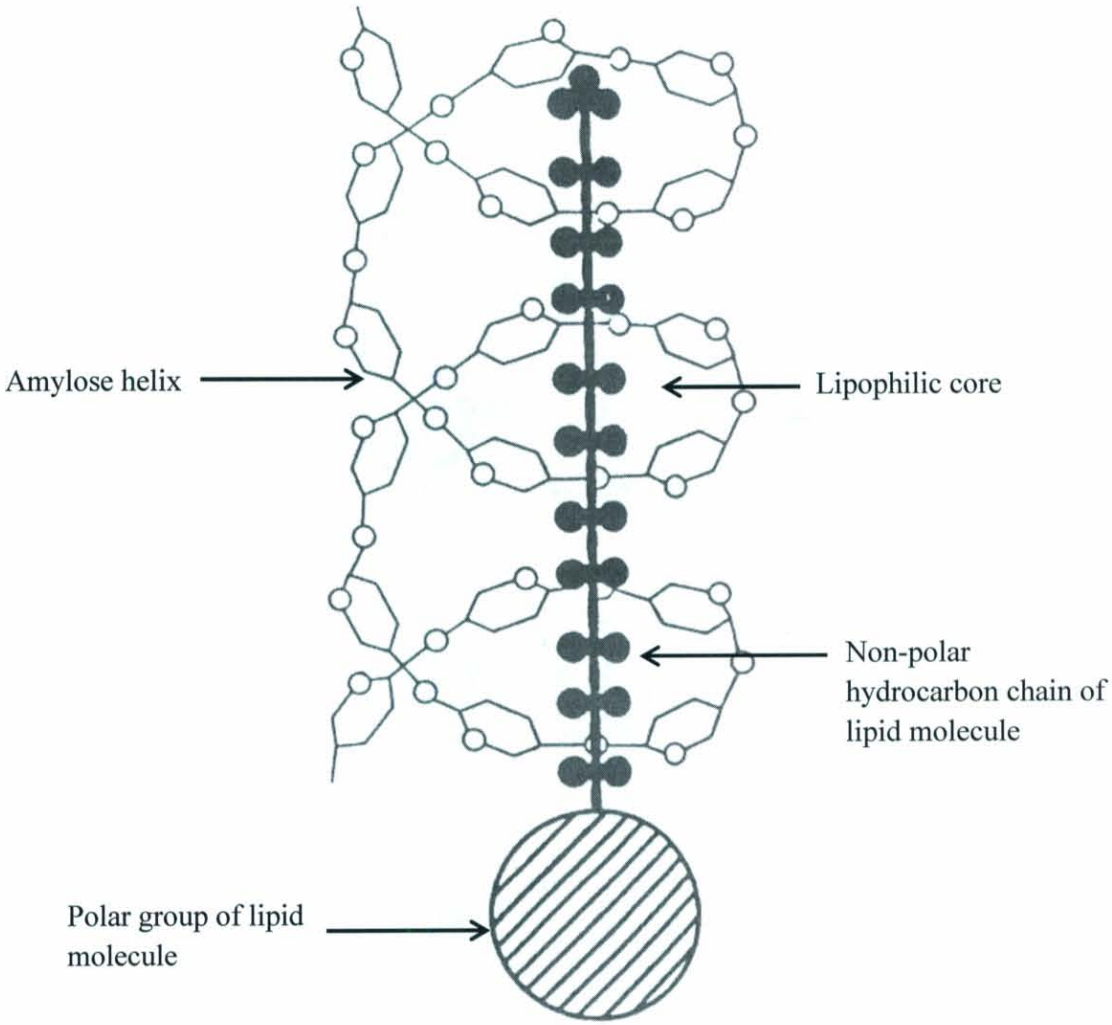
Amylose helix
Lipophilic core
Non-polar
hydrocarbon chain of
lipid molecule
Polar group of lipid
molecule

Fig 2.7 ^{13}C-CP-MAS NMR spectra of V-amylose in waxy barley starch (Chalkey Glen), with inset of the 10-50 ppm region at ×20 scale expansion. The marked resonance is for mid chain methylene carbons of fatty acids in lysophospholipid with a chemical shift of 31.2 ppm (A). Resonance from polysaccharide carbons (B-E) are B = C-6 (61.3 ppm), C = unresolved C-2, C-3, C-5 (71.4 ppm), D = C-4 (80.9 ppm), E = C-1 (100.5 ppm) with some helical amylose (103 ppm) (Morrison *et al.,* 1993b, Copyright Cereal Chemistry, reproduced with permission).

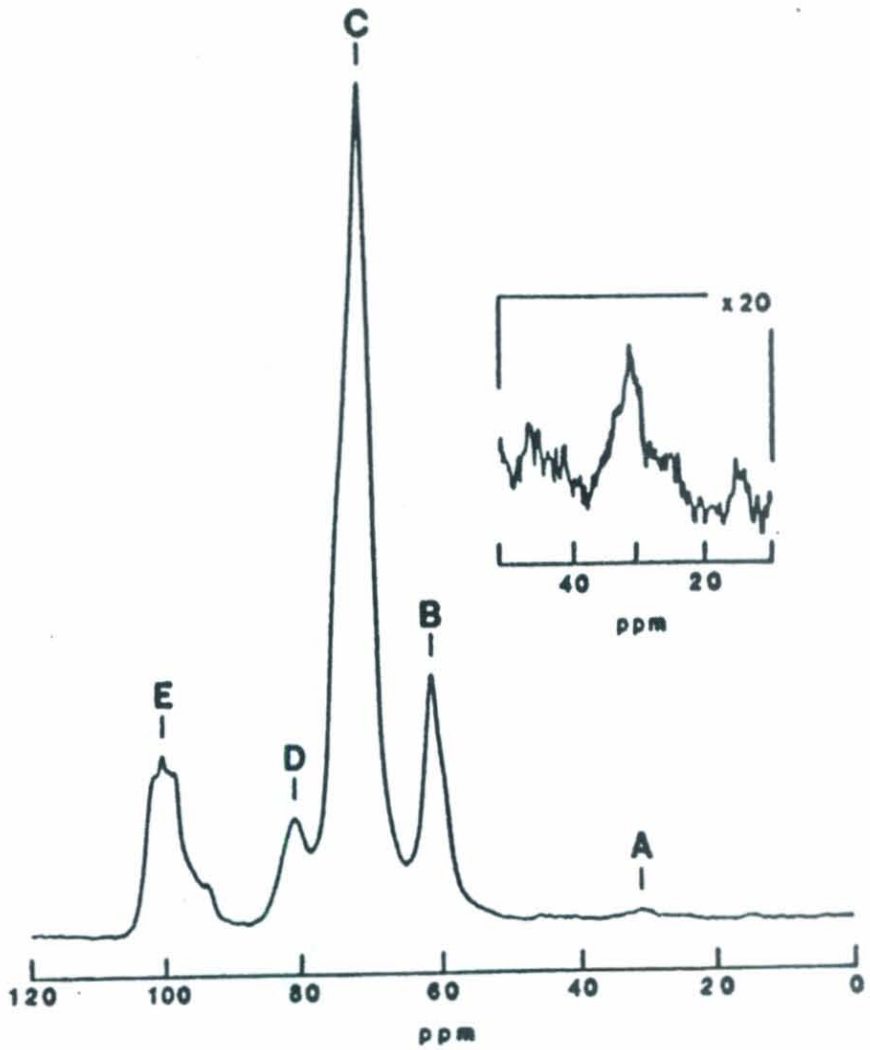
C
x 20
40
20
ppm
B
E
D
A
120
100
80
60
40
20
0
ppm

The amylose-lipid complex in the solid state shows the existence of two structurally different forms: type I (form I) and type II (form II) based on the crystallization conditions (temperature, type of ligand). Type I gives an amorphous X-ray pattern, whereas type II exhibits the typical V-type pattern (Biliaderis and Galloway, 1989; Biliaderis and Seneviratne, 1990). Type I (amorphous complex) is found in most native cereal starches, which display a melting temperature at 94-100°C. The melting temperature of the amylose-lipid complexes increases with the chain length of the fatty acid. Type II lamellar crystalline forms melt at 100-125°C (Fig 2.8) (Karkalas *et al.,* 1995; Raphaelides and Karkalas, 1988). Therefore, the V-type X-ray pattern has not been observed in native starches, except for high (>30%) amylose starches such as wrinkled pea, amylomaize and some other maize genotypes (sugary [su], dull [du]) (Galliard and Bowler, 1987; Gernat *et al.,* 1993). The absence of a V-type pattern in native starches does not necessarily indicate the absence of amylose-lipid complexes. It merely proves that amylose-lipid complexes are not arranged in crystalline domains that can be detected by X-ray diffraction techniques (Hoover, 1998).

Formation of V-type amylose has been observed during swelling and gelatinization of starch granules (Biliaderis *et al.*, 1986b; Morisson, 1988), on heat-moisture treatment (Hoover *et al.,* 1996; Lim *et al.,* 2001), on extrusion cooking of lipid-containing cereal starches (Mercier *et al.,* 1980), and after addition of monoacyl lipids to starch under appropriate conditions (Hoover Hadziyev, 1981). The amylose-lipid inclusion complex has been shown to influence the gelatinization temperature, granular swelling and solubility, amylose leaching, paste viscosity, retrogradation, and enzymatic hydrolysis (Debet and Gidley, 2006; Guraya *et al.*, 1997; Holm *et al.*, 1983; Hoover, 2010, 1998; Tester and Morrison 1990; Vasanthan and Hoover, 1992). These

Fig. 2.8 A typical DSC thermal curve (50% solids) of a cereal starch showing the different melting transitions and the corresponding structural domains undergoing a phase change. M_1 and M_2: melting of amylopectin crystallites at intermediate moisture content; M_3: melting of form 1 amylose-lipid complex; M_4: melting of form II amylose-lipid complex (adapted from Billiaderis, 1998; Biliaderis and Galloway, 1989; Biliaderis and Seneviratne, 1990).

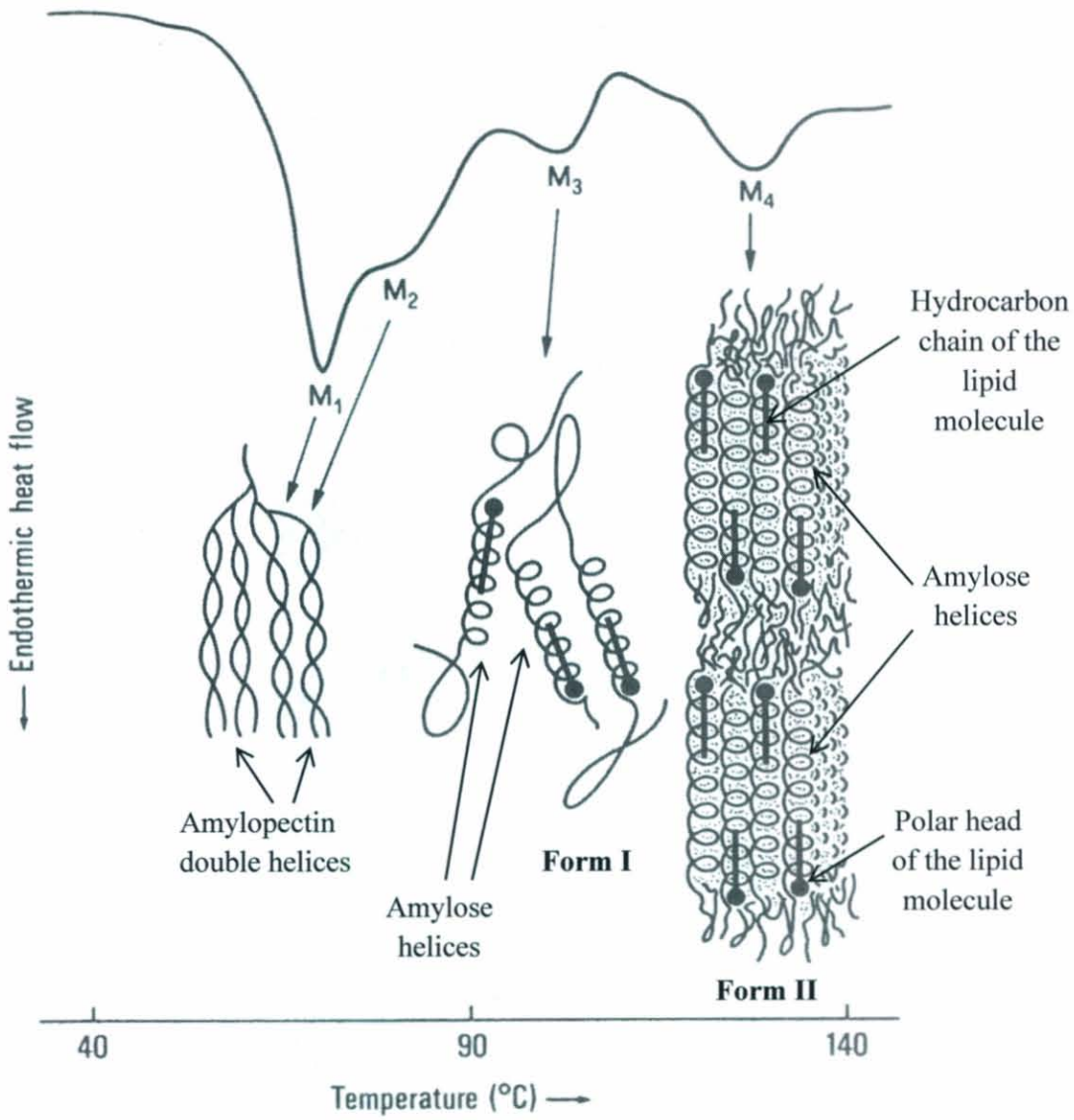
M1
M2
M3
M4
Endothermic heat flow
Hydrocarbon chain of the lipid molecule
Amylose helices
Polar head of the lipid molecule
Amylopectin double helices
Amylose helices
Form I
Form II
40
90
140
Temperature (°C)

inclusion complexes are effective in preventing the stickiness of starch (Hoover and Hadziyev, 1981), improving structural integrity in cereal kernels (parboiled rice) during cooking (Biliaderis *et al.,* 1993), increasing the free-thaw stability and an anti-staling effect in bread and biscuits (Riisom *et al.*, 1984), and improving the texture in products containing extruded starch (Mercier *et al.,* 1980).

2.3.2.3 Proteins

The nitrogen content of starch is a direct indication of crude protein [N×6.25] content. Generally, a starch granule comprises a number of nitrogen fractions such as protein, peptides, free amino acids, amides, enzymes and nucleic acids (Eppendorfer, 1979; Lineback and Rasper, 1988; Swinkels, 1985). Among these nitrogen fractions, pure protein represents on average about 50% of the nitrogen of potato tubers, and may range from 34% to 70% (Shewry, 2003). Maize and waxy maize starches contain a considerable amount of protein (0.25-0.8%) compared to tuber and root starches (potato, 0.06%, and tapioca, 0.01%) (Swinkels, 1985; Buléon *et al.,* 1998). The protein content of purified starch is a good indicator of starch purity.

Proteins are known to be associated with both the surface and the interior of starch granules (Baldwin, 2001). Rahman *et al.* (1995) suggested that the intrinsic proteins are almost entirely enzymes involved in starch synthesis. Approximately 10% of the starch proteins appeared to be associated with the granule surface (Galliard and Bowler, 1987). Surface proteins in starches are often dominated by storage proteins, particularly endosperm storage proteins in cereals (Schofield and Greenwell, 1987; Mu-Forster and Wasserman, 1998). The presence of starch granule surface proteins have been reported for potato and tapioca, (Yoshino *et al.,* 2005), wheat

(Greenwell and Schofield, 1986; Seguchi and Yamada, 1989), maize (Imam, 1989), rice (Villareal *et al.*, 1986), barley (Prentice and Stark, 1992) and mung bean (Oates, 1990) starches. Surface associated proteins of starch granules can be readily extracted with dilute salt (sodium dodecyl sulphate) under mild conditions (Greenwell and Schofield, 1986; Seguchi and Yamada, 1989) that cause no disruption of granules, whereas the internal proteins cannot be extracted without disruption of the granule crystalline structure via chemical or thermal gelatinization (Debet and Gidley, 2006; Gillian *et al.*, 1981; Mu-Forster *et al.*, 1996).

2.3.3 Supramolecular structure

Starch granules consist of concentric alternating amorphous and semicrystalline growth rings (Fig 2.9). They grow by apposition from the hilum of the granule. The number and thickness of these layers depend on the botanical origin of the starch. They are typically 120-400 nm in thickness (French, 1984) and are considered to represent diurnal fluctuations in the deposition of starch in storage tissues (Donald *et al.*, 2001; Gallant *et al.*, 1997; Sevenou *et al.*, 2002). The low-density amorphous rings consist of amylose and amylopectin in a disordered conformation, whereas the dense semicrystalline rings are formed by a lamellar structure of alternating crystalline and amorphous regions with a repeat distance of 9-11 nm (Cameron and Donald, 1992; Donald, 2004; Donald *et al.*, 2001; Yuryev *et al.*, 2004). The crystalline regions of the lamellae are formed mainly by double helices of amylopectin side chains packed laterally into a crystalline lattice, whereas amorphous regions contain amylose and the amylopectin branching points. The longer amylopectin chains are considered to pass from the crystalline region into the amorphous region of the lamellae (Qi *et al.*, 2004).

Fig 2.9 Schematic representation of the starch granule: (a) amorphous and semi-crystalline growth rings in a starch granule, (b) amorphous and crystalline lamellae in a stack and part of an amorphous growth ring, (c) aligned double helices (from amylopectin side chains) within a crystalline lamella and amylopectin branch points within an amorphous lamella (d) blocklet (adapted from Donald *et al.,* 1997; Myers *et al.,* 2000).

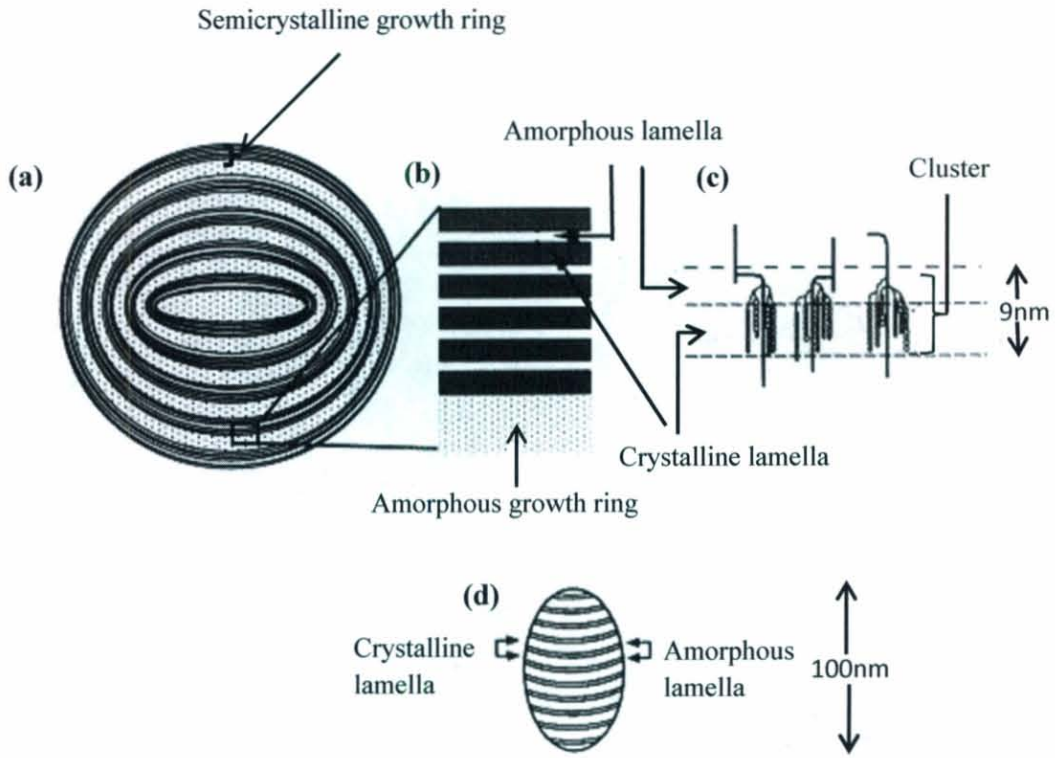
Semicrystalline growth ring
(a)
(b)
Amorphous lamella
(c)
Cluster
9nm
Crystalline lamella
Amorphous growth ring
(d)
Crystalline lamella
Amorphous lamella
100nm

Based on scanning electron microscopy observations, Gallant *et al.* (1997) suggested that both semi-crystalline and amorphous growth rings are subdivided into large (20–500 nm in diameter) and small (25 nm in diameter) spherical blocklets, respectively. On average, two end-to-end blocklets would constitute a single semicrystalline growth ring. These blocklets have an average size of 100 nm in diameter and are proposed to contain 280 amylopectin side chain clusters. In this view, one blocklet in the semi-crystalline growth ring contains several amorphous and crystalline lamellae (Fig. 2.9d) (Le Corre *et al.,* 2010; Vandeputte and Delcour, 2004). Generally, B-type starches (e.g., potato) contain larger (400-500 nm) blocklets than A-type starches (e.g. wheat starch, 25-100 nm in diameter). In potato starch, the granule surface (approximately the outer 10 μm) is predominated by large blocklets (400-500 nm), whereas the granule centre is dominated by small blocklets (Perez and Bertoft, 2010).

Amylopectin clusters may contain amylose tie-chains, which are amylose molecules that pass through both the crystalline and amorphous layers (Jane *et al.,* 2007; Qi *et al.,* 2003). It has been suggested that these amylose tie molecules are in a straightened conformation in crystalline regions and in a disordered conformation in amorphous regions (Fig 2.10a) (Kozlov *et al.*, 2007; Matveev *et al.*, 1998; Yuryev, 2007). Jenkins and Donalds (1995) concluded that an increase in amylose content has the effect of increasing the size of the crystalline lamella and acts to disrupt their packing (Fig 2.10b). Two mechanisms to explain this disruption have been introduced: first, co-crystallization between amylose and amylopectin chains and, second, the penetration of amylose into amorphous regions. However, in high-amylose starches, amylose helices may contribute to the crystallinity of granules (Buleon *et al.,* 1998; Hoover, 2001; Matveev *et al.,* 2001; Tester *et al.,* 2004).

Fig 2.10 Localization of amylose chains in amylopectin clusters. (a) Yeryev's model for amylose chains localization in amylopectin cluster (adapted from Yeryev, 2007); (b) A proposed mechanism to explain the disruption of amylopectin double helical packing by amylose; (A) Amylopectin structure with no amylose present - small crystalline lamellar size; (B) Co-crystallinity between amylose and amylopectin moves a number of the amylopectin chains out of register - increased crystalline lamellar size (Jenkins and Donald, 1995, Copyright Elsevier, reproduced with permission).

a)

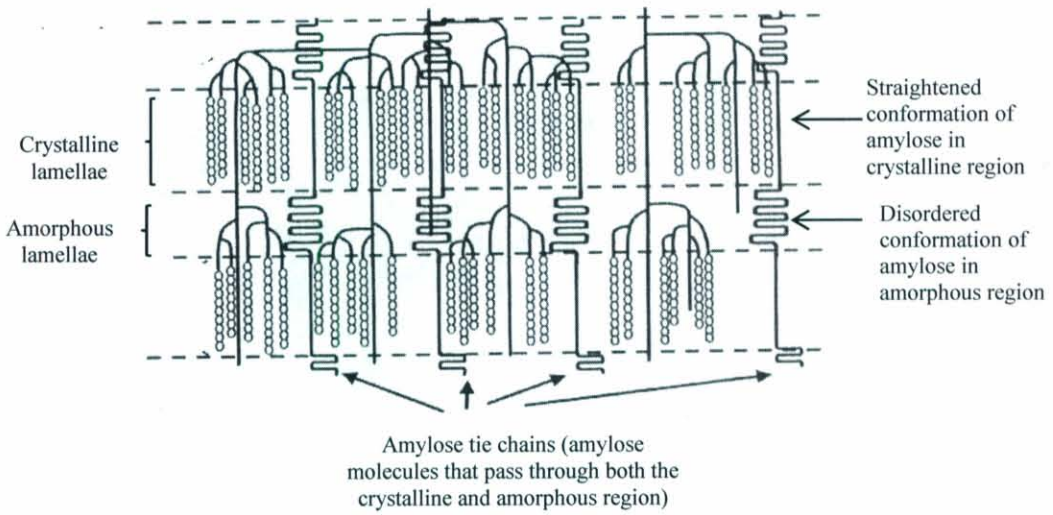
Crystalline lamellae
Amorphous lamellae
Straightened conformation of amylose in crystalline region
Disordered conformation of amylose in amorphous region
Amylose tie chains (amylose molecules that pass through both the crystalline and amorphous region)

b)

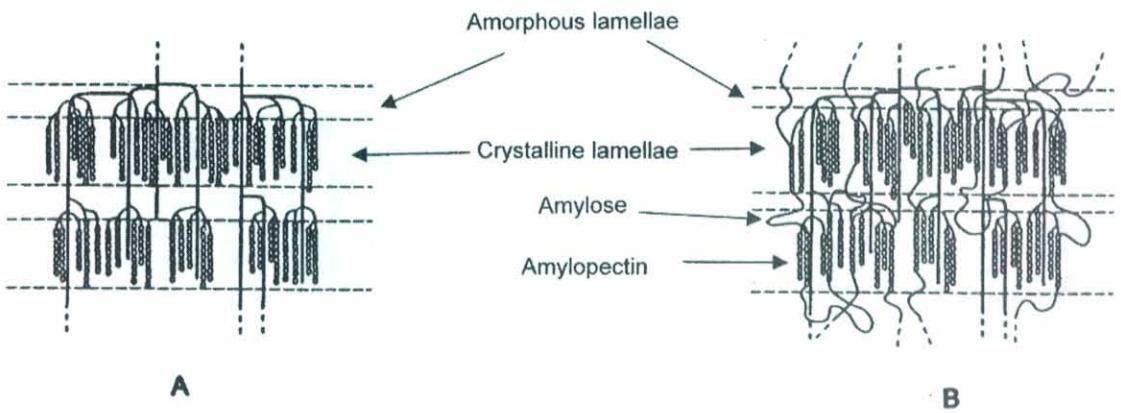
Amorphous lamellae
Crystalline lamellae
Amylose
Amylopectin
A
B

2.3.3.1 Birefringence

The wave model of light describes light waves vibrating at right angles to the direction of propagation with all vibration directions being equally probable. This is referred to as "common" or "non-polarized" white light. In contrast, polarized light waves vibrate in just a single plane (McMohan, 2004). A polarizing filter can convert unpolarized light into polarized light. If two polarizing filters are crossed (oriented at right angles to one another), no light will pass through the second filter. Certain biological materials may act like polarizing filters. The biological material must have a highly ordered internal structure, approaching a crystalline pattern of organization, to partially polarize light. If such materials are placed between crossed filters, some of the light waves are polarized in a new direction and will pass through the second filter. This property is known as birefringence because the material bends or refracts light into two planes. The biological material will be bright against a dark background since the crossed polarizing filters still prevent light from passing through everywhere else (McMahon, 2004).

When starch granules are viewed under cross polarized light, they show birefringence, producing what is often described as the Maltese cross pattern. Birefringence is believed to be due to the radial orientation of the external chains of the amylopectin crystallites in the granule (Evans and Thompson, 2004). According to birefringence maps (French, 1972), the amylopectin chains are symmetrically and radially oriented (Fig 2.11). The Maltese cross pattern is the complementary dark pattern that divides the four light quadrants. The dark regions result when the optic axes in that part of the granule align with one of the polarizing filters (Evans *et al.*, 2003).

Fig 2.11 Schematic model of the organization of a starch granule (Jane, 2009, Copyright Elsevier, reproduced with permission).

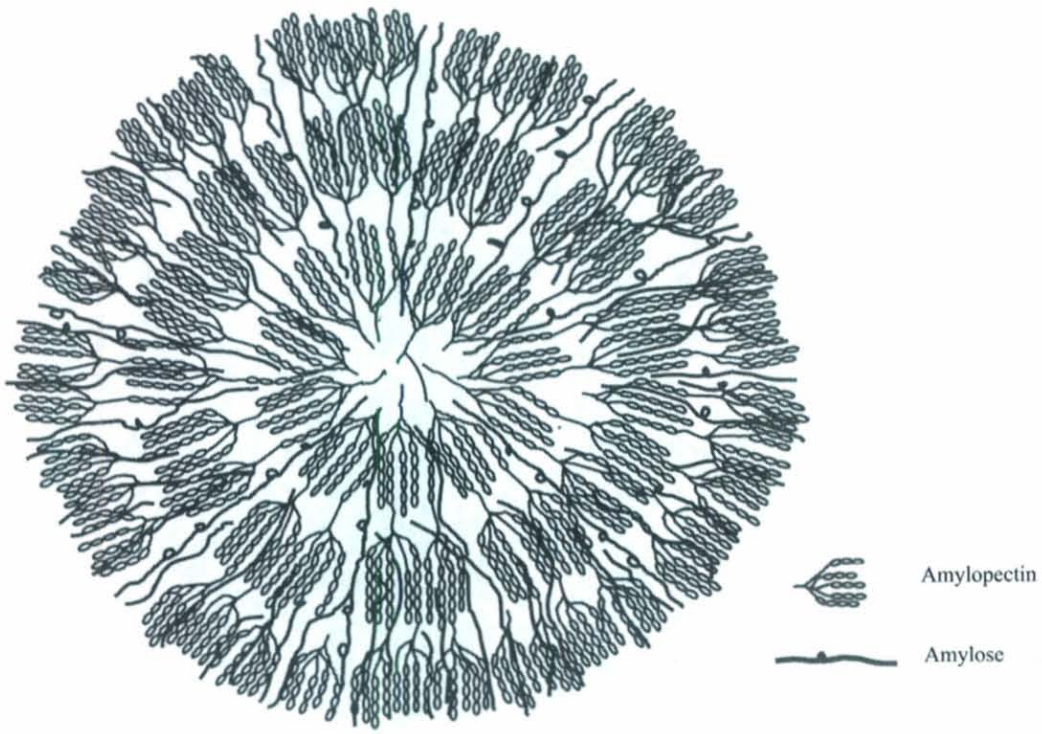
Amylopectin
Amylose

2.3.3.2 Starch crystallinity

Starch crystallinity is attributed to structural elements of amylopectin (Jenkins and Donald, 1995). The unbranched outer A-chains and the shortest inner branched chains (B1) of amylopectin can form double helices, which can crystallize into different crystal types. This crystallization or double helical formation can occur either in the same amylopectin branch cluster or between adjacent clusters in three dimensions and is called the superhelical structure Gallant *et al.,* 1997). Double helical content in starch has been extensively researched by ^{13}C cross polarization magnetic angle spinning nuclear magnetic resonance spectroscopy (^{13}C CPMAS-NMR) (Bogracheva *et al.,* 2001; Lopez-Rubio *et al.,* 2008; Paris *et al.*, 1999; Tamaki *et al.,* 1998; Yusuph *et al.*, 2003). These studies showed that crystallinity of starch increases with increasing double helical content (Table 2.4). Based on this observation, Lopez-Rubio *et al.* (2008) suggested that most of the double helices present in starch granules are packed into crystalline structures.

Wide angle X-ray scattering (WAXS) is widely used to study the structure of semi-crystalline carbohydrate polymers and it provides information of long range order such as the packing of double helices into ordered arrays (Sevenou *et al.,* 2002). Starch granules, depending on their botanical origin and composition (amylose/amylopectin ratio, amylopectin branch length), exhibit two types of WAXS patterns, which are associated with two crystalline polymorphic forms: A-type and B-type. A-type (Fig 2.12A) is mainly found in normal cereal starches and the B-type (Fig 2.12B) is observed in tubers and high amylose starches.

Table 2.4 Double helical content and crystallinity of starches

Starch	% Double helix (NMR)	% Crystallinity
Waxy maize	47	46
Rice	38	37
Potato	44	45
Barley	21	22
Penford wheat	22	23
NB1 wheat	29	25
Gelose 80	26	22
Hylon VII	24	21

(adapted from Lopez-Rubio *et al.*, 2008a)

Fig 2.12 X-ray diffraction patterns of A-, B-, C-type starches with their characteristic d-spacings (adapted from Zobel, 1988b). A-type; B-type; C-type

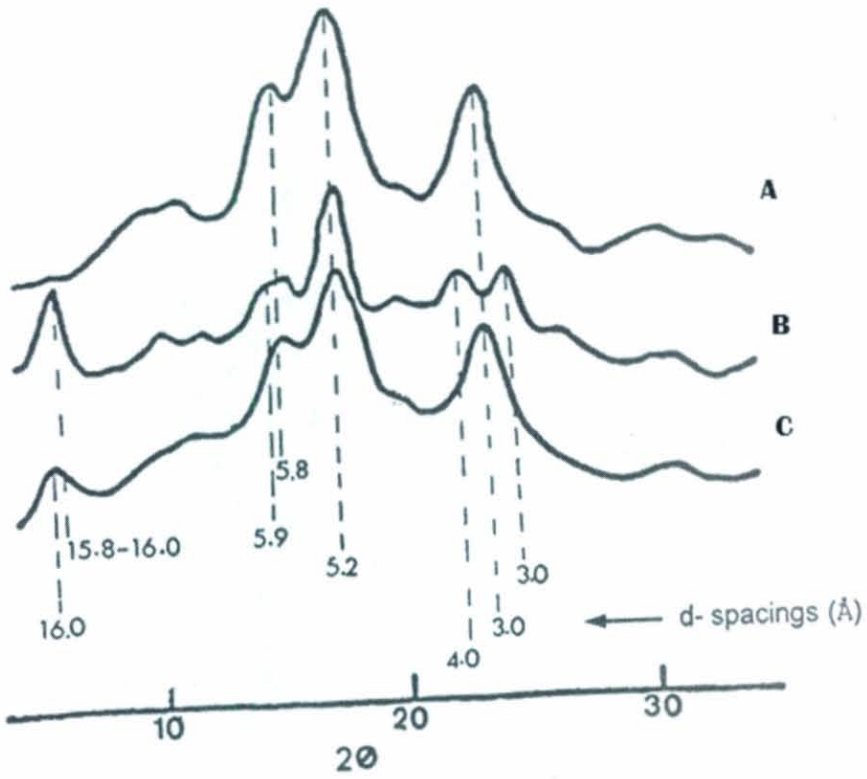
A
B
C
15.8–16.0
16.0
5.8
5.9
5.2
4.0
3.0
3.0
d- spacings (Å)
10
20
30
2Ø

Legume, root and some fruit and stem starches contain significant fractions of both crystalline types, resulting in a combined WAXS pattern referred to as C-type (Fig 2.12C) (Buleon *et al.*, 1998; Zobel, 1988; Cairns *et al.*, 1997; Hizukuri *et al.,* 1985; Imberty *et al.*, 1991; Lineback, 1984; McPherson and Jane, 1999; Sevenou *et al.*, 2002). Another crystal polymorph is often observed in granular starches, the so-called V-type (Fig 2.13) which, in contrast to the double helical nature of the A and B crystal structures, has been described to arise from single amylose helices (Lopez-Rubio *et al.,* 2008a; Saibene *et al.,* 2008), some of which are complexed with endogenous granular lipids (Morrison *et al.,* 1993).

The double helices within the A- and B-type polymorphic forms are essentially identical with respect to helical structure (Gidley and Bulpin, 1987; Imberty *et al.*, 1991). Within the double helix, interstrand stabilization occurs through O-2·····O-6 H-bonding between the two chains as well as through numerous van der Waals interactions. The inner diameter of the double helix cavity is ~ 0.35 nm (i.e., it does not allow any water molecules to pack inside the helix), whereas the outer diameter is ~ 1.03 nm (Biliaderis, 1998). However, the A- and B-type polymorphs, differ in the packing arrangement of the double helices and in the water content. Wu and Sarko (1978a, b) postulated that both A- and B-polymorphs are right-handed, parallel-stranded double helices packed in anti-parallel fashion (Fig 2.14). Later, an improved structure of A- and B-polymorphs was proposed by Imberty *et al.* (1998, 1999). This new model was still based on parallel-stranded double helices, but they were left-handed instead of the previous right-handed ones. In addition, these double helices were packed in a parallel fashion as opposed to Sarko's structure, where the packing was antiparallel.

Fig 2.13 V-type X-ray diffraction pattern of amylose-lipid complex showing characteristic d-spacings (4.4-4.3, 6.5-6.8, 11.3-12) (adapted from Zobel, 1988b).

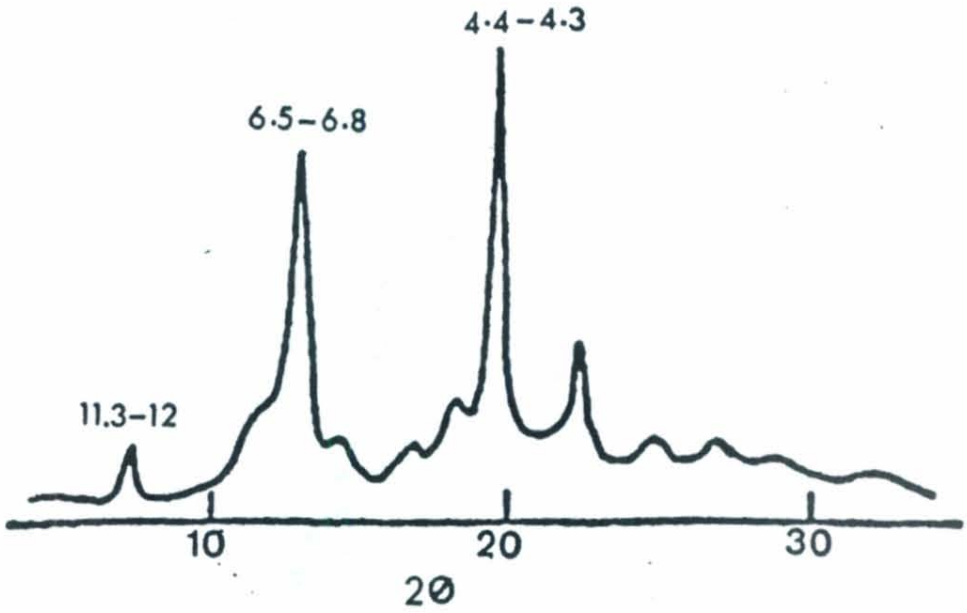
4·4 – 4·3
6·5 – 6·8
11.3–12
10
20
30
2Ø

Fig 2.14 Arrangement of double helices of A-type and B-type crystallites in starch granules (adapted from Wu and Sarko, 1978a; 1978b).

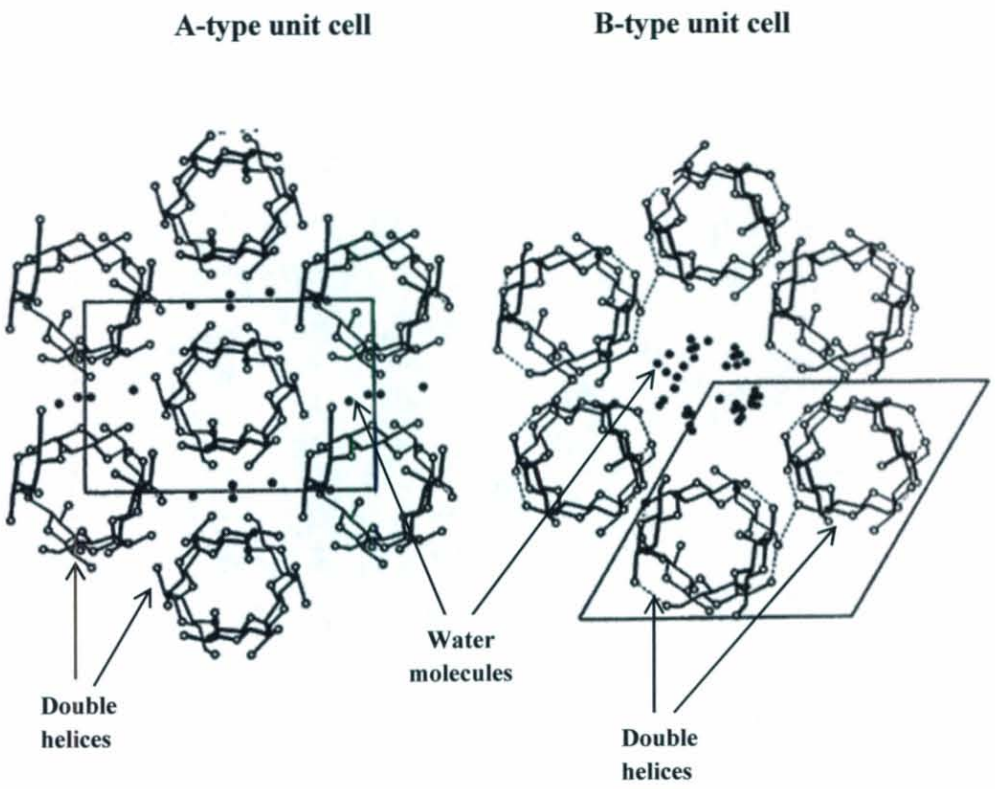
A-type unit cell
B-type unit cell
Water molecules
Double helices
Double helices

For the A-polymorph, chains are crystallized in a monoclinic lattice (unit cell parameters a = 21.24Å, b = 11.72Å, c = 10.69Å and $\alpha = \beta = 90°$, $\gamma = 123.5$) having maltotriose as the repeating (asymmetric) unit and four water molecules per unit cell. The B-polymorph crystallizes in a hexagonal unit cell ($a = b$ = 18.5 Å, c = 10.4 Å and $\alpha = \beta = 90°$, $\gamma = 120$) with a more open hexagonal packing and 36 water molecules per unit cell (Fig 2.15) (Imberty and Perez, 1988, Imberty *et al.,* 1988). The water molecules fill the larger central channel formed by the hexagonically packed double helices; half of the water is tightly bound to the chains, and the other half is connected only to other water molecules (Biliaderis, 1998). The C-polymorphic structure is a mixture of A and B unit cells (the proportions vary among pulse starches) and, therefore, is considered to be intermediate between the A and B forms in packing density and structure (Buleon *et al.*, 1998; Cairns *et al.*, 1997; Hizukuri *et al.,* 1980; Imberty *et al.*, 1991; Lineback, 1984; McPherson and Jane, 1999; Sevenou *et al.*, 2002).

Hizukuri *et al.* (1983) postulated that amylopectin chain length was a determining factor for crystalline polymorphism. The relatively short exterior chains of cereal starch amylopectin molecules (chain length 14-20, or <20) favour the formation of A-type crystalline polymorphs (of double helices), with the longer exterior chains of tuber starches (chain length 16-22, or >22) favouring the formation of B-type polymorphs (Hizukuri *et al.,* 1986). Jane *et al.* (1997) showed that the B-type amylopectin branch points are clustered, forming a smaller amorphous lamella, whereas A-type amylopectin branch points are scattered in both the amorphous and the crystalline regions, giving more flexibility to double helices to pack closely (Fig 2.16).

Fig 2.15 Structure of A- and B-type unit cells.

A] Structure of A- starch. Chains are crystallized in a monoclinic lattice. In the unit cell, 12 glucopyranosyl units are located in two left handed, parallel-stranded double helices, packed in a parallel fashion. For each unit cell, four water molecules are located between the helices. (Imperty *et al.*, 1988, Copyright Elsvier, reproduced with permission).

B] Structure of B-starch. Chains are crystallized in a hexagonal lattice, where they pack as an array of left-handed, parallel-stranded double helices, packed in a parallel fashion. Thirty six water molecules represent 27% hydration. Hydrogen bonds are indicated as broken lines (Imperty and Perez, 1988, Copyright John Wiley and Sons, reproduced with permission).

Projection of the structure onto the (a,b) plane. Hydrogen bonds are indicated as broken lines. Water molecules are indicated by closed circles.

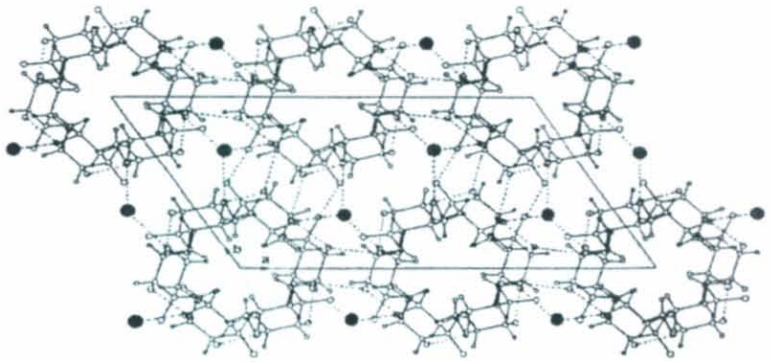

A

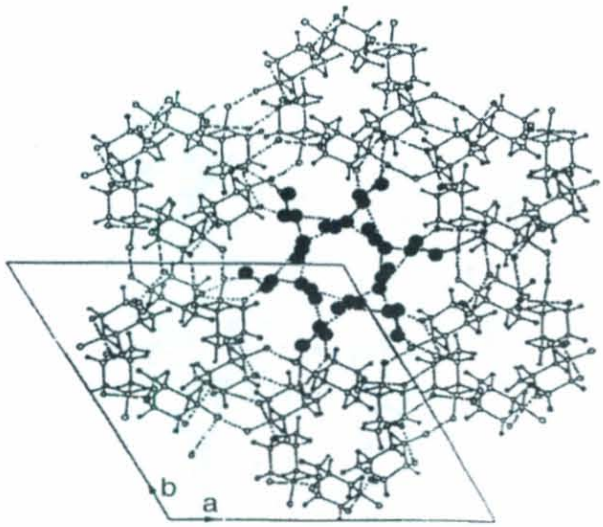

B

Fig 2.16 Proposed models for A-type (waxy maize starch) and B-type (potato starch) amylopectin branching patterns (Jane *et al.,* 1997, Copyright Elsevier, reproduced with permission).

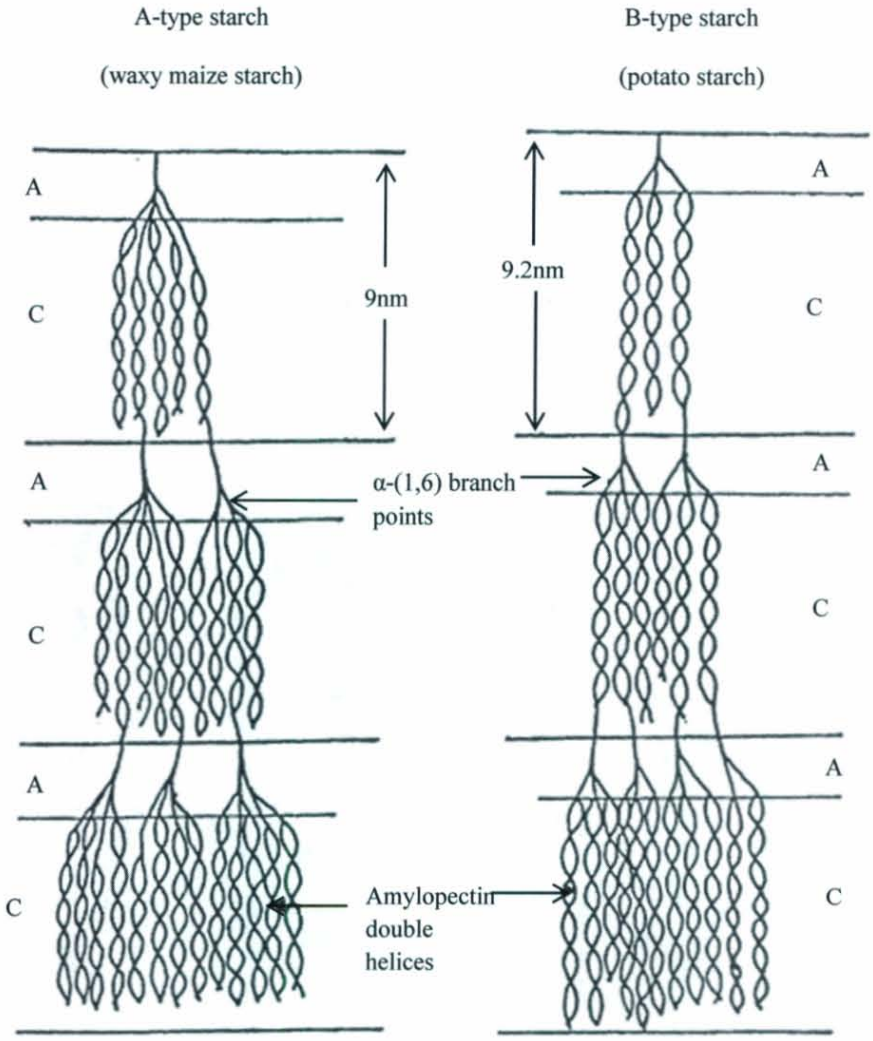

A: amorphous

C: crystalline

Certain pea mutants show different proportions of A- and B-type polymorphs within the starch granule and are used as a model to understand the development of the different polymorphs (Hedley *et al.*, 2002). Microfocus synchrotron WAXS mapping has confirmed that the B-polymorphs occur in the core of smooth pea starches, whereas the A-polymorph is located at the periphery (Buleon *et al.,* 1998). Wang *et al.* (2007a, 2007b) showed by acid hydrolysis that the core part of C-type starch (Chinese yam) was preferentially hydrolyzed and that hydrolyzed starch showed an A-type diffraction pattern, suggesting that B- and A-type are present mainly in the amorphous and crystalline domains respectively. It is now recognized that many regular cereal starches thought to contain only the A-polymorph actually contain small amounts of the B-polymorph (Vermeylen *et al.,* 2004). Ziegler *et al.* (2005) postulated that the hilum region in most granules contains B-type crystallites, and that the overall WAXS pattern is determined by the respective polymorphs contained in the core and periphery, the weight fraction of each region and the ratio of their crystallinity.

2.3.3.2.1 Degree of crystallinity

The degree of crystallinity can be defined as the percentage of the crystalline regions with respect to the total material (Lopez-Rubio *et al.,* 2008a). The amount of crystallinity within starch granules has been reported by many authors. Generally, degree of crystallinity of native starch granules is in the range of 15-45% (Lopez-Rubio *et al.,* 2008a; Zobel, 1988b) depending on the botanical origin, amylose/amylopectin ratio, moisture content and methods used for the crystallinity calculation. The sharpness of the X-ray diffraction pattern of starch granules depends on their water content, B type being more sensitive to hydration than A-type starch (Cleven *et al.,* 1978; Buléon *et al.,* 1982). Studies have shown that there is an optimum moisture

content (about 27%) at which maximum crystallinity is observed, whereas a minimum of 8% water is necessary for the starch to exhibit a X-ray diffraction pattern (Imberty and Perez, 1988). Starch crystallinity was initially calculated by Sterling (1960) and Nara (1978) following the methodologies developed by Hermans (1948) and Wakelin (1959) for cellulose based on the two phase concept, which assumes that relatively perfect crystalline domains (crystallites) are interspersed with amorphous regions. This estimates the degree of crystallinity by separating the diffraction pattern into sharp (crystalline) and diffuse (amorphous) components. Most researchers used this method with slight modifications to calculate starch crystallinity. However, this concept does not fit with the improved understanding of starch structure that encompasses intermediate crystalline objects, chain folding, lamellar crystalline growths and lattice dislocations. Recently, Lopez-Rubio *et al.* (2008a) suggested that a more appropriate way of approaching the crystalline structure of starch is to use the crystal-defect concept as opposed to the two-phase concept. According to the crystal defect concept of polymer structure, a portion of the X-ray scattering from the crystalline domains is diffuse and contributes to the so-called amorphous background.

2.4. Starch properties

2.4.1 Granular swelling

Most starches are insoluble in cold water and undergo a limited reversible swelling due to diffusion and absorption (exothermic process) of small amounts of water into the amorphous region (French, 1984). In the presence of excess water, during heating, the starch granule swells and its volume increases. During this process, crystalline structures of starch molecules are disrupted by increased hydrogen bonding between water molecules and hydroxyl groups, and

this induces granular swelling (Tester and Karkalas, 1996). Therefore, hydration and swelling of starch during heating reflect the magnitude of interaction between the starch chains within the amorphous and crystalline domains. The amylose to amylopectin ratio and the molecular weight/distribution of amylose and amylopectin may affect the extent of this interaction, resulting in variation in the swelling power and solubility of the starch (Gomand *et al.*, 2010; Karim *et al.,* 2007; Ratnayake *et al.*, 2002). Tester and Morrison (1990a) proposed that the swelling property of starch granules is mainly influenced by amylopectin, while amylose acts both as a diluent and as an inhibitor. Furthermore, it has been well documented that minor components of starch, such as phospholipids, monoacylglycerols, phosphate monoesters (Karim *et al.*, 2007; Srichuwong *et al.,* 2005; Roach and Hoseney, 1995; Tester and Morrison, 1990a) and protein (Wang and Seib, 1996), also have enormous effects on swelling properties. Difference in the morphological structures of granules may also be responsible for differences in swelling power and solubility (Singh and Singh, 2001). Sasaki and Matsuki (1998) showed that starches with higher swelling power tended to contain higher proportions of long amylopectin chains ($dp \geq 35$). However, Goman *et al.* (2010) have shown in studies on potato and cassava starches that longer amylopectin chains ($dp > 18$) inhibit swelling, whereas short chains ($dp < 14$) favour swelling.

In general, starches from legumes, roots and tubers exhibit a single stage swelling (Hoover, 2001; Hoover and Sosulski, 1986), whereas normal cereal starches show a two stage swelling (Langton and Hermansson, 1989; Doublier *et al.*, 1987; Leach *et al.*, 1959). Many studies showed that potato starches have higher swelling power than starches from other botanical sources (Eliasson and Gudmundsson, 1996; Swinkels, 1985; Vandeputte *et al.*, 2003). This has

been attributed to the presence of a higher amount of phosphate ester groups on potato amylopectin (Galliard and Bowler, 1987). Waxy starches usually swell to a greater extent than their normal counterparts. The faster swelling of amylose-free starches has been observed for waxy potato (Gomand *et al.*, 2010; Luo *et al.*, 2009; McPherson and Jane, 1999; Visser *et al.*, 1997), waxy barley (Tester and Morrison, 1990b), waxy maize (Li *et al.*, 2001) and waxy rice (Hagenimana and Ding, 2005). The swelling of starch granules is crucial in explaining pasting behaviour and rheological properties (section 2.5.4) (Li and Yeh, 2001).

Starch swelling has been studied by different methods. The classical swelling power (SP) is the ratio of the wet weight of the sedimented gel to its dry weight (Leach *et al.*, 1959). This method shows a disadvantage in that intragranular water cannot be distinguished from intergranular water. Tester and Morrison (1990b) introduced the new concept of swelling factor (SF), which is the ratio of the volume of sedimented gel (volume of swollen granules) to the volume of dry starch granules (initial volume) with a density of 1.4 g/ml. By this technique, the volume of the starch particles is determined from changes in the concentration of a dye, Blue dextran, which by virtue of its high molecular weight (2,000,000) is excluded from the swollen starch granules. Therefore, compared to Leach *et al.* (1959) method, the Blue dextran method has the advantage of measuring intragranular water (Lopez *et al.*, 2004).

2.4.2 Amylose leaching

Amylose leaching mainly occurs at low temperatures, whereas molecules of higher molecular weight leach at higher temperatures (Gomand *et al.*, 2010; Eliasson and Gudmundson, 1996; Ring *et al.*, 1985; Tester and Morrison, 1990). However, amylose can be completely extracted

from granules only at temperatures above 90°C (Banks and Greenwood, 1975). Perez and Bertoft (2010) postulated that these larger amylose chains, which are not easily leached, may participate in double helices with amylopectin (Kasemsuwan and Jane, 1994) or may be entangled within the intricate architecture of the starch granule. In addition to temperature, the extent of amylose leaching has been shown to be influenced by: 1) the extent of interaction between amylose chains (AM-AM) and/or between amylose and outer branches of amylopectin (AM-AMP) (Hoover *et al.,* 2010; Chung *et al.,* 2009; Jayakody *et al.*, 2007; Waduge *et al.*, 2006; Zhou *et al.*, 2004), 2) the amount of lipid-complexed amylose chains (Morrison *et al.*, 1993; Ratnayake *et al.*, 2001; Gunaratne and Hoover, 2002; Nakazawa and Wang, 2004), 3) phosphate content (Gunaratne and Hoover, 2002), and 4) granular size (smaller granules leach more amylose than larger granules) (Lindeboom *et al.*, 2004).

2.4.3 Gelatinization

Starch granules are insoluble in cold water but swell when heated in an aqueous medium. Initially, the swelling is reversible and the optical properties (birefringence) of the granule are retained. But when a certain temperature is reached, starch granules in an aqueous starch suspension undergo an irreversible order-disorder phase transformation termed gelatinization (Donovan, 1979; Lund, 1984). This order-disorder phase transition is associated with the diffusion of water into the granule, hydration and granular swelling, amylose leaching, heat uptake, unravelling and dissociation of double helices, loss of crystalline order and the consequent loss of birefringence, leaching of large molecular weight polymers from the granule (including fragments of amylopectin), and increased viscosity and starch solubilization (Atwell

et al., 1988, Cooke and Gidley, 1992; Donovan, 1979; Jenkins and Donald, 1998; Sakonidou *et al.*, 2003; Sopade, 1990; Stevens and Elton, 1971).

A wide range of techniques (birefringence end point, viscosity, X-ray diffraction, DSC, iodine blue value, enzymatic digestibility, NMR, light extinction, solubility or sedimentation of swollen granules, and absorption of congo red) have been employed to investigate the gelatinization process (Cooke and Gidley, 1992; Derby *et al.*, 1975; Donovan, 1979; Jenkins and Donald, 1998; Liu, *et al.*, 2002; Sopade, 1990; Stevens and Elton, 1971). Birefringence loss could be detected by the Kofler hot stage microscope with polarized light (Leach, 1965; Liu and Zhoa, 1990; Watson, 1964). The temperature at which granules lose their birefringence is referred to as the gelatinization temperature (Lineback, 1986). The birefringence end point temperature (BEPT, i.e. the temperature at which 98% of the granules have lost their birefringence) varies among starches of different origin depending on their composition and the structural organization of their granules. Even within a given starch granule population, the gelatinization temperatures of individual granules might span a 10-15°C range (Biliaderis, 2009).

Differential scanning calorimetry has been widely used to study the phase transitions of aqueous starch suspensions. The gelatinization process is presented in the DSC as an endothermic peak. DSC measures gelatinization transition temperatures (onset [To], peak [Tp] and conclusion [Tc]) and enthalpy (ΔH) of gelatinization. Gelatinization appears as the result of four processes: (1) cleavage of existing starch-starch-OH bonds (endothermic), (2) formation of starch-solvent-OH bonds (exothermic), (3) the unwinding helix-coil transition of amylopectin helices (endothermic) and (4) the formation of amylose-lipid complexes (Colonna and Buleon, 2010). Gelatinization

temperatures are influenced by many factors such as moisture content, botanical source of starch, amylose content, lipid content, starch damage, distribution of amylopectin chains, environmental conditions during growth and the presence of ions and solutes (Hoover and Ratnayake, 2002; Jayakody *et al.*, 2005; Lineback, 1986; Noda *et al.,* 1998; Protserov *et al.,* 2001; Stevenson *et al.,*2006; Tester and Morrison, 1990a; Vandeputte *et al.,* 2003; Visser *et al.,* 1997; Waigh *et al.*, 2000b). Studies on starches with different polymorphic structures showed that A-type crystallites melt at higher temperatures than B-type crystallites (Whittam *et al.,* 1990). The gelatinization temperature of most starches is between 60 and 80 C (Copeland *et al.,* 2009). To has been postulated to represent the melting of the weakest crystallites (Larsson and Eliasson, 1991; Nakazawa and Wang, 2003; Wang *et al.,* 1997). Whereas Tc represents melting of crystallites of high stability (Jacobs *et al.,* 1998). However, there is still no consensus with regard to what ΔH represents during the gelatinization process. Tester and Morrison (1990a) have postulated that ΔH reflects the overall crystallinity (quality and amount of starch crystallites) of amylopectin. Cooke and Gidley (1992) suggested that ΔH primarily reflects loss of double helical order (melting of double helices) rather than loss of crystalline order. According to Lopez-Rubio *et al.* (2008), ΔH reflects melting of imperfect amylopectin-based crystals with potential contributions from both crystal packing and helix melting. Reported gelatinization enthalpies of native starches are generally in the range of 5-20J/g (Biliaderis, 2009).

Starch gives a biphasic endotherm during gelatinization at low moisture levels (water:starch volume fractions less than 0.45) (Donovan, 1979; Evans and Haisman, 1982; Nakazava *et al.,* 1984). Donovan (1979) suggested that in the presence of less water, the endothermic transition

is characterized as a solvent-aided melting of crystallites in the starch granules. The high temperature transition is due to melting of crystallites without adequate moisture. When excess water is present, the high temperature transition disappears (Donovan, 1979). Evans and Haisman (1982) proposed the "cooperative melting theory", which explains the bi-phasic endotherm as a result of crystallite stability within the granules. The granules containing the least stable crystallites start to change first upon heating. Water absorption by the granules lowers the melting points of remaining crystallites. This cooperative process happens quickly when there is sufficient water and gives a narrow or single DSC endotherm. At low moisture content, there is insufficient water for cooperative melting to take place (Evans and Haisman, 1982).

Several gelatinization mechanisms have been proposed to describe the changes occurring during heating of starch granules in excess water (Biliaderis, *et al.,* 1986; Blanshard, 1987; Donovan, 1979; Evans and Haisman, 1982; Liu *et al.*, 2002; Marchant and Blanshard, 1978; Waigh *et al.*, 2000b). Donovan (1979) proposed a model for gelatinization in excess water whereby the swelling of the amorphous regions of the granule facilitated the ''stripping'' of starch chains from the surface of crystallites, thereby disrupting crystalline order. Another approach was developed by Slade and Levine (1988) who introduced the glass transition concept as a key event determining the change in polymer mobility. When the temperature increases, molecular motion is initiated, enabling molecules to slide past one another. At this point, the polymer becomes rubbery and flexible. This physical event reflects an increase in the mobility of short segments (3-20) on the polymer backbone and it is called the glass transition temperature (Tg). Below Tg, segmental mobility of polymer chains is frozen in a random conformation, rendering starch

phases solid and glassy (Slade and Levine, 1988). According to this concept, a glass transition of the amorphous regions will precede the melting of crystallites and gelatinization is controlled by the molecular mobility in the amorphous phase surrounding crystallites (Biliaderis, 1992; Blanshard, 1987).

Waigh *et al.* (2000b) proposed a mechanism for gelatinization based on a side chain liquid crystalline polymeric (SCLCP) model of starch (Donald *et al.*, 2001; Jenkins *et al.*, 1993; Waigh *et al.*, 2000a; Waigh *et al.*, 1998). In this mechanism, depending on the water content and heating rate, gelatinization results from helix-coil transitions and transformations from a glassy nematic phase to a plasticized smectic phase of amylopectin helices. In the SCLCP model, amylopectin is suggested as a structural analogue to a synthetic SCLCP with three distinct components: rigid units (mesogens) corresponding to double helices, flexible spacers and a flexible backbone. In the nematic state, helices are not aligned into lamellae, whereas in the smectic state; as in the granules under native conditions, the mesogens are aligned which leads to a 9 nm repeat between the lamellar lengths.

According to the SCLCP model, the structural phase transitions (mesophases) during gelatinization can be summarized by considering three order parameters: helical ordering (the tendency of helices to line up), lamellar ordering (the amplitude of a sinusoidal density modulation) and the number of helices. At low water content (<5%, w/w), amylopectin helices are in a glassy nematic state and rigid crystalline parts (mesogens) are somewhat disordered and the single peak corresponds to a helix-coil transition.

Fig 2.17 A proposed model for the gelatinization mechanism.

a) The single stage process in the gelatinization of starch at low water contents.

b) The two stage process involved in the gelatinization of starch in limited water.

c) The two stage process involved in the gelatinization of starch in excess water. The first stage involves a slow dissociation of the helices side-by-side. Immediately, a helix-coil transition occurs as a secondary effect (Waigh *et al.,* 2000b, Copyright Elsevier, reproduced with permission).

a) Low water content gelatinization

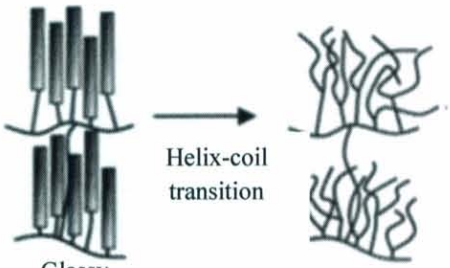

b) Intermediate water content gelatinization

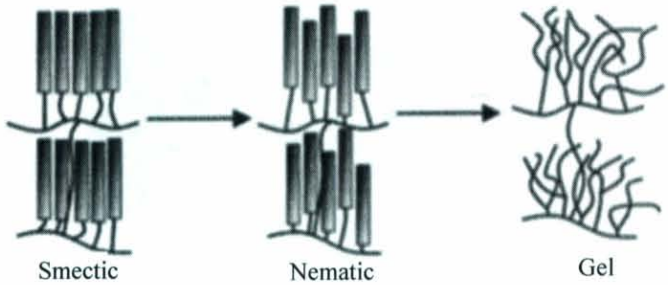

c) Excess water content gelatinization

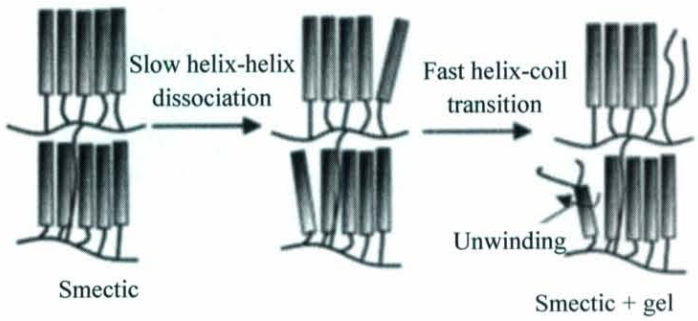

At intermediate water content (>5%, <40%, w/w), the first DSC endotherm is attributed to dislocations between double helices leading to a smectic-nematic transition. The second endotherm is the helix-coil transition with irreversible disentanglement of double helices. Two different processes are shown for A-and B-type starches. It is proposed that the intermediate phase is determined by the length of the amylopectin helices. B-type starch has a much longer amorphous backbone than A-type starch, and because of this, the isotropic structure is formed over gelatinization in the intermediate state, whereas for A-type starch, this takes place during the nematic phase. In excess water (>40%), lamellar break-up and disentanglement of double helices occur simultaneously since free, disassociated helices are unstable (Fig 2.17) (Waigh *et al.*, 2000b).

2.4.4 Pasting properties

Pasting is the phenomenon following gelatinization in the dissolution of starch (Atwell *et al.*, 1988). The granules become increasingly susceptible to shear disintegration as they swell and release soluble material as they disintegrate (Whistler and BeMiller, 1997). The paste that is obtained on gelatinization is a viscous mass consisting of a continuous phase (a molecular dispersion) of solubilized amylose and/or amylopectin and a discontinuous phase of granule remnants (granule ghosts and fragments) (Whistler and BeMiller, 1997). Peak viscosities have been shown to be influenced by several factors, such as granule rigidity, extent of granular swelling, extent of amylose leaching, size distribution of granules, heating rate, shearing rate, stirring rate, heating temperature, starch concentration, the presence of solutes, friction between swollen granules, phosphate monoester content, the proportion of long amylopectin branch chains and the botanical source of the starch (Eerlingen *et al.*, 1997, Evans and Haisman, 1979;

Hagenimana and Ding, 2005; Hoover and Vasanthan, 1994b; Jane *et al.*,1999; Jayakody *et al.*,2007; Ziegler *et al.*, 1993). The pasting profile of starch is commonly monitored using a Rapid Visco™ Analyser (RVA), which is a heating and cooling viscometer configured especially for testing starch-based and other products requiring precise control of temperature and shear (Hagenimana and Ding, 2005).

2.4.5 Retrogradation

When a gelatinized starch suspension is cooled, it begins to retrograde. Retrogradation has been defined as the process which occurs when the molecular chains in gelatinized starches begin to reassociate (hydrogen bonding between starch chains) in an ordered structure (Atwell *et al.*, 1998; Hoover, 2001). During retrogradation, amylose forms double-helical associations of 40-70 glucose units (Jane and Robyt, 1984), whereas amylopectin crystallization occurs by re-association of the outermost short branches (Ring *et al.*, 1987). Retrogradation is accompanied by increases in crystallinity, gel firmness and turbidity, and the appearance of a B-type X-ray diffraction pattern (Hoover, 2010). Miles *et al.* (1985) have shown that the short-term development of gel structure and crystallinity in starch gels is dominated by irreversible ($T<100°C$) gelation and crystallization within the amylose matrix, whereas long-term increases in the modulus of starch gels were linked to a reversible crystallization (within gelatinized granules) involving amylopectin. Miles *et al.* (1985) postulated that crystallization increases granule rigidity and thus enhances their reinforcement of the amylose matrix. The retrogradation of amylose in processed foods is considered to be important for properties related to stickiness, ability to absorb water and digestibility, whereas retrogradation of amylopectin is probably a

more important determinant in the long-term of quality changes in foods such as staling of bread and cakes (Copeland *et al.,* 2009; Miles *et al.*, 1985; Ring *et al.,* 1987).

It has been suggested that the process of retrogradation can be viewed as a temperature-dependent, three-step sequential mechanism of nucleation, propagation, and maturation (Levine and Slade, 1988, 1989). In retrograded starch, the enthalpy value (ΔH) provides a quantitative measure of the energy transformation that occurred during the melting of recrystallized amylopectin (Karim *et al.,* 2000, 2007). The endothermic peak of starches after gelatinization and storage at 4°C appears at lower transition temperatures. Starch retrogradation enthalpies are usually 60-80% smaller than gelatinization enthalpies and transition temperatures are 10-26°C lower than those for gelatinization of starch granules (Baker *et al.,* 1998; White *et al.,* 1989; Yuan *et al.,* 1993). The extent of the decreases in transition temperatures and enthalpy is higher in stored potato starch gels than in corn, rice and wheat gels. This may be attributed to the higher tendency of the potato starch gels toward retrogradation (Singh *et al.,* 2002). Thermal properties of starches after gelatinization and during refrigerated storage could be influenced by the amylose to amylopectin ratio, size and shape of the granules, presence/absence of lipids, and chain length of amylose and amylopectin (Perera and Hoover, 1999; Singh *et al.,* 2003). A greater amount of amylose has generally been linked to a greater retrogradation tendency in starches (Whistler and BeMiller, 1996).

2.4.6 Acid hydrolysis

Acid modification is widely used in the starch industry to produce thin boiling starches for use in the food, paper, textile and other industries (Hoover, 2000). Acid hydrolysis of starches has been

shown to alter granule morphology and crystallinity, gelatinization temperature, gelatinization enthalpy, and viscoelasticity. Several authors have shown that acid hydrolysis could be used as a probe to understand the inner structure of starch granules (Genkina *et al.*, 2009; Hoover, 2010;; Kang *et al.,* 1997; Kim and Ahn, 1996; Osunsam *et al.,* 1989; Shi and Seib, 1992; Virtanen *et al.,* 1993; Wang *et al.,* 2007a and 2007b). This process involves suspending starch in an aqueous solution of hydrochloric acid or sulphuric acid at a certain temperature. Immersion in sulfuric acid (15%) at room temperature produces Nägeli amylodextrins (a low molecular weight acid-resistant fraction), whereas treatment with hydrochloric acid (2.2M) at elevated temperatures (30-40°C) produces Lintnerized starch (a higher molecular weight acid resistant fraction) (Hoover, 2000). In the presence of a strong acid and heat, the glycosidic bonds between monosaccharides in a polysaccharide are cleaved (Hoover, 2000). Two distinct phases are observed in the course of acid hydrolysis of starch as a function of time. The first more rapid phase is attributed to hydrolysis of amorphous regions of the starch granules, whether they be at the surface or in the interior. The second phase is attributed to a slower degradation of less accessible starch molecules present in the crystalline lamellae (Biliaderis *et al.,* 1981; Hoover, 2000; Jacobs *et al.,* 1998; Kainuma and French, 1971; Nakazawa, and Wang, 2003; Robin *et al.,* 1974; Robin *et al.,* 1975; Watanabe and French, 1980).

2.4.7 Enzyme hydrolysis of starch by α-amylase

2.4.7.1 Classification

Amylases are glycoside hydrolases (GHs), which act upon the α-(1,4) and/or α-(1,6)-linkages of starch polymers (Bijttebier *et al.,* 2008; MacGregor *et al.,* 2001). Several GH classification systems exist. One of the simplest classifications is based on substrate specificity. Each enzyme

is characterized by the Enzyme Commission (EC) number based on the recommendations of the International Union of Biochemistry and Molecular Biology. GHs are characterized by the number EC 3.2.1.x, with the x representing the substrate specificity or, in some cases, the molecular mechanism or type of linkage (EC 3.2.1.1, α-amylase; EC 3.2.1.2, β-amylase; EC 3.2.1.3, glucoamylase). This classification does not reflect structural or mechanistic characteristics of enzymes (Bijttebier *et al.,* 2008; Henrissat and Davies, 1997).

The classification of GH families, based on amino acid sequence and structural similarities, is considered the most powerful and common one, since the amino acid sequence of an enzyme gives important structural and mechanistic information about the enzyme (Bijttebier *et al.,* 2008). On this basis, α-amylases are grouped into GH family 13, whereas β-amylases and glucoamylases are grouped into GH family 14 and GH family 15, respectively. GH family 13 amylolytic enzymes include α-amylase (EC 3.2.1.1), maltogenic (EC 3.2.1.133) and other maltooligosaccharide-producing amylases (e.g. EC 3.2.1.60, EC 3.2.1.98) and debranching enzymes (pullulanase/isoamylase) (Bijttebier *et al.,* 2008). Beta-amylase is inverting exo-amylase and hydrolyze the α-(1,4)-linkages at the non-reducing ends of starch molecules. They cannot hydrolyse or pass α-(1,6)-linkages; its action stops at the branch points. Beta-amylase degrades starch to β-maltose and β-limit dextrins (Goesaert *et al.,* 2009). The action of different amylolytic enzymes on starch is illustrated in Figure 2.18.

2.4.7.2 Mechanism for alpha-amylase action

Enzymatic hydrolysis of glycosidic bonds is carried out with one of two stereochemical outcomes, net retention or net inversion of anomeric configuration. Thus, glycosidases are

Fig 2.18 Schematic representation of the action of different amylolytic enzymes on starch (amylopectin) polymers. The gray ring structure represents a reducing glucose residue. (A) Endo-type action of *alpha*-amylase, yielding branched and linear low molecular weight (LMW) dextrins; (B) mainly exo-type action of maltogenic *alpha*-amylase, yielding mainly maltose; (C) debranching enzyme action, yielding linear dextrins; (D) purely exo-type action of *beta*-amylase, yielding maltose and *beta*-limit dextrins; (E) purely exo-type action of glucoamylase, yielding glucose (Goesaer *et al.*, 2009, Copyright Elsvier, reproduced with permission).

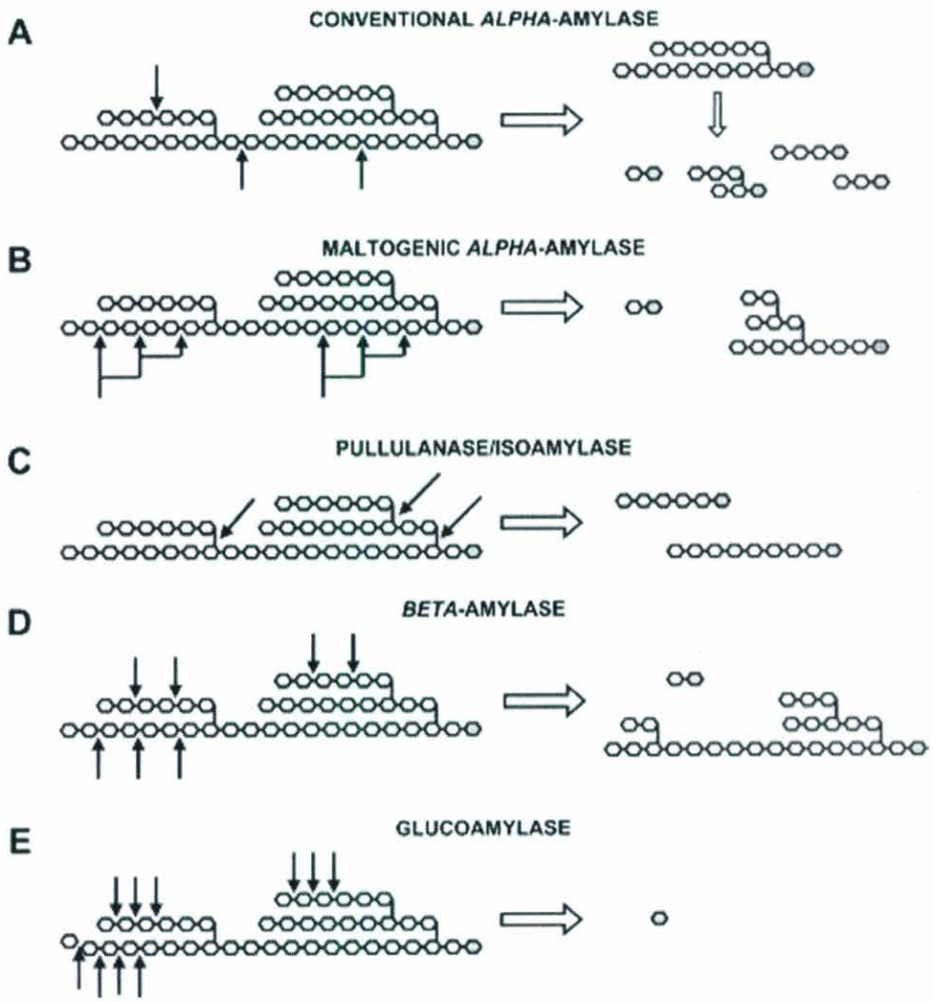
A
CONVENTIONAL *ALPHA*-AMYLASE
B
MALTOGENIC *ALPHA*-AMYLASE
C
PULLULANASE/ISOAMYLASE
D
BETA-AMYLASE
E
GLUCOAMYLASE

classified as either retaining or inverting (Figure 2.19) (Rye and Withers, 2000). All the enzymes of GH family 13 retain the anomeric configuration and work according to the double displacement mechanism (MacGregor, 1993; van der Maarel *et al.,* 2002). This is an acid-base catalysed reaction, requiring a proton donor and a nucleophile, in which a glucosyl-enzyme intermediate is formed (Withers and Aebersold, 1995). Takase *et al.* (1992) have shown that three carboxylic acid groups (one from glutamic acid and two from aspartic acid residues) are essential for catalytic activity. Typically, all endo-acting amylases work according to this action mechanism (Bijttebier *et al.,* 2008). In contrast, exo-acting amylases, such as β-amylases, are inverting amylases and work through the single displacement mechanism (Henrissat and Davies, 1997). The hydrolysis reaction proceeds through an oxocarbenium ion-like transition state (O-anomeric C bond has partial double bond character) (Withers and Aebersold, 1995).

2.4.7.2.1 Double displacement mechanism

In this mechanism, the carboxylate base initiates cleavage of the bond via nucleophilic attack at C-1 of the glucopyranosyl unit undergoing hydrolysis. Simultaneously, the glycosidic oxygen is displaced and protonated by the carboxylic acid group. The attacking carboxylate group forms a covalent β-linked acetal ester, giving a glucopyranosyl-enzyme intermediate. Evidence for the covalent glucopyranosyl-enzyme complex was provided for porcine pancreatic α-amylase, using cryogenic ^{13}C-NMR (Tao *et al.,* 1989). This high energy linkage is subsequently hydrolysed by water. Reaction with water is facilitated by the second asparate carboxylate group at the active sites of these enzymes. The carboxylate group abstracts a proton from water, making the water more nucleophilic for its attack on the β-linked acetal ester. The anomeric carbon atom of the

Fig 2.19 Proposed mechanisms involved in the hydrolysis of glycosidic linkages (adapted from Robyt, 2009).

a) Double displacement (S_N2), mechanism, giving retention of configuration (α-amylases)
   i. Attack on C-1 by a carboxylate group and donation of a proton to the leaving oxygen atom by a carboxyl group
   ii. Attack of water on the covalent β-acetal-carboxyl-ester to give product III with retained configuration at the anomeric end
b) Direct displacement (SN1), mechanism, giving inversion of configuration (β-amylases)
   i. Direct attack on C-1 by water, assisted by a carboxylate group and donation of a proton to the leaving oxygen atom by a carboxyl group.
   ii. Product with inverted configuration

Regeneration of the catalytic groups at the active-site by proton exchange between the two carboxyl groups.

a)

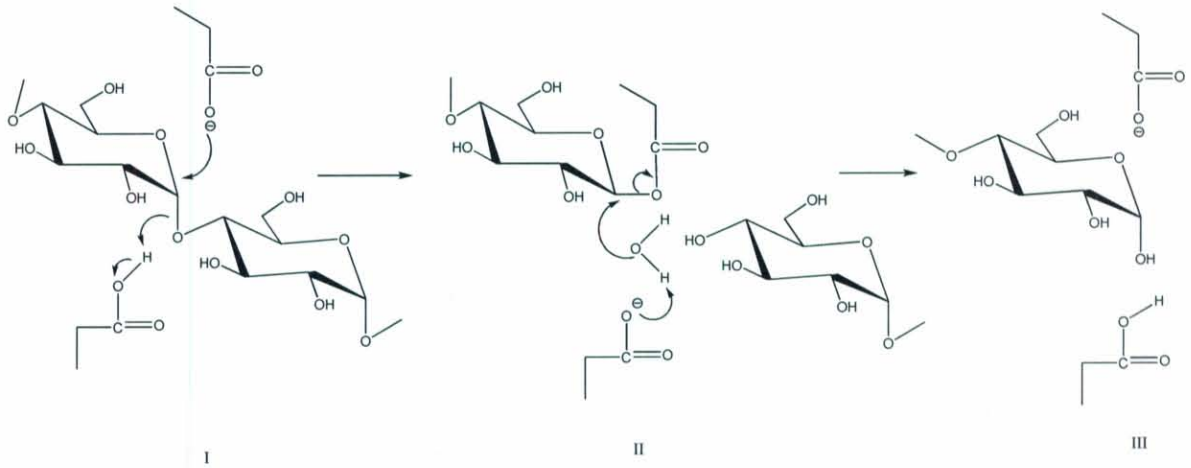

I II III

b)

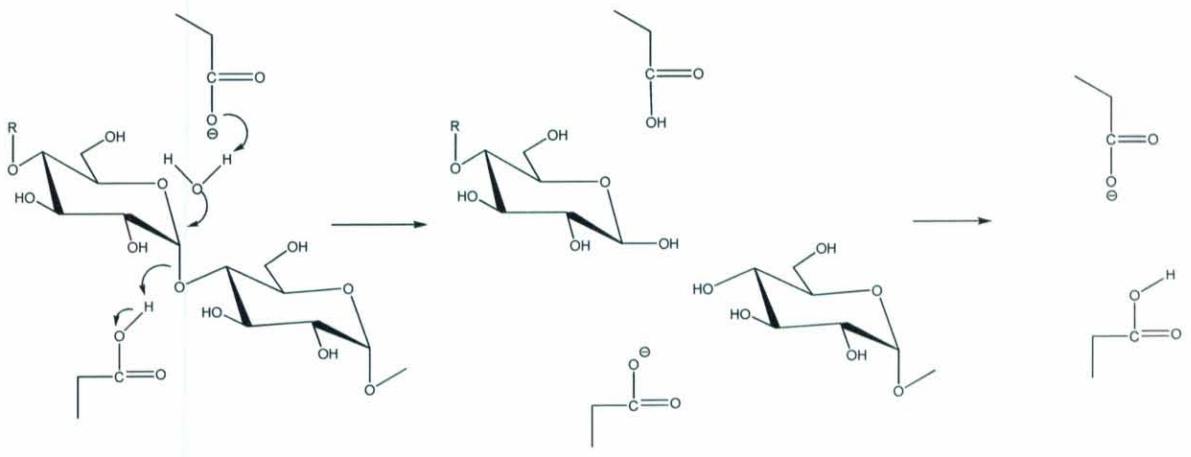

I II III

resulting glucopyranosyl unit that is released from the enzyme complex thus has the α-configuration, giving retention of the configuration of the product at its reducing end (Robyt, 2009).

2.4.7.3 Mode of action of α-amylase

Alpha-amylases have a multiple attack mechanism (Robyt and French, 1970). In this mechanism, an amylase cleaves several glycosidic bonds after the first random hydrolytic attack and then dissociates from the substrate. The direction of multiple attack is from the reducing to the non-reducing end of the molecule (Robyt and French, 1970). Porcine pancreatic α-amylase (endo-amylase, EC 3.2.1.1) has five subsites to bind substrate. Each subsite binds a glucose unit. It requires binding to at least three glucose units before cleaving an α-(1,4) glycosidic linkage. Both amylose and amylopectin are hydrolysed by virtue of binding of their five glucose residues adjacent to the terminal reducing glucose unit to specific catalytic subsites of the α-amylase, followed by cleavage between the second and third α-(1-4) linked glucosyl residue. The final hydrolysis products from α-amylase digestion are mainly maltose, maltotriose and maltotetraose (Gray, 1992). Alpha-amylases have no specificity for α-(1,6) branch linkages in amylopectin. Therefore, their capacity to break α-(1,4) links adjacent to the branching point is decreased, mainly due to steric hindrance (Oates, 1997).

2.4.7.4 Stages of enzymatic reaction

Enzymatic reaction consists of several successive phases: diffusion of the enzyme molecule toward the surface of the solid phase and then inside the granules, adsorption of enzymes on the substrate and finally catalytic reaction (Bird *et al.,* 2009; Dhital *et al.,* 2010; Gallant *et al.,* 1992;

Sujka and Jamroz, 2007). All three stages, diffusion, adsorption and catalysis, are influenced by enzyme-related factors and by the intrinsic properties of the granules. The diffusion is considered as the limiting step of hydrolysis with regard to the macromolecular nature of amylases and the porosity of substrates or associated products in foods. Thus, the surface area accessible to the enzyme and the efficiency of adsorption onto this surface are important kinetic parameters (Bertoft and Manelius, 1992). Smaller granules, by virtue of their higher available surface area per unit mass, facilitate diffusion and adsorption of enzymes, and thus are catalyzed more rapidly than larger granules (Colonna *et al.,* 1992). Adsorption of amylase on the granule is a pre-requisite for subsequent hydrolysis of starch (Slaughter *et al.,* 2001). Upon adsorption, specific forces between the enzyme and the binding sites of the substrate are formed, leading to an enzyme-substrate complex. The number of adsorption sites for the enzyme is essentially dependent on the porosity and accessibility of the substrate (Colonna *et al.,* 1992). The enzyme-catalyzed hydrolysis of α-(1,4) glucosidic bonds involves the enzyme-induced ring distortion of one of the D-glucosyl residues from the $^4C_1$-chair conformation to a 'half chair' conformation (Fig 2.20) (Oates, 1997). Ring distortion decreases the enthalpy of activation and increases the susceptibility of the glycosyl residues. Therefore, chains with restricted mobility, either complexed or crystallized, will be hydrolyzed less readily (Oates, 1997). All of these studies showed that hydrolysis of granular starch can be controlled by influencing each of these steps.

2.4.7.4 Enzyme hydrolysis of native starches

The rate and extent of amylolytic hydrolysis of granular starches depends on the botanical origin of the starch and the α-amylase source (Dona *et al.,* 2010; Gallant *et al.,* 1992; Zhang *et al.,* 2006). Enzyme concentration and reaction time are other factors influencing both rate and extent

of hydrolysis. For a given enzyme and digestion conditions, the degree of hydrolysis of a specific starch will depend only on its structural and molecular organization (Bird *et al.,* 2009). Susceptibility of starch to enzyme attack is influenced by several factors, such as granule size and available specific surface (Franco *et al.*, 1992, 1998; Knutson *et al.*, 1982; Tahir *et al.*, 2010; Tang *et al.*, 2004), surface porosity and channels (Fannon *et al.*, 1992, 1993; Sujka and Jamroz, 2007; Zhang *et al.,* 2006;), amylose and amylopectin content (Blazeck and Copeland, 2010; Hoover and Manuel, 1995; Hoover and Sosulski, 1985; Holm and Bjorck, 1988; Ring *et al.*, 1988), crystalline structure (Chung *et al.*, 2010; Zhou *et al.*, 2004; Gunaratne and Hoover, 2002), extent of branching (long amylopectin branches/branch density) (Dona *et al.*, 2010; Shrestha *et al.*, 2010), distribution pattern of α-(1,6) branch points between the amorphous and crystalline regions (Gunaratne and Hoover, 2002; Jane *et al.*, 1997), degree of crystallinity (Chung *et al.*, 2009a; Zhou *et al.*, 2004), packing of polymers within granules (dense/loose), helical conformation of amylose molecules (Shrestha *et al.*, 2010), presence of non-starch substances (proteins, lipids and phosphorus) (Hoover and Manuel, 1995; Perera and Hoover, 1998) and inhibitors (Colonna *et al.,* 1992; Zhou *et al.*, 2004). The kinetics of α-amylolysis of granular and gelatinized starch are characterized by an initial rapid hydrolysis phase followed by a slower phase. The reduction in the hydrolysis rate is probably caused by product (maltose and maltotriose) inhibition of the α-amylase activity (Colonna *et al.*, 1988).

During α-amylolysis by bacterial or pancreatic enzymes, the amorphous parts generally are thought to be more rapidly digested than the crystalline zones due to the steric incompatibility of the double helix and the active site of α-amylases (Gallant *et al.*, 1992; Planchot *et al.,* 1995).

Fig 2.20 An energy profile (ΔH kcal/mole) for the inter-conversion of the chair to a 'half chair' conformation.

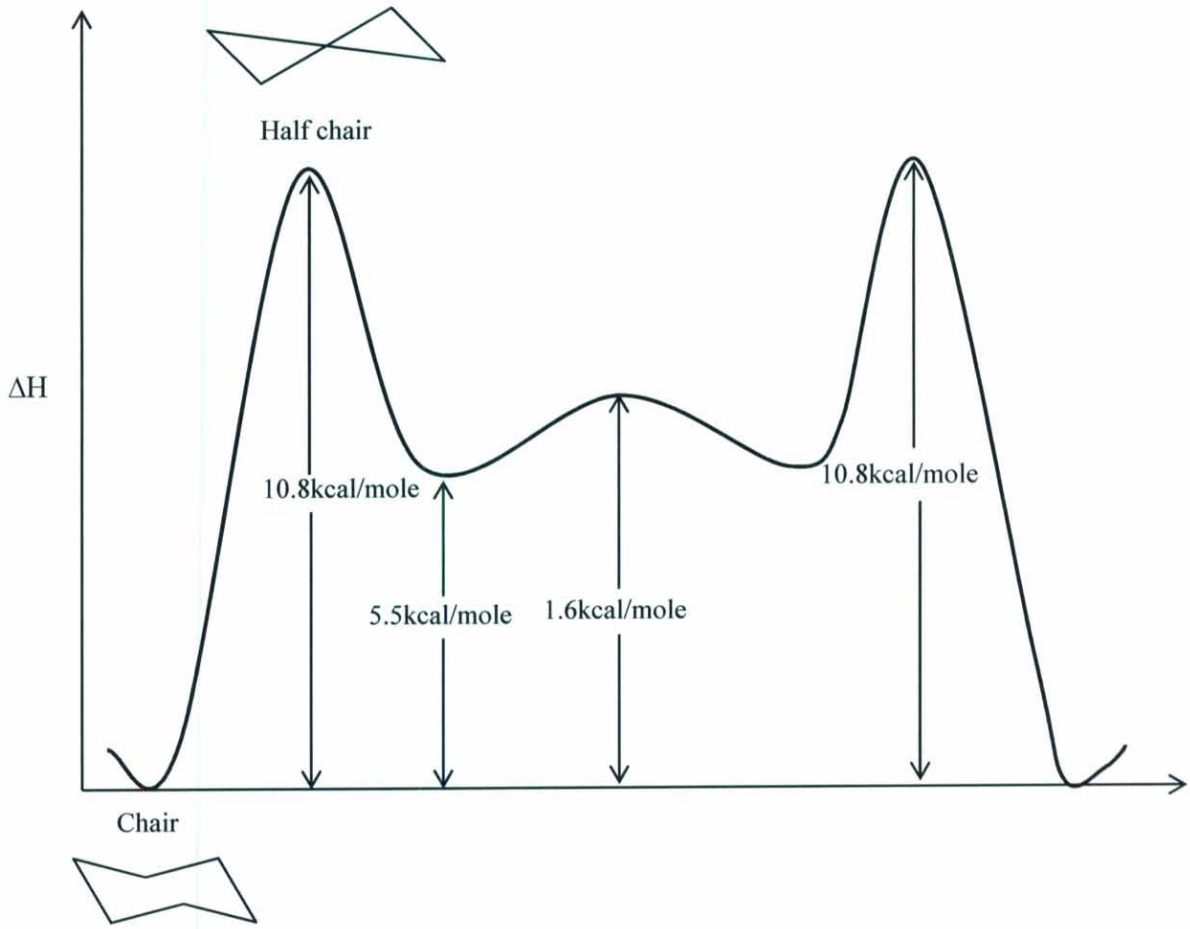
Half chair
ΔH
10.8kcal/mole
5.5kcal/mole
1.6kcal/mole
10.8kcal/mole
Chair

However, Zhang *et al.* (2006) have shown in studies on cereal starches, that the amorphous and crystalline regions are digested simultaneously. A side-by-side and even digestion mechanism that starts from the channels was proposed as the mechanism leading to the simultaneous digestion of crystalline and amorphous regions. The side-by-side digestion mechanism was attributed to strong association between adjacent amorphous and crystalline layers so that the two regions remained together throughout the digestion process.

The susceptibility of starch granules to enzyme hydrolysis can be classified by the intensity and the manner by which the granules are eroded and corroded (Gallant *et al.,* 1992). In general, enzymes either erode the entire granule surface or sections of it (exo-corrosion/exo-pitting) or digest channels at specific locations on the surface towards the centre (endo-corrosion) (Oates, 1997). Many different modes of enzyme attack have been identified, including pinhole, sponge-like erosion, numerous medium sized holes, single holes in individual granules and surface erosion (Sujka and Jamroz, 2007). Planchot *et al.* (1995) showed that the mode of enzymatic degradation depends on the starch and the enzyme used.

Hydrolysis of native cereal starch begins with enlargement of the surface pores and channels with concurrent hydrolysis from the hilum region toward the outside of the granules, an "inside-out" digestion pattern (Zhang *et al.*, 2006). It has been postulated that pores may be the site of initial enzyme attack, openings that allow enzyme molecules direct access to the granule interior (hilum) (Fannon *et al.,* 1993). Planchot *et al.* (1995) observed that normal and waxy maize starch granules were degraded uniformly, with a large range of degradation levels in the granule population, whereas potato and high-amylose maize starch granules were not equally degraded at

a given time. B-type starches without pores shows a different hydrolysis pattern, which is referred to as exo-pitting (Gallant *et al.*, 1992). According to Quingley *et al.* (1998), potato starch hydrolysis is characterized by the formation of a groove along the centre of the granule.

Native cereal starches with A-type crystalline structure (maize) have been shown to be more susceptible to enzymatic hydrolysis than B-type (potato) starches (Planchot *et al.,* 1997). It has been documented that starch granules from waxy maize (Fuwa, Nakajima, Hamada and Glover, 1977), waxy rice (Evers and Juliano, 1976), waxy barley (Fuwa, 1982) and amylose-free sweet potato (Noda *et al.*, 2002) are digested by amylase faster than their normal counterparts, in general. Among non-cereal starches, tapioca starch has relatively higher enzyme susceptibility than other starches such as potato and sweet potato (Zhang and Oates, 1999; Rickard *et al.*, 1991). Potato starch granules are relatively resistant to α-amylolysis, with reasons proposed such as crystallinity and thicker blocklets on the surface (Buleon *et al.,* 1998; Gallant *et al.,* 1997, 1992; Tang *et al.,* 2006). However, Dhital *et al.* (2010) suggested that the dominant reason for the large difference in enzyme hydrolysis between potato and maize starches is the presence of enzyme-accessible channels in maize starch, rather than crystallite polymorph or amylopectin blocklet size differences.

2.5 Heat-moisture treatment

Native starches are not widely used in food applications due to their inconsistency and poor functional properties such as low shear and acid resistance, low thermal resistance, thermal decomposition, and high retrogradation tendency (Hoover, 2010). Therefore, modification of starch is often needed to meet industrial demands. In this respect, physical, chemical or

enzymatic modifications are commonly used to produce starches with desirable properties for specific end uses. Crosslinking and substitution are the two most common chemical modification techniques utilized in the food industry (Luo *et al.,* 2009; Watcharatewinkul *et al.,* 2010).

However, at the present time, physically modified starches prepared by thermal (moisture and heat) or radiation techniques have gained a wider acceptance, especially in the food and pharmaceutical industries (Chung *et al.,* 2009; Hoover, 2010; Watcharatewinkul *et al.,* 2010; Zavareze *et al.*, 2010). Two hydrothermal treatments that modify the physicochemical properties of starch, without destroying granular structure, are annealing and heat-moisture treatment (HMT). Annealing is referred to as treatment of starch in excess water (<65%) or at intermediate moisture (40-55% w/w) for a certain time period at a temperature above the glass transition temperature (Tg) but below the onset temperature of gelatinization (To) (Hoover, 2010; Jacobs and Delcour, 1998). Heat-moisture treatment (HMT) of starches is defined as a physical modification that involves treatment of starch granules at low moisture levels (<35% moisture w/w) over a certain time period (15 min-16 h) and at temperature (80-130°C) above the glass transition temperature (T_g) but below the gelatinization temperature (Hoover, 2010; Jacobs and Delcour, 1998; Kulp and Lorenz, 1981; Sair, 1967). HMT has been shown to influence morphology, X-ray diffraction pattern, crystallinity, granule swelling, amylose leaching, gelatinization parameters, viscosity, retrogradation and susceptibility towards acid and α-amylase hydrolysis of the starch granule. However, the type and extent of change depends on the botanical origin (e.g. cereal, tuber, root or legume), starch composition (e.g., amylose-amylopectin ratio and lipid content) and treatment conditions (temperature, moisture and

duration of heating) (Abraham, 1993; Adebowela *et al.,* 2005a, 2005b, 2005c, 2003; Anderson *et al.,* 2002; Anderson and Guraya, 2006; Chung *et al.,* 2009a, 2009b; Brumovsky *et al.,* 2009; Brumovsky and Thompson, 2001; Collado and Corke, 1999; Collado *et al.*, 2001; Donova *et al.,* 1983; Eerlingen *et al.*, 1996, 1997; Franco *et al.*, 1995; Gunaratne and Hoover, 2002; Gunaratne and Corke, 2007; Hoover, 2010; Hoover and Manuel 1996; Hoover and Vasanthan, 1994a, 1994b; Hoover *et al.*, 1994; Jacobs and Delcour, 1998; Kawabata *et al.*, 1994; Kurakake *et al.*, 1996; Kweon *et al.,* 2000; Kulp and Lorenz, 1983; Lawal, 2005; Lawal and Adebowale, 2005; Lim et al., 2001; Lorenz and Kulp, 1981, 1982, 1983; Lu *et al.*, 1996; Moorthy, 1999; Olayinka, *et al.*, 2008; Perera *et al.*, 1997; Perera and Hoover, 1998, 1999; Purwani *et al.*, 2006; Sang and Seib, 2006; Schierbaum and Kettlitz, 1994; Singh *et al.,* 2009; Stute, 1992; Takaya *et al.*, 2000; Vermeylen *et al.,* 2006; Watcharatewinkul *et al.,* 2010; Wongsagonsup, 2009; Wu and Sarko, 1978b; Zavareze *et al.,* 2010).

2.5.1 Impact of HMT on granule morphology

HMT temperature has been shown to influence the granule morphology of potato (Kawabata *et al.,* 1994; Vermeylen *et al.,* 2006), maize (Kawabata *et al.,* 1994) and pulse (Chung *et al.,* 2009a) starches. Chung *et al.* (2009a) observed that HMT at 120°C decreased the birefringence intensity and causes loss of birefringence at the granular centre (hilum region). In potato starches, disappearance of birefringence at the granular centre (hilum region) has been shown to increase with increasing HMT temperature (Vermeylen *et al.,* 2006). However, the granule periphery in potato and maize starches was found to remain highly birefringent even after HMT (Kawabata *et al.,* 1994; Vermeylen *et al.,* 2006). The disappearance of birefringence (loss of radial orientation of AMP chains) at the granular centre has been attributed to the formation of

voids surrounding the hilum (Vermeylen *et al.,* 2006). Several studies have shown that HMT has no effect on the size and shape of the starch granule (Adebowala *et al.,* 2005; Gunaratne and Hoover, 2002; Hoover and Vasanthan, 1994a; Hoover and Manuel, 1996; Khunae *et al.,* 2007; Lawal, 2005; Singh *et al.,* 2009; Watcharatewinku *et al.*, 2009).

2.5.2 Impact of HMT on X-ray pattern and crystallinity

HMT has been shown to change the X-ray pattern (WAXS) of B-type starches from B-to A+B- or A-type (Donovan *et al.,* 1983; Gunatratne and Hoover, 2002; Kulp and Lorenz, 1981; Sair, 1967; Stute, 1992; Hoover and Vasanthan, 1994; Vieira and Sarmento, 2008). The extent of change has been shown to be influenced by the HMT conditions (temperature, moisture and duration of heating) (Vermeylen *et al.,* 2006). However, Lorenz and Kulp (1982) observed a shift from C-to A-type in arrowroot and cassava starches. The A-type pattern of cereal starches has been shown to remained unchanged on HMT (Donovan *et al.,* 1983; Hoover and Vasanthan, 1994a; Sair, 1967). The change in X-ray pattern of B-type starches on HMT has been attributed to dehydration of the 36 water molecules in the central channel of the B-type unit cell and to the movement of a pair of double helices into the central channel (that was originally occupied by the water molecules) (Fig 2.21) (Gunaratne and Hoover, 2002).

The X-ray intensity of peaks has been shown to decrease in potato (Hoover and Vasanthan, 1994a; Lim *et al.,* 2001; Miyoshi, 2002), cassava (Abraham, 1993), yam (Hoover and Vasanthan, 1994a), barley (Lorenz and Kulp, 1982; Singh *et al.,* 2005), triticale (Lorenz and Kulp, 1982), pea (Hoover and Manuel, 1996) and bean (Lawal and Adebowale, 2005; Adebowale and Lawal, 2003) starches. However, cereal starches generally exhibit either increased or unchanged

Fig 2.21 A model of the polymorphic transition from B-type to A-type unit cell in the solid state (adapted from Imberty *et al.*, 1991).

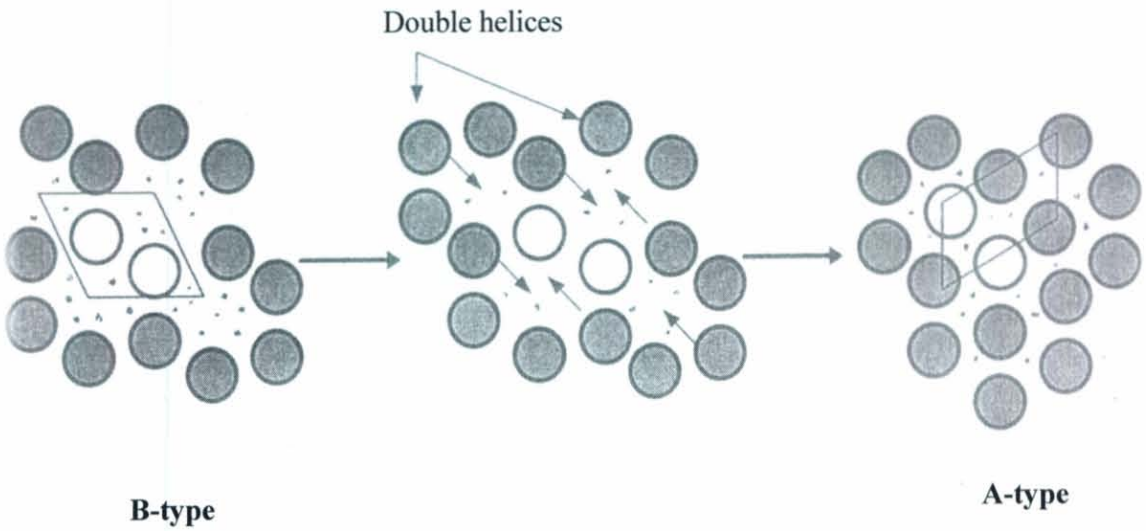
Double helices
B-type
A-type

intensities after heat-moisture treatment (Sair, 1967; Donavan *et al.,* 1983; Hoover and Vasanthan, 1994a; Hoover and Manuel, 1996).

The relative crystallinities of potato (Gunartane and Hoover, 2002; Lim *et al.,* 2001; Vermeylen *et al.,* 2006), cassava (Jyothi *et al.,* 2010) pulse (Chung *et al.,* 2009a), rice (Khunae *et al.,* 2007; Zavareze *et al.,* 2010) and maize (Lim *et al.,* 2001) starches have been shown to decrease on HMT. The decrease in relative crystallinity on HMT has been attributed to the disruption of hydrogen bonds between and among double helices (Chung *et al.,* 2009a). An increase in crystallinity has been reported for sweet potato and arrowroot starches subjected to HMT at 120°C (Jyothi *et al.,* 2010) and potato starch subjected to HMT at 130°C (Vermeylen *et al.,* 2006). Vermeylen *et al.* (2006) suggested that the breaking of covalent linkages by excessive heating decouples the double helices from the amylopectin backbone and renders them sufficiently mobile to become organized in more perfect/ larger crystallites. The crystallinity and intensity of some A-type tuber starches, such as new cocoyam have been shown, to remain unchanged on HMT (Lawal, 2005). The interaction of free lipids present in native starch granules with amylose chains has been shown to occur during HMT. This is reflected by the decrease in the apparent amylose content of wheat and potato starches on HMT (Hoover and Vasanthan, 1994a; Hoover and Manuel, 1996) and by the increase in intensity of the X-ray diffraction peak centered at 20° 2θ (represents crystalline V-amylose lipid complexes) with an increase in moisture content (due to an increase in mobility of V-amylose-lipid complex chains), which facilitates the formation of larger assemblies that are detectable by X-ray diffraction in rice starches (Zavareze *et al.,* 2010; Khunae *et al.*, 2007).

2.5.3 Impact of HMT on granular swelling and amylose leaching

Regardless of starch origin, HMT reduces granular swelling and amylose leaching of many starches (Chung *et al.,* 2009; Gunaratne *et al.,* 2010; Gunaratne and Hoover, 2002; Hoover *et al.,* 1994; Hoover and Manuel, 1996; Hoover and Vasanthan, 1994a; Hormdok, and Noomhorm, 2007; Olayinka *et al.,* 2008; Sair, 1967; Zavareze *et al.,* 2010). However, in some cereal starches, such as rye, barley, triticale, finger millet and wheat, amylose leaching has been shown to be increased on HMT, inspite of reduced granular swelling (Adebowale *et al.,* 2005a; Kulp and Lorenz, 1981; Kurakake *et al.*, 1996). Furthermore, an increase in amylose leaching has been reported for corn starches subjected to HMT at 120°C (Chung *et al.,* 2009b). The increase in amylose leaching on HMT at higher temperatures reflects leaching of both loosely-packed amylose chains and short chains resulting from the disrupted crystallites (occurs mainly at temperatures exceeding 120°) (Chung *et al.,* 2009b). The reduction in granular swelling and amylose leaching on HMT has been attributed to amylose-amylose (AM-AM), amylose-amylopectin (AM-AMP), amylopectin-amylopectin (AMP-AMP) interactions (these interactions reduce the number of free hydroxyl groups available for interaction with water), amylose-lipid interactions, crystalline stability, an increase in crystallinity, and polymorphic transformation (B→A+B) [the ingress of water during swelling would be more rapid and higher in the B-type polymorph, due to double helices being more compactly packed in the A-type polymorph] (Chung *et al.,* 2009a, 2009b; Gunaratne *et al.,* 2010; Gunaratne and Hoover, 2002; Hoover and Vasanthan, 1994b).

2.5.4 Impact of HMT on gelatinization parameters

Heat moisture treatment has been shown to increase the gelatinization transition temperatures (onset [To], mid-point [Tp] and conclusion [Tc]) and broaden the gelatinization temperature

range (To-Tc), whereas the enthalpy of gelatinization (ΔH) either decreases or remains unchanged on HMT (Chung *et al.,* 2009a, 2009b; Gunaratne and Hoover, 2002; Hoover and Vasanthan, 1994a; Kweon *et al.,* 2000; Vermeylen *et al.*, 2006). The increase in gelatinization temperatures has been attributed to interactions between amylose-amylose (AM-AM), amylose-amylopectin (AM-AMP) chains and amylose-lipid interactions (Gunaratne and Hoover, 2002; Hoover and Vasanthan, 1994a) and polymorphic transformation (B→A+B) and destabilization of crystallites (Gunaratne *et al.*, 2010; Gunaratne and Hoover, 2002). Hoover and Manuel (1996) and Kweon *et al.* (2000) have shown that the increase in To, Tp and Tc on HMT in normal and waxy maize starches is lower in the latter due to the absence of AM-AM and AM-AMP interactions. The reduction in enthalpy of gelatinization on HMT has been attributed to interaction between amylose-amylose (AM-AM) and/or amylose-amylopectin (AM-AMP) chains, decoupling of double helices and disruption of crystallites (Gunaratne *et al.*, 2010; Gunaratne and Hoover, 2002). Gunaratne and Hoover (2002) and Hoover and Vasanthan (1994a) postulated that an increase in the peak temperature is a reflection of melting of crystallites, which are formed because of AM-AM and AM-AMP interactions along the chains, which is stronger in heat-moisture treatments. This suppresses the swelling of the granule, leading to delayed gelatinization and high onset, peak and conclusion temperatures. Furthermore, HMT has been shown to increase the enthalpy associated with melting of the amylose-lipid complex in corn starch (see sec 2.7.2) (Lim *et al.,* 2001).

Several authors showed that the decrease in enthalpy on HMT is more pronounced in tuber starches than in cereal starches (Collado and Corke, 1999; Donavn *et al.,* 1993; Eerlington *et al.,* 1996; Gunaratne *et al.,* 2010; Hoover and Vasanthan, 1994a). This variation could be explained

by the influence of two factors, namely the packing arrangement of double helices and phosphate monoester content. In B-type starches (potato), the packing of double helices is less compact than in A-type starches (cereal). Furthermore, B-type unit cells contain more water molecules (thirty-six) than A-type unit cells (four) (Wu and Sarko, 1978b). Therefore, double helices of tuber starches would be more mobile and more prone to disruption than those in cereal starches (Gunaratne *et al.,* 2010; Hoover 2010). Tuber starches, such as potato, have been shown to have a higher phosphate monoester content than cereal starches (Hizukuri *et al.*, 1970). The presence of higher phosphate monoester content would hinder strong interaction between double helices (due to repulsion between negatively charged phosphate groups on adjacent amylopectin chains) during HMT in tuber starches (Gunaratne and Hoover, 2002). Hoover and Manuel (1996) have shown in studies on amylomaize (B-type) starches that the ΔH remains unchanged on HMT. This suggests that the disruptive effect of HMT on amylopectin is influenced more by the phosphate monoester content than by unit cell structure (Hoover, 2010).

2.5.5 Impact of HMT on pasting properties

Heat-moisture treatment of many starches, including potato (Kulp and Lorenz, 1981; Stute, 1992; Hoover and Vasanthan, 1994a; Purwani *et al.*, 2006; Gunaratne and Corke, 2007; Svegmark *et al.*, 2002), sweetpotato (Collado and Corke, 1999; Singh *et al.*, 2005), cassava (Lorenz and Kulp, 1981; Abraham, 1993), yam (Hoover and Vasanthan, 1994a; Moorthy, 1999; Lawal, 2005), cana (Watcharatewinkul *et al.* 2009; 2010), maize (Chung *et al.,* 2009b; Franco *et al.*, 1995; Hoover and Manuel, 1996; Loisel *et al.*, 2006), rice (Anderson and Guraya, 2006; Shih *et al.*, 2007; Zavareze *et al.,* 2010), sorghum (Olayinka *et al.*, 2008), oat (Hoover and Vasanthan, 1994a), lentil (Hoover and Vasanthan, 1994a), mucuna bean (Adebowale and Lawal, 2003),

pigeon pea (Hoover *et al.*, 1993), amaranth (Gunaratne and Corke, 2007) has been shown to increase pasting temperature and decrease paste viscosity and breakdown. However, peak viscosity of waxy maize and wheat starches remained unchanged or increased after HMT (Hoover and Manuel, 1996; Hoover and Vasanthan, 1994a). Hoover and Vasanthan (1994a) claimed that structural rearrangement contributed to these changes. Recently, Watcharatewinkul *et al.* (2010) have shown in studies on canna starches, that pasting properties of HMT (moisture 22% and 25%, 100°C, 16 h) starches are equivalent to those of canna starches crosslinked with sodium trimetaphosphate (0.2 and 0.5%).

2.5.6 Impact of HMT on enzyme hydrolysis

Several authors have shown that HMT parameters such as moisture content, temperature, duration of heating, botanical origin and starch composition influence the susceptibility of starches towards α-amylase (Hoover, 2010; Jacobs and Delcour, 1998). HMT (100°C, 30% moisture, 16 h) of pulse starches (field pea, wrinkled pea, pigeon pea, black bean, lentil) (Hoover and Manuel, 1996) and tuber and root starches (potato, taro, new cocoyam, cassava, yam) (Kawabata *et al.*, 1994; Hoover and Vasanthan, 1994a; Perera and Hoover, 1998; Gunaratne and Hoover, 2002) has been shown to increase susceptibility towards α-amylase. Lorenz and Kulp (1983) have shown that digestibility of potato starch increased with increasing moisture content prevailing during HMT (100°C, 16 h, 18 and 27% moisture content).

In cereal starches, the digestibility of normal and waxy maize starches by a mixture of PPA and amyloglucosidase was shown to decrease on HMT (100°C/16 h) at 18% moisture content (Franco *et al.*, 1995), whereas the digestibility of normal and waxy maize starches increased on

HMT (100°C/16 h) at 27% moisture content (Franco *et al.*, 1995). Hoover and Manuel (1996) showed that digestibility of normal, waxy, and Hylon V maize starches after 72 h of incubation with pancreatic porcine α-amylase (PPA) decreased on HMT (100°C/16 h/30% moisture). Kweon *et al.* (2000) reported that the digestibility of normal and Hylon V (57% amylose), HylonVII (70% amylose) and waxy maize starches by PPA decreased on HMT (110°C/16 h) at 15-21% moisture content. However, starch digestibility increased on HMT (110°C/16 h) at moisture contents in the range 24-27% in normal and Hylon V starches, and at 27% moisture in a waxy and Hylon VII starches. In this study (Kweon *et al.*, 2000), the lowest digestibility was observed after HMT at 18% moisture content. However, the extent of this increase was most pronounced after HMT at 27% moisture content. A similar trend has been reported by Zavareze *et al.* (2010) on HMT (110°C, 1h, 15, 20 and 25% moisture content) of high, medium and low amylose rice starches hydrolyzed by bacterial α-amylase. Anderson *et al.* (2002) studied the digestibility of HMT (20% moisture content) normal and waxy rice starches at their melting temperature and reported that the digestibility decreased by 25 and 10%, respectively, for HMT normal and waxy rice starches relative to untreated controls. However, the extent of hydrolysis of Hylon V and Hylon VII maize starches on HMT at 100°C by heat stable bacterial α-amylase from *Bacillus licheniformis* has been shown to decrease with increasing moisture levels (15 to 27%) (Kweon *et al.*, 2000). The reasons for the different kinetic profiles of amylolysis are likely to be ascribed to variations in the magnitude of interactions between AM-AM, AM-AMP, AMP-AMP and AM-lipid, polymorphic transformation (B→A+B), crystallite disruption, crystallite reorientation, and formation of fissures and cracks on the granule surface during HMT (Hoover, 2010).

2.5.7 Uses of HMT starches

HMT starch has important properties for the food industry. HMT has been shown to improve thermal stability and decrease the extent of set-back (Hoover, 2010). Therefore, HMT starches could be utilized in the canned and frozen food industries for their respective advantages (Zavareze *et al.,* 2010). The decrease in granular swelling and amylose leaching, and the increase in the thermal, acid and shear stability that occur on HMT, are all desirable properties for the production of noodles, retort foods (soups and sauces), dressings, baked foods, batter products, confections, dairy products, creams and fat minetics (Hormdok and Noomhorm, 2007; Kurahashi and Yoshino, 2000). Thus, HMT could be used as an alternative to chemical modification (Yoshino *et al.,* 1994).

HMT has been shown to manipulate the digestibility (rate and extent of PPA hydrolysis) of many starches (Hoover, 2010). For nutritional purposes, starch is classified into three general types based on rate of digestion: rapidly digestible starch (RDS), slowly digestible starch (SDS) and resistant starch (RS) (Englyst *et al.,* 1992). Starch that resists digestion is of nutritional importance because of its reduced glycemic and insulinemic responses, as well as its hypocholesterolemic and improved gut health effects (Lim *et al.,* 2005; Sajilata, *et al.,* 2006; Grabitske and Slavin, 2009; Singh *et al.,* 2010). HMT has been used to modify the amount of RDS, SDS and RS in various native starches (Brumovsky and Thompson, 2001; Mutungi, *et al.,* 2009; Sang and Seib, 2006; Shin *et al.*, 2005; Wongsagonsup *et al.,* 2009).

SDS is considered beneficial for dietary management of metabolic disorders, including diabetes and hyperlipidemia (Wolever and Mehling, 2002). A high proportion of SDS relative to RDS in

a starchy food indicates a food with a low glycemic index (GI). Consumption of foods containing SDS improves overall blood glucose control in patients suffering from diabetes mellitus (Brand *et al.*, 1991) and attenuates total serum cholesterol levels in hyperlipidemic patients (Jenkins *et al.*, 1987). Therefore, much attention is being given to SDS as a new functional ingredient (Wongsagonsup *et al.*, 2009; Shin *et al.*, 2004). Heat-moisture treatment has been shown to increase SDS in pulse (pea, lentil and navy bean) starches (Chung *et al.*, 2009c).

RS has been defined as the fraction of starch that escapes digestion in the small intestine of healthy individuals and arrives in the colon, where it is fermented to short chain fatty acids (Englyst and Cummings, 1985). The health benefits of RS have been reported as prevention of colon cancer, hypoglycemic effects, substrate for growth of probiotic microorganisms, reduction of gall stone formation, hypocholesterolemic effects, inhibition of fat accumulation and increased absorption of minerals (Sajilata *et al.*, 2006). This has stimulated research on RS fractions in food products. Several studies showed that HMT increases the RS content in high amylose starches (Brumovsky and Thompson, 2001; Jacobasch *et al.*, 2006; Sang and Seib, 2006). Brumovsky *et al.* (2009) have shown in studies on corn, potato, cassava and wheat starches, that HMT increased the boiling-stable RS content in starches of corn, potato and wheat in relation to the corresponding native starches, but not in cassava starch, which exhibited a decrease in the content of RS after HMT. Further, they reported that corn starch subjected to HMT for 60 minutes at 120°C produced the highest content of RS (4.2%, w/w), followed by potato starch (3.1%, w/w) with identical treatment.

CHAPTER 3

MATERIALS AND METHODS

3.1 Materials

Normal potato starch and crystalline porcine pancreatic α-amylase (PPA) (EC 3.2.1.1, type 1A) were purchased from Sigma Chemical Co. (St. Louis, MO, USA). Waxy potato starch (Eliane 100) was a gift from Louise Lynch (Chemroy Canada, Inc., Laval, QC, Canada). APTS (8-aminopyrene-1,3,6-trisulfonic acid, trisodium salt), sodium cyanoborohydride and Pro-Q Diamond phosphoprotein gel stain were purchased from Molecular Probes, Eugene, OR, USA. All chemicals and solvents were of ACS certified grade.

3.2 Methods

3.2.1 Chemical composition

3.2.1.1 Moisture content

The moisture contents of starch samples were quantitatively determined according to Method 44-15A of the AACC (2000).

3.2.1.2 Nitrogen content

The nitrogen content was determined by the Micro Kjeldahl method (AACC, 2000).

3.2.1.3 Phosphorous content

The phosphorus contents of potato starches were determined as phosphomolybdic Blue complexes according to the procedure described by Morrison (1964). Starch (5 mg, db) was placed in a hard glass test tube (15-20 mL capacity) accurately calibrated at the 5 mL level.

Sulphuric acid (0.3 mL, 98%) was added and the contents were gently heated over a small micro burner flame until charring was completed, and the climbing film of acid on the walls of the tubes was no longer viscous with partially charred organic matter. One drop of hydrogen peroxide (H_2O_2, 30%, w/v) was then added to contact the walls of the tubes just above the acid, and the tubes were shaken. (If the acid was not clear, the process was repeated using one drop of peroxide at a time). When clear, the tubes were gently boiled for 1min and then allowed to cool. The contents were diluted to approximately 4mL with deionized water to wash down the walls of the tubes. Sodium sulphite ($Na_2SO_3.7H_2O$, 33%, w/v) solution (0.1 mL) was then added and the tubes shaken to acidify the lower walls of the tube. Ammonium molybdate [$(NH_4)_6Mo_7O_{24}.4H_2O$, 2%, w/v] solution (1 mL) was added directly into the acid, (taking care not to touch the walls of the tube) followed by the addition of ascorbic acid (0.001 g). The tubes were then heated at 100°C for 10min and cooled. The volume of the solution was adjusted to 5 mL, the tube was stoppered and shaken, and the optical density at 822 nm was measured against water. The optical density of the blank was also determined at 822 nm. A standard curve (Appendix 4) of phosphorus (µg) versus optical density (822 nm) was prepared using a standard phosphorus solution (1.0068 g $NaH_2PO_4.2H_2O$/L contains 200 µg/mL) and used to calculate the phosphorus content of the samples.

3.2.1.4 Ash content

The ash contents of starch samples were determined by Method 08-17 of the AACC (2000).

3.2.1.5 Lipid Content

3.2.1.5.1 Surface Lipid

The surface lipid contents of the starch samples were determined according to the procedure described by Vasanthan and Hoover (1992b). The lipids were extracted at ambient temperature (25-27°C) by mixing a starch sample (5 g, db) with 100 mL of chloroform/methanol (2:1, v/v). The contents were mixed thoroughly for 1 h and the solution was filtered carefully using Whatman No. 4 filter paper into a 250 mL round bottom flask. The residue was thoroughly washed out with chloroform/methanol solution. The lipid solvent mixture was evaporated to dryness using a rotary evaporator (Rotovapor-R110, Büchi Laboratorimus-Technik AG, Flawill/Schweiz, Switzerland). The crude lipid extracts were purified by the method of Bligh and Dyer (1959) before quantification.

3.2.1.5.2 Bound Lipid

Bound lipids in the starch samples also were determined according to the method of Vasanthan and Hoover (1992b). The residues from the chloroform/methanol extractions were refluxed with *n*-propanol:water (3:1, v/v) in a Soxhlet apparatus at 85°C for 7 h. The solvent was evaporated to dryness using a rotary evaporator and the crude lipid residue was purified by the method of Bligh and Dyer (1959) before quantification.

Crude lipid purification (Bligh and Dyer,1959; Vasanthan and Hoover, 1992b):

The crude lipid extracts were purified by extraction in a separatory funnel with chloroform: methanol:water [1:2:0.8(v/v/v)]. The round bottom flask containing the crude lipid extract was washed with chloroform:methanol:water mixture and the washings were transferred to separatory funnel and chloroform and water were added further to form a biphasic layer. The heavy

chloroform layer at the bottom of separatory funnel, which contained the purified lipid, was withdrawn into a pre-weighted round bottom flask and evaporated to dryness in a rotary evaporator. The round bottom flask with purified lipid was then removed and the contents dried at 60°C for 1 h in forced-air oven. The dried lipid was cooled to room temperature in a desiccator and weighed.

$$Lipid\ (\%) = \frac{W_2 - W_1}{W_0} \times 100$$

Where,

W_0- sample weight (g, db)

W_1- weight of tare round bottom flask (g)

W_2- weight of round bottom flask and lipid after drying (g)

3.2.1.6 Amylose content

The amylose contents of normal and waxy potato starches were determined by the colorimetric method of Hoover and Ratnayake (2004).

3.2.1.6.1 Apparent amylose content

Starch (20 mg, db) was weighed into a round bottom, screw cap tube and solubilized by adding dimethylsulfoxide (90% DMSO, 8 mL). The contents were vortexed vigorously and heated for 15 min in a water bath at 85°C with intermittent mixing. The tubes were then allowed to cool at

room temperature and diluted to 25mL in volumetric flask. One millilitre of the diluted solution was mixed with water (40 mL) and I_2/KI solution (5 mL, [0.0025M I_2 and 0.0065M KI mixture]) and vortexed. The final volume was adjusted to 50 mL in a volumetric flask and the contents were allowed to stand in the dark for 15 min at room temperature. The absorbance measurements were taken at 600 nm using a UV-visible spectrophotometer and the amylose contents of the samples were calculated from the standard curve obtained with pure amylose and amylopectin mixtures, over the range of 0% to 100%.

3.2.1.6.2 Total amylose content

Defatted starch was prepared by Soxhlet extraction with 75% aqueous *n*-propanol at 85°C for 7 h and the amylose content of the defatted starch was determined by the procedure described above.

3.3 Heat-moisture treatment (HMT)

Starch samples were equilibrated at room temperature to a water activity of 0.97 in a desiccator over saturated K_2SO_4 solution for up to one month. Following equilibration, the moisture contents (~27%) of the samples were determined by AACC (2000). The starch samples were then heated at 80, 100, 120 and 130°C for 16 h in a forced-air oven. The HMT starches were subsequently air dried to a uniform moisture content (~10%). In the text of this thesis, normal and waxy potato starches in their native state are referred to as NP and WP, respectively, whereas NP80, NP100, NP120 NP130, WP, WP80, WP100, WP120 and WP130 represent NP and WP starches after HMT at 80, 100, 120 and 130°C.

3.4. Polarized light microscopy

Native and HMT starch suspensions (water-glycerol, 50:50, v/v) were observed under bright field light and crossed polarized light (magnification 400×) using a binocular microscope (Nikon Microscope, Eclipse 80i) equipped with real time viewing (Q-capture Pro™). A QImaging digital camera (QICAM fast 1394, Canada) was used for image capture.

3.5. Scanning electron microscopy (SEM)

The granule morphologies of native and HMT normal and waxy potato starches were analyzed before and after amylolysis (24 h) using a Hitachi S570 scanning electron microscope (Nissei Sangyo Inc., Rexdale, ON, Canada) at an accelerating potential of 15kV. Dry starch samples were brushed onto the surface of double-sided carbon adhesive tape mounted on an aluminium stub and then coated with a thin film (20 nm) of gold in an argon atmosphere.

3.6. Confocal laser scanning microscopy (CLSM)

The molecular distribution of amylose and amylopectin, morphological changes during HMT and the degradation pathway of PPA into the granule interior were visualized by staining with APTS (Molecular Probes, Eugene, OR, USA) according to the method described by Blennow *et al.* (2003). Phosphorus was stained with Pro-Q Diamond stain (Molecular Probes) based on the method of Glaring *et al.* (2006). Starch samples (10-15 mg) were stained in 10 μL of freshly made APTS solution (20 mM APTS in 15% acetic acid) and 10 μL of 1M sodium cyanoborohydride at 30 °C for 15 h. The APTS-stained starch granules were washed five times with deionized water and then dispersed in 0.5 mL of Pro-Q Diamond solution at room

temperature for 1 h. After thoroughly washing five times with deionized water, the stained starch granules were suspended in 0.5 mL of 50% glycerol for CLSM observation.

Stained starch granules in 50% glycerol (10 μL) were dropped into a glass bottom culture dish (MatTek Corporation, Ashland, MA, USA), mixed with 0.1 mL of deionized water, covered with a glass slip, and then visualized with a confocal laser scanning microscope (Zeiss LSM 710, Carl Zeiss MicroImaging GmbH, Jena, Germany) equipped with a 40x/1.3 oil objective lens. The excitation wavelength achieved with a diode laser was 488 nm for APTS and 561 nm for Pro-Q Diamond with an emission light interval of 490-560 nm. Laser power capacity and master gain were adjusted to maximum saturation. Images of optical sections of starch granules were recorded with ZEN 2009 software (Carl Zeiss MicroImaging GmbH). For each starch sample, a population of granules was examined with 15-20 images, with approximately 10-15 granules in each image.

3.7. Iodine binding

The ability of iodine to complex starch chains before and after HMT was determined by equilibrating starch samples at 100% RH for 2 h. To determine iodine binding, a thin layer of the equilibrated starch sample (0.1 g) was spread on a plastic dish and exposed for 24 h at room temperature to iodine vapour generated from 2 g of iodine crystals placed in the desiccator containing the starch samples. The desiccator was covered with aluminum foil to avoid light exposure. The reflectance spectra of iodine stained starches were determined using the Kubelka and Munk (1931) equation:

$$\frac{K}{S} = \frac{(1-R)^2}{2R}$$

where K is an absorption coefficient, S is a scattering coefficient representing the fraction of light that is scattered when the incident light strikes a sufficiently thick layer of starch granules, and R is the reflectance expressed as fraction between 0 and 1. The K/S value of the starches (represents the absorption corrected to the light scattering) was measured over the wavelength range of 360 to 740 nm (CM 3500-d spectrophotometer, Konica Minolta, Mahwah, NJ, USA) at 10 nm intervals.

3.8. Fluorophore-assisted capillary electrophoresis (FACE)

The AMP chain length distributions of native and HMT starches were analysed by FACE as described by Morell *et al.* (1998). Starches were debranched (at 37°C for 2 h) with isoamylase (10U) and labelled with APTS (Fig 3.1) (O'Shea *et al.*, 1998). FACE was conducted using the Beckman Coulter Proteome Lab PA800 equipped with 488 nm laser module. The N-CHO (PVA) capillary with a preburned window (50 μm ID and 50.2 cm total length) was used for separation of debranched samples. Maltose was used as an internal standard. Separation was conducted at 10°C for 30 min. Data was recorded and analysed using 32-Karat software. The degree of polymerization, (DP) was assigned to peaks based on the migration time of maltose.

Figure 3.1 Labelling reaction of glucose with 8-aminopyrene-1,3,6-trisulphonic acid (APTS) (adapted from O'Shea *et al.*, 1998).

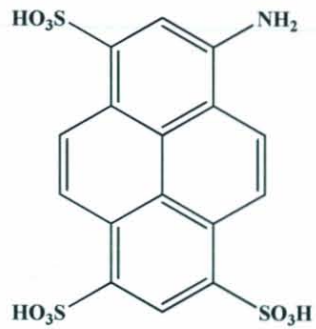

8-aminopyrene-1,3,6-trisulphonic acid
[APTS]

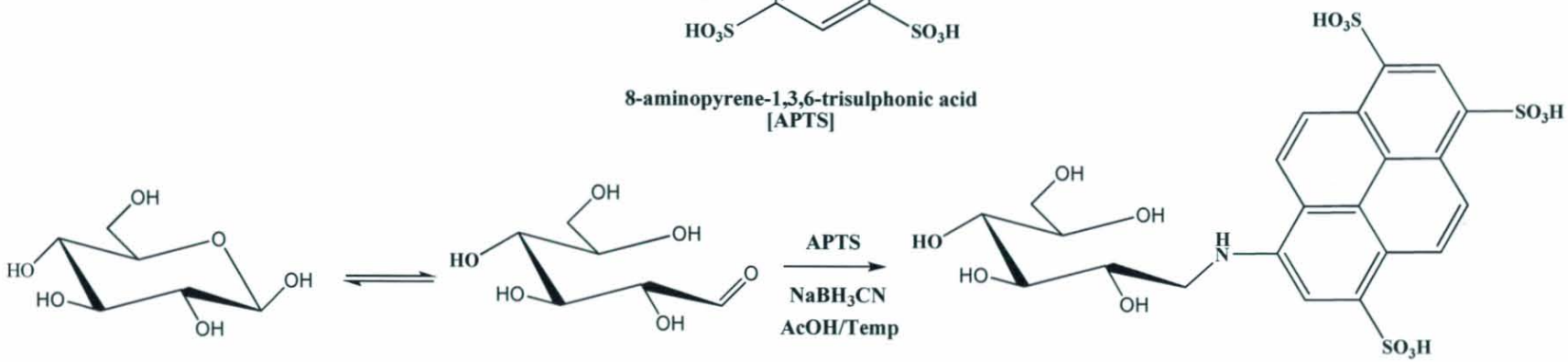

Labelled glucose

3.9. Attenuated total reflectance Fourier transform infrared spectroscopy (ATR-FTIR)

The ATR-FTIR spectra of native and HMT starches were recorded on a Digilab FTS 7000 spectrophotometer (Digilab USA, Randolph, MA, USA) equipped with a thermoelectrically cooled deuterated triglycine sulphate (DIGS) detector using an attenuated total reflectance (ATR) accessory at a resolution of 4 cm^{-1} and 128 scans. Spectra were base-line-corrected and then deconvoluted by drawing a straight line between 1200 and 800 cm^{-1} (using Win-IR Pro software). A half-band width of 15 cm^{-1} and a resolution enhancement factor of 1.5 with Bessel apodization were employed. Intensity measurements were performed on the deconvoluted spectra by recording the peak height of the absorbance bands from the base-line.

3.10. Wide angle X-ray diffraction (WAXS)

Native and HMT normal and waxy potato starches were kept in a desiccator over saturated K_2SO_4 solutions (a_w-0.97) at room temperature for 14 days prior to X-ray diffraction measurements. The hydrated native and HMT starches were then packed tightly into a round aluminum holder. X-ray diffractograms were obtained with a Rigaku Ultima IV X-ray diffractometer with operating conditions of target voltage, 40 kV, current, 44 mA, scanning range, 3–35°, scan speed, 1.00°/min, step time, 0.95, divergence slit width, 0.5°, scatter slit width, 0.5°, sampling width, 0.03° and receiving slit width, 0.3 mm. IGOR pro 6.1 software (WaveMetrics Inc. Oregon, USA) was used to calculate the relative crystallinity (RC), half height peak width, also called full width at half maximum height (FWHM) using the curve fitting procedure (Appendix 1) described by Lopez-Rubio *et al.* (2008a). A Gaussian function was used for curve fitting. Peak height and FWHM were calculated after subtracting the amorphous

background. A- and B-type polymorphic composition of the starches was calculated as described by Ratnayake *et al.* (2001).

3.11. Amylose leaching (AML)

Starch samples (20 mg, db) in deionized water (10 mL) were heated at 60–95°C in volume-calibrated sealed tubes for 30 min (tubes were shaken by hand every 5 min to suspend the starch slurry). The tubes were then cooled to room temperature and centrifuged at 2000 × *g* for 10min. The supernatant liquid (1 mL) was withdrawn and the amylose content determined as described by Hoover and Ratnayake (2004). AML was expressed as the percentage of amylose leached per 100 g of dry starch. Three replicate samples were used in the determination.

3.12. Swelling factor (SF)

The SF of the native and HMT starches when heated to 60-95°C in excess water (5 mL) was determined according to the method of Tester and Morrison (1990). Starch samples (50 mg, db) were weighed into screw cap tubes, 5 mL deionized water was added, and the tubes were heated in a shaking water bath at the appropriate temperature for 30 min. The tubes were then cooled rapidly to 20°C in an ice water bath and 0.5 mL of Blue Dextran (Pharmacia MW 2×10^6, 5 mg/mL) was added and the contents mixed by inverting the closed tubes several times. The tubes were centrifuged at 1500 × *g* for 10min and the absorbance of the supernatant was measured at 620 nm. The absorbance of the reference tube that contained no starch was also measured. Three replicate samples were used in the determination. The swelling factor was reported as the ratio of the volume of the swollen starch granules to the volume of the dry starch.

Calculation of swelling factor (SF) was based on starch weight corrected to moisture content, assuming a density of 1.4 g/mL. Free or interstitial-plus-supernatant water (FW) is given by:

$$FW\ (mL) = 5.5(A_R/\ A_S) - 0.5 \quad (1)$$

The initial volume of the starch (V_O) of weight W (mg) is

$$V_0\ (mL) = W/1400 \quad (2)$$

The volume of absorbed intragranular water (V_1) is thus

$$V_1 = 5.0 - FW \quad (3)$$

Hence, the volume of the swollen starch granules (V_2) is

$$V_2 = V_0 + V_1 \quad (4)$$

$$SF = V2/V0 \quad (5)$$

This can be expressed by the single equation

$$SF = 1 + \{(7700/w) \times [(A_s - A_r)/A_s]\}$$

3.13 Differential scanning calorimetry (DSC)

Gelatinization parameters of native and HMT starches were measured using a Mettler Toledo differential scanning calorimeter (DSC1/700/630/GC200) equipped with a thermal analysis data station and data recording software (STAR@ SW 9.20). Deionized water (11 µl) was added with a micro syringe to starch (3.0 mg, db) in the DSC pans, which were then sealed, reweighed and allowed to stand overnight at room temperature before DSC analysis. The scanning temperature

range and the heating rates were 30-110°C and 10°C/min, respectively. In all measurements, the thermogram was recorded with an empty aluminum pan as a reference. During the scans, the space surrounding the sample chamber was flushed with dry nitrogen to avoid condensation. The transition temperatures reported are the onset (To), peak (Tp) and conclusion (Tc) temperatures. The enthalpy of gelatinization (ΔH) was estimated by integrating the area between the thermogram and a base line under the peak and was expressed in terms of J/g of dry starch. Three replicates per sample were analyzed.

3.14 Rapid Visco™ Analyser (RVA)

A Rapid Visco™ Analyzer RVA-4 (Newport Scientific Pty. Ltd., Warriewood, NSW, Australia) was employed to measure the pasting properties of native and HMT starches (5% db, 25 g total weight). The samples were equilibrated at 50°C for 1 min, heated at 6°C/min to 95°C, held at 95°C for 5 min, cooled at 6°C/min to 50°C, and held at 50°C for 2 min. The speed was 960 rpm for the first 10s, then 160 rpm for the remainder of the experiment.

3.15 Enzymatic hydrolysis

Enzymatic digestibility studies on native and HMT starches were conducted using a crystalline suspension of porcine pancreatic α-amylase (PPA) in 2.9M sodium chloride containing 3mM calcium chloride, in which the concentration of α-amylase was 26 mg protein/mL and the specific activity was 1128 units/mg protein. One unit was defined as the α-amylase activity which liberates 1 mg maltose in 3min at 20°C at pH 6.9. The procedure was essentially that of Knutson *et al.* (1982) with a slight modification. Starch (20 mg) was added with 5mL deionized water and 4mL of 0.1M phosphate buffer (pH 6.9) containing 0.006M NaCl. The slurry was pre-

warmed for 30 min at 37°C and gently stirred before adding PPA suspension (12 units/mg starch). The samples were analysed after 3, 6, 12, 24, 48, and 72 h of incubation at 37°C in a constant temperature water bath (New Brunswick Scientific, G76D, Edison, NJ, USA). The reaction mixtures were vortexed on a daily basis to resuspend the deposited granules. Samples were taken at specific time intervals and the digestion reaction was terminated by adding 2mL of 95% ethanol. The hydrolysate was recovered for microscopic study by centrifugation (2000 × *g*, 5min) of the mixture and aliquots of the supernatant were analysed for soluble carbohydrate (Bruner, 1964). Controls without PPA but subjected to above experimental conditions were run concurrently. The degree of hydrolysis was defined as the reducing sugars generated in the supernatant, expressed as mg maltose equivalents released per 100mg dry starch. The hydrolysate was washed three times by suspending it in 10mL deionized water and recovered by centrifugation (2000 × *g*, 5min). The hydrolysates were then dried at 25°C for 2 days. The sugar content of the supernatant was determined as follows.

Determination of reducing value by 3, 5-dinitrosalicylic acid (DNS):

3,5-DNS (2 mL) was taken into a glass tube and placed in an ice-water bath to chill for 5 min. An aliquot of the sample (1 mL) was pipetted into 2 mL of the chilled 3,5-DNS and the reaction mixture was then diluted to 4mL with deionized water. The contents were mixed by rapid swirling and returned to the ice-water bath until thoroughly chilled and then the contents were heated in a boiling water bath for exactly 5 min for colour development. After that, the contents were returned to the ice-water bath prior to colour measurement. After chilling, the final volume was adjusted to 8mL with deionized water at room temperature. The contents were mixed by rapid swirling before taking the absorbance measurement at 540 nm. If the sample relative

absorbance exceeded 1.5 at 540 nm, the spectrophotometer was reset to 590 nm without delay and the relative absorbance was measured at that wavelength. The apparent sugar content of the sample was determined by calculation from the appropriate regression equation of the standard curves.

$$Enzyme\ Hydrolysis\ (\%) = \frac{Reducing\ sugar\ (as\ maltose) \times 0.95 \times 100}{Initial\ starch\ weight\ (g,db)}$$

3.16 Statistical analysis

Analytical determinations for the samples were done in triplicate and standard deviations were reported. A comparison of the means was ascertained by Tukey's test, to a 5% level of significance using analysis of the variance (ANOVA).

CHAPTER 4

RESULTS AND DISCUSSION

4.1 Composition

Data on the chemical composition of the potato starches are presented in Table 4.1. The purity of the starches was judged on the basis of low nitrogen (0.13% [normal potato], 0.14% [waxy potato]) and low ash (0.22% [normal potato], 0.21% [waxy potato]) levels. There was no significant difference between the starches with respect to their total phosphorus (0.07-0.08%), free lipid (0.02%) and bound lipid (0.05-0.08%) contents (Table 1). However, the starches differed significantly with respect to apparent amylose (32.3% [normal potato], 3.4% [waxy potato]) and total amylose content (33.5% [normal potato], 3.4% [waxy potato]). The total phosphorus content, which is mainly in the form of phosphate monoesters (McPherson and Jane, 1999) was in agreement with those reported in the literature (Gunaratne and Hoover, 2002; McPherson and Jane, 1999).

4.2 Morphology

Morphological characteristics such as phosphate and amylose distribution, growth rings, surface characteristics and birefringence patterns of native and HMT starches were determined by microscopy.

4.2.1 Scanning electron microscopy (SEM)

Scanning electron micrographs of native NP and WP starches are presented in Fig 4.1. The granule surface of normal potato starch appeared to be smooth with no evidence of pores, indentations or fissures. However, in WP starch, pores were present (mainly in the peripheral regions) of some granules, whereas others were devoid of pores (Fig 4.1 [WP]).

Table 4.1 Chemical composition (%) of normal and waxy potato starches [a]

Characteristics	Composition (%)	
	Normal potato	Waxy potato
Moisture	17.01 ± 0.04^{p}	15.20 ± 0.04^{q}
Ash	0.22 ± 0.01^{p}	0.21 ± 0.01^{p}
Nitrogen	0.13 ± 0.01^{p}	0.14 ± 0.03^{p}
Phosphorus	0.08 ± 0.01^{p}	0.07 ± 0.01^{p}
Amylose content		
Apparent[b]	32.3 ± 0.2^{p}	3.4 ± 0.5^{q}
Total[c]	33.5 ± 0.3^{p}	3.4 ± 0.3^{q}
Lipid content		
CM[d]	0.02 ± 0.01^{p}	0.02 ± 0.01^{p}
PW[e]	0.08 ± 0.03^{p}	0.05 ± 0.02^{p}

[a]All data reported on a dry basis and represent the means of three determinations. Means of normal and waxy starches with different superscripts within the same row are significantly different ($p < 0.05$)

[b]Determined by iodine binding without removal of free and bound lipids

[c]Determined by iodine binding after removal of free and bound lipids

[d]Lipid extracted from the starch by chloroform-methanol (CM) 2:1(v/v) at 25°C (mainly free lipids)

[e]Lipid extracted by hot 1-propanol-water (PW) 3:1(v/v) from the residue left over CM extraction (mainly bound lipids)

Fig. 4.1 Scanning electron micrographs of native normal (NP) and native waxy (WP) potato starches.

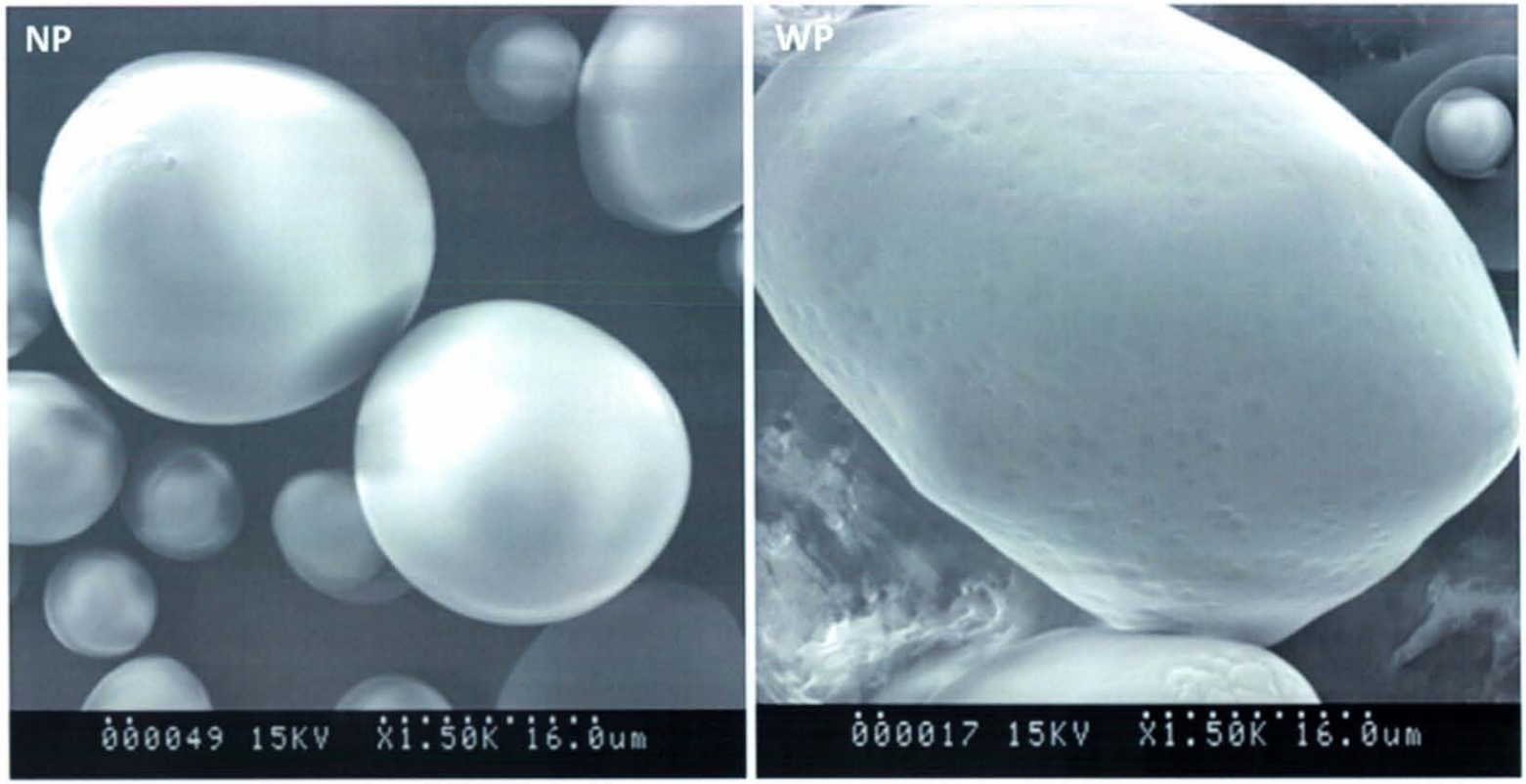
NP
000049 15KV X1.50K 16.0um
WP
000017 15KV X1.50K 16.0um

4.2.2 Confocal laser scanning microscopy (CLSM)

4.2.2.1 Phosphate distribution

Pro-Q Diamond dye is a metallo-organic fluorophore that recognizes accessible phosphate groups in native starch granules. The distribution of Pro-Q fluorescence reflects phosphate distribution pattern in the granule (Glaring *et al.,* 2006). Pro-Q staining of native NP and WP granules followed by visualization using CLSM revealed that both NP and WP starches were stained brightly near the peripheral regions (Fig 4.2). Smaller granules were stained more brightly (indicating a higher concentration of accessible phosphate groups) than larger granules (Fig 4.2 [NP, WP]). No staining occurred in the granule interior of either starch (Fig 4.2).

Glaring *et al.* (2006) have shown by Pro-Q staining of cereal and tuber starch granules (representing a wide range in starch bound phosphate content) that fluorescence intensity is positively correlated to phosphate content. The absence of phosphate in the granule interior was surprising (Fig 4.2 [NP, WP]), since Jane and Shen (1993) have shown by surface gelatinization studies that phosphate monoesters are more concentrated at the core (hilum) than in the periphery of normal potato starch granules. Therefore, hypothesized that either the Pro-Q dye is too large (molar mass and structure of this dye is not known) to diffuse into the granule and/or the phosphate groups are buried within the amylopectin clusters and hence not available for interacting with the dye. In order, to test this hypothesis, NP and WP starches were hydrolysed with PPA (72 h). The residues left after hydrolysis were then stained with Pro-Q Diamond dye. As shown in Fig 4.2 (NP72, WP72), the region near the hilum was stained brightly indicating that PPA hydrolysis may have opened a pathway for the Pro-Q Diamond dye into the amorphous and crystalline regions within the granule interior.

Fig 4.2 Confocal laser scanning microscopy of Pro-Q Diamond stained granules of native normal potato (NP), native waxy potato (WP), PPA hydrolysed (72 h) normal potato (NP72) and PPA hydrolysed (72 h) waxy potato (WP72) starches.

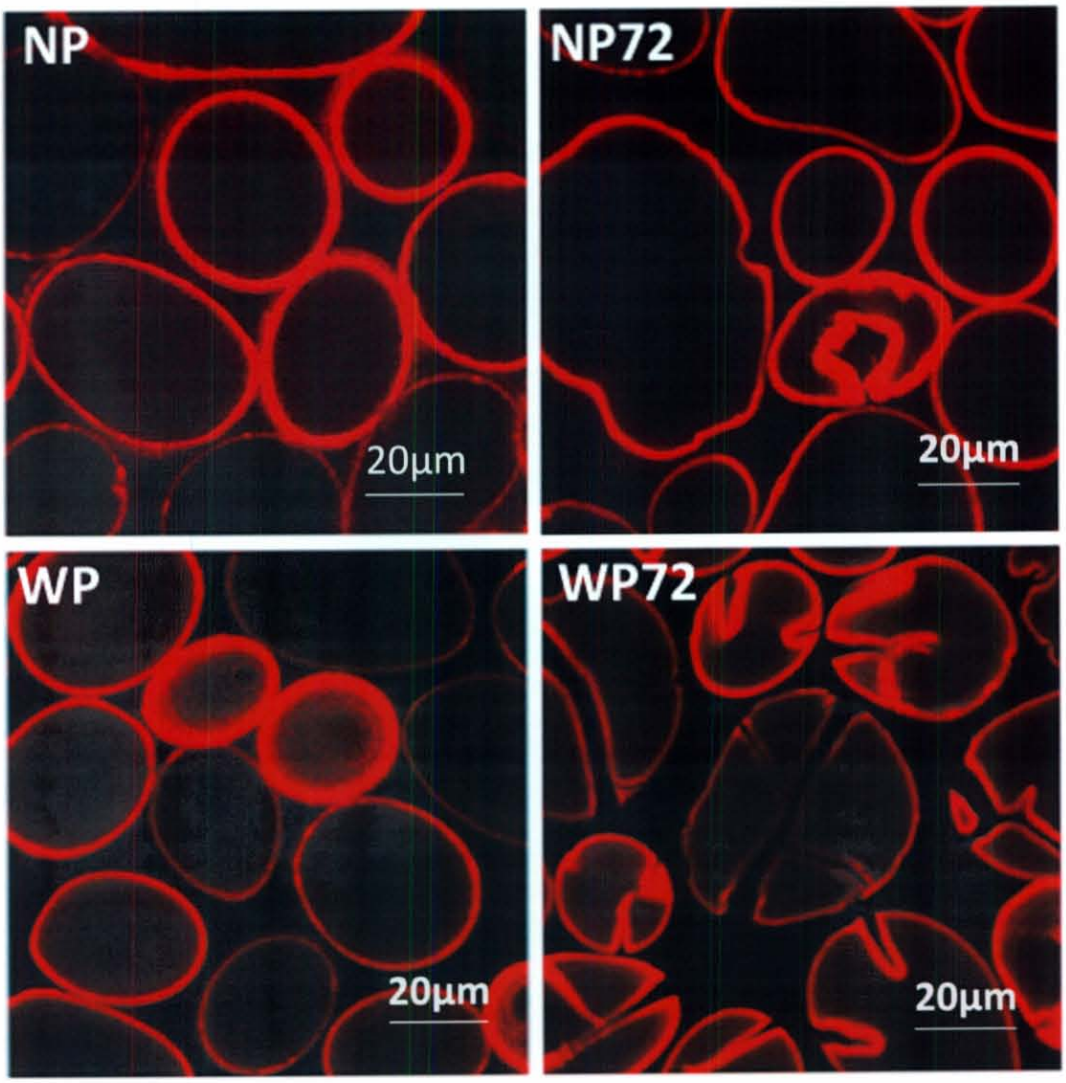
NP
20μm
NP72
20μm
WP
20μm
WP72
20μm

4.2.2.2 Growth rings and amylose distribution

The growth rings and amylose distribution in native and HMT starches stained with APTS was visualized by CLSM. Glaring *et al.* (2006) have shown that APTS reacts specifically with the reducing ends of starch molecules leading to a 1:1 stoichiometric ratio of starch molecular labelling. Because of its smaller size, amylose (AM) contains a much higher molar ratio of reducing ends per glucose residue than amylopectin (AMP). This results in a higher by-weight labelling of AM enabling the distinction of the two molecules by CLSM.

The CLSM images (Fig 4.3) revealed that both the growth rings and the hilum appeared much sharper and exhibited higher fluorescence in NP than in WP starches. This could be attributed to the higher AM concentration in NP starch. The area near the hilum was disrupted on HMT, resulting in the formation of voids at HMT temperatures of 100°C (Fig 4.3 [NP100, WP100]) and 130°C (Fig 4.3 [NP130, WP130]). Voids were more evident (WP>NP) at 130°C (Fig 4.3 [NP130, WP130]). Buléon *et al.* (1998) have suggested that surrounding the hilum is a core which is semicrystalline with a lower degree of organization relative to the more crystalline layers at the periphery. The concentration of AM has been shown to increase from the hilum to the periphery (Buléon *et al.,* 1998).

We speculate that the thermal energy imparted during HMT may have disorganized the double helical organization of starch chains present in the core surrounding the hilum region, leading to the formation of voids near the hilum (Fig 4.3). This is reflected in the extent of disorganization in both NP and WP starches being greater at 130°C (Fig 4.3 [NP130, WP130]) than at 100°C (Fig 4.3 [NP100, WP100]).

Fig 4.3 Confocal laser scanning microscopy of APTS stained granules of native normal potato (NP), NP heat-moisture treated at 100°C (NP100), NP heat-moisture treated at 130°C (NP130), native waxy potato (WP), WP heat-moisture treated at 100°C (WP100) and WP heat-moisture treated at 130°C (WP130).

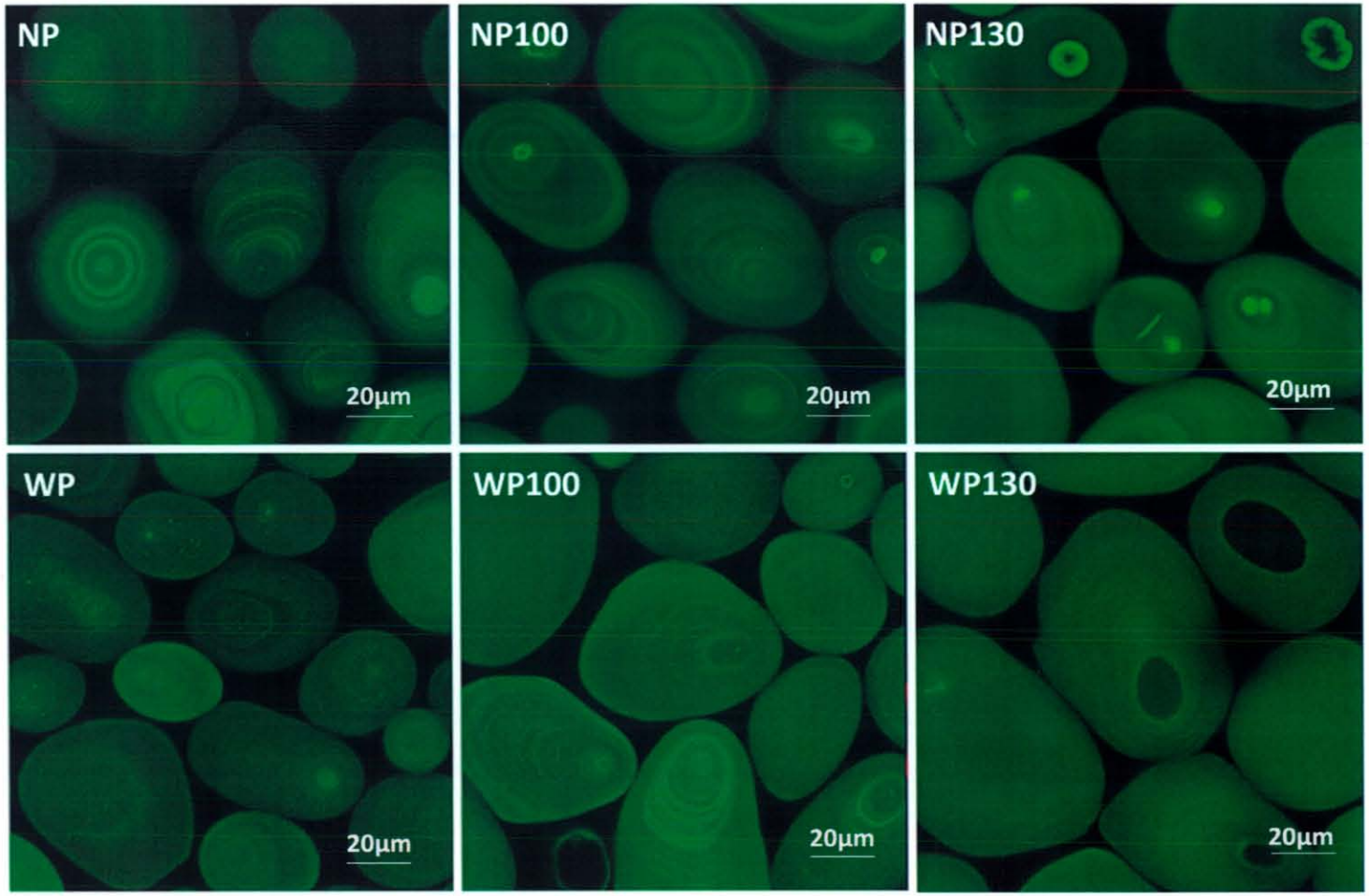
NP
20μm
NP100
20μm
NP130
20μm
WP
20μm
WP100
20μm
WP130
20μm

4.2.3 Polarized and bright field microscopy

The birefringence patterns of NP and WP starches before and after HMT are shown in Fig 4.4. Birefringence indicates that the average orientation of helical structures is radial. The intensity of birefringence is influenced by granule shape and by the orientation of the granule with respect to the light beam (Buléon *et al.,* 1998). Both NP and WP starches (Fig 4.4) exhibited strong birefringence intensity.

However, the birefringence intensity of both starches decreased with an increase in HMT temperature; the effect was most pronounced in NP130 and WP130 starches (Fig 4.4). The decrease in birefringence intensity was reflected by the formation of voids (depicted by arrows) at the granule centers. This suggests that the increase in starch chain mobility accompanying an increase in HMT temperature disrupted the radial orientation of AMP double helices that were loosely organized around the hilum. Similar observations have been reported for pulse (Chung *et al.,* 2010) and normal potato (Vermeylen *et al.,* 2006) starches. When viewed under bright field microscopy, both HMT NP and WP starches displayed dark areas (voids) near the hilum region in both large and small granules. The size of these voids (representing the extent of disorganization of AMP double helices near the vicinity of the hilum) increased with HMT temperature (Fig 4.4). Furthermore, at 130°C, voids in WP starch were larger and more numerous than in NP130 starch.

Fig 4.4 Polarized light microscopy of native and HMT normal potato (NP) and waxy potato (WP) starches. For NP and WP starches, the same field is shown for bright field (left frame) and between cross polarized light (right frame). The arrows depict the regions in the granules that were disorganized during HMT.

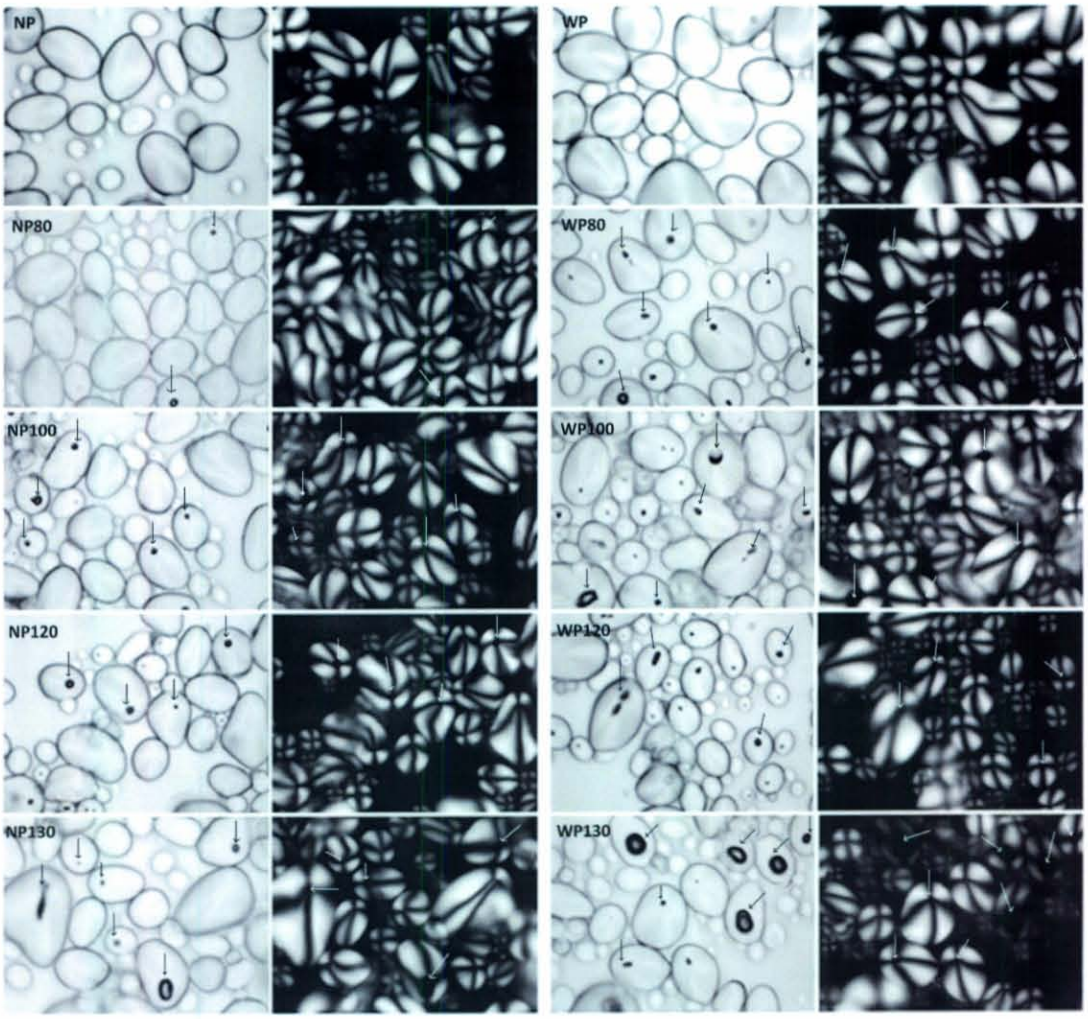
NP
WP
NP80
WP80
NP100
WP100
NP120
WP120
NP130
WP130

4.3 Amylopectin chain length distribution

The amylopectin chain length distributions (determined by fluorophore assisted capillary electrophoresis) of both native and HMT starches remained unchanged at all HMT temperatures (Table 4.2). This suggests that covalent linkages of AMP were not broken under the HMT conditions (27% moisture, 16 h, 80-130°C) used in this study. However, Vermeylen *et al.,* (2006) reported degradation of amylopectin crystallites (indicated by an increase in the proportion of chains with DP<6) during HMT of NP starch at 23% moisture for 24 h at 130°C. This discrepancy may have been due to the longer period of HMT used in their study.

4.4 X-ray diffraction

NP (Fig 4.5a) and WP (Fig 4.5b) starches exhibited the typical B-type X-ray pattern with reflection intensities centred at 5.5°, 17.1° and 22-24° 2θ. The peak height (PH) and the peak width at half height, also called full width at half maximum height (FWHM) [Table 4.3] of the 5.5° 2θ peak (typical of B-type crystallites; Hizukuri *et al.,* 1983) for NP and WP starches were 178.6 and 0.9 and 106.6 and 1.0, respectively. PH and FWHM have been shown to represent the amount of ordered crystallites and crystallite size and/or crystallite perfection, respectively (Suryanarayana and Norton, 1998). This suggests a higher content of ordered B-type crystallites in NP starch, which are larger in size than those of WP starch. In WP starch, the doublet centred at 22-24° 2θ was less well resolved (Fig 4.5b) than in NP starch (Fig 4.5a). This is indicative of the presence of both A- and B-type unit cells in WP starch. Both NP and WP starches exhibited a peak centred at 20° 2θ, which reflects single left handed linear starch chains arranged in a V-type crystalline array (Lopez-Rubio *et al.,* 2008a; Saibene *et al.,* 2008). The PH and FWHM of the 20° 2θ peak for NP and WP starches were 51 and 0.6 and 47.7 and 0.9, respectively.

Table 4.2 Amylopectin chain length distribution of native and HMT normal and waxy potato starches as determined by fluorophore-assisted capillary electrophoresis (FACE)

Starch source	Treatment	Distribution percentage			
		DP 6-8	DP 9-13	DP 14-35	DP 36-49
Normal potato	Native	7.95 ± 0.27^{p}	29.37 ± 1.39^{p}	59.50 ± 1.59^{p}	3.18 ± 0.47^{p}
	NP80	6.84 ± 0.54^{p}	27.27 ± 1.09^{p}	61.49 ± 0.33^{p}	4.40 ± 0.22^{p}
	NP100	7.11 ± 1.11^{p}	26.01 ± 2.97^{p}	61.56 ± 1.39^{p}	5.32 ± 2.70^{p}
	NP120	8.38 ± 0.02^{p}	28.04 ± 0.06^{p}	58.88 ± 0.36^{p}	4.70 ± 0.45^{p}
	NP130	8.63 ± 0.24^{p}	27.64 ± 0.82^{p}	58.76 ± 0.76^{p}	4.97 ± 0.29^{p}
Waxy potato	Native	6.43 ± 0.95^{p}	26.83 ± 1.01^{p}	60.37 ± 0.72^{p}	6.09 ± 0.45^{p}
	WP80	7.51 ± 0.42^{p}	29.00 ± 0.60^{p}	58.96 ± 0.10^{p}	4.53 ± 1.13^{p}
	WP100	7.14 ± 0.65^{p}	27.37 ± 1.94^{p}	60.00 ± 1.04^{p}	5.49 ± 1.56^{p}
	WP120	6.76 ± 0.72^{p}	29.78 ± 3.23^{p}	58.35 ± 3.94^{p}	5.11 ± 0.01^{p}
	WP130	6.43 ± 0.95^{p}	25.87 ± 0.43^{p}	61.97 ± 1.04^{p}	5.73 ± 0.34^{p}

Means within the same column with different superscripts for native and its HMT counterparts are significantly different ($p<0.05$)

This suggests a higher content of ordered V-type crystallites in NP starch, which are larger in size than those of WP starch. It is highly unlikely that the V-type crystallites are indicative of starch-lipid complexes, since both starches contained only trace quantities of bound lipids (<0.08%). HMT, at all temperatures, changed the X-ray pattern (B→A+B) and decreased the relative crystallinity (RC) and B-polymorphic content (Fig 4.5). The extent of these changes increased progressively with an increase in HMT temperature. The change in X-ray pattern has been attributed to dehydration of the 36 water molecules in the central channel of the B-type unit cell and to the movement of a pair of double helices into the central channel that was originally occupied by the water molecules (Gunaratne and Hoover, 2002). This would explain the increase in A-type unit cells with an increase in HMT temperatures. The increase in A-type unit cells was reflected in the decrease in PH of the reflections centred at 5.6° 2θ (NP>WP), 17.1 2θ (NP>WP), merging of the doublet centred at 22-24° 2θ (WP>NP) and broadening of the 17.1° 2θ peak (WP> NP) [Fig 4.5, Table 4.3]. The increase in peak width of the reflection centred at 5.5° 2θ in NP and WP starches on HMT (Fig 4.5, Table 4.3) suggests a reduction in the size of B-type crystallites and/or dissociation of these crystallites within the crystalline lattice during the polymorphic transformation. HMT at 80°C decreased the PH of the reflection centred at 20° 2θ (NP80>WP80) (Table 4.3 Fig 4.5). The size of the crystallites (Table 4.3, Fig 4.5) forming this peak remained unchanged in NP80 starch, but decreased in WP80 starch. The decrease in PH at 80°C indicates that the ordered crystallites of the V-type helices (representing single AM chains and/or the outer branches of AMP) may have been disrupted due to an increase in chain mobility. The 20° 2θ reflection was not visible in NP100, NP120, NP130, WP100, WP120 and WP130 starches (Fig 4.5).

Fig 4.5 X-ray diffraction patterns of NP (a), WP (b), NP80 (c), WP80 (d), NP100 (e), WP100 (f), NP120 (g), WP120 (h), NP130 (i) and WP130 (j) starches.

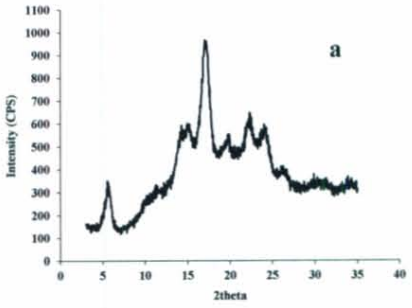
a
Intensity (CPS)
2theta

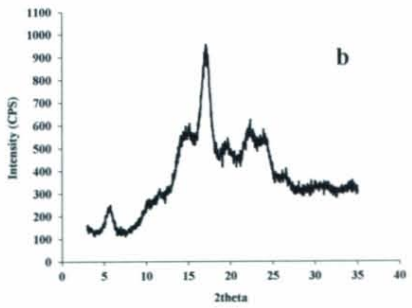
b
Intensity (CPS)
2theta

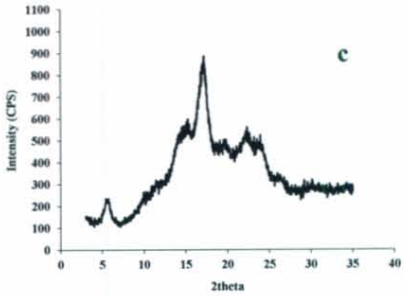
c
Intensity (CPS)
2theta

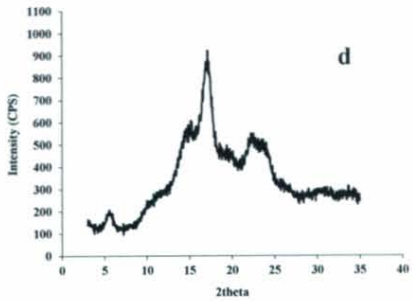
d
Intensity (CPS)
2theta

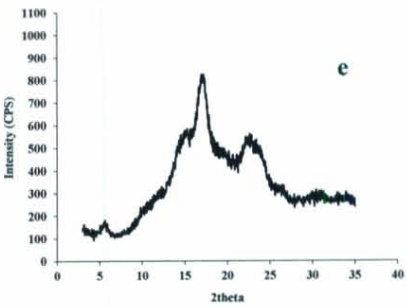
e
Intensity (CPS)
2theta

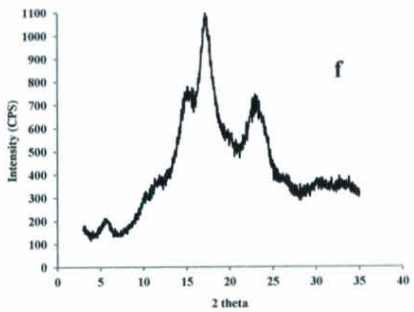
f
Intensity (CPS)
2 theta

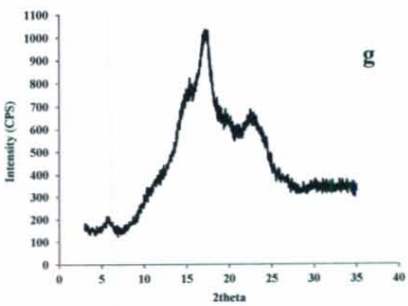
g
Intensity (CPS)
2theta

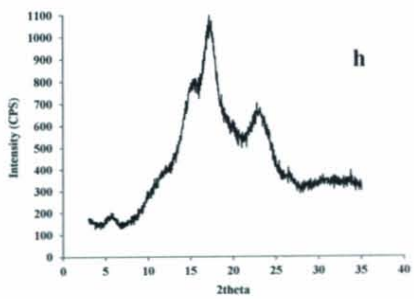
h
Intensity (CPS)
2theta

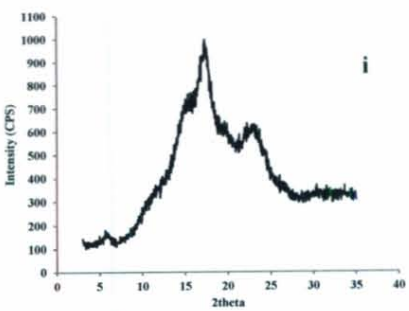
i
Intensity (CPS)
2theta

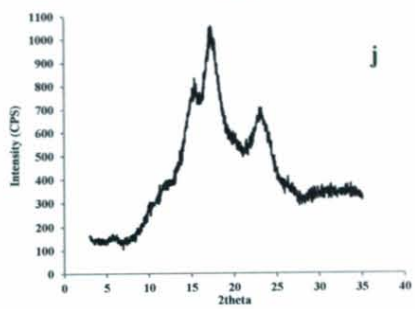
j
Intensity (CPS)
2theta

4.5 ATR-FTIR spectroscopy

The ATR-FTIR spectral data for native and HMT starches are presented in Table 4.4. This technique is considered as a short-range probe, measuring order at the level of individual helices. That is, it distinguishes helices either in or out of the crystalline registry, unlike X-ray diffraction, which is related to the packing of double helices into ordered crystalline arrays. In the spectrum of native potato starch obtained by the FTIR method, the following bands can be distinguished (Cael *et al.,* 1973, 1975; van Soest *et al.,* 1995): 2,900-3,000 cm^{-1} (stretching vibration of CH), 1,150, 1,124 and 1,103 cm^{-1} (stretching vibrations of CO, CC and COH), 1,047, 1,022, 994 and 928 cm^{-1} (bending vibrations of COH and CH_2), 861 cm^{-1} (symmetric stretching vibrations of COC and deformation vibrations of CH). Sevenou *et al.* (2002) have shown that ATR-FTIR yields information on the structural organization of starch chains near the granule surface, since the IR beam penetrates only to a depth of 2 μm into the granule. The above authors showed that FTIR differences between starch varieties are related only to variations in the ratios of the amounts of ordered to unordered fractions within the starch granule.

The FTIR spectrum of starch has been attributed to three main vibrational modes with maximum absorbances at 995, 1022 and 1047 cm^{-1}. The IR bands at 1048 cm^{-1} and 1016 cm^{-1} have been shown to be associated with ordered and amorphous structures of starch, respectively (van Soest *et al.,* 1995). Studies on normal potato starch have shown that the band at 1048 cm^{-1} increases with an increase in crystallinity (van Soest *et al.,* 1995). The band at 1016 cm^{-1} has been attributed to vibrational modes within the amorphous domains of starch granules [since this band has been observed to decrease with an increase in crystallinity (Capron *et al.,* 2007)].

Table 4.4 Short range molecular order of native and heat-moisture treated potato starches measured by attenuated total reflectance-Fourier transform infrared spectroscopy (ATR-FTIR)

Starch source	Treatment	Ratio (1048/1016 cm^{-1})[a]
Normal potato	Native	1.146 ± 0.011^{p}
	HMT 80	1.078 ± 0.002^{q}
	HMT 100	1.000 ± 0.000^{r}
	HMT 120	0.889 ± 0.000^{s}
	HMT 130	0.886 ± 0.005^{s}
Waxy potato	Native	1.167 ± 0.011^{p}
	HMT 80	1.095 ± 0.000^{q}
	HMT 100	1.000 ± 0.000^{r}
	HMT 120	0.917 ± 0.039^{r}
	HMT 130	0.927 ± 0.032^{r}

[a]Ratio of the ordered crystalline (1048 cm^{-1}) to amorphous domains (1016 cm^{-1}).

Means within each column with different superscripts for the native potato starch and its heat-moisture treated counterparts are significantly different ($P < 0.05$)

Thus, the ratio of the bands at 1048cm^{-1} and1016 cm^{-1} reflects the proportions of ordered starch and amorphous starch. The band at 995 cm^{-1} which is mainly due to COH bending vibrations, is especially sensitive to water content and these vibrations involve water-starch interaction, such as hydrogen bonding, which influence the COH bending modes.

HMT at all temperatures decreased the IR ratio (1048cm^{-1}/1016 cm^{-1}) in both NP and WP starches by nearly the same amount, the extent of this reduction being more pronounced at 120° and 130°C (Table 4.4). There was no significant difference in the IR ratio (1048 cm^{-1}/1016 cm^{-1}) between NP120 and NP130 starches. The progressive decrease in the IR ratio (1048 cm^{-1}/1016 cm^{-1}) with an increase in HMT temperature reflects the interplay between: 1) the extent of polymorphic transformation (B→A+B), 2) disruption of hydrogen bonds, and 3) disorganization of double helices within AMP clusters.

4.6 Amylose leaching (AML)

The extent of AML in the temperature range of 60-95°C is presented in Fig 4.6. In both native and HMT starches, AML increased with increase in temperature. HMT of NP starch at 80° and 100°C decreased AML. The extent of this decrease followed the order: NP80>NP100>NP (Fig 4.6). AML in NP80 starch was detectable only at temperatures exceeding 75°C. NP120 and NP130 starches exhibited higher AML than NP starch in the temperature range 60-75°C, but lower AML than NP starch in the temperature range 75°-95°C (Fig 4.6). There was no significant difference in the extent of AML between NP120 and NP130 starches in the temperature range 60-95°C.

Fig 4.6 Amylose leaching of native and heat-moisture treated normal potato (NP) starches at 60-95°C.

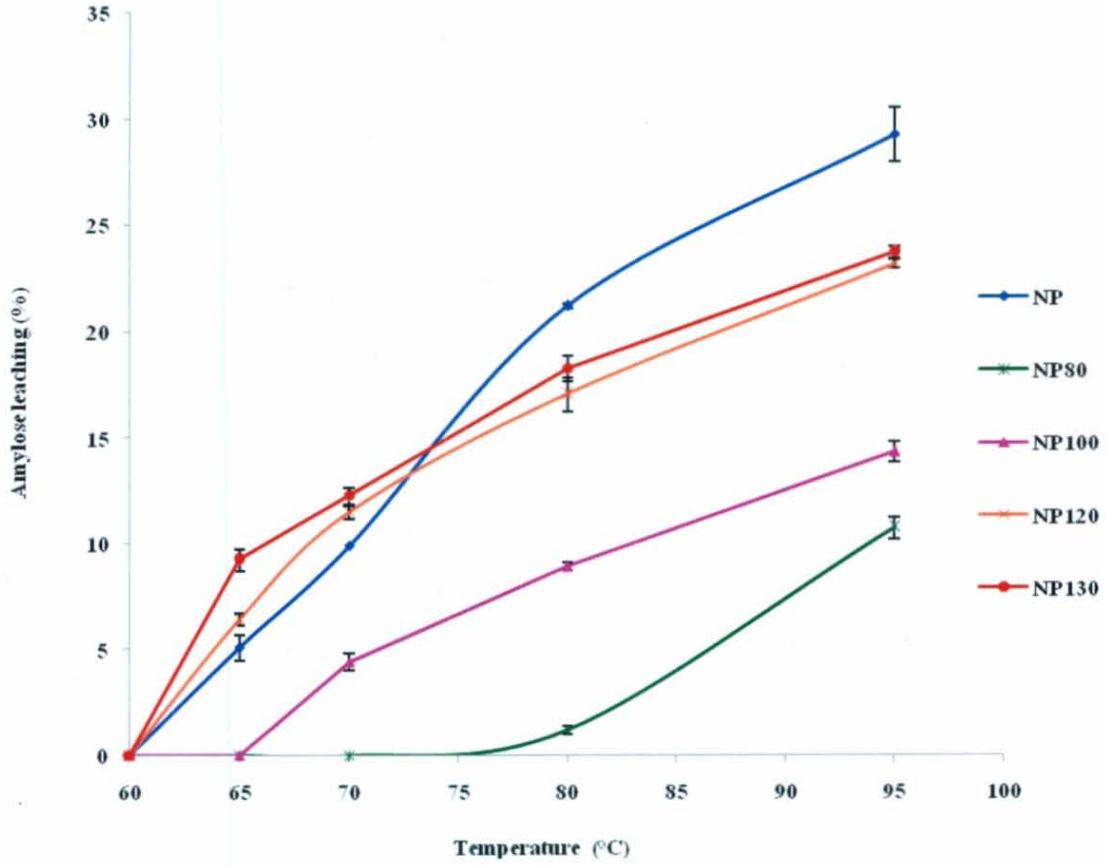
35
30
25
20
15
10
5
0
Amylose leaching (%)
60
65
70
75
80
85
90
95
100
Temperature (°C)
NP
NP80
NP100
NP120
NP130

The reduction in AML on HMT has been attributed to the interplay of: 1) additional interactions between AM-AM and/or AM-AMP chains, 2) a decrease in granular swelling and 3) an increase in V-amylose lipid content (Hoover and Vasanthan, 1994b). In this study, only factors 1 and 2 influence AML, since lipids were present only in trace (<0.08%) quantities (Table 4.1) in NP starch. The results showed that AM-AM and/or AM-AMP interactions were most extensive in NP80 starch. This indicates that due to the lower degree of chain mobility at 80°C, starch chains are better aligned for interaction. The order of AML in the temperature range 60-75°C (NP120~NP130>NP) indicates that at 120°C and 130°C, hydrogen bonds between co-crystallized AM and AMP chains may have been disrupted. However, the extent of AML in NP120 and NP130 starches was lower than in NP starch (NP>NP120~NP130) in the temperature range 75-95°C. This could be attributed to lower granular swelling in NP120 and NP130 starches (Fig 4.7). A decrease in granular swelling would reduce AML.

4.7 Swelling factor (SF)

The swelling factor in the temperature range 60-95°C of NP and WP starches before and after HMT are presented in Figs 4.7. The SF of native NP starch (Fig 4.7a) increased progressively with an increase in temperature. The extent of this increase was most pronounced in the temperature range 60-70°C. However, in WP starch, SF increased only until 70°C, and then decreased thereafter (Fig 4.7b). The SF of starches has been shown to be influenced by amylopectin content and structure and starch-lipid complexes (Gomand *et al.,* 2010; Chung *et al.,* 2009a). Since there was no difference in chain length distribution of amylopectin (Table 4.2) or bound lipid content (Table 4.1) between the starches, the higher SF of waxy potato in the temperature range 60-70°C reflects its higher amylopectin content. The lower SF of waxy potato

starch at higher temperatures (>70°C) suggests that the higher granular swelling at lower temperatures rendered the granules very fragile and thus susceptible to partial disintegration at higher temperatures.

HMT reduced the SF of NP starches at all temperatures (Fig 4.7a). Reduction in SF on HMT has also been reported in cereals, pulses and tuber starches (Chung *et al.,* 2009; Hoover *et al.,* 2010; Jayakody *et al.,* 2007). The extent of SF reduction (in the temperature range 70-95°C) followed the order: NP100~NP130>NP120>NP80. The reduction in SF on HMT has been attributed to : 1) AM-AM, AM-AMP and AMP-AMP interactions (these interactions reduces the number of free hydroxyl groups available for interaction with water) and 2) polymorphic transformation (B→A+B) [the ingress of water during SF measurements would be more rapid and higher in the B-type polymorph (Hoover and Vasanthan, 1994b) due to double helices being more compactly packed in the A-type polymorph]. X-ray data (Fig 4.5) showed that the amount of A-type polymorph in the HMT starches followed the order: NP130>NP120>NP100>NP80. In order to explain the variation in SF reduction on HMT, it is necessary to consider both AML (Fig 4.6) and DSC (Table 4.5) data. AML data showed that starch chain interactions (AM-AMP, AMP-AMP) followed the order: NP80>NP100>NP120>NP130. The large decrease in ΔH at 130°C showed disorganization of crystallite packing. Thus, the differences in SF among the HMT NP starches (Fig4.7a) reflect the interplay between the following factors: 1) extent of interaction among AM-AMP and AMP-AMP chains, 2) the amount of A-type unit cells, 3) crystalline stability and 4) the extent of organization of double helical packing within the amylopectin clusters.

Fig 4.7 Swelling factor in the temperature range 60-90°C of native and heat-moisture treated normal potato (NP) (a) and waxy potato (WP) (b) potato starches.

a)

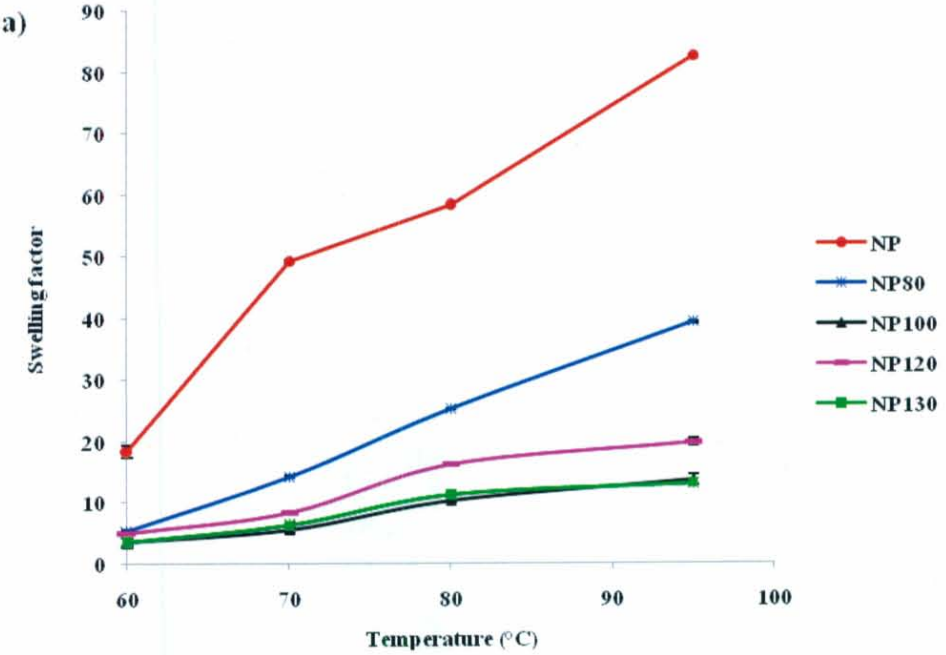
Swelling factor
90
80
70
60
50
40
30
20
10
0
60
70
80
90
100
Temperature (°C)
NP
NP80
NP100
NP120
NP130

b)

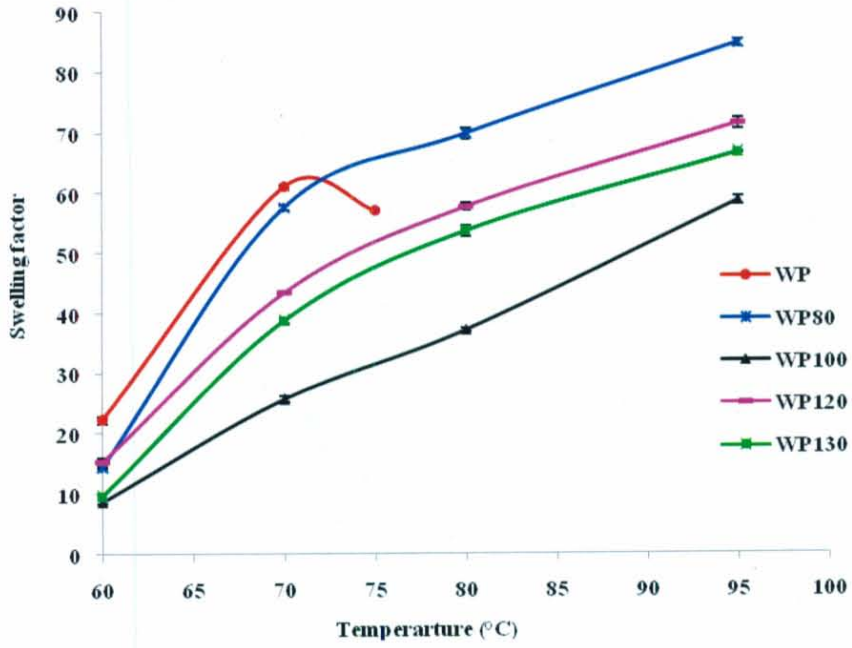
Swelling factor
90
80
70
60
50
40
30
20
10
0
60
65
70
75
80
85
90
95
100
Temperarture (°C)
WP
WP80
WP100
WP120
WP130

In the WP starches (Fig4.7b), SF of WP starch increased up to 70°C and then decreased due to the disruption of highly swollen granules. The rapid increase in SF in the low temperature range reflects the higher AMP content of WP starch. The difference in SF between WP80 and WP100 starches reflects the higher content of A-type unit cells in the latter (Fig 4.5). The differences in SF between WP120 and WP130 starches reflect not only the presence of more A-type unit cells but also the greater loss in crystallite packing (Table 4.5) in the latter.

4.8 K/S spectral analysis

The K/S spectra provide information about the intensity of the colour developed in granular starch when it complexes with iodine, forming V-type crystallinity (Saibene and Seetharaman, 2010; Saibene *et al.*, 2006). Saibene *et al.* (2006) and Waduge *et al.* (2010) have shown that iodine binding in a starch granule requires a certain minimum level of mobility of the linear molecules, and that the water content would plasticize the starch, thus increasing the ability to bind iodine by the formation of single helices.

Gidley and Bulpin (1987) have shown that all α-1,4-glucans form helical inclusion complexes with iodine to some degree. The extent of the iodine binding depends upon the degree of helix formation which can be attained. A single helix, capable of supporting complex formation, has been shown to require six glucose molecules per turn. As the length of the glucan chain, and hence the number of helical turns, increases, the number of iodine molecules which can be accommodated also increases, so that the iodine binding capacity is enlarged. This increased binding has been shown to result in a shift in the wavelength of maximum absorbance; $1/\lambda_{max}$ has been shown to be directly proportional to 1/DP up to a DP of about 100 (Banks *et al.,* 1971) The

formation of inclusion complexes between granular starches and iodine vapour has been shown to depend on the accessibility of segments of glucan polymers (segments of AM molecules which are not trapped in the crystalline lamellae, AM molecules that are not in double helices with AMP branch chains and long segments of AMP branches) to iodine (Waduge and Seetharaman, 2010). Therefore, the structural organization of starch chains within the amorphous and crystalline domains will influence the extent of iodine binding. The major structural changes during HMT at different temperatures and the availability of glucan polymers for iodine complexing before and after HMT are presented schematically in Fig 4.8.

The K/S spectra of NP and WP starches before and after HMT (80, 100, 120, 130°C) following equilibration at 100% relative humidity are presented in Fig 4.9. NP and NP120 starches exhibited maximum K/S absorption of 39.0 and 42.0, respectively, at 590 nm. However, NP80, NP100 and NP130 starches exhibited K/S maxima of 38.2, 31.0 and 37.5, respectively, at 570 nm. The decrease in K/S maxima and λ_{max} (590 to 570 nm) shown by NP80 starch indicates that AM-AM and/or AM-AMP interactions during HMT decrease the population of glucan polymers (decreases the K/S maxima) and chain length (decreases λ_{max}) available for iodine complexing. AML data (Fig 4.6) showed that interactions between AM-AM and AM-AMP chains were most pronounced in NP80 starch. Consequently, these interactions would decrease chain mobility, thereby hindering the ability of AM chains to form helical complexes with iodine. AML data (Fig 4.6) also showed that NP100 starch exhibited a higher degree of AML than NP80 starch. Theoretically, NP100 starch should have exhibited a higher K/S maxima than NP80 starch due to the availability of additional free AM chains for iodine complexing.

Fig 4.8 Schematic model for structural changes on HMT at different temperatures (**A**) and their impact on iodine binding (**B**).

A] Arrangement of amylose and amylopectin chains in the native starch granule (a) and after HMT at 80-100°C (b), 120°C (c), 130°C (d)

B] Iodine complexing ability of glucan polymers before (a) and after HMT at 80-100°C (b), 120°C (c), 130°C (d)

At low temperatures (80-100°C) - AM-AM, AM-AMP and AMP-AMP interactions reduce the availability of glucan polymers for iodine complexing

At 120°C - disruption of hydrogen bonds between co-crystallized AM and AMP chains and between AMP-AMP chains increases the availability of glucan polymers for iodine complexing

At 130°C - 1) disruption of hydrogen bonds between co-crystallized AM and AMP chains and between AMP-AMP chains increases the availability of glucan polymers for iodine complexing 2) formation of interrupted helices reduces the availability of glucan polymers for iodine complexing

A

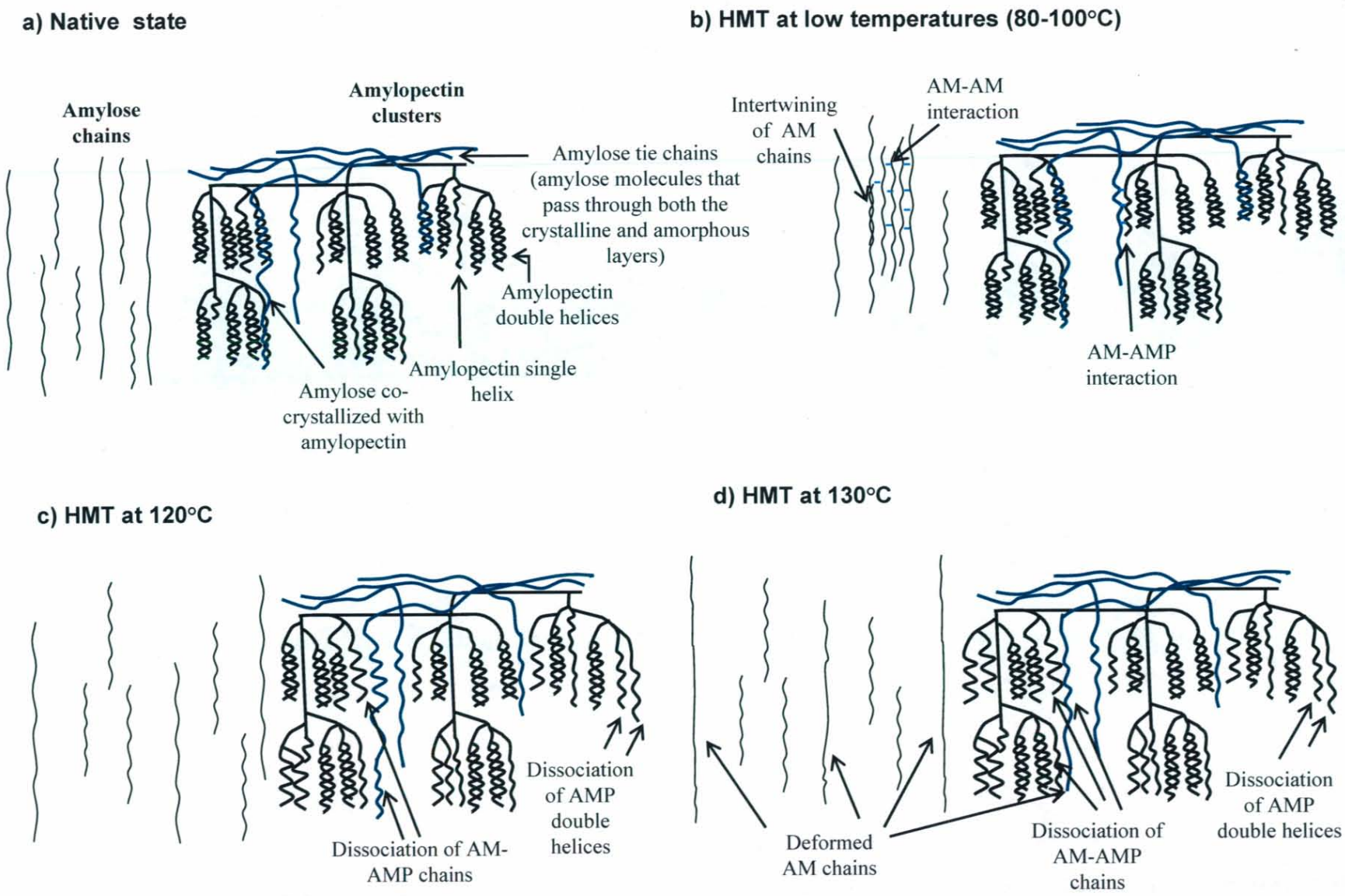
a) Native state
Amylose chains
Amylopectin clusters
Amylose tie chains (amylose molecules that pass through both the crystalline and amorphous layers)
Amylopectin double helices
Amylopectin single helix
Amylose co-crystallized with amylopectin
b) HMT at low temperatures (80-100°C)
Intertwining of AM chains
AM-AM interaction
AM-AMP interaction
c) HMT at 120°C
Dissociation of AM-AMP chains
Dissociation of AMP double helices
d) HMT at 130°C
Deformed AM chains
Dissociation of AM-AMP chains
Dissociation of AMP double helices

B

a) Native state

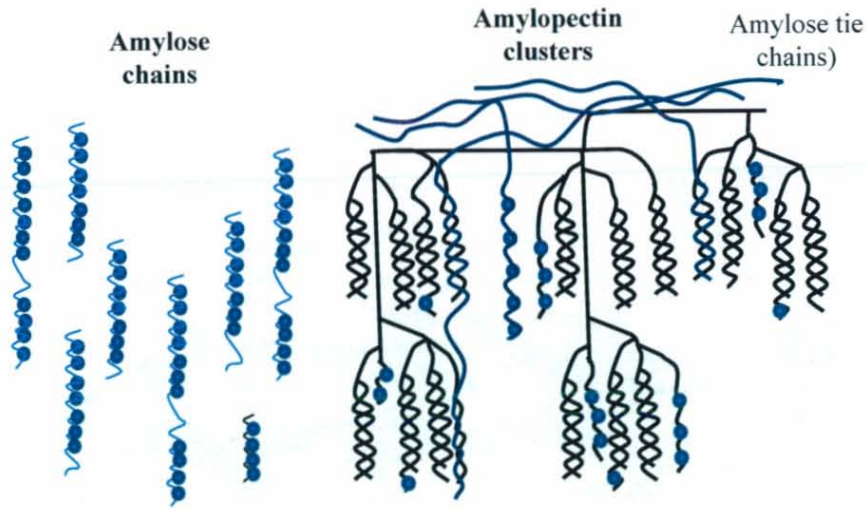

b) HMT at low temperatures (80-100°C)

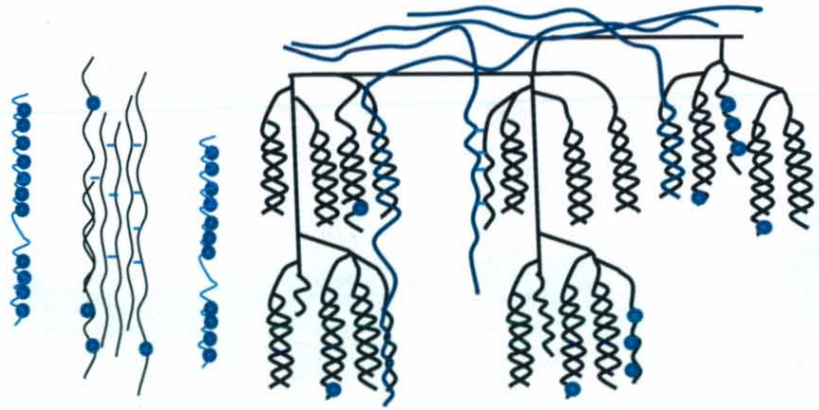

c) HMT at 120°C

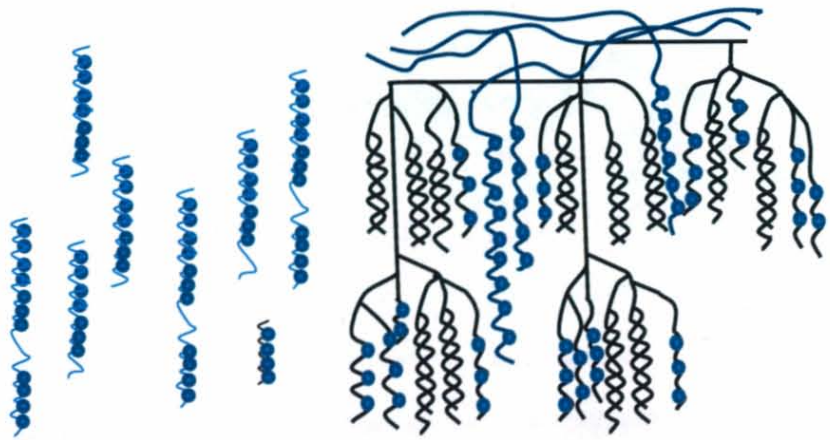

d) HMT at 130°C

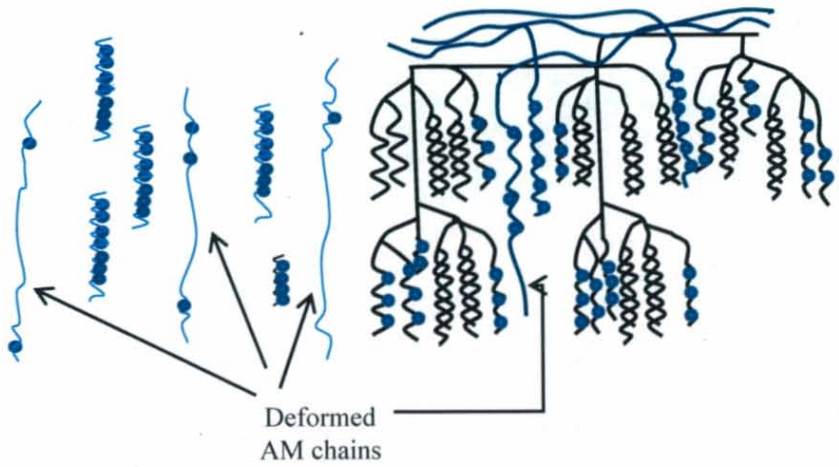

However, as shown in Fig 4.9a, the iodine complexing ability of NP100 starch was much lower than that of NP80 starch. As discussed earlier, the polymorphic transformation during HMT is accompanied by the loss of water from the central channel of the B-type unit cell (Gunaratne and Hoover, 2002). Consequently, the extent of starch chain plasticization would decrease with an increase in HMT temperature. This in turn would decrease iodine binding ability. Thus, the difference in K/S maxima between NP80 and NP100 starches, and the decrease in λ_{max} at HMT temperatures of 80° and 100°C stands explained. The difference in K/S maxima (Fig 4.9a) between NP120 (42.0) and NP (39.0) starches at the same λ_{max} (590 nm) is indicative of the availability of a greater population of glucan polymers for iodine complexing in NP120 starch. This seems to suggest that the iodine binding ability of NP120 starch is not influenced by the lower degree of plasticization of its starch chains. DSC data (Table 4.5) showed that AM-AMP interactions were disrupted at 120°C and 130°C. These disruptions would free AM and AMP chains, thereby increasing their mobility and hence their ability to bind iodine. This would then account for the difference in K/S maxima between NP120 and NP100 starches. On this basis, one would have expected the K/S maximum of NP130 starch to be higher than that of NP120 starch. However, the lower K/S maxima of NP130 starch and the shift to a lower λ_{max} (570 nm) at 130°C, suggests that intra molecular hydrogen bonds stabilizing the helical region may have been disrupted, resulting in interrupted single helices with limited regions of random coil interspaced between helical segments. A helix to coil transformation would decrease the number of helical turns required to form the typical deep blue colour with iodine. It is highly unlikely that a coil →helix transition could occur on the addition of iodine vapour to NP130 starch, since an aqueous medium would be required for such a transformation (Cheetham and Tao, 1998).

Fig 4.9 Reflectance spectra of native and heat-moisture treated normal potato (NP) (a) and waxy potato (WP) (b) starches.

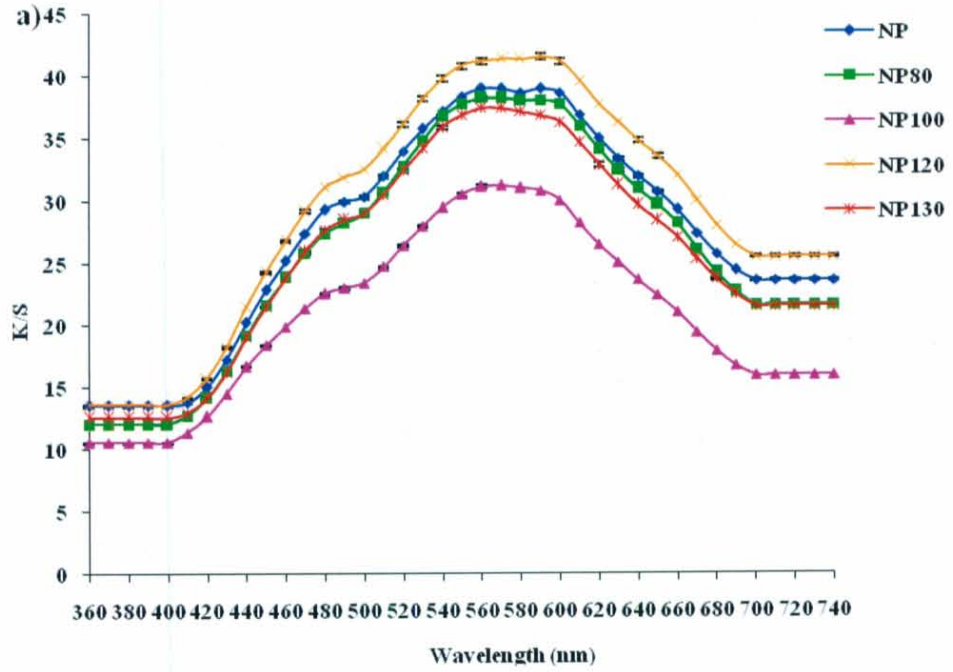
a)
45
40
35
30
25
20
15
10
5
0
K/S
NP
NP80
NP100
NP120
NP130
360 380 400 420 440 460 480 500 520 540 560 580 600 620 640 660 680 700 720 740
Wavelength (nm)

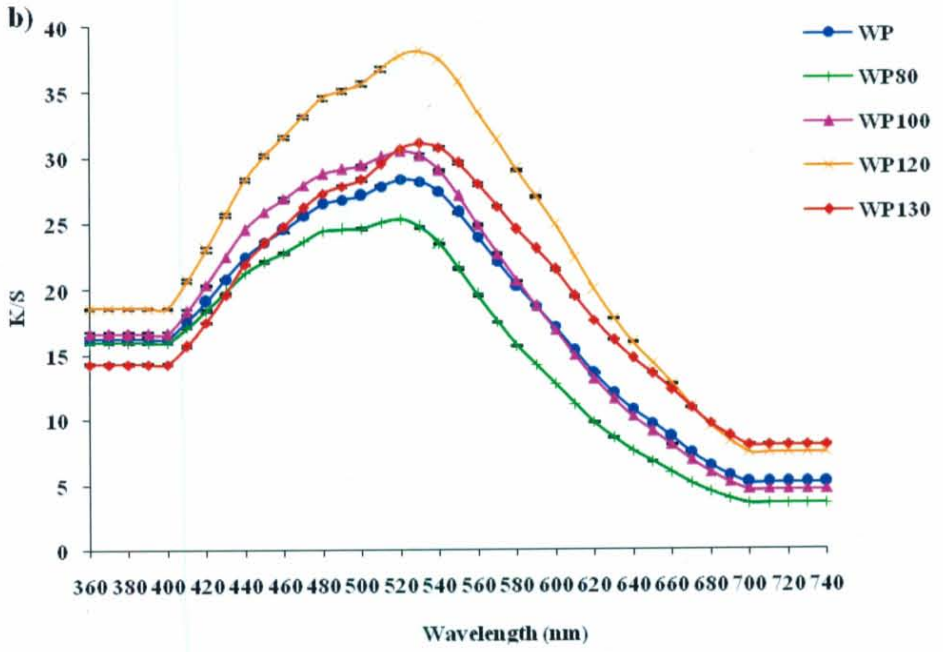
b)
40
35
30
25
20
15
10
5
0
K/S
WP
WP80
WP100
WP120
WP130
360 380 400 420 440 460 480 500 520 540 560 580 600 620 640 660 680 700 720 740
Wavelength (nm)

WP and WP80 starches exhibited a K/S maxima of 28 and 25, respectively, at 520nm. However, HMT at 100, 120 and 130°C increased the K/S maximum (WP100 [30 at 520 nm], WP120 [38 at 530 nm] and WP130 [31 at 530 nm]). The decrease in K/S maxima at 80°C is indicative of interactions between AMP-AMP chains. Disruption of hydrogen bonds between AMP-AMP chains at higher temperatures of HMT (>80°C) may have rendered the outer branches of AMP more flexible for complexing iodine. The difference in K/S maxima between WP120 and WP130 starches is indicative of the presence of a higher content of interrupted helices in the latter. It was interesting to observe that the K/S maximum of NP100 starch was lower than that of NP starch (Fig 4.9a), whereas that of WP100 starch was greater than that of WP starch (Fig 4.9b). This could be attributed to strong interactions between AM-AM and/or AM-AMP chains during HMT of NP starch at 100°C, and to decreased starch chain plasticization at this temperature. The presence of only trace quantities of AM in WP starch may have facilitated the disruption of hydrogen bonds between AMP chains during HMT at 100°C, thereby increasing the ability of WP100 starch to bind more iodine than WP starch.

4.9 Gelatinization characteristics

The gelatinization temperatures ([To-onset], [Tp-midpoint], [Tc-conclusion]), the gelatinization temperature range (Tc-To) and the enthalpy of gelatinization (ΔH) of normal potato (NP) and waxy potato (WP) starches, before and after HMT, are presented in Table 4.5. To, Tp and Tc are influenced by the structural organization of the AMP clusters. ΔH has been suggested to reflect the following: 1) melting of double helices (Cooke and Gidley, 1992), 2) overall crystallinity (quantity and amount of AMP crystallites) (Tester and Morrison, 1990) and 3) melting of imperfect amylopectin-based crystals with potential contributions from both crystal packing and

helix melting enthalpies (Lopez-Rubio *et al.*,2008b). HMT of NP and WP starches at 80 and 100°C increased Tp and Tc. The extent of this increase being higher at 100°C (Table 4.5). However, this trend was reversed at 120 and 130°C, where the extent of increase in Tp and Tc was lower than at 100°C. An increase in Tp and Tc on HMT of tuber starches has been shown to represent melting of : a) B-type crystallites present in the native granule, b) A-type crystallites formed during the polymorphic transformation, and c) crystallites formed from interaction between AM-AMP and AMP-AMP chains (Hoover, 2010).

The increase in A-type crystallites on HMT in both NP and WP starches (Fig 4.5), when considered along with compact packing of double helices in A-type crystallites, should have theoretically resulted in Tp and Tc of NP120, NP130, WP120 and WP130 starches being higher than their respective counterparts at 100°C (NP100, WP100). This suggests that the higher chain mobility prevailing at 120° and 130°C may have hindered the expected increase in Tp and Tc by decreasing the extent of interaction between AM-AMP and AMP-AMP chains and/or by disrupting hydrogen bonds between co-crystallized AM and AMP chains (decreases crystalline stability).

HMT decreased ΔH in both NP and WP starches (Table 4.5). The extent of this decrease for NP and WP starches followed the order: NP130>NP120~NP100>NP80 and WP130>WP120>WP100>WP80, respectively. The decrease in ΔH for NP80, NP100, WP80 and WP100 starches can be attributed to interactions between AM-AMP and/or AMP-AMP chains on HMT that strengthen double helical associations (Fig 4.6).

Table 4.5 Gelatinization parameters of native and HMT normal and waxy potato starches

Starch source	Treatment	Gelatinization transition parameters[a]				
		To (°C)[b]	Tp (°C)[b]	Tc (°C)[b]	Tc- To (°C)[c]	ΔH (J/g)[d]
Normal potato	Native	62.08 ± 0.3^{p}	66.92 ± 0.1^{p}	72.59 ± 0.0^{p}	10.51 ± 0.3^{p}	13.20 ± 0.2^{p}
	NP80	64.32 ± 0.2^{q}	70.09 ± 0.1^{q}	76.06 ± 0.6^{q}	11.75 ± 0.4^{p}	10.73 ± 0.3^{q}
	NP100	63.87 ± 0.3^{q}	72.98 ± 0.1^{r}	80.39 ± 0.2^{r}	16.52 ± 0.2^{q}	9.05 ± 0.4^{r}
	NP120	61.72 ± 0.3^{p}	67.89 ± 0.2^{p}	75.33 ± 0.4^{q}	13.61 ± 0.1^{r}	9.02 ± 0.6^{r}
	NP130	60.65 ± 0.2^{r}	67.14 ± 0.5^{p}	76.54 ± 0.9^{q}	15.89 ± 0.6^{q}	7.36 ± 0.4^{s}
Waxy potato	Native	63.21 ± 0.1^{p}	68.38 ± 0.0^{p}	73.85 ± 0.3^{p}	10.64 ± 0.4^{p}	14.50 ± 0.2^{p}
	WP80	63.15 ± 0.2^{p}	69.33 ± 0.0^{q}	$75.41 \pm 0.1^{p, r}$	12.26 ± 0.1^{q}	12.24 ± 1.0^{q}
	WP100	61.67 ± 0.1^{q}	74.63 ± 0.1^{r}	81.54 ± 0.1^{s}	19.88 ± 0.0^{r}	11.86 ± 0.6^{q}
	WP120	61.30 ± 0.1^{q}	67.70 ± 0.0^{s}	75.89 ± 0.3^{r}	14.58 ± 0.4^{s}	10.01 ± 0.2^{r}
	WP130	61.65 ± 0.1^{q}	68.32 ± 0.1^{p}	79.98 ± 0.8^{t}	18.33 ± 0.7^{t}	8.46 ± 0.3^{s}

[a]All data reported on dry basis. Means within each column with different superscripts for native and waxy potato starches and their heat moisture treated counterparts are significantly different ($P < 0.05$) by Tukey's HSD test

[b]To, Tp, Tc represent the onset, mid-point and conclusion temperature respectively

[c](Tc-To) represents the gelatinization temperature range

[d]Gelatinization enthalpy of starch expressed in J/g of dry starch

Consequently, the number of helices that disrupt, unwind and melt during gelatinization would decrease on HMT. Tp and Tc data (Table 4.5) revealed that starch chain interactions at HMT temperatures of 120° and 130°C were weaker than at 100°C (Table 4.5). This suggests that the decrease in ΔH at 120° and 130°C reflect mainly disruption of hydrogen bonds present in: 1) double helices formed between AM and AMP chains, and 2) double helices forming the AMP clusters.

It was interesting to observe, that although ΔH values were different for WP100 and WP120 starches (Table 4.5), both NP120 and NP100 starches exhibited nearly similar ΔH values (Table 4.5). This suggests that the presence of AM co-crystallized with AMP chains in NP starch may have resisted hydrogen bond disruption during HMT at 120°C. Consequently, the extent of double helical disorganization may have been too small to be detectable by DSC. This seems plausible, since the K/S iodine absorption spectra showed that the difference in the extent of iodine absorption between NP and NP120 starches (Fig 4.9a) was smaller (due to a lower extent of double helical disruption on HMT) than between WP and WP120 starches (Fig 4.9b).

4.10 Pasting properties

The pasting properties of native and HMT normal and waxy potato starches measured using a Rapid Visco™ Analyser (RVA) are presented in Fig 4.10 and Table 4.6. All RVA parameters were higher in native normal potato starch. Studies have shown that peak viscosities are influenced by amylose content, extent of amylose leaching, granular swelling, friction between swollen granules, phosphate monoester content and/or the proportion of long amylopectin branch chains (Jayakody *et al.*, 2007; Jane *et al.*, 1999). As shown in Tables 4.1 and 4.2, there was no

significant difference in phosphate monoester content and in the proportion of long amylopectin chains (DP 37-50), between native normal and waxy potato starches. Therefore, the difference in peak viscosity (normal>waxy) between the two native starches could be attributed to AML (normal potato) (Fig 4.6) negating the effect of granular swelling (waxy>normal) (Fig 4.7) on peak viscosity. McPherson and Jane (1999) also showed that normal potato starch displays a larger peak viscosity than waxy potato starch. This was attributed to AM-AMP interactions within native normal potato starch, which confers granule rigidity, thereby enabling granules to swell and to attain a higher peak viscosity than waxy potato starch.

Higher granule fragility (resulting from higher granular swelling) may have been responsible for the extent of viscosity breakdown being higher in normal potato starch (Fig 4.10). The higher set-back of native normal potato starch reflects more extensive amylose leaching (Fig 4.6). In both starches, HMT (100, 120, 130°C) decreased peak viscosity (normal > waxy), breakdown viscosity (normal>waxy) and increased the pasting temperature (normal>waxy). Set-back decreased in normal potato starch, but increased in waxy potato starch on HMT (Fig 4.10). However, HMT at 80°C increased peak viscosity, breakdown viscosity, final viscosity and pasting temperature and decreased set-back in waxy potato starch. In normal potato starch, HMT at 80°C increased breakdown viscosity and decreased set-back.

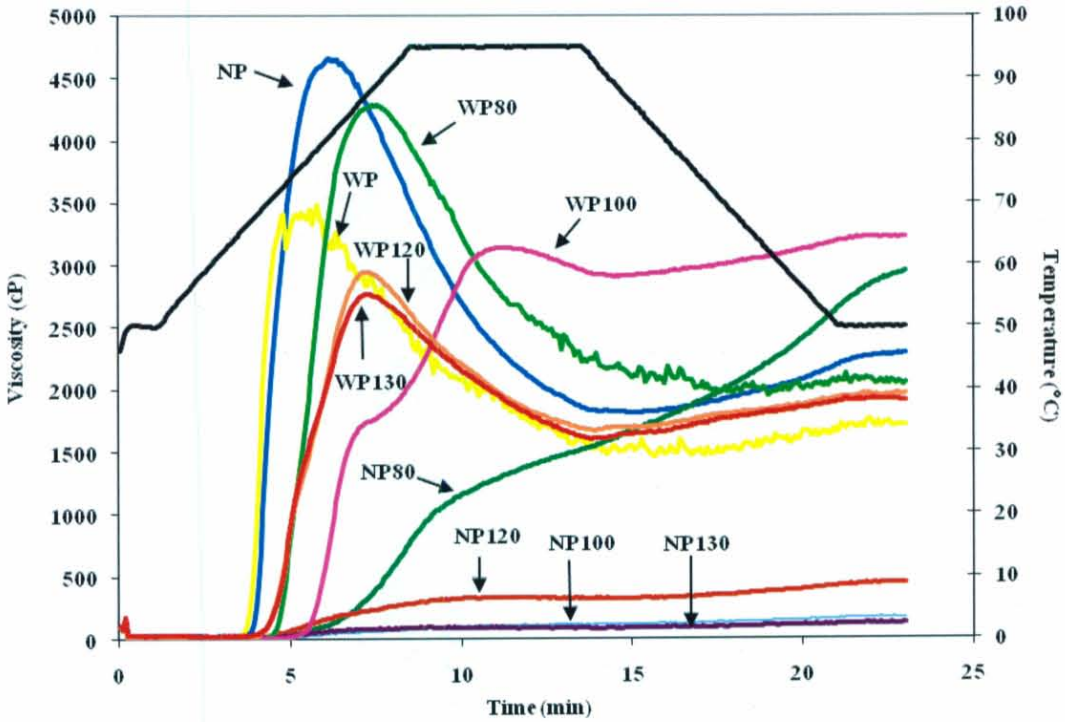
Viscosity (cP)
Temperature (°C)
Time (min)
NP
WP80
WP
WP100
WP120
WP130
NP80
NP120
NP100
NP130
5000
4500
4000
3500
3000
2500
2000
1500
1000
500
0
100
90
80
70
60
50
40
30
20
10
0
0
5
10
15
20
25

Table 4.6 RVA parameters* of native and heat-moisture treated normal and waxy potato starches

Sample	Peak (cP)	Trough (cP)	Breakdown (cP)	Final viscosity (cP)	Setback (cP)	Peak Time (min)	Pasting T° (°C)
NP	4605 ± 75^{p}	1800 ± 14^{p}	2805 ± 61^{p}	2277 ± 14^{p}	477 ± 0.0^{p}	6.23 ± 0.1^{p}	66.6 ± 0.3^{p}
NP80	1466 ± 9^{q}	1467 ± 15^{q}	-1 ± 6^{q}	2937 ± 18^{q}	1470 ± 3^{q}	13.00 ± 0.0^{q}	84.3 ± 0.0^{q}
NP100	116 ± 1^{r}	108 ± 1^{r}	8 ± 0^{r}	165 ± 0^{r}	58 ± 1^{r}	12.80 ± 0.1^{q}	–
NP120	332 ± 1^{s}	317 ± 2^{s}	16 ± 1^{s}	449 ± 1^{s}	132 ± 3^{s}	11.90 ± 0.1^{q}	–
NP130	93 ± 5^{t}	78 ± 1^{t}	15 ± 6^{s}	121 ± 3^{t}	44 ± 4^{t}	9.13 ± 0.0^{r}	–
WP	3506 ± 29^{p}	1462 ± 3^{p}	2044 ± 26^{p}	1693 ± 31^{p}	231 ± 34^{p}	5.30 ± 0.7^{p}	65.4 ± 0.3^{p}
WP80	4291 ± 11^{q}	1949 ± 3^{q}	2342 ± 8^{q}	2057 ± 2^{q}	108 ± 5^{q}	7.47 ± 0.1^{q}	70.7 ± 0.0^{q}
WP100	3119 ± 30^{r}	2884 ± 32^{r}	235 ± 1^{r}	3209 ± 17^{r}	326 ± 15^{r}	11.40 ± 0.0^{q}	76.6 ± 0.0^{r}
WP120	2978 ± 51^{r}	1691 ± 35^{s}	1287 ± 16^{s}	1982 ± 28^{s}	291 ± 8^{s}	7.27 ± 0.1^{q}	69.20 ± 0.1^{s}
WP130	2790 ± 35^{s}	1639 ± 55^{s}	1151 ± 21^{t}	1922 ± 13^{t}	283 ± 42^{s}	7.33 ± 0.1^{q}	69.53 ± 0.0^{s}

*Values are means of two determinations. Means within each column with different superscripts for native and waxy potato starches and their heat moisture treated counterparts are significantly different ($P < 0.05$) by Tukey's HSD test

In normal potato starch, the reduction in peak viscosity (NP130>NP100>NP120>NP80) on HMT reflects decreased AML (Fig 4.6) and SF (Fig 4.7) as a result of enhanced interaction between AM-AM, AM-AMP and AMP-AMP chains and polymorphic transformation (B→A+B). Reduction of peak viscosity on HMT (WP130>WP120>WP100) in waxy potato starches could be attributed to lower granular swelling because of AMP-AMP interactions and polymorphic transformation (B→A+B). Reduction of peak viscosity is lower in waxy potato starch, since the extent of granular swelling is very high (Fig 4.7b). Starch interactions are also responsible for the increase in pasting temperature on HMT being higher in normal potato starch. Jayakody *et al.* (2007) have shown that both amylose gelation and the presence of rigid swollen granules embedded within the leached amylose network influence the extent of set-back. SF (Fig 4.7) and AML (Fig 4.6) data showed that HMT decreased the SF and AML of normal potato starch, but increased SF of waxy potato starch. This suggests that the increased setback on HMT of waxy potato (WP100, WP120, WP130) starch reflects an increase in the proportion of swollen intact granules (provides increased resistance to shearing during the cooling cycle in the RVA).

4.11 Enzyme Hydrolysis

Hydrolysis of native and HMT starches by PPA are presented in Figs 4.11. In their native state, NP was hydrolysed to a greater extent than WP starch. HMT at 80°C, decreased hydrolysis in NP starch (Fig 4.11a) but did not significantly influence hydrolysis in WP starch (Fig 4.11b). However, HMT at 100, 120 and 130°C increased hydrolysis of both NP and WP starches nearly to the same extent. The extent of this increase in NP and WP starches, was more pronounced between 120 and 130°C. It is difficult to compare these results with those reported in the literature for normal potato starch due to differences in moisture content, duration of HMT and

HMT temperatures (Hoover, 2010). The granular architecture and, more specifically the surface organization has been shown to be one of the main factors determining kinetics and degree of hydrolysis (Bird *et al.*, 2009). Thus the extent of decrease in molecular order that occurs at or near the granule surface on HMT of NP starch (NP130~NP120>NP100>NP80) (Table 4.4) should have theoretically increased hydrolysis in the same order. However, the observed order of hydrolysis (NP130>NP120>NP100>NP>NP80), suggests that interactions between starch chains on HMT (Fig 4.6), which are more prevalent at 80 and 100°C (80>100°C) than at 120 and 130°C may have also been a contributory factor influencing hydrolysis. At this stage, it might be instructive to consider the conformational changes in glucosyl residues during PPA hydrolysis. Oates (1997) has shown that PPA catalyzed hydrolysis of α (1→4) glycosidic bonds involves the enzyme –induced ring distortion of one of the D-glucosyl residues from the $^4C_1$chair conformation to a 'half chair' conformation. Ring distortion decreases the enthalpy of activation and increases the susceptibility of the glucosyl residues to hydrolysis. The ability of PPA to unwind double helices is driven by the influence of ring distortion on neighbouring units. Chains with restricted mobility, either complexed or crystallized will be hydrolysed less readily because their constituent glucose units are more firmly locked into a specific configuration.

Jane *et al.* (1997) have shown that in A-type starches, the branch points are scattered in both amorphous and crystalline regions. Consequently, there are many short chains derived from branch linkages located inside the crystalline region, which produces an inferior crystalline structure. This inferior crystalline structure containing α (1→6) branch points and the short double helices are more susceptible to PPA hydrolysis leading to a 'weak points' in starches containing the A-type unit cells. These weak points are readily attacked by PPA.

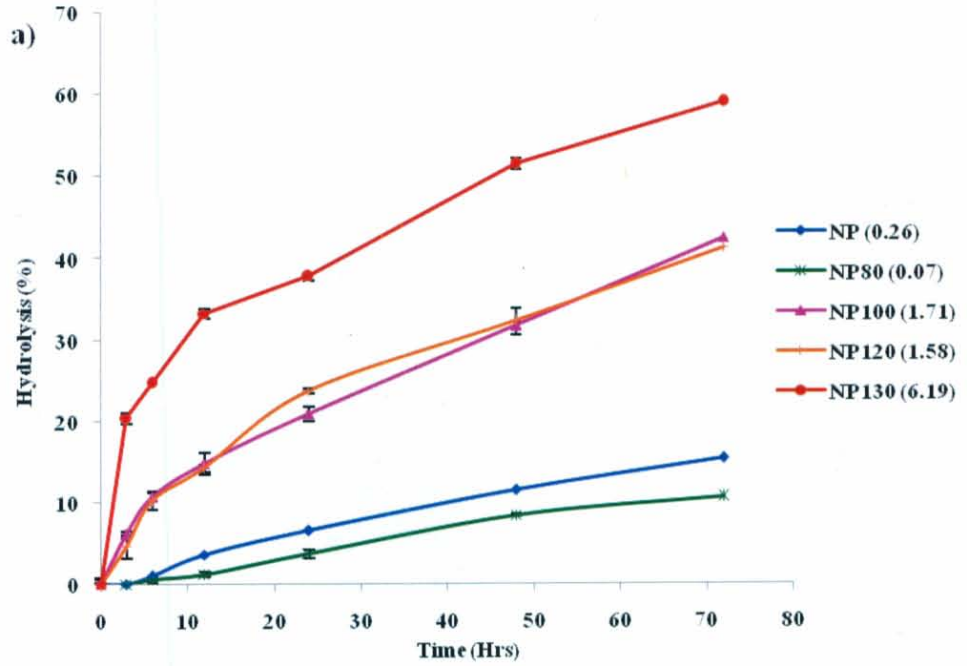
a)
Hydrolysis (%)
Time (Hrs)
NP (0.26)
NP80 (0.07)
NP100 (1.71)
NP120 (1.58)
NP130 (6.19)

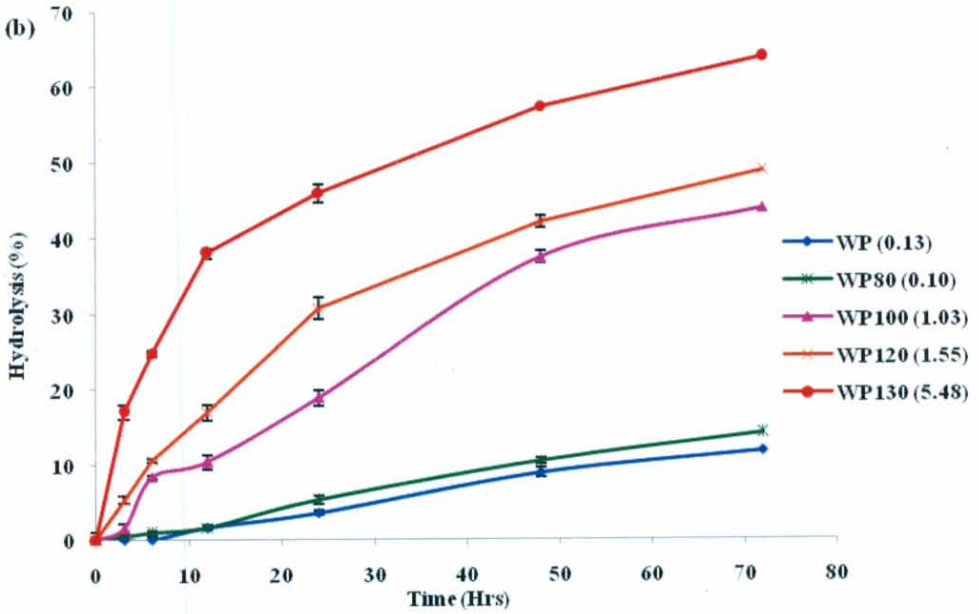
(b)
Hydrolysis (%)
Time (Hrs)
WP (0.13)
WP80 (0.10)
WP100 (1.03)
WP120 (1.55)
WP130 (5.48)

However, in B-type starches more branch points are clustered in the amorphous region, and furthermore, there are fewer short branch chains. Consequently, the crystalline structure is superior to that of the A-type starches, and hence more resistance to PPA. Ratnayake *et al.* (2001) have shown by studies on pulse starches that resistance to PPA increases with increase in B-type unit cell content. X-ray data (Fig 4.5) showed the formation of A-type unit cells on HMT of NP starch at 80°C. ATR-FTIR data (Table 4.4) indicated structural disorganization of starch chains near the granule surface of NP80 starch. Thus, both of the above factors should have theoretically increased the susceptibility of NP80 starch towards PPA. The observed hydrolysis (NP>NP80), suggests that the extensive interaction between starch chains (AM-AM, AM-AMP) during HMT at 80°C (Fig 4.6) may have hindered the accessibility of PPA towards the glycosidic oxygen. This suggests that the structural disorganization near the granule surface as observed by ATR-FTIR data (Table 4.4) mainly reflects disorganization of AMP helices. The large increase in hydrolysis on HMT of NP starch at 100°C (Fig 4.11a) reflects an increase in A-type crystallites (Fig 4.6) and greater degree of structural disorganization near the granule surface (Table 4.4). This seems plausible, since the extent of interaction involving AM chains at 100°C was much weaker than at 80°C (Fig 4.6). The marginal difference in hydrolysis between NP100 and NP120 starches was rather surprising, since compared to NP100 starch, NP120 starch exhibited higher structural disorganization near the granule surface (Table 4.4), weaker interaction between AM-AM and AMP-AMP chains (Fig 4.7) and disruption of hydrogen bonds between co-crystallized AM and AMP chains (Table 4.5). Consequently, NP120 starch should have been hydrolysed to a greater extent than NP100 starch. This suggests that the increase in the amount of A-type unit cells (NP120>NP100) formed on HMT (Fig 4.5, Table 4.3) may have been the causative factor influencing the difference in hydrolysis between NP120 and NP100

starches. Several studies (Lopez-Rubio *et al.,* 2008b; O'Brien and Wang, 2008; Oates 1997) have shown that the double helical conformation hinders enzyme hydrolysis, since in this form only a maximum linear portion of three glucose units is available; this is insufficient for complete subsite binding. This suggests that the large difference in hydrolysis between NP120 and NP130 starches (Fig 4.11a,b) reflects helix to coil transformation and the greater content of A-type unit cells in the latter (Fig 4.5, Table 4.3).

X-ray (Fig 4.5, Table 4.3) and ATR-FTIR (Table 4.4) data showed an increase in A-type crystallites and structural disorganization (near the granule surface), respectively, on HMT of WP starch at 80°C. On this basis, WP80 starch should have been hydrolysed to a greater extent than WP starch. The nearly similar hydrolysis values for WP and WP80 starches (Fig 4.11b) is indicative that AMP-AMP interactions during HMT at 80°C, may have negated the expected increase in hydrolysis by hindering the accessibility of glycosidic oxygen to PPA. In comparison with NP100 and NP120 starches, the difference in hydrolysis between WP100 and WP120 starch (WP120> WP100) was very significant (Fig 4.11b). This could be attributed to greater disruption of H-bonds between AMP chains at 120°C, which renders the AMP chains more susceptible to α-amylolysis (sec 4.8). The large difference in hydrolysis between WP120 and WP130 starches reflects the presence of more A-type crystallites (Fig 4.5, Table 4.3) and to the presence of interrupted helices in the latter (sec 4.8). The results indicate that reactivity of PPA towards HMT starches is influenced by the interplay of :1) interactions between starch chains, 2) structural disorganization near the granular surface, 3) amount of A-type crystallites, 4) double helical organization within the AMP crystallites.

Bright field (BFM) and cross-polarized light microscopy of (CPLM) of PPA hydrolysed (24h) residues of NP and WP starches before and after HMT at 100° and 130°C are presented in Fig 4.12. CPLM showed decreased birefringence intensity at the granule centre of both hydrolysed residues of NP (Fig 4.12A) and WP (Fig 4.12B) starches. BFM (Fig 4.12A) and CLSM (Fig 4.13) showed peripheral exocorrosion in hydrolysed NP starch. Whereas, SEM (Fig 4.14) showed the presence of pitting and roughened surface that varied from granule to granule. Hydrolysed WP starch showed extensive splitting (Fig 4.12B, Fig 4.13) but very little peripheral exocorrosion. SEM of hydrolysed WP starch (Fig 4.14) revealed the presence of numerous pores that were larger in diameter than the pores present in unhydrolysed granules (Fig 4.1) (largely confined to the exterior regions of the granule). Granule splitting and roughened surfaces were also seen in many granules (Fig 4.14).

Fig 4.12 Microscopy of hydrolysed (pancreatic α-amylase/24h) residues of native and HMT (100° and 130°C) normal potato (NP) [A] and waxy potato (WP) [B] starches. For NP and WP starches the same field is shown for bright field (upper frame) and between cross polarized light (lower frame).

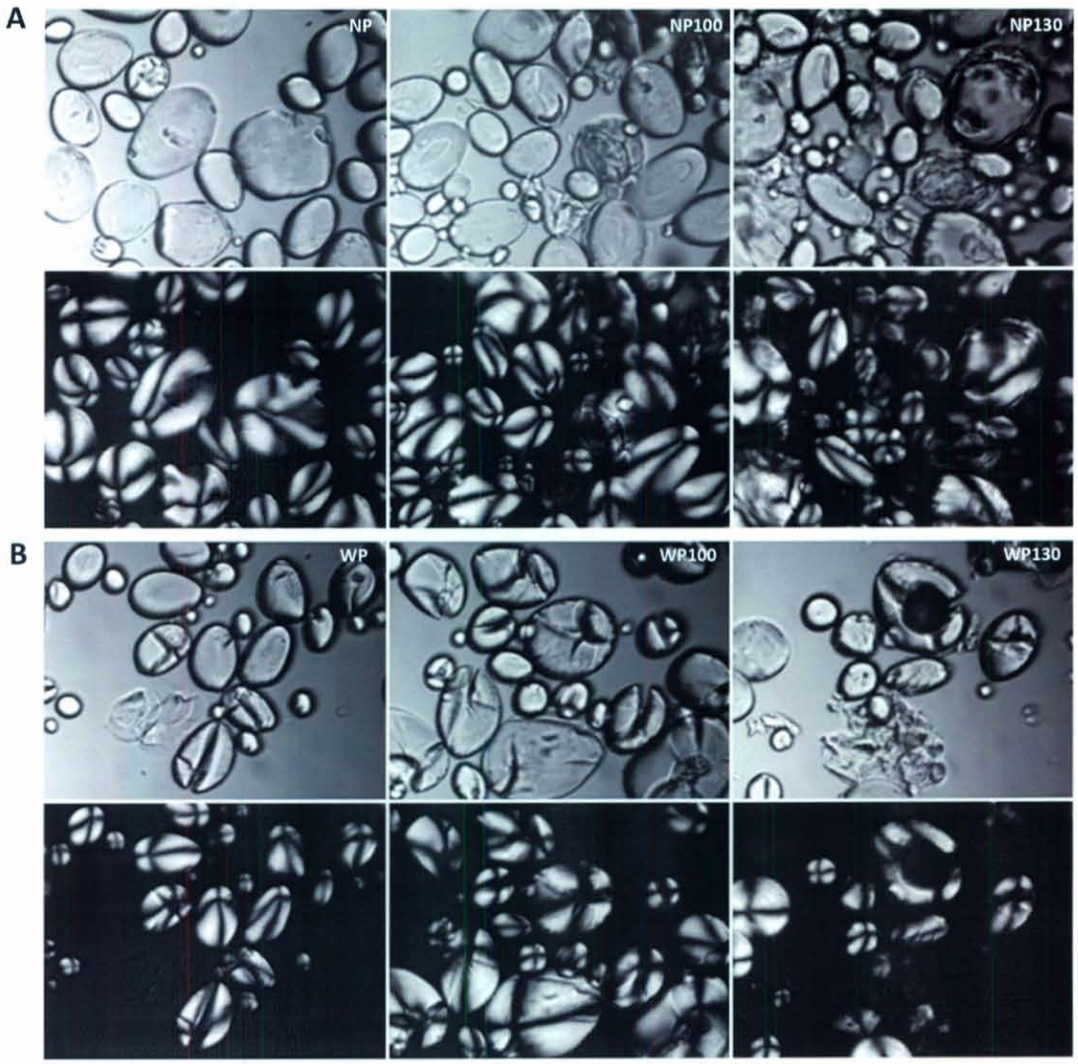
A
NP
NP100
NP130
B
WP
WP100
WP130

Fig 4.13 Confocal laser scanning microscopy (APTS stained) of porcine pancreatic α-amylase (PPA) hydrolysed (24h) granules of native normal (NP), NP heat-moisture treated at 100°C (NP100), NP heat-moisture treated at 130°C (NP130), native waxy potato (WP), WP heat-moisture treated at 100°C (WP100) and WP heat-moisture treated at 130°C (WP130).

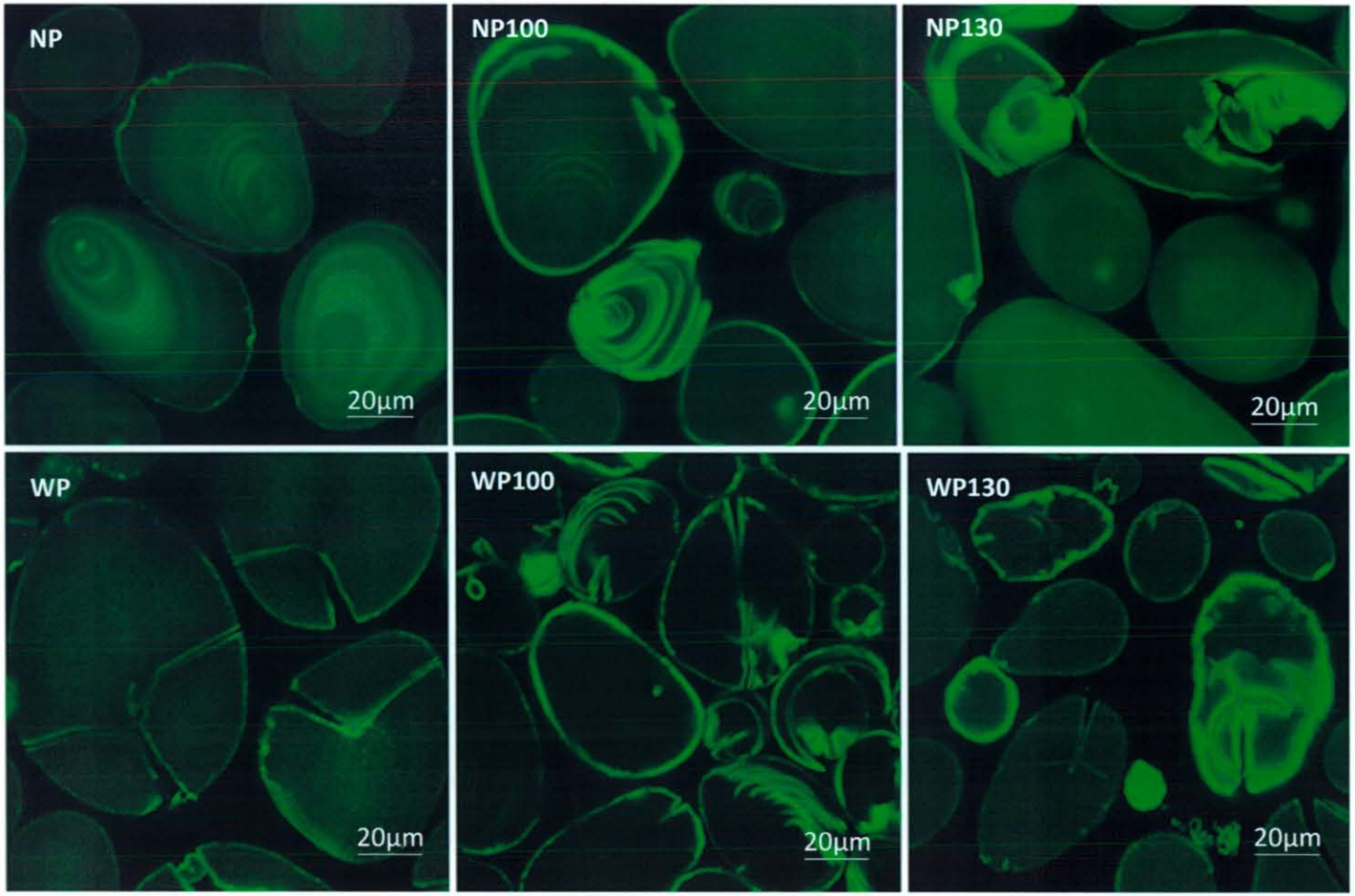
NP
20μm
NP100
20μm
NP130
20μm
WP
20μm
WP100
20μm
WP130
20μm

Fig 4.14 Scanning electron microscopy of porcine pancreatic α-amylase (PPA) hydrolysed (24h) granules of native normal (NP), NP heat-moisture treated at 100°C (NP100), NP heat-moisture treated at 130°C (NP130), native waxy potato (WP), WP heat-moisture treated at 100°C (WP100) and WP heat-moisture treated at 130°C (WP130).

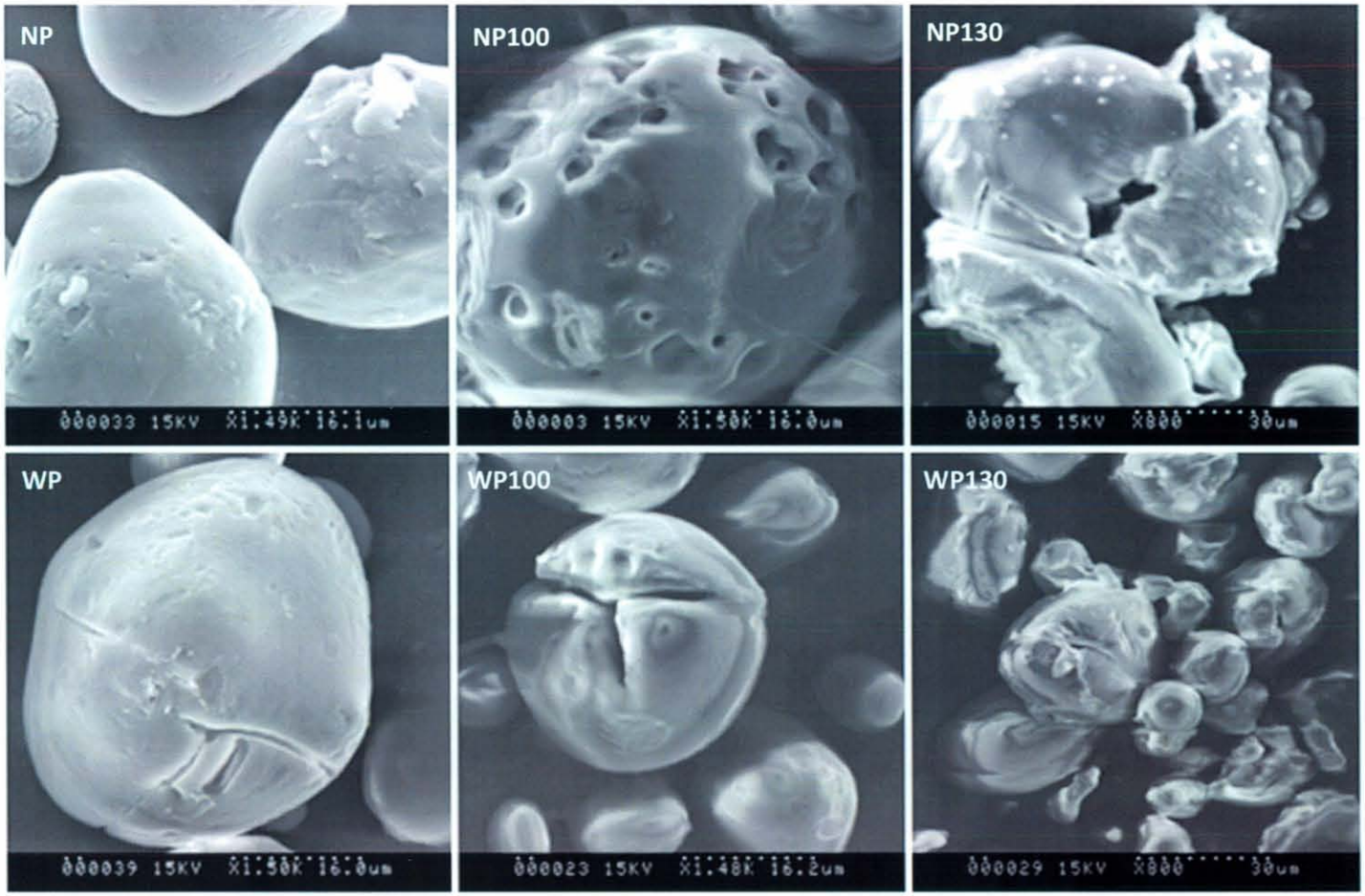
NP
NP100
NP130
WP
WP100
WP130

Blazec and Copeland (2010) have shown by studies on waxy and high amylose wheat starches that growth ring structures are more readily digested in waxy starch granules than in amylose rich maize starches. They attributed this to the absence of amylose in the amorphous layers of waxy starch granules that would allow them to absorb water more readily, thereby facilitating the entry of α-amylase into the granule interior. This suggest that the difference in granule morphology between hydrolysed NP and WP starches could be attributed both to the presence of pores and higher granular swelling (Fig 4.7b,c) in WP starch. In both NP and WP starches, the loss in birefringence intensity on hydrolysis was more pronounced after HMT (Fig 4.12A, B). BFM of NP100 starch showed increased exocorrosion, and some degree of internal degradation near the hilum. A few granules of NP100 starch were deformed (Fig 4.11A). However, granules of WP100 starch (Fig 4.12B) exhibited extensive splitting. The extent of splitting varied among the granules (Fig 4.12B). SEM of NP100 starch showed numerous large pores on the granule surface, which appeared spongy. Whereas, WP100 starch showed many split granules. CLSM of NP100 starch revealed more extensive peripheral exocorrosion than in NP starch and some degree of internal degradation (Fig 4.13). Whereas, WP100 showed many split granules and peripheral exocorrosion. In both NP130 and WP130 starches, the loss in birefringence intensity was more pronounced than at 100°C (Fig 4.12A, B). BFM showed that granules of both NP130 (Fig 4.12A) and WP130 (Fig 4.12B) starches were more extensively degraded than at 100°C. Granules of NP130 starch showed the presence of holes on granule surfaces, internal degradation and granule deformation (Fig 4.12A). However, in WP130 starch, granules were split and some were disintegrated (Fig 4.12B). SEM revealed granule splitting in some granules of NP130 and WP130 starches (Fig 4.14). The extent of this splitting being more pronounced in the latter. CLSM of NP130 and WP130 starches (Fig 4.13), revealed extensive degradation near the hilum,

whereas, some granules were not degraded. The above data showed that granules of both NP and WP starches exhibited heterogeneity in degradation (NP>WP) in their native and HMT states. This could reflect differences within each granule with respect to: 1) molecular order near the granule surface, 2) variation in granule size, 3) extent to which B-type crystallites were converted to A-type crystallites during HMT, 4) extent of disorganization of the region surrounding the hilum during HMT, 5) extent to which double helical chains unravel during HMT and 6) arrangement of amylose and amylopectin within the granule interior. The greater level of heterogeneity in NP starch could be attributed to its higher amylose content.

CHAPTER 5

SUMMARY AND CONCLUSIONS

The data obtained from X-Ray, ATR-FTIR, K/S spectra, SF, AML, DSC, RVA showed that structural and property changes on HMT of NP and WP starches were mainly influenced by differences in starch chain mobility at the different temperatures of HMT. Starch chain mobility, in turn was influenced by the interplay between the extent to which B-type crystallites were transformed into A+B-type crystallites and the kinetic energy imparted to starch chains.

HMT at all temperatures (80, 100, 120 and 130°C) changed the X-ray pattern (B→A+B) of both NP and WP. The extent of this transformation increased with increase in HMT temperature. The decrease in AML and K/S intensity on HMT at low temperatures (80-100°C) can be attributed to additional interaction between starch chains. The increase in AML on HMT at higher temperatures (120 and 130°C) is indicative that at 120°C and 130°C, hydrogen bonds between co-crystallized AM and AMP chains may have disrupted. The decrease in ΔH at 120° and 130°C reflect mainly disruption of hydrogen bonds present in: 1) double helices formed between AM and AMP chains, and 2) double helices forming the AMP clusters. Lower K/S maxima of NP130 starch and the shift to a lower λ_{max} (570nm), suggests that intra molecular hydrogen bonds stabilizing helical region may have disrupted on HMT at 130°C. AMP chain length distribution of both native and HMT starches remained unchanged at all HMT temperatures. This suggests that covalent linkages of AMP were not broken under the HMT conditions (27% moisture, 16h, 80-130°C) used in this study.

Therefore, the main type of structural changes that had great impact on physicochemical properties at different temperatures of HMT were polymorphic transition (B → A+B), AM-AM, AM-AMP and AMP-AMP interactions (80 and 100°C), disruption of hydrogen bonds between co-crystallized AM and AMP chains and between AMP-AMP chains (120 and 130°C), disorganization of AMP chains near the vicinity of the hilum (100, 120 and 130°C), and formation of interrupted helices (130°C). The extent of changes to starch structure and properties on HMT was different in normal and waxy starches due to differences in their amylose content and amylopectin chain mobility.

The susceptibility of NP and WP starches towards PPA hydrolysis decreased with HMT at 80°C, but increased with HMT at 100-130°C. This suggested that PPA hydrolysis of HMT starches was influenced by the interplay of: 1) the amount of A-type crystallites, 2) starch chain interactions and 3) changes to the double helical conformation. There are differences between the mode of attack by pancreatic α-amylase on NP and WP starch granules. These differences in granule morphology in PPA hydrolyzed NP and WP starches were largely influenced by the presence of pores and higher granular swelling in the latter. NP and WP starches exhibited heterogeneity in degradation (NP>WP) in both their native and HMT states. This suggests that within each granule, variations exist with respect to molecular order, double helical packing arrangement of AM and AMP and the proportion of A- to B-type unit cells.

DIRECTIONS FOR FUTURE RESEARCH

- Heat-moisture treatment of starch is of interest due to its possible applications in the food industry, either for use alone or in combination with other types of starch modifications. Studies showed that HMT changes starch structure and its physicochemical properties. The type and extent of these changes are influenced by starch source, starch composition and treatment conditions. However, the exact molecular mechanisms of HMT still remains poorly understood. This study provided only a partial glimpse into the molecular mechanism of HMT. In order to further understand the molecular mechanism of HMT, experiments must be conducted at different levels of time/moisture/temperature combinations on starches varying widely in amylose content (maize, barley and rice).

- Presently, there is an interest in developing starches with modified digestion (slowly digestible starch [SDS], and resistant starch [RS]) characteristics. These modified products have the potential to benefit human health through moderation of the glycemic response and as a source of prebiotic carbohydrate. Results showed that starch digestibility is influenced by HMT temperature. Thus, HMT may be a tool for modifying starch digestibility.

- Acid hydrolysis has been used as a tool to modify starch properties. This is due to the preferential attack of H_3O^+ on the amorphous domain. Thus, it would be worthwhile to investigate how acid hydrolysis followed by HMT and HMT followed by acid hydrolysis would influence starch properties in normal, waxy and high amylose starches.

REFERENCES

AACC (2000). Approved methods of the AACC (10th ed.), St. Paul, MN, USA: American Association of Cereal Chemists.

Abraham, T. E. (1993). Stabilization of paste viscosity of cassava starch by heat–moisture treatment. *Starch, 43,* 131–135.

Absar, N., Zaidul, I. S. M., Takigawa, S., Hashimoto, N., Matsuura-Endo, C., Yamauchi, H. and Noda, T. (2009). Enzymatic hydrolysis of potato starches containing different amounts of phosphorus. *Food Chemistry, 112*, 57-62.

Acker, L. (1977). The lipids of starch—Research between carbohydrates and lipids. *Fette Seifen Anstrichmittel, 79*, 1-9.

Adebowale, K. O. and Lawal, O. S. (2003). Microstructure, physicochemical properties and retrogradation behaviour of mucuna bean (*Mucuna puriens*) starch on heat moisture treatment. *Food Hydrocolloid, 17*, 265–272.

Adebowale, K. O., Afolabi, T. A. and Olu-Owolabi, B. I. (2005a). Hydrothermal treatment of finger millet (*Eleusine coracana*) starch. *Food Hydrocolloids, 19*, 974–983

Adebowale, K. O., Afolabi, T. A., Olu-Owolabi, B. I., Olawum, E. K., and Lawal, O. S. (2005b). Functional properties of native, physically and chemically modified breadfruit (Artocarpus artilis) starch. *Industrial Crops and Products, 21*, 343–351.

Anderson, A. K., Guraya, H. S. (2006). Effects of microwave heat-moisture treatment on properties of waxy and non-waxy rice starches. *Food Chemistry, 97*, 318–323.

Anderson, A. K., Guraya, H. S., James, C. and Salvaggio, L. (2002). Digestibility and pasting properties of rice starch heat-moisture treated at the melting temperature (*T*m). *Starch, 54,* 401-409.

Ao, Z., Simsek, S., Zhang, G., Venkatachalam, M., Reuhs, B. L. and Hamaker, B. R. (2007). Starch with a slow digestion property produced by altering its chain length, branch density, and crystalline structure. *Journal of Agricultural and Food Chemistry, 55*, 4540–4547.

Atkin, N. J., Cheng, S. L., Abeysekera, R. M. and Robards, A. W. (1999). Localisation of amylose and amylopectin in starch granules using enzyme-gold labeling. *Starch, 51*, 163-172.

Atwell, W. A., Hood, L. F., Lineback, D. R., Varriano-Marston, E. and Zobel, H. E. (1988). The terminology and methodology associated with basic starch phenomena. *Cereal Foods World, 33*, 306–311.

Badenhuizen, N.P. (1969). The biogenesis of starch granules in higher plants. Appleton Crofts, NY.

Bailey, 1. M. and Whelan, W. J. (1961). Physical properties of starch. *Journal of Biological Chemistry, 236,* 969-973.

Baker, A. A., Miles, M. J. and Helbert, W. (2001). Internal structure of the starch granule revealed by AFM. *Carbohydrate Research, 330*, 249–256.

Baker, L. A. and Rayas-Duarte, P. (1998). Freeze-thaw stability of amaranth starch and the effects of salt and sugars. *Cereal Chemistry, 75*, 301–303.

Baldwin, P. M., Davies, M. C., and Melia, C. D. (1997). Starch granule surface imaging using low-voltage scanning electron microscopy and atomic force microscopy. *Biological Macromolecules, 21*, 103-107.

Banks, W. and Greenwood, C. T. (1967). The fractionation of laboratory- isolated cereal starches using dimethyl sulphoxide. *Starch, 19*, 394–398.

Banks, W. and Greenwood, C. T. (1971). Amylose: a non helical biopolymer in aqueous solution. *Polymer, 12,* 141-145

Banks, W. and Greenwood, C. T. (1975). *Starch and its Components*, Chapter 4, Edinburgh University Press, Edinburgh

Banks, W., Greenwood, C. T. and Khan, K. M. (1971). The interaction of linear amylose oligomers with iodine. *Carbohydrate Research, 17*, 25-33.

Baum, B. R. and Bailey, L. G. (1987). A survey of endosperm starch granules in the genus Hodeum: a study using image analytic and numerical taxonomic techniques. *Canadian Journal of Botany, 65*, 1563–1569.

Bay-Smidt, A. M., Wischmann, B., Olsen, C. E. and Nielsen, T. H. (1994). Starch bound phosphate in potato as studied by a simple method for determination of organic phosphate and 31P-NMR. *Starch, 46,* 167–172.

Benmoussa, M., Hamaker., B. C., Huang, C. P., Sherman, D. M., Weil, C. F. and BeMiller, J. N. (2010). Elucidation of maize endosperm starch granule channel proteins and evidence for plastoskeletal structures in maize endosperm amyloplasts. *Journal of Cereal Science, 52*, 22-29

Bertoft, E. (2004). Lintnerization of two amylose-free starches of A- and B- crystalline types, respectively. *Starch*, 56, 167-180.

Bertoft, E. (1991). Investigation of the fine structure of alpha-dextrins derived from amylopectin and their relation to the structure of waxy-maize starch. *Carbohydrate Research, 212,* 229–244.

Bertoft, E. and Manelius, R. (1992). A method for the study of the enzymic hydrolysis of starch granules. *Carbohydrate Research, 227*, 269–283.

Bertoft, E. and Qin, Z. (1993). Studies on the Structure of Pea Starches Part 4: Intermediate material of wrinkled pea starch. *Starch, 45,* 420-425.

Bijttebier, A., Goesaert, H. and Delcour, J. A. (2008). Amylase action pattern on starch polymers. *Biologia, 63,* 989-999.

Biliaderis (1998). Structures and phase transitions of starch polymers. In R. H. Walter (Ed), *Polysaccharide association structures in food,* (pp. 57-168). Marcell Dekker, Inc. NY

Biliaderis, C. G. (1992). Structures and phase transitions of starch in food systems. *Food Technology, 46*, 98–109.

Biliaderis, C. G. (2009). Structural transitions and related physical properties of starch. In J. BeMiller, and R. Whistler (Eds), *Starch:Chemistry and Technology*, (pp 293-359). Academic Press, NY.

Biliaderis, C. G. and Seneviratne, H. D. (1990). On the supermolecular structure and metastability of glycerol monostearate-amylose complex. *Carbohydrate Polymers, 13*, 185-206.

Biliaderis, C. G. Grant, D. R. and Vose, J. R. (1981). Structure characterization of legume starches. II. Studies on acid treated starches. *Cereal Chemistry, 58*, 502–507.

Biliaderis, C. G. and Galloway, G. (1989). Crystallization behaviour of amylose-V complexes: structure-property relationships. *Carbohydrate Research*, 189, 31-48.

Biliaderis, C. G. and Seneviratne, H. D. (1990). On the supermolecular structure and metastability of glycerol monostearate-amylose complex. *Carbohydrate Polymers*, 13, 185-206.

Biliaderis, C. G., Page, C. M., Maurice, T. J. and Juliano, B. O. (1986a). Thermal characterization of rice starches: a polymeric approach to phase transition of granular starch. *Journal of Agricultural and Food Chemistry, 34,* 6–14.

Biliaderis, C. G., Tonogai, J. R., Perez, C. M. and Juliano, B. O. (1993). Thermophysical properties of milled rice starch as influenced by variety and parboiling method. *Cereal Chemistry, 70*, 512-516.

Biliaderis, C. G. (1998). Structures and phase transitions of starch polymers. In R. H. Walter, (Ed), *Polysaccharide Association Structures in Foods*, (pp. 57–168). Marcel Dekker, NY.

Biliaderis, C. G., Page, C. M. and Maurice, T. J. (1986b). Non-equilibrium melting of amylose-V complexes. *Carbohydrate Polymers, 6*, 269–288.

Bird, A. R., Lopez-Rubio, A., Shrestha, A. K. and Gidley, M. J. (2009). Resistant starch in vitro and in vivo: Factors determining yield, structure, and physiological relevance. In S.

Kasapis, I. T. Norton, and J. B. Ubbink (Eds.), *Modern biopolymer sciences* (pp. 449–512). Academic Press, London.

Blanshard, J. M. V. (1987). Starch granule structure and function: a physicochemical approach. In T. Galliard (Ed.), Starch: Properties and potential (pp. 16). Chichester: John Wiley and Sons.

Blaszczak, W. Fornal, J. and Amarowicz, R. (2003). Lipids of wheat, corn and potato starch. *Journal of Food Lipids, 10*, 301-312.

Blazeck, J. and Copeland, L. (2010). Amylolysis of wheat starches. II. Degradation pattern of native starch granules with varying functional properties. *Journal of Cereal science*, doi:10.1016/j.jcs.2010.06.011.

Blennow, A., Bay-Smidt, A. M., Olsen, C. E. and Møller, B. L. (2000). The distribution of covalently bound phosphate in the starch granule in relation to starch crystallinity. *International Journal of Biological Macromolecules, 27,* 211–218.

Blennow, A., Bay-Smidt, A. M., Wischmann, B., Olsen, C. E. and Lindberg-Møller, B. (1998). The degree of starch phosphorylation is related to the chain length distribution of the neutral and the phosphorylated chains of amylopectin. *Carbohydrate Research, 307*, 45–54.

Blennow, A., Hansen, M., Schulz, A., Jørgensen, K., Donald, A. M. and Sanderson, J. (2003). The molecular deposition of transgenically modified starch in the starch granule as imaged by functional microscopy. *Journal of Structural Biology, 143*, 229– 241

Bogracheva, T. Y. Wang Y. L. and Hedley, C. L. (2001). The effect of water content on the ordered/disordered structures in starches. *Biopolymers, 58*, 247–259.

Bogracheva, T. Y., Morris, V. J., Ring, S. G. and Hedley, C. L. (1998). The granular structure of C-type pea starch and its role in gelatinization. *Biopolymers, 45*, 323–332.

Brand, J. C., Colagiuri, S., Crossman, S., Allen, A. and Truswell, A. S. (1991). Low glycemic index carbohydrate foods improve glucose control in non-insulin dependent diabetes mellitus (NIDDM). *Diabetes Care 14*, 95–101.

Brumovsky, L. A., Brumovsky, J. O., Fretes, M. R. and Peralta, J. M. (2009). Quantification of resistant starch in several starch sources treated thermally. *International Journal of Food Properties, 12*, 451-460.

Brumovsky, J. O. and Thompson,D. B. (2001). Production of boiling stable granular resistant starch by partial acid hydrolysis and hydrothermal treatments of high amylose maize starch. *Cereal Chemistry, 79*, 680–689.

Bruner, R. L. (1964). Determination of reducing value. In R.L. Whistler (Ed), *Methods in Carbohydrate Chemistry*: *Starch* (Vol. IV, pp. 67-71). Academic Press, NY.

Buléon, A. Colonna, P. Planchot V. and Ball, S. (1998). Starch granules: Structure and biosynthesis. *International Journal of Biological Macromolecules 23*, 85–112.

Buléon, A., Bizot, H., Delage, M. M. and Multon, J. L. (1982). Evolution of Crystallinity and Specific Gravity of Potato Starch versus Water Ad- and Desorption. *Starch, 34*, 361–366.

Bulpin, P. V., Welsh, E. J. and Morris, E. R. (1982). Physical characterization of amylose-fatty acid complexes in granules and in solution. *Starch, 34,* 335.

Burrell, M. M. (2003). Starch: the need for improved quality or quantity—an overview.*Journal of Experimental Botany, 54,*451-456.

Cairns, P., Bogracheva, T. Y., Ring, S. G., Hedley, C. L. and Morris, V. J. (1997). Determination of the polymorphic composition of smooth pea starch. *Carbohydrate Polymers, 32*, 275–282.

Calabrese, V. T. and Khan, A., (1999). Amylose–iodine complex formation without KI: evidence for absence of iodide ions within the complex. *Journal of Polymer Science: Part A, 37*, 2711–2717.

Cameron, R. E. and Donald, A. M., (1992). A small-angle X-ray scattering study of the annealing and gelatinisation of starch. *Polymer*, *33*, 2628–2635.

Cao, H. and Shannon, J. C. (1997). BT1, a possible adenylate translocator, is developmentally expressed in maize endosperm but not detected in starchy tissues from several other species. *Physiologia Plantarum, 100*, 400–406.

Capron, I., Robert, P., Colonna, P., Brogly, M. and Planchot, V. (2007). Starch in rubbery and glassy states by FTIR spectroscopy. *Carbohydrate Polymers*, 68, 249-259.

Cardoso, M. B., Putaux, J. L., Nishiyama, Y., Helbert, W., Hytch, M., Silveira, N. P. and Chanzy, H. (2007). Single crystals of V-amylose complexed with α-naphthol *Biomacromolecules, 8,* 1319-1326.

Carlson, T. L. G., Larsson, K., Dinh-Nguyen, N. and Krog, N. (1979). A study of the amylose–monoglyceride complex by Raman spectroscopy. *Starch, 31*, 222–224.

Cheetham, N. W. H. and Tao, L. P. (1998a). Solid state NMR studies on the structural and conformational properties of natural maize starches. *Carbohydrate Polymers, 36*, 285–292.

Cheetham, N. W. H. and Tao, L. P. (1998b) Amylose conformational transitions in binary DMSO/water mixtures. *Carbohydrate Polymers, 35*, 287–295.

Chung, H. J., Hoover, R. and Liu, Q. (2009b). The impact of single and dual hydrothermal modifications on the molecular structure and physicochemical properties of normal corn starch. *International Journal of Biological Macromolecules*, *44*, 203–210.

Chung, H. J., Liu, Q. and Hoover, R. (2009a). Impact of annealing and heat-moisture treatment on rapidly digestible, slowly digestible and resistant starch levels in native and gelatinized corn, pea and lentil starches. *Carbohydrate Polymers, 75,* 436–447.

Chung, H. J., Liu, Q. and Hoover, R. (2010). Effect of single and dual hydrothermal treatments on the crystalline structure, thermal properties and nutritional fractions of pea, lentil and navy bean starches. *Carbohydrate Polymers, 43*, 501–508.

Cleven, R., van den Berg, C. and van der Plas, L. (1978). Crystal Structure of Hydrated Potato Starch. *Starch, 30*, 223–228.

Collado, L. S. and Corke, H. (1999). Heat-moisture treatment effects on sweet potato starches differing in amylose content. *Food Chemistry, 65*, 339–346

Colonna, P. and Buleon, A. (2009). Thermal transitions of starches. In A. C. Bertolini, (Ed), Starches: Characterization, properties and applications, (pp 72-95). CRC Press, Boca Raton, FL.

Colonna, P., Buléon, A. and Lemarié, F. (1988), Action of *Bacillus subtilis* α-amylase on native wheat starch. *Biotechnology and Bioengineering, 31*, 895–904.

Colonna, P., Leloup, V. and Buleon, A. (1992). Limiting factors of starch hydrolysis. *European Journal of Clinical Nutrition, 46*, S17-S32.

Cooke, D. and Gidley, M. (1992). Loss of crystallinity and molecular order during starch gelatinization: origin of the enthalpic transition. *Carbohydrate Research*, 227, 103-112.

Copeland, L., Blazek, J., Salman, H. and Tang, M. C. (2009). Form and functionality of starch, *Food Hydrocolloids, 23*, 1527-1534

Cowie, J. M. G. (1961). Studies on amylose and its derivatives. I. Molecular size and configuration of amylose molecules in various solvents. *Die Makromoleculare Chemie, 42*, 230-247.

Craig, S. A. S., Maningat, C. C., Seib, P. A. and Hoseney, R. C. (1989). Starch paste clarity. *Cereal Chemistry 66*, 173–182.

Davis, H. and Khan, A. (1994). Determining the chromophore in the amylopectin-iodine complex by theoretical and experimental studies. *Journal of Polymer Science Part A: Polymer Chemistry, 32,* 2257-2265.

Davis, H., Skrzypek, W. and Khan, A. (1994). Iodine binding by amylopectin and stability of the amylopectin-iodine complex. *Journal of Polymer Science Part A: Polymer Chemistry, 32*, 2267-2274.

Davis, J. P., Supatcharee, N., Khanddelwal, R. L. and Chibbar, R. N. (2003). Synthesis of novel starches in Planta: Opportunities and challenges. *Starch, 55*, 107-120.

Debet, M. R. and Gidley, M. J. (2006). Three classes of starch granule swelling: Influence of surface proteins and lipids. *Carbohydrate Polymers, 64,* 452-465.

Dona, A. C., pages, G., Gilbert, R. G. and Kuchel, P. W. (2010). Digestion of starch: In vivo and in vitro kinetic models used to characterise oligosaccharide or glucose release. *Carbohydrate Polymers, 80,* 599-617.

Donald, A. M. (2004). Understanding starch structure and functionality. In: A-C. Eliasson, (Ed), *Starch in food: Structure, function and applications* (pp. 156-184). Woodhead Publishing Limited/CRC Press LLC, Cambridge/Boca Raton.

Donald, A. M. Kato, K. L., Perry, A. P and Waigh, T. A. (2001). Scattering studies of internal structure of starch granules. *Starch, 53,* 504–512.

Donovan, J. W. (1979). Phase transitions of the starch-water system. *Biopolymers 18,* 263–275.

Donovan, J. W. and Mapes, C. J. (1980). Multiple phase transitions of starches and Naegeli amylodextrins. *Starch, 32,*190-193.

Doublier, J. L. (1987). A rheological comparison of wheat, maize, faba bean and smooth pea starches. *Journal of Cereal Science, 5,* 247–262.

Eerlingen, R. C., Jacobs, H., Block, K. and Delcour, J. A. (1997). Effects of hydrothermal treatments on the rheological properties of potato starch. *Carbohydrate Research, 297,* 347–356.

Eerlingen, R.C., Jacobs, H., Van Win, H. and Delcour, J. A. (1996). Effect of hydrothermal treatment on the gelatinization properties of potato starch as measured by differential scanning calorimetry. *Journal of Thermal Analysis, 47,* 1229-1246.

ELIANE™ (2006), http://www.agfdt.de/loads/st06/semeiabb.pdf (2010-09-28).

Eliasson, A. C. and Gudmundsson, M. (1996). Starch: physicochemical and functional aspects. In A. C. Eliasson, (Ed), *Carbohydrates in food* (pp. 431–503). Marcel Dekker.

Eliasson, A. C. and Krog, N. (1985). Physical properties of amylose-monoglyceride complexes. *Journal of Cereal Science, 3,* 239–248.

Englyst, H. N., Kingman, S. M. and Cummings, J. H. (1992). Classification and measurement of nutritionally important starch fractions. *European Journal of Clinical Nutrition, 46*: 533–550.

Eppendorfer, W. H., Eggum, B. O. and Bille, S. W. (1979). Nutritive value of potato crude protein as influenced by manuring and amino acid composition. *Journal of Science Food and Agriculture 30*, 361-368.

Evans, A. and Thompson, D. B. (2004). Resistance to amylase digestion in four native high-amylose maize starches. *Cereal Chemistry 81*, 31–37.

Evans, A., McNish, N. and Thompson, D. B. (2003). Polarization colors of lightly iodine-stained maize starch for amylose-extender and related genotypes in the W64A inbred line. *Starch, 55,* 250–257.

Evans, I. D. and Haisman, D. R. (1982). The effect of solutes on the gelatinization temperature range of potato starch. *Starch, 34,* 224–231.

Evans, I. D., and Haisman, D. R. (1979). Rheology of gelatinized starch suspensions. *Journal of Textural Studies, 10*, 347–370.

Evers, A. D. and Juliano, B. O. (1976). Varietal Differences in Surface Ultrastructure of Endosperm Cells and Starch Granules of Rice. *Starch, 28*, 160–166.

Fannon J. E., Hauber R. J., and BeMiller J. N., 1992. Surface pores of starch granules. *Cereal Chemistry*, *69*, 284-288.

Fannon, J. E., Gray, J. A., Gunawan, N., Huber, K. C. and BeMiller, J. N. (2004). Heterogeneity of starch granules and the effect of granule channelization on starch modification. *Cellulose, 11,* 247-254.

Fannon, J. E., Shull, J. M. and BeMiller, J. N. (1993). Interior channels of starch granules. *Cereal Chemistry, 70,* 611-613.

Franco, C. M. L., Ciacco, C. F. and Tavares, D. Q. (1995). Effect of the heat- moisture treatment on the enzymatic susceptibility of corn starch granules. *Starch, 47,* 223–228.

French, D. (1972). Fine structure of starch and its relationship to the organization of starch granules. *Starch 19*, 8-25.

French, D. (1984). Organization of starch granules. In R. L. Whistler, J. N. Bemiller, and E. F. Paschall, (Eds), *Starch: Chemistry and Technology*, (pp. 183-247). Academic Press, Orlando, FL.

Fujii, M., Honda, K. and Fujita, H. (1973). Dilute solution of amylose in dimethylsulfoxide. *Biopolymers, 12*, 1177-1195.

Fuwa, H. (1982). Enzymic degradation of starch granules. *Journal of Japanese Society of Starch Science*, *29*, 99–106.

Fuwa, H., Nakajima, M., Hamada, A. and Glover, D. V. (1977). Comparative susceptibility to amylases of starches from different plant species and several single endosperm mutants and their double-mutant combinations with OPAQUE-2 inbred Oh43 maize. *Cereal Chemistry*, *54*, 230–237.

Gallant, D. J., Bouchet, B. and Baldwin, P. M. (1997). Microscopy of starch: evidence of a new level of granule organization. *Carbohydrate Polymers, 32*, 177–191.

Gallant, D. J., Bouchet, B., Buléon A. and Pérez, S. (1992). Physical characteristics of starch granules and susceptibility to enzymatic degradation. *European Journal of Clinical Nutrition, 46,* S3–S16.

Galliard, T. (1987). *Starch: properties and potential*. (Vol 13): John Wiley, Chichester, U.K.

Galliard, T. and Bowler, P. (1987). Morphology and composition of starch. In T. Galliard, (Ed), *Starch, Properties and Potential,* (pp. 55-78) . John Wiley, Chichester, UK.

Genkina, N. K., Kiseleva, V. I. and Noda, T. (2009). Comparative investigation on acid hydrolysis of sweet potato starches with different amylopectin chain-length. *Starch,* 61, 321–325.

Gerard, C., Barron, C., Colonna, P. and Planchot, V. (2001). Amylose determination in genetically modified starches. *Carbohydrate Polymers, 44*, 19–27.

Gerard, C., Colonna, P. Buleon, A. and Planchot, V. (2002). Order in maize mutant starches revealed by mild acid hydrolysis. *Carbohydrate Polymers*, *48,* 131–141.

Gerard, C., Colonna, P., Buleon, A. and Planchot, V. (2001). Amylolysis of maize mutant starches. *Journal of Science and Food Agriculture, 81*, 1281-1287.

Gernat, Ch., Radosta, S., Anger, H. and Damaschun, G. (1993). Crystalline parts of three different conformations detected in native and enzymatically degraded starches. *Starch/Starke, 45*, 309–314.

Gidley, M. J., and Bulpin, P. V. (1987). Crystallisation of malto-oligosaccharides as model of the crystalline forms of starch: Minimum chain-length requirement for the formation of double helices. *Carbohydrate Research, 161*, 291–300.

Gidley, M. J. and Bociek, S. M. (1985). Molecular organization in starches: A ^{13}C.CP/MAS NMR study. *Journal of the American Chemical Society*, *107*, 7040-7044.

Gillian, D. A. Sargent, J. G. and Schofield, J. D. (1981). Wheat starch granule proteins: the isolation and characterization of a salt-extractable protein from starch granules. *Journal of the Science of Food and Agriculture, 32,* 371–377.

Glaring, M. A., Koch, C. B. and Blennow, A. (2006). Genotype-specific spatial distribution of starch molecules in the starch granule: a combined CLSM and SEM approach, *Biomacromolecules, 7,* 2310–2320

Godet, M. C., Bizot, H. and Buléon, A. (1995). Crystallization of amylose-fatty acid complexes prepared with different amylose chain lengths. *Carbohydrate Polymers*, *27*, 47–52.

Goesaert, H., Slade, L., Levine, H. and Delcour, J. A. (2009). Amylases and bread firming – an integrated view. *Journal of Cereal Science*, *50,* 345-352.

Gomand, S. V., Lamberts, L., Visser, R. G. F. and Delcour, J. A. (2010). Physicochemical properties of potato and cassava starches and their mutants in relation to their structural properties. *Food Hydrocolloids*, *24*, 424-433.

Grabitske, A. H. and Slavin, J. L. (2009). Gastrointestinal effects of low digestible carbohydrates. *Critical Review in Food Science and Nutrition, 49*, 327–360.

Gray, G. M. (1992). Starch digestion and absorption in nonruminants. *Journal of Nutrition, 122*, 172–177.

Gray, J. A. and BeMiller, J. N. (2004). Development and utilization of reflectance confocal laser scanning microscopy to locate reaction sites in modified starch granules. *Cereal Chemistry, 81*, 278–286.

Greenwell, P. and Scofield, J. D. (1986). A starch granule protein associated with endosperm softness in wheat. *Cereal Chemistry, 63*, 379-380.

Greenwood, C. T. and Thompson, J. (1962). Physiochemical studies on starches. XXIV. Fractionation and characterization of starches of various plant origins. *Journal of Chemical Society, 42,* 222-229.

Gunaratne, A. and Corke, H. (2007). Gelatinizing, pasting and gelling properties of potato and amaranth starch mixtures. *Cereal Chemistry, 84*, 22–29.

Gunaratne, A. and Hoover, R. (2002). Effect of heat-moisture treatment on the structure and physicochemical properties of tuber and root starches. *Carbohydrate Polymers*, *40*, 425-437.

Gunaratne, A., Kong, X. and Corke, H. (2010). Functional properties and retrogradation of heat-moisture treated wheat and potato starches in the presence of hydroxypropyl β-cyclodextrin. *Starch, 62*, 69–77.

Guraya, H. S., Kadan, R. S. and Champagne, E. T. (1997). Effect of rice starch–lipid complexes on in vitro digestibility, complexing index, and viscosity. *Cereal Chemistry, 74*, 561–565.

Hagenimana, A. and Ding, X. (2005). A comparative study on pasting and hydration properties of native rice starches and their mixtures. *Cereal Chemistry, 82*, 72–76.

Hall, D. M., and Sayre, J. G. (1970). A scanning electron microscope study of starches. II. Cereal starches. *Textile Research Journal, 40,* 256-266.

Han, X. Z. and Hamaker, B. R. (2002). Location of starch granule-associated proteins revealed by confocal laser scanning microscopy. *Journal of Cereal Science, 35*, 109–116.

Han, X. Z., Benmoussa, M., Gray, J. A., BeMiller, J. N. and Hamaker, B. R. (2005). Detection of proteins in starch granule channels. *Cereal Chemistry, 82*, 351-355.

Hanashiro, I., Tagawa, M., Shibahara, S., Iwata, K., Takeda, Y. (2002). Examination of molar-based distribution of A, B and C chains of amylopectin by fluorescent labelling with 2-aminopyridine. *Carbohydrate Research, 337*, 1211–1215.

Hanes, C. S. (1937). The action of amylases in relation to the structure of starch and its metabolism in the plant. Parts I-III. *New Phytologist, 36,* 101–141.

Hedley, L., Bogracheva, T. Y. and Wang, T. L. (2002). A genetic approach to studying the morphology, structure and function of starch granules using pea as a model. *Starch, 54,* 235–242.

Helbert, W. and Chanzy, H. (1994). Single-crystals of V-amylose complexed with n-butanol or n-pentanol structural features and properties. *International Journal of Biological Macromolecules, 16*, 207-213.

Hermans, P. H. and Weidinger, A. (1948). Quantitative X-ray investigations on the crystallinity of cellulose fibres. A background analysis. *Journal of Applied Physics, 19*, 419–506.

Hizukuri, S. (1985). Relationship between the distribution of the chain length of amylopectin and the crystalline structure of starch granules. *Carbohydrate Research, 141*, 295–306.

Hizukuri, S. (1986). Polymodal distribution of the chain lengths of amylopectins, and its significance. *Carbohydrate Research, 147,* 342–347.

Hizukuri, S., Kaneko, T. and Takeda, Y. (1983). Measurement of the chain length of amylopectin and its relevance to the origin or crystalline polymorphism of starch granules. *Biochemica et Biophysica Acta, 760*, 188–191.

Hizukuri, S., Tabata, S. and Nikuni, Z. (1970). Studies on starch phosphate. Part 1. Estimation of glucose-6-phosphate residues in starch and the presence of other bound phosphate(s). *Starch, 22*, 338-343.

Hizukuri, S., Takeda, Y., Shitaozono, T., Abe, J., Ohtakara, A., Takeda, C. and Suzuki, A. (1988), Structure and Properties of Water Chestnut (*Trapa natans* L. var. *bispinosa* Makino) Starch. *Starch, 40*, 165–171

Hizukuri, S., Takeda, Y., Yasuda, M. and Suzuki, A. (1981). Multibranched nature of amylose and the action of de-branching enzymes. *Carbohydrate Research, 94*, 205–213.

Holm, J. and Bjorck, I. (1988). Effect of thermal processing of wheat on starch. II. Enzymic availability. *Journal of Cereal Science, 8*, 261–268.

Holm, J., Bjorck, I., Ostrowska, S., Eliasson, A. C., Asp, N. G., Larsson, K. and Undquist, I. (1983). Digestibility of amylose–lipid complexes in-vitro and in-vivo. *Starch, 35*, 294–297.

Hoover, R. (1998). Starch- Lipid Interactions. In R. H. Walter (Ed), *Polysaccharide association structures in food,* (pp. 227-256). Marcell Dekker, Inc. NY.

Hoover, R. (2000). Acid treated starches. *Food Review International, 16*, 369–392.

Hoover, R. (2001). Composition, molecular structure, and physico-chemical properties of tuber and root starches: a review. *Carbohydrate Polymers, 45,* 253–267.

Hoover, R. (2010). The impact of heat-moisture treatment on molecular structures and properties of starches isolated from different botanical sources. *Critical Reviews in Food Science and Nutrition, 50*, 1-13.

Hoover, R. and Hadziyev, D. (1981). Characterization of potato starch and its monoglyceride complexes. *Starch, 33*, 290–330.

Hoover, R. and Manuel, H. (1996). The effect of heat-moisture treatment on the structure and physicochemical properties of normal maize, waxy maize, dull waxy maize and amylomaize V starches. *Journal of Cereal Science, 23*, 153-162.

Hoover, R. and Manuel, H. (1995). A comparative study of the physicochemical properties of starches from two lentil cultivars. *Food Chemistry, 53*, 275-284.

Hoover, R. and Ratnayake, W.S. (2004). Determination of total amylose content of starch. In Wrolstad *et al.* (Eds.), *Handbook of Food Analytical Chemistry – Water, protein, enzymes, lipids, and carbohydrates* (pp. 689-691). Wiley-Interscience, Hoboken, NJ.

Hoover, R. and Sosulski, F. (1986). Effect of cross linking on functional properties of legume starches. *Starch, 38*, 149–155.

Hoover, R. and Sosulski, F. W. (1985). Studies on the functional characteristics and digestibility of starches from *Phaseolus vulgaris* biotypes. *Starch, 37*, 181–191.

Hoover, R. and Vasanthan, T. (1994c). The effect of annealing on the physicochemical properties of the wheat, oat, potato and lentil starches. *Journal of Food Biochemistry, 17*, 303–325.

Hoover, R. and Vasanthan, T. (1994a). Effect of heat-moisture treatment on the structure and physicochemical properties of cereal, legume and tuber starches. *Carbohydrate Research, 252*, 33-53.

Hoover, R. and Vasanthan, T. (1994b). The flow properties of native, heat– moisture treated and annealed starches from wheat, oat, potato and lentil. *Journal of Food Biochemistry, 18*, 67–82.

Hoover, R., Hughes, T., Chung, H. J. and Liu, Q. (2010). Composition, molecular structure, properties and modification of pulse starches: A review. *Food Research International, 43*, 399–413.

Hoover, R., Swamidas, G. and Vasanthan, T. (1993). Studies on the physico- chemical properties of native, defatted, and heat-moisture treated pigeon pea (Cajanus cajan L.) starch. *Carbohydrate Research, 246*, 185–203.

Hoover, R., Vasanthan, T., Senanayake, N. J., and Martin, A. M. (1994). The effects of defatting and heat–moisture treatment on the retrogradation of starch gels from wheat, oat, potato and lentil. *Carbohydrate Research, 26*, 13–24.

Hormdok, R. and Noomhorm, A. (2007). Hydrothermal treatments of rice starch for improvement of rice noodle quality, *LWT – Food Science and Technology, 40*, 1723–1731.

Huber, K. C. and BeMiller, J. N. (1997). Visualization of channels and cavities of corn and sorghum starch granules. *Cereal Chemistry, 74*, 537–541.

Huber, K. C. and BeMiller, J. N. (2000). Channels of maize and sorghum starch granules. *Carbohydrate Polymers, 41*, 269-276.

Imam, S. H. (1989). A tightly bound M_r 55,000 polypeptide in cornstarch associated with the amylose portion of the granule. *Journal of cereal Science, 9*, 231-236.

Imberty, A. and Pérez, S. (1988). A revisit to the three dimensional structure of B-type starch. *Biopolymers, 27*, 308–325.

Imberty, A., Buléon, A., Tran, V. and Pérez, S. (1991). Recent advances in knowledge of starch structure. *Starch, 43*, 375–384.

Imberty, A., Chanzy, H., Pérez, S., Buléon, A. and Tran, V. (1988). The double helical nature of the crystallline part of A-starch. *Journal of Molecular Biology, 201*, 365–378.

Jacobasch, G., Dongowski, G., Schmiedl, D., and Schmehl, K. M. (2006). Hydrothermal treatment of Novelose 330 results in high yield of resistant starch type 3 with beneficial prebiotic properties and decreased secondary bile acid formation in rats. *British Journal of Nutrition, 95*, 1068–1074.

Jacobs, H. and Delcour, J. A. (1998). Hydrothermal modifications of granular starch, with retention of the granular structure: a review. *Journal of Agricultural Food Chemistry, 46*, 2895–2905.

Jacobs, H., Eerlingen, R. C., Rouseu, N., Colonna, P. and Delcour, J. A. (1998). Acid hydrolysis of native and annealed wheat, potato and pea starches—DSC melting features and chain length distributions of lintnerised starches. *Carbohydrate Research, 308*, 359-371

Jane, J. L. (2007). Structure of starch granules. *Journal of Applied Glycoscience, 54*, 31–36.

Jane, J. L. and Robyt, J. F. (1984). Structure studies of amylose V complexes and retrogradaded amylose by action of alpha amylase, a new method for preparing amylodextrins. *Carbohydrate Research, 132*, 105–110.

Jane, J. L., Wong, K. S. and McPherson, A. E. (1997). Branch-structure difference in starches of A- and B-type X-ray patterns revealed by their Naegeli dextrins. *Carbohydrate Research, 300*, 219–227.

Jane, J. L., Chen, Y. Y., Lee, L. F., McPherson, A. E., Wong, S., Radosavlievic, M. and Kasemsuwan, T. (1999). Effects of amylopectin branch chain length and amylose content on the gelatinization and pasting properties of starch. *Cereal Chemistry, 76*, 629–637.

Jane, J., Kasemsuwan, T., Chen, J. F. and Juliano, B. O. (1996). Phosphorus in rice and other starches. *Cereal Foods World, 41*, 827–832.

Jane, J., Kasemsuwan, T., Leas, S., Zobel, H. and Robyt, J. F. (1994). Anthology of starch granule morphology by scanning electron microscopy. *Starch, 46*, 121–129.

Jane, J. L., Xu, A., Radosavljevic, M. and Seib, P. A. (1992). Location of amylose in normal starch granules. I: susceptibility of amylose and amylopectin to cross-linking reagents. *Cereal Chemistry, 69,* 405– 409

Jane, J. L. and Shen, J. J. (1993). Internal structure of potato starch granule revealed by chemical gelatinization. *Carbohydrate Research*, 247, 279-290.

Jane, J. L. (2009). Structural features of starch granules II. In J. BeMiller, and R. Whistler (Eds), *Starch:Chemistry and Technology*, (pp 193-236). Academic Press NY:

Jayakody, L., Hoover, R., Liu, Q. and Donner, E. (2007). Studies on tuber starches. II. Molecular structure, composition and physicochemical properties of yam (*Dioscorea* Sp.) starches grown in Sri Lanka. *Carbohydrate Polymers, 69*, 148-163.

Jenkins, D. J. A., Wolever, T. M. S., Collier, G. R., Ocana, A., Rao, A. V., Buckely, G., Lam, Y., Mayer, A., and Thompson, L. U. (1987). Metabolic effects of a low-glycemic-index diet. *American Journal of Clinical and Nutrition, 46*, 968-975.

Jenkins, D. J. A., Wolever, T. M. S., Taylor, R. H., Barker, H., Fielder, H., Baldwin, J. M., Bowling, A. C., Newman, H. C., Jenkins, A. L. and Goff, D. V. (1981). Glycemic index of foods: a physiological basis of carbohydrate exchange. *American Journal of Clinical Nutrition, 34,* 362-366.

Jenkins, P. J. and Donald, A. M. (1995). The influence of amylose on starch granule structure. *International Journal of Biological Macromolecules, 17*, 315–321

Jenkins, P. J. and Donald, A. M. (1998). Gelatinisation of starch – a combined WAXS/SAXS/DSC and SANS study. *Carbohydrate Research, 308,* 133–147.

Jenkins, P. J., Cameron, R. E. and Donald, A. M. (1993). A universal feature in the structure of starch granules from different botanical sources. *Starch, 45,* 417–420.

John, M., Schmidt, J. and Kneifel, H. (1983). Iodine-maltosaccharide complexes: relation between chain-length and colour. *Carbohydrate Research, 119*, 254-257.

Jouquand, C., Ducruet, V. and Le Bail, P. (2006). Formation of amylose complexes with C6-aroma compounds in starch dispersions and its impact on retention. *Food Chemistry, 96,* 461 470.

Juszczaka, L., Fortuna, T. and Krok, F. (2003). Non-contact Atomic Force Microscopy of Starch Granules Surface. Part I. Potato and Tapioca Starches. *Starch, 55*, 1–7.

Jyothi, A. N., Sajeev, M. S. and Sreekumar, J. N. (2010). Hydrothermal modifications of tropical tuber starches. 1. Effect of heat-moisture treatment on the physicochemical, rheological and gelatinization characteristics. *Starch, 62,* 28-40.

Kainuma, K. and French, D. (1971). Nageli amylodextrin and its relationship to starch granule structure. 1. Preparation and properties of amylodextrins from various starch types. *Biopolymers*, *10,* 1673–1680.

Kainuma, K. (1988). Structure and chemistry of starch granule. In P. K. Stumpf and E. E. Conn, (Eds), *The biochemistry of plants*, (pp. 141–180). Academic Press, NY.

Kang, K. J., Kim, S., Lee, S. K. and Kim, S. K. (1997). Relationship between molecular structure of acid-hydrolyzed rice starch and retrogradation. *Korean Journal of Food Science and Technology*, *29*, 876–881.

Karim, A. A., Norziah, M. H. and Seow, C. C. (2000). Methods for the study of starch retrogradation. *Food Chemistry, 71*, 9–36.

Karim, A. A., Toon, L. C., Lee, V. P., Ong, W. Y., Fazilah, A. and Noda, T. (2007). Effects of phosphorus contents on the gelatinization and retrogradation of potato starch. *Journal of Food Science, 72,* C132-138.

Karkalas, J., Ma, S., Morrison, W. and Pethrick, R. A. (1995). Some factors determining the thermal properties of amylose inclusion complexes with fatty acids. *Carbohydrate Research, 268*, 233–247.

Karkalas, J., Ma, S., Morrison, W. R. and Pethrick, R.A. (1995). Some factors determining the thermal properties of amylose inclusion complexes with fatty acids. *Carbohydrate Research, 268*, 233–247.

Kasemsuwan, T. and Jane, J. (1994). Location of amylose in normal starch granules. II. Location of phosphodiester cross-linking revealed by phosphorous-31 nuclear magnetic resonance. *Cereal Chemistry, 71*, 282–287

Kawabata, A., Takase, N., Miyoshi, T., Sawayama, S., Kimura, T. and Kudo, K. (1994). Microscopic observation and X-ray diffractometry of heat-moisture treated starch granules. *Starch,* 48, 463-469.

Khunae, P., Tran, T., and Sirivongpaisal, P. (2007). Effect of heat-moisture treatment on structural and thermal properties of rice starches differing in amylose content. *Starch, 59*, 593–599.

Kim, H. and Huber, K. (2008). Channels within soft wheat starch A- and B-type granules. *Journal of Cereal Science, 48*, 159–172.

Kim, R. E. and Ahn, S. Y. (1996). Gelling properties of acid-modified red bean starch gels. *Agriculture Chemistry and Biotechnology, 39*, 49–53.

Kitamura, S. and Kuge, T. (1989). A differential scanning calorimetric study of the conformational transitions of schizophyllan in mixture of water and dimethylsulfoxide. *Biopolymers, 28*, 639–654.

Klucinec, J. D. and Thompson, D. B. (1998). Fractionation of high amylose maize starches by differential alcohol precipitation and chromatography of the fractions. *Cereal Chemistry, 75*, 887–896.

Knutson, C. A., Khoo, U., Cluskey, J. E. and Inglett, G. E. (1982). Variation in enzyme digestibility and gelatinization behaviour of corn starch granule fractions. *Cereal Chemistry, 59*, 512-515.

Kotting, O., Pusch, K., Tiessen, A., Geigenberger, P., Steup, M. and Ritte, G. (2005). Identification of a novel enzyme required for starch metabolism in Arabidopsis leaves. The phosphoglucan, water dikinase. *Plant Physiology, 137*, 242–252.

Kozlov, S. S., Noda, T., Bertoft, E. and Yuryev, V. P. (2006). Structure of starches exctracted from near-isogenic wheat lines. Part I. Effect of different GBSS I combinations. *Journal of Thermal Analysis and Calorimetry, 86*, 291–301.

Kozlov, S. S., Blennow, A., Krivandin, A. V. and Yuryev, V. P. (2007). Structural and thermodynamic properties of starches extracted from GBBS and GWD suppressed potato lines. *International Journal of Biological Macromolecules, 40*, 449-460.

Kubelka, P. and Munk, F. (1931). An article on optics of paint layers. *Physik, 12*, 593–601.

Kugimiya, M. and Donovan, J. W. (1981). Calorimetric determination of the amylose content of starches based on the formation and melting of the amylose-lysolecithin complex. *Journal of Food Science, 46,* 765.

Kulp, K. and Lorenz, K. (1981). Heat-moisture treatment of starches. I. Physicochemical properties. *Cereal Chemistry, 58*, 46–48.

Kurahashi, Y. and Yoshino, Z. (2000). HMT starch: Its production, properties, and uses (in Japanese). *Oyo Toshitsu Kagaku 47*, 125-132.

Kurakake, M., Tachibana, Y., Masaki, K. and Komaki, T. (1996). Adsorption of alpha-amylase on heat-moisture treated starch. *Journal of Cereal Science, 23*, 163–168.

Kweon, M., Haynes, L., Slade, L. and Levine, H. (2000). The effect of heat and moisture treatments on enzyme digestibility of AeWx, Aewx and aeWx corn starches. *Journal of Thermal Analytical Calorimetry*, 59, 571-586.

Langton, M. and Hermasson, A. M. (1989). Microstructural changes in wheat starch dispersions during heating and cooling. *Food Microstructure, 8*, 29-39.

Lansky, S., Kooi, M. and Schoch, T. J. (1949). Properties of the fractions and linear subfractions from various starches. *Journal of the American Chemical Society, 71*, 4066-4075.

Lawal, O. S. (2005). Studies on the hydrothermal modifications of new cocoyam (Xanthosoma sagittifolium) starch. *International Journal of Biological Macromolecules, 37*, 268–277.

Lawal, O. S. and Adebowale, K. O. (2005). An assessment of changes in thermal and physicochemical parameters of jack bean (*Canavalia ensiformis*) starch following hydrothermal modifications. *European Food Research and Technology, 221*, 631–638.

Le Corre, D., Bras, J. and Dufresne, A. (2010). Starch Nanoparticles: A Review *Biomacromolecules*, *11*, 1139–1153.

Leach, W., McCowen, D. and Schoch, T. J. (1959). Structure of the starch granule. I. Swelling and solubility patterns of various starches. *Cereal Chemistry, 36*, 534–544.

Lee, S. H. and BeMiller, J. N. (2008). Lysophosphatidylcholine identified as channel-associated phospholipid of maize starch granules. *Cereal Chemistry, 85,* 776–779.

Levine, H. and Slade, L. (1988). Non-equilibrium behaviour of small carbohydrate-water systems. *Pure Applied Chemistry, 60*, 1841.

Levine, H. and Slade, L. (1989). Influence of glassy and rubbery states on the thermal, mechanical, and structural properties of doughs and baked products. In H. Fairidi, J. M Faubion, (Eds), *Dough rheology and baked product texture*, (pp 157–300). Van Nostrand Reinhold, NY.

Li, J. H., Vasanthan, T., Rossnagel, B. and Hoover, R. (2001). Starch from hull-less barley: I. Granule morphology, composition, and amylopectin structure. *Food Chemistry, 74*, 395–405.

Li, J-Y. and Yeh, An-I. (2001). Relationships between thermal, rheological characteristics and swelling power for various starches. *Journal of Food Engineering, 50*, 141-148.

Lim, C. C., Ferguson, R. L. and Tannock G. W. (2005). Dietary fibres as "prebiotics": Implications for colorectal cancer. *Molecular Nutrition and Food Research, 49,* 609–619.

Lim, S. T., Chang, E. H. and Chung, H. J. (2001). Thermal transition characteristics of heat-moisture treated maize and potato starches. *Carbohydrate Polymers, 46*, 107–115.

Lim, S., Kasemsuwan, T. and Jane, J. (1994). Characterization of phosphorus in starch by 31P-nuclear magnetic resonance spectroscopy. *Cereal Chemistry, 71*, 488-493.

Lin, P.-Y. and Czuchajowska, Z. (1998). Role of Phosphorus in Viscosity, Gelatinization, and Retrogradation of Starch. *Cereal Chemistry, 75*, 705-709.

Lindeboom, N., Chang, P. R. and Tylera, R. T (2004). Analytical, biochemical and physicochemical aspects of starch granule size, with emphasis on small granule starches: A review. *Starch, 56*, 89–99.

Lineback, D. R. (1986). Current concepts of starch structure and its impact on properties. *Journal of Japanese Society of Starch Science, 33*, 80–88.

Lineback, D. R. (1984). The starch granule organisation and properties. *Bakers Digest, 13*, 16-21.

Lineback, D. R. and Rasper, V. F. (1988). Wheat carbohydrates. In Y. Pomeranz, (Ed), *Wheat, Chemistry and Technology*, (pp. 277–372). AACC, St Paul, MN.

Liu, J. and Zhoa, S. (1990). Scanning Electron Microscope Study on Gelatinization of Starch Granules in Excess Water. *Starch, 42,* 96-98.

Liu, Q., Charlet, G., Yelle, S. and Arul, J. (2002). Phase transition in potato starch–water system. I. Starch gelatinisation at high moisture level. *Food Research International, 35,* 397–407.

Liu, Q., Gu, Z., Donner, E., Tetlow, L. and Emes, M. (2007). Investigation of digestibility *in vitro* and physicochemical properties of A and B-type starch from soft and hard wheat flour. *Cereal Chemistry, 84,* 15-21.

Loisel, C., Maache–Rezzoug, Z., Esneault, C. and Doublier, J. L. (2006). Effect of hydrothermal treatment on the physical and rheological properties of maize starches. *Journal of Food Engineering, 71,* 45–54.

Lopez, E. C., Rolee, A. and Le Meste, M. (2004). Study of starch granules swelling by the blue dextran method and by microscopy. *Starch, 56,* 576-581.

Lopez-Rubio, A., Flanagan, B. M., Gilbert, E. P., and Gidley, M. J. (2008a). A novel approach for calculating starch crystallinity and its correlation with double helical content: A combined XRD and NMR study. *Biopolymers, 89,* 761-768.

Lopez-Rubio, A., Flanagan, B. M., Shrestha, A. K., Gidley, M. J. and Gilbert, E. P. (2008b). Molecular rearrangement of starch during in vitro digestion: towards a better understanding of enzyme resistant starch formation in processed starch. *Biomacromolecules, 9,* 1951-1958.

Lorberth, R., Ritte, G., Willmitzer, L. and Kossmann, J. (1998). Inhibition of a starch-granule-bound protein leads to modified starch and repression of cold sweetening. *Nature Biotechnology, 16,* 473-477.

Lorenz, K. and Kulp, K. (1981). Heat-moisture treatment of starches. II. Functional properties and baking potential. *Cereal Chemistry, 58,* 49–52.

Lorenz, K., and Kulp, K. (1982). Cereal and root starch modification by heat–moisture treatment. 1. physicochemical properties. *Starch, 34,* 50–54.

Lu, S., Chen, C.Y. and Lii, C.Y. (1996). Gel chromatography fractionation and thermal characterization of rice starch affected by hydrothermal treatment. *Cereal Chemistry, 73,* 5-11.

Lund, D. (1984). Influence of time, moisture, ingredients, and processing conditions on starch gelatinization. *Critical Review in Food Science and Nutrition, 20,* 249–273.

Luo, F.-X., Huang, Q., Fu, X., Zhang, L. X. and Yu, S.-J. (2009). Preparation and characterisation of crosslinked waxy potato starch. *Food Chemistry, 115,* 563–568

MacGregor, E. A., Janeček, Š. and Svensson, B. (2001). Relationship of sequence and structure to specificity in the α-amylase family of enzymes. *Biochimica et Biophysica Acta, 1546,* 1–20.

Marchant, J. L. and Blanshard, J. M. V. (1978). Studies of the dynamics of the gelatinization of starch granules employing a small angle light scattering system, *Starch/Stärke, 30,* 257–264.

Matveev, Y. I., Elankin, N. I., Kalistratova, E. N., Danilenko, A. N., Niemann, C. and Yuryev, V. P. (1998). Estimation of contributions of hydration and glass transition to heat capacity changes during melting of native starches at excess water. *Starch, 50,* 141–147.

Matveev, Y. I., van Soest, J. J. G., Nieman, C., Wasserman, L. A., Protserov, V. and Ezernitskaja, M. *and.* Yuryev, V. P. (2001). The relationship between thermodynamic and structural properties of low and high amylose maize starches. *Carbohydrate Polymers, 44,* 151–160.

McPherson A. E. and Jane, J. (1999). Comparison of waxy potato with other root and tuber starches. *Carbohydrate Polymers, 40,* 57–70.

Mercier, C., Charbonnier, R. Grebaut, J. and De La Gueriviere, J. F. (1980). Formation of amylose lipid complexes by twin-screw extrusion cooking of manioc starch. *Cereal chemistry, 57,* 4-9.

Mikkelsen, R., Baunsgaard, L., Blennow, A. (2004). Functional characterization of alpha-glucan,water dikinase, the starch phosphorylating enzyme. *Biochemistry Journal, 377*, 525– 532.

Miles, M. J., Morris, V. J., Oxford P. D. and Ring, S. G. (1985). The roles of amylose and amylopectin in the gelation and retrogradation of starch. *Carbohydrate Research, 135,* 271–281.

Mishra, S and Raj, T. (2006). Morphology and functional properties of corn, potato and tapioca starches. *Food Hydrocolloids, 20*, 557-566.

Miyoshi, E. (2002). Effect of heat–moisture treatment and lipids on gelatinization and retrogradation of maize and potato starches. *Cereal Chemistry, 79*, 72-77.

Moorthy, S.N. (1999). Effect of steam pressure treatment on the physicochemical properties of dioscorea starches. *Journal of Agricultural and Food Chemistry, 47*, 1695–1699.

Morell, M. K., Samuel, M. S. and O'Shea, M. G. (1998). Analysis of starch structure using fluorophore-assisted carbohydrate electrophoresis. *Electrophoresis, 19*, 2603-2611.

Morrison, W. R. (1981). Starch lipids: A reappraisal. *Starch, 33*, 408-410.

Morrison, W. R. (1985). Extraction of lipids from cereal starches with hot aqueous alcohols. *Starch, 37,* 83-87.

Morrison, W. R. (1988). Lipids in cereal starches: A review. *Journal of Cereal Science, 8*, 1-15

Morrison, W. R. and Karkalas, J. (1990). Starch. In P.M. Dey, (Ed), *Methods in plant biochemistry: carbohydrates*, (pp. 252–323). Academic Press, London, UK.

Morrison, W. R., Milligan, T. P. and Azudin, M. N. (1984). A relationship between the amylose and lipid contents of starches from diploid cereals. *Journal of Cereal Science, 2*, 257-271.

Morrison, W. R., Tester, R. F., Snape, C. E., Law, R. and Gidley, M. J. (1993a). Swelling and gelatinization of cereal starches: IV. Some effects of lipid complexed amylose and free amylose in waxy and normal barley starches. *Cereal Chemistry, 70*, 385–391

Morrison, W. R. (1964). A fast simple and reliable method for the micro determination of phosphorus in biological material. *Analytical Biochemistry*, *7*, 218-224.

Morrison, W. R., Law, R. V. and Snape, C. E. (1993b). Evidence for inclusion complexes of lipids with V-amylose in maize, rice and oat starches. *Journal of Cereal Science*, *18*, 107-109.

Mua, J. P. and Jackson, D. S. (1997). Fine structure of corn amylose and amylopectin fractions with various molecular weights. *Journal of Agricultural and Food Chemistry*, *45*, 3840–3847.

Mu-Forster, C. and Wasserman, B. P. (1988). Surface localisation of zein storage proteins in starch granules from maize endosperm. Proteolytic removal by thermolysin and in-vitro cross-linking of granule associated polypeptides. *Plant Physiology, 116,* 1563–1571.

Mu-Forster, C., Huang, R., Powers, J. R., Harriman, R.W., Knight, M., Singletary, G. W., Keeling P. L. and Wasserman, B. P. (1996). Physical association of starch biosynthetic enzymes with starch granules of maize endosperm. Granule-associated forms of starch synthase I and starch branching enzyme II. *Plant Physiology, 111*, 821–829.

Mutungi, C., Rost, F., Onyango, C., Jaros, D. and Rohm, H. (2009). Crystallinity, thermal and morphological characteristics of resistant starch type III produced by hydrothermal treatment of debranched cassava starch. *Starch, 61*, 634-645.

Myers, A. M., Morell, M. K., James, M. G. and Ball, S. G. (2000). Recent progress toward understanding biosynthesis of the amylopectin crystal. *Plant Physiology, 122*, 989–997

Nakazawa Y. and Wang, Y. J. (2004). Effect of annealing on starch–palmitic acid interaction. *Carbohydrate Polymers, 57*, 327–335.

Nakazawa, Y. and Wang, J-J. (2003). Acid hydrolysis of native and annealed starches and branch-structure of their Naegeli dextrins. *Carbohydrate Research, 338*, 2871-2882.

Nara, S., Mori, A. and Komiya, T. (1978). *Starch, 30,* 111–114.

Nguyen, Q. T., Aptel, P and Neel, J. (1976). *Biopolymers, 15,* 2097

Noda, T., Kimura, T., Otani, M., Ideta, O., Shimada T., Saito, A. and Suda, I. (2002). Physicochemical properties of amylose-free starch from transgenic sweet potato. *Carbohydrate Polymers, 49*, 253–260.

Noda, T., Takigawa, S., Matsuura-Endo, C., Kim, S.-J., Hashimoto, N., Yamauchi, H., Hanashiro, I. and Takeda, Y. (2005). Physicochemical properties and amylopectin structures of large, small, and extremely small potato starch granules. *Carbohydrate Polymers, 60*, 245–251.

O'Brien, S. O. and Wang, Y. J. (2008). Susceptibility of annealed starches to hydrolysis by α-amylase and glucoamylase. *Carbohydrate Polymers, 72*, 597–607.

O'Shea, M. G., Samuel, M. S., Konik, C. M. and Morell, M. K. (1998). Fluorophore-assisted carbohydrate electrophoresis (FACE) of oligosaccharides— Efficiency of labelling and high-resolution separation. *Carbohydrate Research, 307*, 1-12

Oates, C. G. (1990). Evidence for protein crosslinks in mung-bean starch. In G. O. Phillips, D. J. Wedlock, and P. A. Williams, (Eds). *Gums and Stabilisers for the Food Industry*, (pp 203-206). IRL Press, Oxford, UK.

Oates, C. G. (1997). Towards an understanding of starch granule structure and hydrolysis. *Trends in Food Science and Technology, 82,* 375-382.

Olayinka, O., Adebowale, K. O. and Olu-Owolabi, B. I. (2008). Effect of heat-moisture treatment on physicochemical properties of white sorghum starch. *Food Hydrocolloids, 22,* 225–230.

Osunsam, A. T., Akingbala, J. O., and Oguntimein, G. B. (1989). Effect of storage on starch content and modification of cassava starch. *Starch, 41*, 54–57.

Paris, M., Bizot, H., Emery, J., Buzare, J. Y. and Buleon, A. (2001). NMR local range investigations in amorphous starchy substrates I. Structural heterogeneity probed by ^{13}C CP-MAS NMR. *International Journal of Biological Macromolecules, 29*, 127–136.

Peat, S., Whelan,W. J., Thomas,G. J. (1952). Evidence of multiple branching in waxy maize starch, (pp. 4546-4548). *Journal of the Chemical Society Chemical Communications,* London.

Peng, M., Gao, M., Abdel-Aal, E. S. M., Hucl, P. and Chibbar, R. N. (1999). Separation and characterization of A- and B-type starch granules in wheat endosperm. *Cereal Chemistry, 76,* 375–379.

Perera, C. and Hoover, R. (1998). The reactivity of porcine pancreatic α-amylase towards native, defatted and heat-moisture treated potato starches before and after hydroxypropylation. *Starch, 50,* 206-213.

Pérez, S. and Bertoft, E., (2010). The molecular structures of starch components and their contribution to the architecture of starch granules: A comprehensive review. *Starch, 62,* 389-420.

Peroni, F. H. G., Rocha, T. S. and Franco, C. M. L. (2006). Some Structural and Physicochemical Characteristics of Tuber and Root Starches. *Food Science and Technology International, 12,* 505–513.

Perry, P. A. and. Donald, A. M. (2002). The effect of sugars on the gelatinisation of starch. *Carbohydrate Polymers, 49,* 155–165.

Planchot V., Colonna, P., Gallant D. J., and Bouchet, B. (1995). Extensive degradation of native starch granules by á–amylase from *Aspergillus fumigatus*. *Journal of Cereal Science, 21,* 163-171.

Planchot, V., Colonna, P., Buleon, A. and Gallent, D. (1997). Amylolysis of starch granules and α-glucan crystallites. In R. J. Frazier, A. M. Donald and P. Richmond, (Eds), *Starch structure and functionality,* (pp. 141–152). Royal Society of Chemistry, Cambridge, UK.

Prentice, R. D. and Stark, J. R. (1992). Granule residues and "ghosts" remaining after heating A-type barley-starch granules in water. *Carbohydrate Research, 227,* 121-130.

Purwani, E. Y., Widaningrum, R., Thahir, and Muslich (2006). Effect of heat- moisture treatment of sago starch on its noodle quality. *Indonesian Journal of Agricultural Science, 7*, 8–14.

Qi, X., Tester, R. F., Snape, C. E. and Ansell, R. (2003). Molecular basis of the gelatinisation and swelling characteristics of waxy rice starches grown in the same location during the same season. *Journal of Cereal Science, 37*, 363–376.

Qi, X., Tester, R. F., Snape, C. E., Yuryev, V., Wasserman, L. A. and Ansell, R. (2004). Molecular basis of the gelatinisation and swelling characteristics of waxy barley starches grown in the same location during the same season. Part II. Crystallinity and gelatinisation characteristics. *Journal of Cereal Science, 39,* 57–66.

Quigley, T. A., Kelly C. T., Doyle E. M. and Fogarty W. M. (1998). Patterns of raw starch digestion by the glucoamylase of *Cladosporium gossypiicola* ATCC 38026. *Process Biochemistry, 33*, 677-681

Rahman, S., Kosar-Hashemi, B., Samuel, M. S., Hill, A., Abbot, D. C., Skerritt, J. H., Preiss, J., Appels, R. and Morell, M. K. (1995). The major proteins of wheat endosperm starch granules. *Australian Journal of Plant Physiology, 22,* 793 -803.

Rao, V. S. R. and Foster, J. F. (1963). Studies of the conformation of amylose in solution. *Biopolymers, 1,* 527-544.

Raphaelides, S. and Karkalas, J. (1988). Thermal dissociation of amylose–fatty acid complexes. *Carbohydrate Research, 172*, 65–82.

Rappenecker, G. and Zugenmaier, P. (1981). Detailed refinement of the crystal structure of Vh-amylose. *Carbohydrate Research, 89,* 11–19.

Ratnayake W. S., Hoover, R., Shahidi, F., Perera, C. and Jane, J. (2001). Composition, molecular structure and physicochemical properties of starches from four field pea (Pisum sativum L.) cultivars. *Food Chemistry, 74*, 189-202.

Ratnayake, W. S., Hoover, R. and Warkentin, T. (2002). Pea starch: composition, structure and properties - A Review. *Starch, 54*, 217-234.

Rendleman, J. A. J. (2003). The reaction of starch with iodine vapor. Determination of iodide-ion content of starch-iodine complexes. *Carbohydrate Polymers, 51*, 191–202.

Rickard, J. E., Asaoka, M. and Blanshard, J. M. V. (1991). Review of the physicochemical properties of cassava starch. *Tropical Science, 31*, 189–207.

Ridout, M. J., Gunning, A. P., Parker, M. L., Wilson, R. H. and Morris, V. J. (2002). Using AFM to image the internal structure of starch granules. *Carbohydrate Polymers, 50*, 123–132.

Riisom, T., Krog, N., and Eriksen, J. (1984). Amylose complexing capacities of cis- and trans-unsaturated monoglycerides in relation to their functionality in bread. *Journal of Cereal Science, 2*, 105–118.

Ring, S. G., Gee, M. J., Whittam, M., Orford P. and Johnson, I. T. (1988). Resistant starch: its chemical form in foodstuffs and effect on digestibility *in vitro*. *Food Chemistry, 28*, 97–109.

Ring, S. G., Collona, P., Panson, K. J., Kalicheversky, M. T., Miles, M. J., Morris, V. J. and Oxford, P. D. (1987). The gelation and crystallization of amylopectin. *Carbohydrate Research, 162,* 277–293.

Ring, S. G., L'Anson, K. J. and Morris, V. J. (1985). Static and dynamic light scattering studies of amylose solutions. *Macromolecule, 18*, 182-188.

Ritte, G., Heydenreich, M., Mahlow, S., Haebel, S., Kötting, O. and Steup, M. (2006). Phosphorylation of C6- and C3-positions of glucosyl residues in starch is catalyzed by distinct dikinases. *FEBS Letters, 580,* 4872–4876.

Ritte, G., Lloyd, J., Eckermann, N., Rottmann, A., Kossmann, J. and Steup, M. (2002). The starch-related R1 protein is an α-glucan, water dikinase. *Plant Biology, 99*, 7166–7171

Roach, R. R. and Hoseney, R. C. (1995). Effect of certain surfactants on the swelling, solubility and amylograph consistency of starch. *Cereal Chemistry, 72*, 571–577.

Robin, J. P., Mercier, C., Charbonnière, R. and Guilbot, A. (1974). Lintnerized starches. Gel-filtration and enzymatic studies of insoluble residues from prolonged acid treatment of potato starch. *Cereal Chemistry, 51*, 389–406.

Robin, J. P., Mercier, C., Duprat, F., Charbonnière, R. and Guilbot, A. (1975). Lintnerized starches. Chromatographic and enzymatic studies of insoluble residues from acid hydrolysis of various cereal starches, particularly, waxy maize starch. *Starch, 27,* 36–45

Robyt, J. F and French, D. (1970). The action pattern of porcine pancreatic α-amylase in relationship to the substrate binding site of the enzyme. *Journal of Biological Chemistry, 245*, 3917-3927.

Robyt, J. F. (2009). Enzymes and their action on starch. In J. BeMiller, and R. Whistler (Eds), *Starch:Chemistry and Technology*, (pp 238-284). Academic Press, NY:

Rundle R. E. (1947). The Configuration of Starch in the Starch-Iodine Complex. V. Fourier Projections from X-Ray Diagrams. *Journal of American Chemical Society, 69*, 1769–1772.

Rundle, R. E. and French, D. (1943). The configuration of starch in the starch–iodine complex. III. X-ray diffraction studies of the starch–iodine complex. *Journal of the American Chemical Society, 65*, 1707–1710.

Rye, C. S and Withers, S. G. (2000). Glycosidase mechanisms. *Current Opinion in Chemical Biology, 4*, 573-580.

Saenger, W. (1984). The structure of the blue starch-iodine complex. *Naturwissenschaften, 71,* 31-36.

Saibene D. and Seetharaman, K. (2006). Segmental mobility of polymers in starch granules at low moisture contents. *Carbohydrate Polymers, 64,* 539–547.

Saibene, D. and Seetharaman, K. (2010). Amylose involvement in the amylopectin clusters of potato starch granules. *Carbohydrate Polymers, 82*, 376-383.

Saibene, D., Zobel, H. F., Thompson, D. B. and Seetharaman, K. (2008). Iodine binding by granular corn and potato starch: Evidence for differential location of amylose. *Starch, 60*, 165–173.

Sair, L. (1967). Heat–moisture treatment of starch. *Cereal Chemistry, 44*, 8–26

Saitô, H., Yamada, J., Yukumoto, T., Yajima, H. and Endo, R. (1991). Conformational stability of V-amyloses and their hydration induced conversion to B-type form as studied by high-resolution solid-state C13 NMR-spectroscopy. *Bulletin of the Chemical Society of Japan, 64,* 3528–3537.

Sajilata, M. G. Singhal, R. S. and Kulkarni, P. R. (2006). Resistant starch-A review. *Comprehensive Reviews in Food Science and Food Safety, 5,* 1–17.

Sakonidou, E. P., Karapantsios, T. D. and Raphaelides, S. N. (2003). Mass transfer limitations during starch gelatinization. *Carbohydrate Polymers, 53*, 53–59.

Sang, Y., and Seib, P. A. (2006). Resistant starchesfrom amylosemutants of corn by simultaneous heat–moisture treatment and phosphorylation. *Carbohydrate Polymers, 63,* 167–175.

Sasaki, T. and Matsuki, J. (1998). Effect of wheat starch structure on swelling power. *Cereal Chemistry, 75*, 525–529.

Satin, M. (1998). Functional properties of starches. In Spolight tropical starch misses market. *AGSIreport, Agriculture21, FAO-Magazine*, 11p.

Satin, M. (2000). Functional properties of starches. In: International Symposium on Tropical Root and Tuber Crops, Thiruvananthapuran (Trivandrum).

Schoch, T. J. (1942). Non-carbohydrate substance in the cereal starches. *Journal of American Chemical Society*, *64*, 2954-2956.

Schoch, T. J. and Maywald, E. C. (1956). Microscopic examination of modified starches. *Analytical Chemistry, 28*, 382-387

Schofield, J. D. and Greenwell, P. (1987). Wheat starch granules and their technological significance. In I. D. Morton, (Ed), *Cereals in a European context*, (pp. 407–420). Elis Horwood/VCH, England/Weinheim.

Schwall, G. P., Safford, R., Westcott, R. J., Jeffcoat, R., Tayal, A., Shi, Y. C., Gidley, M. J. and Jobling, S. A. (2000). Production of very-high-amylose potato starch by inhibition of SBE A and B. *Nature of Biotechnology, 18*, 551– 554

Seguchi, M. and Yamada, Y. (1989). Study of proteins extracted from the surface of wheat starch granules with sodium dodecyl sulphate. *Cereal Chemistry, 66*, 193-196.

Seneviratne, H. D. and Biliaderis, C. G. (1991). Action of α-amylases on amylose-lipid complex superstructure. *Journal of Cereal science, 13*, 129-141.

Senior, M. B. and Hamori, E. (1973). Investigation of the effect of amylose/ iodine complexation on the conformation of amylose in aqueous solution. *Biopolymers, 12,* 65-78.

Sevenou, O., Hill, S. E., Farhat, I. A., Mitchell, J. R. (2002). Organization of the external region of the starch granule as determined by infrared spectroscopy. *International Journal of Biological Macromolecules*, 31, 79-85.

Shannon, J. C. and Garwood, D. L. (1984). Genetics and physiology of starch development. In R. L. Whistler, J. N. Bemiller, and E. F. Paschall, (Eds), *Starch: Chemistry and Technology*, (pp. 25-86). Academic Press, Orlando, FL.

Shannon, J. C., Pien, F. M., Cao, H. and Liu, K. C. (1998). Brittle-1, an adenylate translocator, facilitates transfer of extraplastidial synthesized ADP-glucose into amyloplasts of maize endosperms. *Plant Physiology, 117,* 1235–1252.

Shewry, P. R. (2003). Tuber storage proteins. *Annals of Botany*, *91*, 755-769.

Shi, Y.-C. and Seib, P. A. (1992). The structure of four waxy starches related to gelatinization and retrogradation. *Carbohydrate Research, 227*, 131–145.

Shih, F., King, J., Daigle, K., An, H. J., and Ali, R. (2007). Physicochemical properties of rice starch modified by hydrothermal treatments. *Cereal Chemistry, 84*, 527–553.

Shin, S. I., Choi, H. J., Chung, K. M., Hamaker, B. R., Park, K. H., and Moon, T. W. (2004). Slowly digestible starch from debranched waxy sorghum starch: Preparation and properties. *Cereal Chemistry, 81*, 404-408.

Shin, S. I., Kim, H. J., Ha, H. J., Lee, S. H., and Moon, T. W. (2005). Effect of hydrothermal treatment on formation and structural characteristics of slowly digestible non–pasted granular sweet potato starch. *Starch, 57*, 421–430.

Shogren, R. (2007). Effect of Orientation on the Physical Properties of Potato Amylose and High-Amylose Corn Starch Films. *Biomacromolecules, 8,* 3641–3645.

Shogren, R. L., Fanta, G. F. and Felker, F. C. (2006). X-ray diffraction study of crystal transformations in spherulitic amylose/lipid complexes from jet-cooked starch. *Carbohydrate Polymers, 64,* 444-451.

Singh, J. and Singh, N. (2001). Studies on the morphological, thermal and rheological properties of starch separated from some Indian potato cultivars. *Food Chemistry 75*, 67–77.

Singh, J. Dartois, A. and Kaur, L. (2010). Strach digestibility in food matrix: a review. *Trends in Food Science and Technology, 21*, 168-180.

Singh, J., McCarthy, O. J. and Singh, H. (2006). Physico-chemical and morphological characteristics of New Zealand Taewa (Maori potato) starches. *Carbohydrate Polymers, 64,* 569–581.

Singh, J., Singh, N. and Saxena, S. K. (2002). Effect of fatty acids on the rheological properties of corn and potato starch. *Journal of Food Engineering, 52*, 9–16.

Singh, N., Singh, J., Kaur, L., Sodhi, N. S. and Gill, B. S. (2003). Morphological, thermal and rheological properties of starches from different botanical sources. *Food Chemistry, 81,* 219-231.

Singh, S., Raina, C. S., Bawa, A. S., and Saxena, D. C. (2005). Effect of heat- moisture treatment and acid modification on rheological, textural, and differential scanning calorimetry characteristics of sweet potato starch. *Journal of Food Science, 70*, E373–E378.

Slade, L. and Levine, H. (1988). Non-equilibrium melting of native granular starch. Part I. Temperature location of the glass transition associated with gelatinization of A-type cereal starches. *Carbohydrate Polymers, 8*, 183–208.

Slaughter, S. L., Ellis, P. R. and Butterworth, P. J. (2001). An investigation of the action of porcine pancreatic α-amylase on native and gelatinised starches. *Biochimica et Biophysica Acta, 1525*, 29–36.

Smith, O. (1987). Effect of cultural and environmental conditions on potatoes for processing. In Talburt, William, F. and Smith, Ora, (Eds), *Potato processing*, Van Nostrand, Reinhold, NY.

Sopade, P. A. (1990). Starch gelatinisation and retrogradation in food systems with special references to baked foods. In A. J. Rayar, B. K. Kaigama, J. O. Olukosi and A. B. Anaso (Eds), Wheat in Nigeria: Production, processing and utilization (pp. 251–261).

South, J. B. Morrison, W. R. and Nelson, O. E. (1991). A relationship between the amylose and lipid contents of starches from various mutants for amylose content in maize. *Journal of Cereal Science, 14*, 267-278.

Srichuwong, S, Sunarti, T. C, Mishima, T., Isono, N. and Hisamatsu, M. (2005). Starches from different botanical sources. II: Contribution of starch structure to swelling and pasting properties. *Carbohydrate Polymers, 62*, 25–34.

Srichuwong, S., Sunarti, T. C. Mishima, T., Isono, N and Hismatsu, M. (2005). Starches from different botanical sources. I: Contribution of amylopectin fine structure to thermal properties and enzyme digestibility. *Carbohydrate Polymers, 60*, 529-538.

Sterling, C. (1960). Crystallinity of potato starch. *Starch, 12*, 182.

Sterling, C. (1973). Pore size in potato starch. *Starch, 25*, 115- 118.

Stevens, D. J. and Elton, G. A. H. (1971). Thermal properties of the starch/water system. Part I. Measurement of heat of gelatinisation by differential scanning calorimetry. *Starch, 23,* 8–11.

Stoddard, F. L. (1999). Survey of starch particle-size distribution in wheat and related species, *Cereal Chemistry, 76*, 145–149.

Stute, R. 1992). Hydrothermal modification of starches: The difference between annealing and heat-moisture-treatment. *Starch, 44,* 205-214

Sujka, M. and Jamroz, J. (2007). Starch granule porosity and its changes by means of amylolysis. *International Agrophysics*, *21*, 107-113.

Sujka, M. and Jamroz, J. (2009). α-Amylolysis of native potato and corn starches – SEM, AFM, nitrogen and iodine sorption investigations. *LWT - Food Science and Technology, 42*, 1219-1224.

Suryanarayana, C. and Norton, M. G. (1998). Practical aspects of X-ray diffraction. In: C. Suryanarayana and M.G. Norton, Editors, X-ray diffraction: A practical approach, Plenum Press, NY (1998), pp. 63–94.

Svegmark, K. and Hermansson, A. M. (1993). Microstructure and rheological properties of composites of potato starch granules and amylose: a comparison of observed and predicted structure. *Food Structure, 12*, 181–193.

Svegmark, K., Helmersson, K., Nilsson, G., Nilsson, P. O., Anderson, R., and Svenson, E. (2002). Comparison of potato amylopectin starches and potato starches–influence of year and variety. *Carbohydrate Polymers, 47*, 331–340.

Swinkels, J. J. M. (1985). Composition and properties of commercial native starches. *Starch, 37,* 1–5.

Tabata, S. and Hizukuri, S (1971). Studies on starch phosphate. 2. *Starch, 23*, 267–272.

Tahir, R., Ellis, P. R. and Butterworth, P. J. (2010). The relation of physical properties of native starch granules to the kinetics of amylolysis catalysed by porcine pancreatic α-amylase. *Carbohydrate Polymers, 81*, 57-62.

Takase, K., Matsumoto, T., Mizuno, H. and Yamane, K. (1992). Site-directed mutagenesis of active site residues in Bacillus subtilis α-amylase. *Biochimica Biophysica Acta, 1120*, 281-288.

Takeda Y. and Hizukuri, S. (1981). Re-examination of the action of sweet potato beta amylase on phosphorylated (1–4) α-glucan. *Carbohydrate Research, 89*, 174–178.

Takeda Y. and Hizukuri, S. (1982). Location of phosphate groups in potato amylopectin. *Carbohydrate Research, 102,* 321–327.

Takeda, Y., Hizukuri, S., Takeda, C., and Suzuki, A. (1987). Structures of branched molecules of amyloses of various origins and molar fractions of branched and unbranched molecules. *Carbohydrate Research, 165*, 139–145.

Tamaki, S., Hisamatsu, M., Teranishi, K., Adachi, T. and Yamada, T. (1998). Structural Change of maize starch granules by ball-mill treatment. *Starch, 50*, 342–348.

Tang, M. C. and Copeland, L. (2007). Analysis of complexes between lipids and wheat starch. *Carbohydrate Polymers, 67,* 80-85.

Tao, B. Y., Reilly, P. J. and Robyt, J. F. (1989). Detection of covalent intermediate in the mechanism of action of porcine pancreatic α-amylase by using 13C nuclear magnetic resonance. *Biochimica et Biophysica Acta, 995*, 214-220.

Tatge, H., Marshall, J., Martin, C., Edwards, E. A. and Smith, A. M. (1999). Evidence that amylose synthesis occurs within the matrix of starch granules. *Plant Cell Environment, 22*, 543-550.

Tester, R. F. and Karkalas, J. (1996). Swelling and gelatinization of oat starches. *Cereal Chemistry*, *73*, 271–273.

Tester, R. F. and Karkalas, J. (2002). Starch In A. Steinbüchel (series Ed), E. J. Vandamme, S. De Baets, and A. Steinbüchel (volume Eds), *Biopolymers Volume 6, Polysaccharides II: Polysaccharides from Eukaryotes* (pp. 381–438). Wiley-VCH, Weinheim.

Tester, R. F. and Morrison, W. R. (1990a). Swelling and gelatinization of cereal starches. 1. Effects of amylopectin, amylose, and lipids, *Cereal Chemistry, 67,* 551–557.

Tester, R. F., Karkalas, J. and Qi, X. (2004). Starch – composition, fine structure and architecture. *Journal of Cereal Science*, *39*, 151–165.

Tester, R.F. and Morrison, W. R. (1990b). Swelling and gelatinization of cereal starches II. Waxy rice starches. *Cereal Chemistry, 67*, 558–563.

Thoma, J. A. and French, D. (1960). The starch–iodine–iodide interaction. Part I. Spectrophotometric investigations. *Journal of the American Chemical Society, 82*, 4144–4147.

Thompson, D. B. (2000). On the non-random nature of amylopectin branching. *Carbohydrate Polymers, 43*, 223–239.

van Soest, J. J. G., Tournois, H., de Wit, D., Johannes, F.G. and Vliegenthart, J. F. G. (1995). Short-range structure in (partially) crystalline potato starch determined with attenuated total reflectance Fourier-transform IR spectroscopy. *Carbohydrate Research*, *279*, 201-214.

Vandeputte, G. E. and Delcour, J. A. (2004). From sucrose to starch granule to starch physical behavior: A focus on rice starch. *Carbohydrate Polymers, 58,* 245–266.

Vandeputte, G. E., Derycke, V., Geeroms, J., and Delcour, J. A. (2003). Rice starches. II. Structural aspects provide insight into swelling and pasting properties. *Journal of Cereal Science, 38*, 53–59.

Vasanthan, T. and Hoover, R. (1992). A comparative study of the composition of lipids associated with starch granules from various botanical sources. *Food Chemistry*, *43*, 19-27.

Vermeylen, R., Goderis, B. and Delcour, J. A. (2006). An X-ray study of hydrothermally treated potato starch. *Carbohydrate Polymers*, *64*, 364-375.

Vermeylen, R., Goderis, B., Reynaers, H. and Delcour, J. A. (2004). Amylopectin molecular structure reflected in macromolecular organization of granular starch. *Biomarcomolecules, 5*, 1775–1786.

Villareal, C. P., Juliano, B. O. and Banos, L. (1986). Waxy gene factor and residual protein of rice starch granules. *Starch, 38*, 118-119.

Virtanen, T., Autio, K., Suortti, T., and Poutanen, K. (1993). Heat-induced changes in native and acid-modified oat starch paste. *Journal of Cereal Science, 17*, 137–145

Visser, R. G. F., Somhorst, I., Kuipers, G. J., Ruys, N. J., Feenstra, W. J. and Jacobsen, E. (1991). Inhibition of the expression of the gene for granule-bound starch synthase in potato by antisense constructs. *Molecular Genetics and Genomics*, *225*, 289–296.

Visser, R. G. F., Suurs, L. C. J. M., Steeneken, P. A. M. and Jacobsen, E. (1997). Some physicochemical properties of amylose-free potato starch. *Starch, 49,* 443–448.

Waduge, R. N., Hoover, R., Vasanthan, T., Gao, J. and Li, J. (2006). Effect of annealing on the structure and physicochemical properties of barley starches of varying amylose content. *Food Research International*, *39*, 59–77.

Waduge, R. N., Xu, S. and Seetharaman, K. (2010). Iodine absorption properties and its effect on the crystallinity of developing granules. *Carbohydrate Polymers,* doi:10.1016/J.Carb. Pol.2010.05.093.

Waigh, T. A., Gidley, M. J., Komanshek B. U. and Donald, A. M. (2000b). The phase transformations in starch during gelatinisation: a liquid crystalline approach. *Carbohydrate Research, 328*, 165–176.

Waigh, T. A., Kato, K. L., Donald, A. M., Gidley, M. J., Clarke, C. J. and Riekel, C. (2000a). Side-chain liquid-crystalline model for starch. *Starch, 52*, 450–460.

Waigh, T. A., Perry, A. P., Riekel, C., Gidley, M. J. and Donald, A.M. (1998). Chiral side-chain liquid-crystalline polymeric properties of starch. *Macromolecules, 31,* 7980–7984.

Wakelin, J. H., Virgin, H. S. and Crystal, E. (1959). Development and comparison of two X-ray methods for determining the crystallinity of cotton cellulose. *Journal of Applied Physics, 30*, 1654–1662.

Wang, L. and Seib, P. A. (1996). Australian salt-noodle flours and their starches compared to US wheat flours and their starches. *Cereal Chemistry, 73*, 167–175.

Wang, L. Z. and White, P. J. (1994). Structure and properties of amylose, amylopectin and intermediate material of oat starches. *Cereal Chemistry, 71*, 263–268.

Wang, S. J., Yu, J. L., Gao, W. Y., Pang, J. P. and Liu, H. Y. (2007). Particle structural changes in native Chinese Yam (Dioscorea opposite Thunb var. Anguo) starches during acid hydrolysis. *Carbohydrate Polymers, 69*, 286–292.

Wang, S. J., Yu, J. L., Yu, J. G., Chen, H. X. and Pang, J. P. (2007). The effect of acid hydrolysis on morphological and crystalline properties of Rhizoma Dioscorea starch. *Food Hydrocolloids, 21*, 1217–1222.

Wang, Y.-J., White, P., Pollak, L. and Jane, J. (1993). Amylopectin and intermediate materials in starches from mutant genotypes of the Oh43 inbred line. *Cereal Chemistry, 70*, 521–525.

Watanabe, T. and French, D. (1980). Structural features of nageli amylodextrin as indicated by enzymic degradation. *Carbohydrate Research, 84,* 115–123.

Watcharatewinkul, Y., Puttanlek, C., Rungsardthong, V. and Uttapap, D. (2009). Pasting properties of a heat-moisture treated canna starch in relation to its structural characteristics. *Carbohydrate Polymers, 75,* 505-511.

Watcharatewinkul, Y., Uttapap, D., Puttanlek, C. and Rungsardthong, V. (2010). Enzyme digestibility and acid/shear stability of heat–moisture treated canna starch. *Starch, 62,* 205–216.

Watson, S. A. (1964). Determination of starch gelatinization temperature. In R. L. Whistler, R. J. Smith, M. L. Wolfrim (Eds). *Methods in Carbohydrate Chemistry,* (pp 286-288). Academic Press, NY.

Wei, C., Qin, F., Zhu, L., Zhou, W., Chen, Y., Wang, Y., Gu, M. and Liu, Q. (2010). Microstructure and ultrastructure of high-amylose rice resistant starch granules modified by antisense RNA inhibition of starch branching enzyme. *Journal of Agricultural Food Chemistry, 58*, 1224-1232.

Whistler, R. L. and BeMiller, J. N. (1996). Starch. In: R. L. Whistler and J. N. BeMiller (Eds), *Carbohydrate Chemistry for Food Scientists*, (pp. 117–151). Eagan Press, St. Paul, MN.

Whistler, R. L. and BeMiller, J. N. (1997). Starch. In R. L. Whistler and J. N. Be-Miller (Eds), *Carbohydrate Chemistry for Food Scientists,* (pp 117–151). American Association of Cereal Chemists. St Paul.

White, P. J., Abbas, I. R. and Johnson, L. J. (1989). Freeze-thaw stability and refrigerated-storage retrogradation of starches. *Starch, 41*, 176–180.

Widya, Y., Gunawan, N., BeMiller, J. N. (2010). Methods for determining relative average number of channels per maize starch granule and digestion of raw granules of mutant maize cultivars by amyloglucosidase. *Cereal Chemistry, 87,* 194-203.

Withers, S. G. and Aebersold, R. (1995). Approaches to labeling and identification of active-site residues in glycosidases. *Protein Science, 4*, 361-372.

Wolever, T. M. S. and Mehling, C. (2002). High-carbohydrate–low glycemic index dietary advice improves glucose disposition index in subjects with impaired glucose tolerance. *British Journal of Nutrition, 87,* 477-487.

Wongsagonsup, R., Varavinit, S. and James BeMiller, N. (2009). Increasing slowly digestible starch content of normal and waxy maize starches and properties of starch products. *Cereal Chemistry, 85*, 738–745.

Wu, H. C. H. and Sarko, A. (1978a). The double helical molecular structure of crystalline B-amylose. *Carbohydrate Research, 61*, 7–25.

Wu, H. C. H., and Sarko, A. (1978b). The double helical molecular structure of crystalline A-amylose. *Carbohydrate Research, 61*, 27–40.

Yamamoto, M. Sano, T. and Yasunaga, T. (1982). Interaction of amylose with iodine. I. Characterization of cooperativity binding isotherms for amyloses. *Bulletin of the Chemical Society of Japan, 55*, 1886–1889.

Yamashita, Y. and Monobe, K. (1971). Single crystals of amylose V complexes. 3. Crystals with 81 helical configuration. *Journal of Polymer Science Part B: Polymer Physics, 9,* 1471.

Yashushi, Y. B., Takenouchi, T. and Takeda, Y. (2002). Molecular structure and some physicochemical properties of waxy and low-amylose barley starches. *Carbohydrate Polymers, 47*, 159–167.

Yoon, J.-W., Lim, S.-T. (2003). Molecular fractionation of starch by density-gradient ultracentrifugation. *Carbohydrate Research, 338*, 611–617.

Yoshimoto, Y., Tashiro, J., Takenouchi, T. and Takeda, Y. (2000). Molecular structure and some physicochemical properties of high-amylose barley starch. *Cereal Chemistry, 77*, 279–285.

Yoshino, Y., Hayashi, M. and Seguchi, M. (2005). Presence and Amounts of Starch Granule Surface Proteins in Various Starches. *Cereal Chemistry, 82,* 739–742.

Yoshino, Z., Komaki, T., and Kurahashi, Y. 1994. Process for producing HMT starch. *US. patent 5*, 362329.

Yu, X., Houtman, C. and Atalla, R. H. (1996). The complex of amylose and iodine. *Carbohydrate Research, 292*, 129-141.

Yuan, R. C., Thompson, D. B. and Boyer, C. D. (1993). Fine structure of amylopectin in relation to gelatinization and retrogradation behaviour of maize starches from three wax-containing genotypes in two inbred lines. *Cereal Chemistry, 70*, 81–89.

Yuryev, V. P., Krivandin, A. V., Kiseleva, V. I., Wasserman, L. A., Genkina, N. K. and Fornal, J., Blaszczak, W. and Schiraldi, A. (2004). Structural parameters of amylopectin clusters

and semi-crystalline growth rings in wheat starches with different amylose content. *Carbohydrate Research, 339*, 2683–2691.

Yuryev, V. P., Kozlov, S. S., Noda, T., Bertoft, E. and Blennow, A. (2007). Influence of different GBSS1 and GWD combinations on the amylose localization within wheat and potato starch granules. In V. P. Yuryev, P. Tomasik and E. Bertoft, (Eds), Starch: Achievements in Under-standing of Structure (pp. 1–47). Nova Science, NY.

Yusuph, M., Tester, R. F., Ansell, R. and Snape, C. E. (2003). Composition and properties of starches extracted from tubers of different potato varieties grown under the same environmental conditions. *Food Chemistry, 82,* 283–289.

Zavareze, E. R., Storck, C. R., Castro, L. A. S., Schirmer, M. A. and Dias, A. R. G. (2010). Effect of heat-moisture treatment on rice starch of varying amylose content. *Food Chemistry, 121*, 358-365

Zhang, G., Ao, Z. and Hamaker, B. R. (2006). Slow digestion property of native cereal starches. *Biomacromolecules*, *7*, 3252-3258.

Zhang, T. and Oates, C. G. (1999). Relationship between α-amylase degradation and physico-chemical properties of sweet potato starches. *Food Chemistry, 65*, 157–163.

Zhou, Y., Hoover, R. and Liu, Q. (2004). Relationship between α-amylase degradation and the structure and physicochemical properties of legume starches. *Carbohydrate Polymers*, 57, 299-317.

Ziegler, G. R., Creek, J. A. and Runt, J. (2005). Spherulitic crystallization in starch as a model for starch granule initiation. *Biomacromolecules, 6,* 1547–1554.

Ziegler, G. R., Thompson, D. B. and Casasnovas, J. (1993). Dynamic measurement of starch granule swelling during gelatinisation. *Cereal Chemistry, 70*, 247–261.

Zobel, H. F. (1988a). Molecules to granules: A comprehensive starch review. *Starch, 40*, 44–50.

Zobel, H. F., (1988b). Starch crystal transformations and their industrial importance. *Starch, 40,* 1-7.

PUBLICATIONS

Varatharajan, V., Hoover, R, Liu, Q., Seetharaman, K. (2010). The impact of heat-moisture treatment on the molecular structure and physicochemical properties of normal and waxy potato starches. *Carbohydrate Polymers, 81,* 466-475.

Varatharajan, V., Hoover, R., Jihong, L., Vasanthan, T., Nantanga K. K. M., Seetharaman, K., Liu, Q., Donner, E., Jaiswal, S. and Chibbar, R. N. (2010). Impact of structural changes at different temperatures of heat-moisture treatment on the susceptibility of normal and waxy potato starches towards hydrolysis by porcine pancreatic alpha amylase. (In-review- *Food Chemistry*).

SCHOLARSHIPS AND AWARDS

- School of Graduate Studies (SGS) Merit Award (2008), Memorial University of Newfoundland
- First place in the Graduate Student Competition (Carbohydrate Division) at the Institute of Food Technologists' (IFT) Conference held in Anaheim, CA, June 6-9, 2009
- Barrowman Biochemistry Travel Award for 2009, Memorial University of Newfoundland
- Fellow of the School of Graduate Studies (2009-2010), Memorial University of Newfoundland
- AACC International Student Travel Award (2010), AACC International Annual Meeting in Savannah GA, USA (Oct-24-27, 2010)
- University of Guelph/Ontario Ministry of Agriculture, Food and Rural Affairs (OMAFRA)/ High Quality Personnel (HQP) Scholarship (2010-2011)
- University International Graduate Scholarship (UIGS) (2010-2011), University of Guelph

APPENDICES

Appendix 1

Curve fitting for XRD using Gaussian function

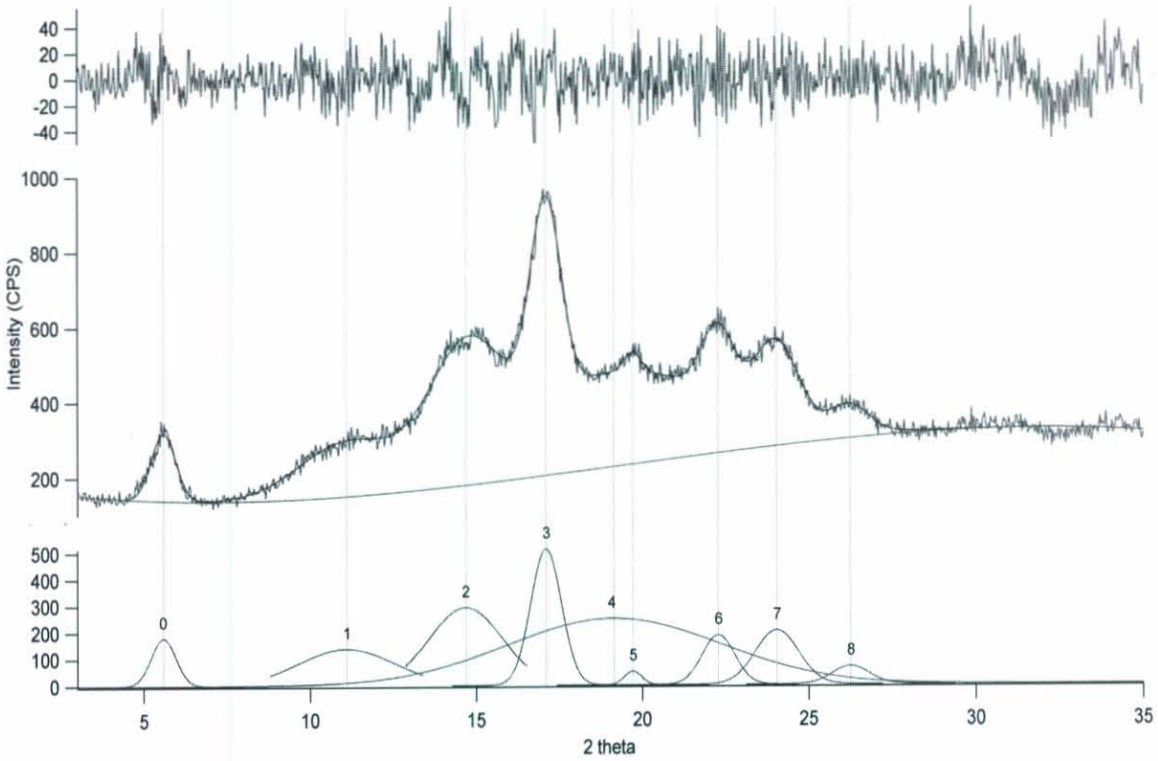

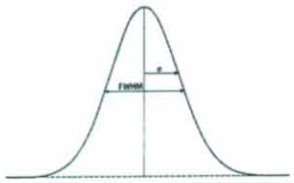

- Peak height and FWHM were calculated after subtracting the amorphous (peak 4) background

Appendix 2

Standard curve for determination of amylose content (Hoover and Ratnayake, 2004)

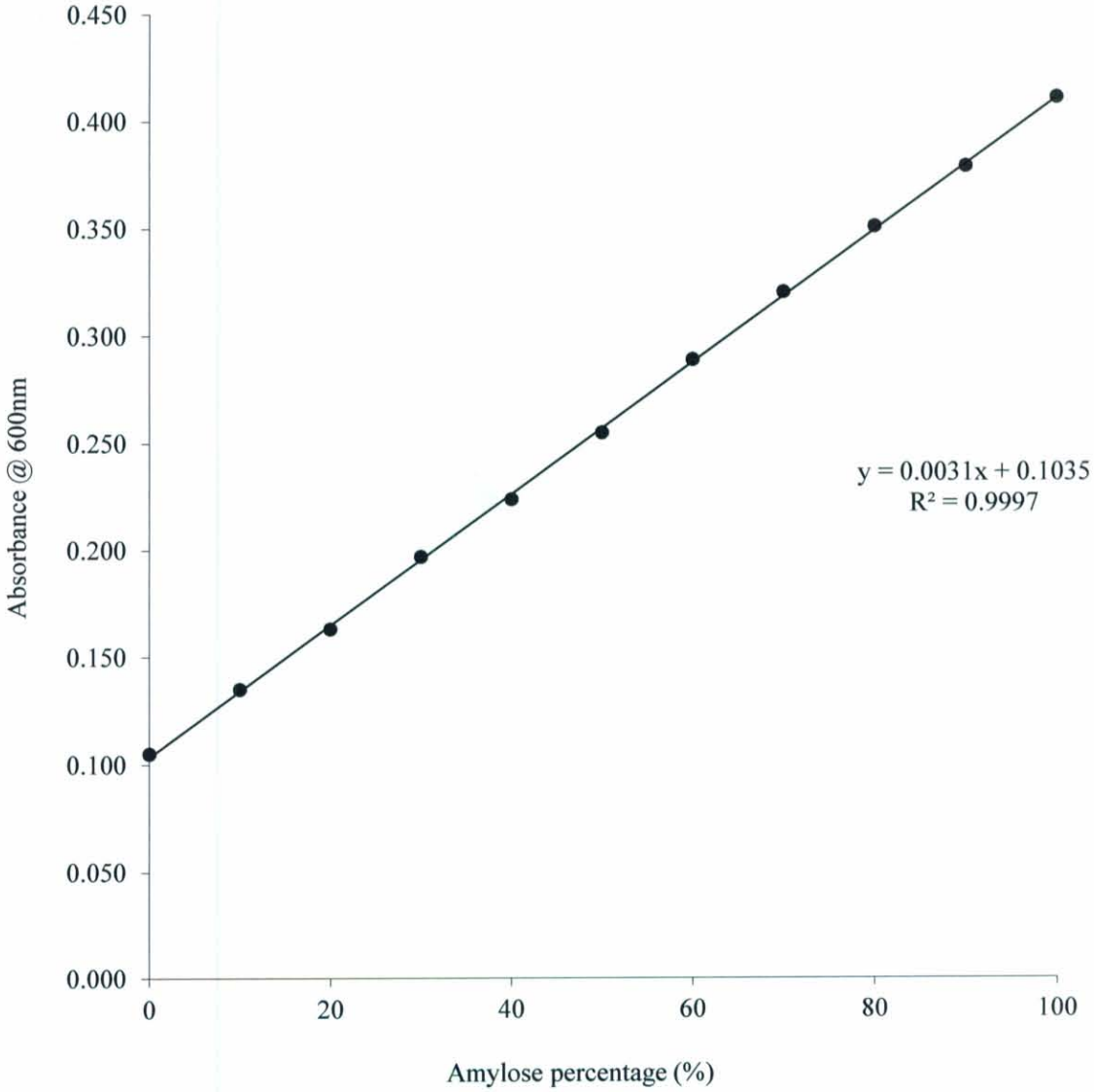
0.450
0.400
0.350
0.300
0.250
0.200
0.150
0.100
0.050
0.000
Absorbance @ 600nm
0
20
40
60
80
100
Amylose percentage (%)
y = 0.0031x + 0.1035
R² = 0.9997

Appendix 3

Standard curve for determination of reducing sugar as maltose (Bruner, 1964)

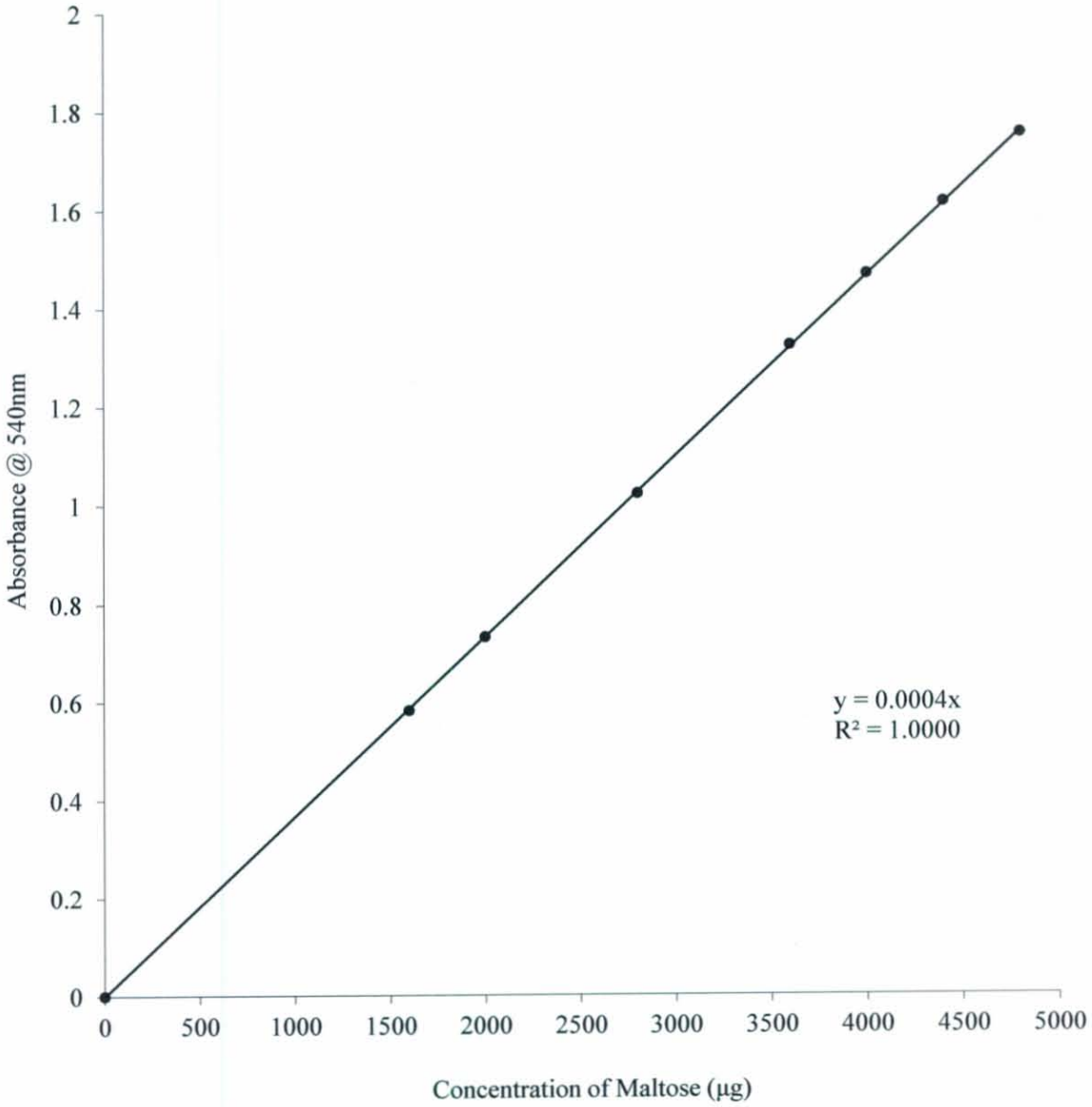
Absorbance @ 540nm
2
1.8
1.6
1.4
1.2
1
0.8
0.6
0.4
0.2
0
0
500
1000
1500
2000
2500
3000
3500
4000
4500
5000
y = 0.0004x
R² = 1.0000
Concentration of Maltose (µg)

Appendix 4

Phosphorus calibration curve (Morrison, 1964)

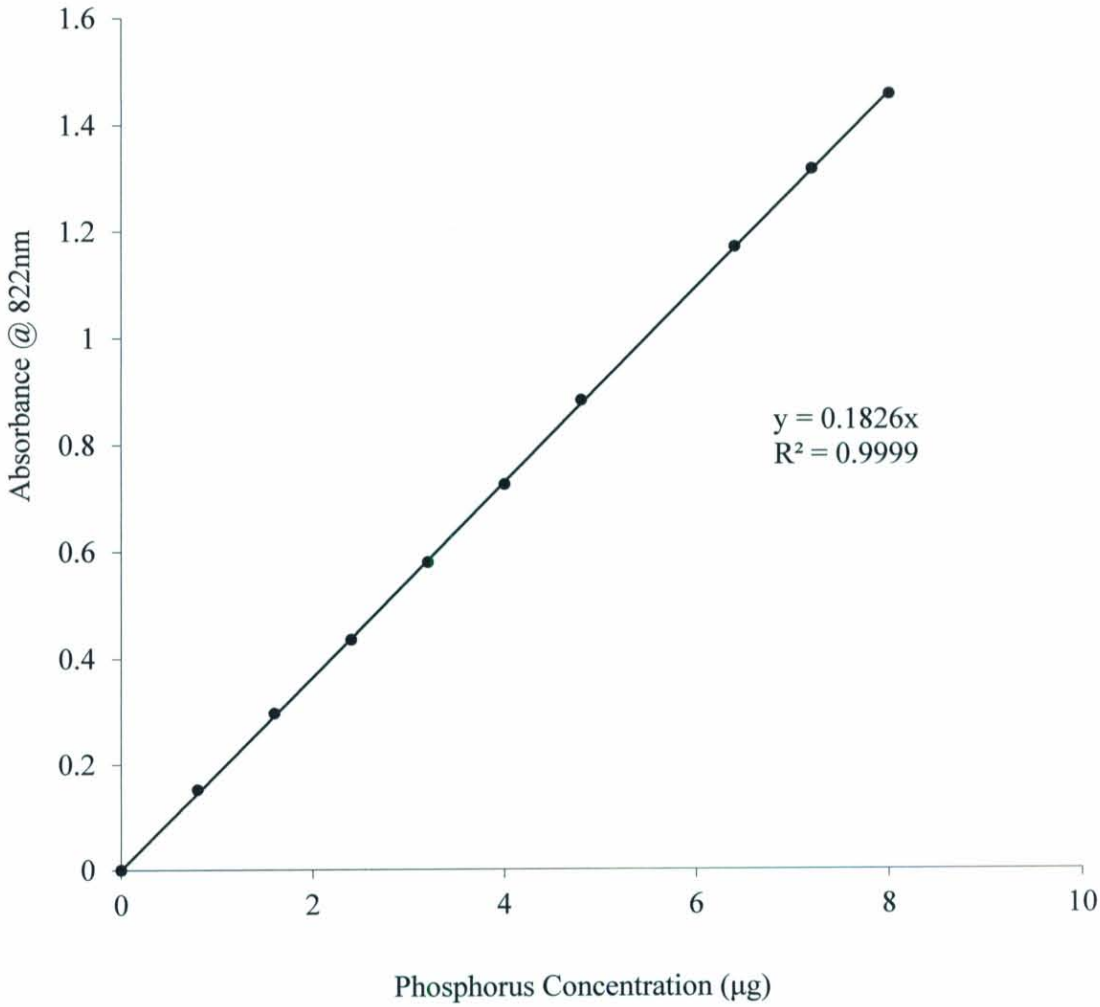
1.6
1.4
1.2
1
0.8
0.6
0.4
0.2
0
Absorbance @ 822nm
y = 0.1826x
R² = 0.9999
0
2
4
6
8
10
Phosphorus Concentration (µg)